Synthesis of Nitrosyl Molybdenum and Tungsten Complexes and their Application in Catalytic Ionic Hydrogenations

DISSERTATION

zur

Erlangung der naturwissenschaftlichen Doktorwürde

(Dr. sc. nat.)

vorgelegt der

Mathematisch-naturwissenschaftlichen Fakultät

der

Universität Zürich

von

Alexander Dybov

aus

Russland

Promotionskomitee

Prof. Dr. Heinz Berke (Vorsitz und Leitung)

Prof. Dr. Roger Alberto

Prof. Dr. Roland Sigel

Zürich 2010

List of the Used Abbreviations

δ	chemical shift
μ	descriptor of bridging
ν	frequency
BAr^F_4	tetrakis(3,5-bis(trifluoromethyl)phenyl)borate
Cy	cyclohexyl
d	doublet
dcype	1,2-bis(dicyclohexylphosphino)ethane
dippe	1,2-bis(dicyclohexylphosphino)ethane
dippf	1,1'-bis(diphenylphosphino)ferrocene)
depe	1,2-bis(diethylphosphino)ethane
dippp	1,3-bis(diisopropylphosphino)propane
dppe	1,2-bis(diphenylphosphino)ethane
ee	enantiomeric excess
Et	ethyl
Et_2O	ethyl ether
Hz	hertz
iPr	isopropyl
IR	infrared
m	multiplet (NMR)
Me	methyl
Mes	1,3,5-trimethylphenyl
MS	mass spectra
NMR	Nuclear Magnetic Resonance
Ph	phenyl
ppm	part per million
quart	quartet
quint	quintet
r.t.	room temperature
s	singlet
t	triplet

THF tetrahydrofuran

(*S*,*S*)-dmpcp 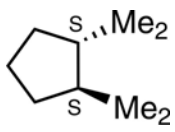

(*S*,*S*)-dippcp 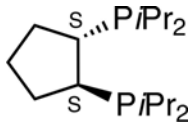

List of the Prepared Compounds

(dippe)W(NO)$(Cl)_3$(dippe)$(Cl)_3$(NO)W(dippe) (**1**)

W(NO)$(Cl)_3$(dippe) (**2**)

W$(dippe)_2$(NO)(Cl) (**3**)

Mo$(dippe)_2$(NO)(Cl) (**4**)

W$(dippe)_2$(Cl)(NO···$LiBH_4$) (**5**)

W$(dippe)_2$(H)(NO···$LiBH_4$) (**6**)

W$(dippe)_2$(NO)H (**7**)

Mo$(dippe)_2$(NO)H (**8**)

W$(dippe)_2$(NO)(O(CH)O) (**9**)

Mo$(dippe)_2$(NO)(O(CH)O) (**10**)

[W$(dippe)(H)_2$(dippe)(NO)][$BAr^F{}_4$] (**11**)

[W$(dippe)(H)_2$(dippe)(NO)][BF_4] (**12**)

[Mo$(dippe)_2$(NO)][$BAr^F{}_4$] (**13**)

[Mo$(dippe)_2$(NO)][BF_4] (**14**)

W$(dppe)_2$(NO)(Cl) (**15**)

W$(dppe)_2$(NO···$AlCl_3$)Cl (**16**)

Mo$(depe)_2$(NO)(Cl) (**17**)

Mo$(depe)_2$(NO)H (**18**)

[(Mo(NO)$(depe)_2)_2$(μ-N_2)][$BAr^F{}_4$]$_2$ (**19**)

[(dippe)(NO)Mo(μ-$Cl)_3$Mo(NO)(dippe)][BF_4] (**20**)

Mo(dcype)Cl_3(NO) (**21**)

Mo(dcype)(dippe)(NO)Cl (**22**)

Mo(dcype)(dippe)(NO)H (**23**)

[Mo(dippe)(dcype)(NO)][$BAr^F{}_4$] (**24**)

Mo(dippp)$(CO)_2$(NO)Cl (**25a**)

Mo(dippe)$(CO)_2$(NO)Cl (**25b**)

Mo(dippf)$(CO)_2$(NO)Cl (**25c**)

Mo(dcype)$(CO)_2$(NO)Cl (**25d**)

W(dippp)$(CO)_2$(NO)Cl (**26a**)

Mo(dippp)$(CO)_2$(NO)H (**27a**)

$Mo(dippe)(CO)_2(NO)H$ (**27b**)

$Mo(dippf)(CO)_2(NO)H$ (**27c**)

$Mo(dcype)(CO)_2(NO)H$ (**27d**)

$W(dippp)(CO)_2(NO)H$ (**28a**)

$[Mo(dippp)(CO)_2(NO)(THF)][BAr^F{}_4]$ (**29a**)

$[W(dippp)(CO)_2(NO)(THF)][BAr^F{}_4]$ (**30a**)

$[Mo(dippp)(CO)_2(NO)(THF)][B(C_6F_5)_4]$ (**31a**)

$Mo(PiPr_3)_2(NO)(CO)_2Cl$ (**32**)

$Mo(PiPr_3)_2(NO)(CO)_2H$ (**33**)

$[Mo(PiPr_3)_2(NO)(CO)_2(THF)][BAr^F{}_4]$ (**34**)

$Mo((S,S)\text{-dmpcp})_2(OPh)(NO)$ (**35**)

$Mo((S,S)\text{-dippcp})_2(NO)(Cl)$ (**36**)

Content

Content

1 Introduction

The discovery of the first hydride complex $H_2Fe(CO)_4$ in 1931 by Hieber[1, 2] opened a new era in organometallic chemistry. Nowadays hydrides are widely used in organic, pharmaceutical and agricultural industries. They are widely used in catalytic hydrogenations of olefins,[3, 4] aldehydes, ketones[5, 6] and imines,[7] as well as hydrosilylation[8-10] and polymerization.[11-13] Some of the hydride complexes show high selectivity and efficiency in homogenous catalyses. [14-16] Moreover, the hydride formation is a key step in dozens of hydrogenation reactions. The commonly known Wilkinson's catalyst $RhCl(PPh_3)_3$,[17] a complex lacking hydride ligands, cleaves hydrogen via oxidative addition and forms dihydride complex with subsequent β-H shift of hydride towards a coordinated substrate and reductive elimination of the reaction product.[18] Ruthenium complex catalyzing the hydrogenation of maleic acid with the similar mechanism was first reported in 1960 by Halpern, Harrod and James.[19] Schrock and Osborn developed a Rh complex that is active in ketone hydrogenation reactions.[20] All the above mentioned examples demonstrated wide appreciation of studies concerning hydrides. Hereinafter the main aspects of the hydride chemistry are discussed in more detail.

1.1 Proton and hydride transfer of metal hydrides

The term "hydride" implies the presence of a metal-hydrogen bond in an organometallic complex. However, it does not reflect the chemical reactivity of the hydride ligand. The classical approach based on electronegativities considers a M−H bond of the transition metal hydrides as a polar covalent bond with a polarization toward the hydrogen site ($M^{\delta+}-H^{\delta-}$).[21, 22] Nevertheless, it does not signify that the hydrides always react as a base or a nucleophile. The detailed mechanism of hydride transfer to the substrate is discerned through fundamental kinetic and mechanistic studies. One of the fascinating aspects of metal hydrides is the diversity of their reactivity patterns.[23] The metal-hydride bond can be cleaved by all three ways of formal bond rupture shown in Scheme 1.1.

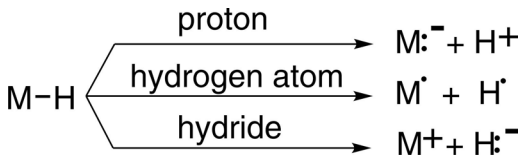

Scheme 1.1 Modes of bond cleavage of metal hydrides.

There are several examples whereby the same hydrides can exhibit all three formal modes of M−H bond cleavage. Metal hydrides such as $[W(Cp)(CO)_3H]$, $[Mo(Cp)(CO)_3H]$, $[Mo(Cp)(CO)_2(PPh_3)H]$, $[Mn(CO)_5H]$, $[Re(CO)_5H]$, and others can undergo cleavage of their metal-hydride bond as proton, hydrogen atom, or hydride depending on the substrate, reaction condition, the structure, ligand coordination sphere, etc.[24-27] For instance, complex $[W(Cp)(CO)_3H]$ was shown to act as a H^+ source toward simple bases and as a source of H^- in the presence of acids.[28]

There are two general ways of dihydrogen delivery to the substrate proceeding in a formal homolytic or heterolytic fashion (Scheme 1.1), depending on how dihydrogen (H_2) is transferred to the substrate. The first one, so-called Wilkinson type of hydrogenation, implies homolytic splitting of the hydrogen and hydrogen atom transfer towards a substrate.[29] The ionic mechanism of hydrogenation operating with heterolytic H_2 cleavage involves a principally new approach[30, 31] of the hydride (H^-) or proton (H^+) transfer to the substrate.[24] The Wilkinson hydrogenation can be efficiently used for hydrogenation of olefinic compounds, whereas the ionic hydrogenation possesses better activity towards unsaturated polar organic compounds such as ketones and imines. This approach is very formal since classical Wilkinson type catalysts were found to be active in ketone hydrogenation.[32] On the contrary, olefinic compounds were hydrogenated via ionic transfer reaction.[30, 33, 34] Nevertheless, it is necessary to discern homolytic and heterolytic hydrogenations as in the most cases it can be definitely identified which system is related to which mechanism.

This review will be mostly focused on the ionic transfer hydrogenation. There are two types of ionic hydrogenations, stoichiometric and catalytic. The simplest metal monohydrides can donate the H^-, and are normally incapable of the hydride to be restored after the reaction, which can be attributed to the stoichiometric type. The catalysts operating with ionic hydrogenation mechanism are often based on precious

metal and after the hydride transfer these complexes retain the capability to reform the hydride by activation of hydrogen gas or other hydrogen sources.

1.2 Stoichiometric ionic hydrogenation

The first ionic hydrogenation was observed by Kursanov *et al.*[30] Stoichiometric amounts of CF_3CO_2H acid as a proton donor and Et_3SiH as a hydride source were used. Further investigations revealed Et_3SiH to be much weaker hydride donor compared to most of transition metal hydrides. Another advantage of using transitional metal hydrides is the potential of catalytic developments, in which H_2 can be used as a source of both H^+ and H^-. The ability of some metal complexes to form a M−H bond via the interaction with the hydrogen is a key step in catalytic hydrogenation reactions (the hydrogen activation reaction is discussed in Chapter 1.4 in more detail). The way how metal hydrides interact with acids can be also considered as an advantage over $HSiEt_3$. While $HSiEt_3$ evolves hydrogen immediately after protonation, many metal hydrides are able to produce a stable product after the protonation. Protonation at the M−H bond produces a dihydrogen complex in which an H_2 ligand is bound to the metal, while protonation at the metal gives a dihydride complex (Scheme 1.2).[35]

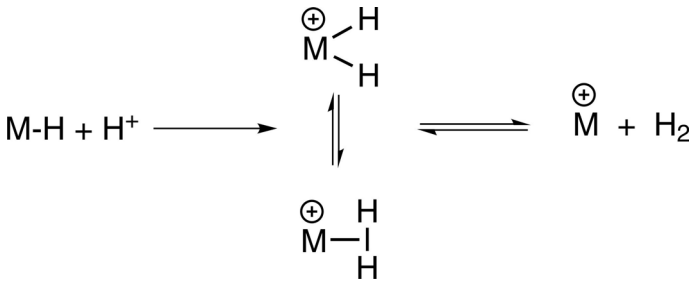

Scheme 1.2 Protonation of a metal hydride and subsequent H_2 formation.

Dihydrogen complexes generally have a higher kinetic acidity in comparison to the corresponding dihydrides.[36] It might be expected that dihydrogen complexes act as a better proton donors in ionic hydrogenations. In fact it does not make a big difference whether a dihydride or a dihydrogen complex (or an equilibrium mixture of the two) is

the proton donor, as long as this species are sufficiently acidic. In both cases hydride transfer from neutral metal hydride generate the product.

Based on Kursanov's investigations, in which combination of $HSiEt_3$ and CF_3SO_3H was used in alkene ionic hydrogenation, many hydrides were tested in the similar reactions.[28, 37] Our group also reported the hydrogenation pair $W(NO)(CO)_2(PMe_3)_2H$ and 8-hydroxyquinoline that selectively reduces the olefin functionality and does not attack the C=O bond in PhCH=CH(C(O)Ph).[38] The combination of $W(Cp)(CO)_3H$ and CF_3SO_3H is another example of olefin ionic hydrogenation to mention.[33, 37]

Many transition metal hydrides were also reported to be active in the stoichiometric ketone and aldehyde ionic hydrogenation. One of the pioneering works in this field was performed by Darensbourg and co-workers in 1985.[39] Group VI metal hydrides $[HM(CO)_4L]^-$ (M = Cr, W; L = CO, $P(OMe)_3$ and PPh_3) were shown to successfully hydrogenate variety of ketones, aldehydes and epoxides. The mechanism for these reductions appears to involve nucleophilic attack of the carbonyl by hydride. For aldehydes, this leads to a straightforward observation of alkoxides in the absence of acid. No such intermediates were observed for reduction of ketones. The group VI hydrides are, evidently, not hydridic enough and consequently requires a strong acid for successful ionic hydrogenation.

El-Omrani and co-workers investigated the applications of group VI binuclear hydrido anions $Et_4N[\mu\text{-}HM_2(CO)_{10}]$ (M = Mo and W) in combination with acetic acid. The authors confirmed the chemioselective reduction of the carbon-carbon double bond of α,β-unsaturated ketones.[40]

Ionic hydrogenation implies the delivery of a hydride and a proton to the substrate. The question rose up whether the H^- transfer or the H^+ delivery occurs first. If the reaction rate is limited by the proton transfer, a ketone must undergo a fast insertion into M−H bond with alkoxide formation. However, the kinetics exhibited the reaction to be second-order overall, first order in aldehyde, and first order in metal hydride while the acidity was held constant by a buffer. Consequently, a proton transfer reaction followed by a rate-determining hydride transfer takes place (Scheme 1.3).[41] This fundamental

result was confirmed by determination of pK_a values of some metal hydrides and protonated ketones.[42, 43]

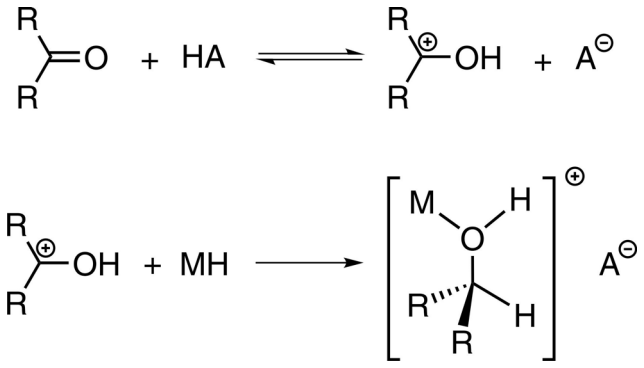

Scheme 1.3 Mechanism of stoichiometric ionic hydrogenation.

The ionic hydrogenation of different substrates leaded to new complexes in which the hydrogenated organic product is bound to the tungsten. Reaction of α,β-unsaturated ketones and $[W(Cp)(CO)_3H]$/HOTf results in hydrogenation of the C=C double bond and formation of $[W(Cp)(CO)_3(\eta^1\text{-ketone})][OTf]$ complexes as a product.[44] Coordinated ethers were obtained in the reaction of acetals. In particular, $[W(Cp)(CO)_3(PhCH_2OCH_3)][OTf]$ was formed as a reaction product of $PhCH(OCH_3)_2$, $[W(Cp)(CO)_3H]$, and HOTf interaction.[45]The reaction of PhC(O)Cl, $[W(Cp)(CO)_3H]$, and HOTf produces the aldehyde complex $[W(Cp)(CO)_3(\eta^1\text{-PhCHO})][OTf]$ and HCl.[44]

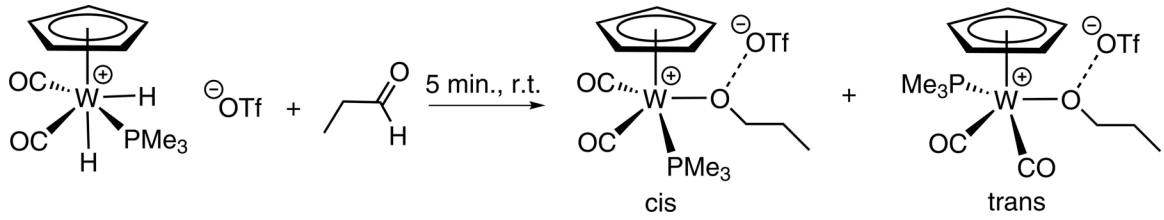

Equation 1.1

The stoichiometric ionic hydrogenation involving $[W(Cp)(CO)_2(PMe_3)(H)_2]^+$ was investigated by Bullock's group. It was found that addition of aldehydes or ketones to the tungsten dihydride cation results in fast stoichiometric hydrogenation at room temperature (Equation 1.1).[46] The initial products of the hydrogenation were *cis* and *trans* isomers of the alcohol complex $[W(Cp)(CO)_2(PMe_3)(ROH)]$, which then released alcohol

slowly. The mechanism of this process is identical to the one observed for separated hydride/proton source pairs. The reaction involves H^+ transfer from a cationic dihydride to the oxygen followed by an H^- transfer from the neutral metal hydride to the carbon atom.

The stoichiometric ionic hydrogenation reactions have been studied in our group for a variety of tungsten and molybdenum complexes. The crucial influence of ligand situated *trans* to hydride atom was shown. All complexes bearing a nitrosyl ligand exhibited higher ionicity of M−H bond that was proven by NMR, IR, and kinetic studies.[47] Also the strong influence of σ-donating abilities of equatorial situated ligands was demonstrated. The increasing polarization of W−H in the series $W(PMe_3)_2(CO)_2(NO)(H)$,[48-50] $W(PMe_3)_3(CO)(NO)(H)$,[51] $W(PMe_3)_4(NO)(H)$[52] was observed. Similar tendency was found in the molybdenum complexes. For instance, $Mo(dmpe)_2(H)(NO)$ (dmpe = 1,2-bis(diethylphosphanyl)ethane)[53] possesses a stronger hydridic character of the Mo−H bond than that of $Mo(CO)(H)(NO)(PMe_3)_3$.[54] It was quantitatively demonstrated by DQCC and bond ionicity determinations of the corresponding deuterides. These parameters were obtained from T_{1min} measurements in solution and in solid state from the Pake doublets of static ^2H NMR spectra. These hydrides exhibited a high propensity to undergo hydride transfer reactions in agreement with their enhanced hydridic properties. It was demonstrated by the reactions with simple ketones and metal carbonyls yielding alkoxy or formyl compounds.

1.3 Catalytic ionic hydrogenation

The stoichiometric ionic hydrogenation provides a metal-based source of H^+ and H^-. However, the completion of catalytic cycle requires direct hydrogen gas reaction with the metal complex (i.e. M−H bonds can be derived from H_2). Bullock *at al.* reported a series of complexes with formula $[M(Cp)(CO)_2(PR_3)(O{=}CEt_2)][BAr^F{}_4]$ (M = W, Mo, Ar^F = 3,5-bis(trifluoromethyl)phenyl), which were shown to be the catalyst precursors for ionic hydrogenation of $Et_2C{=}O$.[55, 56] As it was reported, molybdenum metal exhibited higher catalytic activity than analogous tungsten complexes. The hydrogenation was

performed under mild conditions at 23 °C and 4 atm of H_2 with a maximum about 2 turnovers/hour. The proposed mechanism is shown in Scheme 1.4.

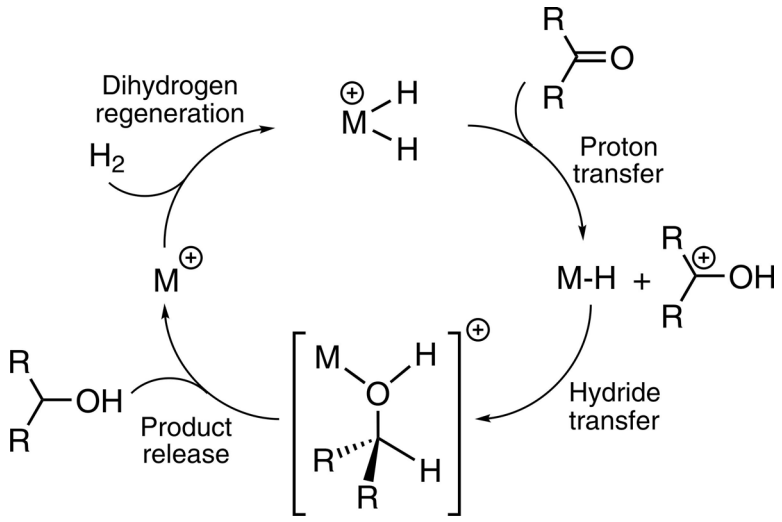

Scheme 1.4 Proposed mechanism for catalytic ionic hydrogenation of ketones.

During this catalytic ionic hydrogenation reaction the increasing amount of the alcohol complexes $[W(Cp)(CO)_2(PR_3)(Et_2CHOH)]^+$ was directly observed by NMR spectroscopy. The limiting step of this reaction was thought to be displacement of the ketone (or alcohol) ligand by H_2 forming the dihydride. For both Mo and W complexes, the rates increase with the steric bulk of the phosphine with the order of catalytic activity being $PCy_3 > PPh_3 > PMe_3$. The big disadvantage of the catalytic system is the instability of the complexes, since phosphonium cations (HPR^{3+}) were observed in the reaction mixtures indicating dissociation of the phosphine and, consequently, decomposition of the catalyst.

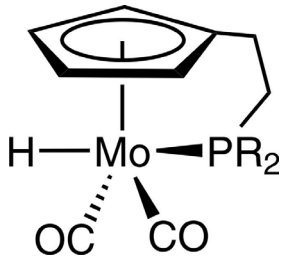

Figure 1.1

The observation of decomposition led to the improvement of the catalytic system. A new complex where the phosphine ligand was bound to the cyclopentadienyl ring via an ethylene bridge was used as a catalyst precursor (Figure 1.1).

Hydrogenation of liquid ketones can be carried out under solvent-free conditions at low catalyst loadings. For example, neat $Et_2C=O$ was completely hydrogenated to the alcohol (eight days at 50 °C, 55 atm. H_2 pressure) using $[MoH(CO)_2(\eta^5:\eta^1\text{-}C_5H_4)\text{-}(CH_2)_2PCy_2)]$ (0.35 mol%) as the catalyst precursor.[57]

Catalytic ionic hydrogenations are believed to be involved in the selective deoxygenation of 1,2-propanediol to n-propanol (Equation 1.2).[58]

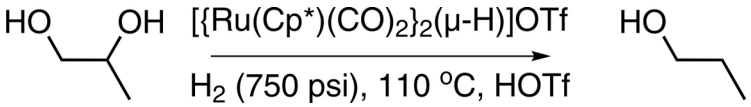

Equation 1.2

The initial step of the deoxygenation of diols is dehydration of the diol producing aldehyde, which then undergoes ionic hydrogenation to yield the alcohol product. Following the discovery of this hydrogenation step in the deoxygenation reaction, it was independently discoved that aldehydes and ketones are hydrogenated using $[\{Ru(Cp^*)(CO)_2\}_2(\mu\text{-}H)]OTf$ as a catalyst precursor under H_2. This apparently occurs via dihydrogen complex $[Ru(Cp^*)(CO)_2(H_2)]^+$ originating from the bimetallic complex under H_2 in the presence of HOTf.

Norton and co-workers reported the Ru catalyst with chiral phosphines which were successfully tested in the enantioselective hydrogenation of C=N double bonds of iminium cations (Equation 1.3).[59]

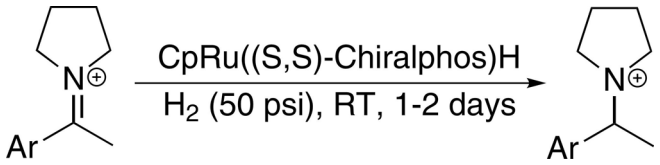

Equation 1.3

The mechanism of the hydrogenation is believed to be similar to the one proposed for ketone hydrogenation (Scheme 1.4). However, NMR monitoring of the reaction

revealed the limiting step to be a hydride transfer. These stoichiometric H^- transfers become faster as the chelate ring in CpRu(P-P)H becomes smaller or as more electron donating substituents are introduced onto the phosphine.[59, 60] Interestingly, the reaction showed expected preference for the hydrogenation of C=N over the hydrogenation of C=C, although a terminal C=C can block the coordination of another H_2 after H^- transfer. With an α,β-unsaturated iminium cation the initial H^- transfer gives an enamine, that is further protonated and hydrogenated to an ammonium cation.[61]

In the 1980s, Shvo and co-workers developed a bimetallic ruthenium complex (Scheme 1.5) served as a catalyst precursor for the hydrogenation of C=O and C=C bonds. The two metals were joined by both a bridging hydride as well as an C−O−C bridge. The catalytic ketone hydrogenations were carried out at 145 °C under an initial H_2 pressure of 500 psi.[62-64]

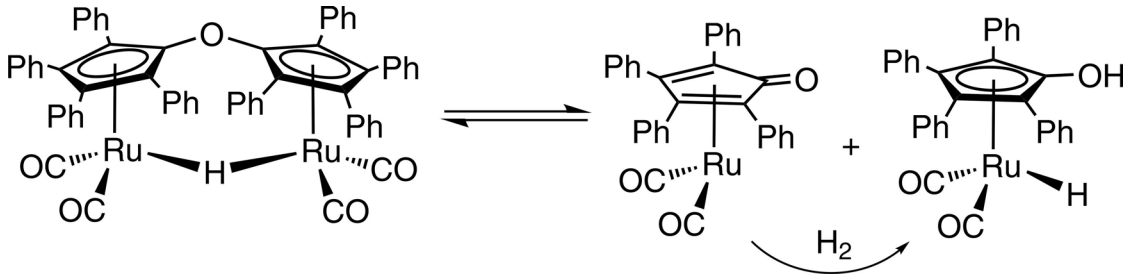

Scheme 1.5 Shvo's bimetallic ruthenium catalyst precursor and catalyst.

Cleavage of the bimetallic complex under these conditions produces an 18-electron complex with a Ru−H and an O−H bond that carries out the hydrogenations. Additionally, the unsaturated 16-electron intermediate capable to cleave the hydrogen molecule forms the same 18-electron complex. Baeckvall and co-workers found that Shvo catalyst can be used at 70 °C for the transfer hydrogenation of imines.[65] Moreover, it was found that the isopropanol can play a role of hydrogen source. After the dissociation 16-electron species interacts with the alcohol producing 18-electron active complex. The reaction is highly efficient with turnover frequencies of over 800 per hour.

Efforts to find catalysts that do not require noble metals were done by Casey and co-workers in 2007. An efficient and chemoselective iron catalyst was reported to be

tested in ketone hydrogenations (Figure 1.2).[66, 67] The hydrogenations can take place at room temperature under low hydrogen pressure.

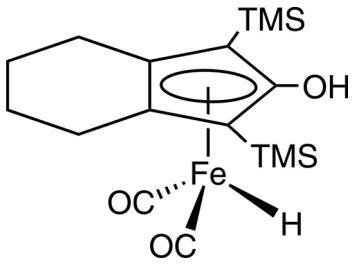

Figure 1.2

The catalyst operates with the similar to the Shvo's Ru catalyst mechanism. Proton transfer from the O−H group followed by hydride transfer from the Fe−H group, accomplishes the overall transfer of H_2 to the C=O bond. Regeneration of the catalyst is complete by heterolytic cleavage of H_2 to produce O−H and Fe−H bonds, possibly via an undetected η^2-H_2 dihydrogen complex. This discovery of the iron catalyst that is active under mild conditions is a good example of the progress in seeking catalysts that do not require noble metals.

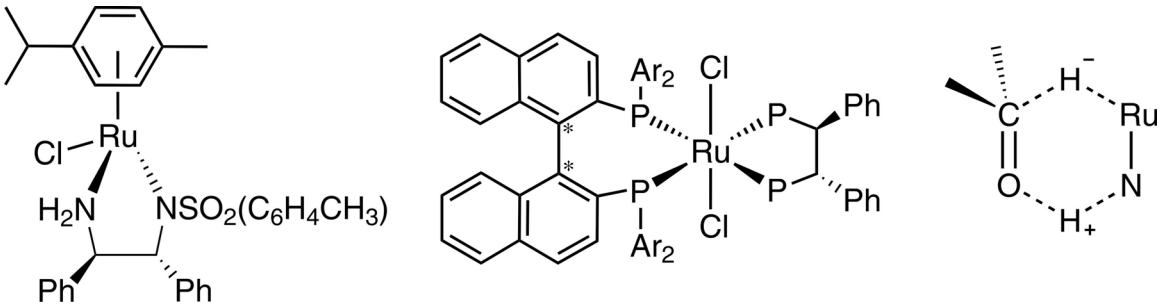

Figure 1.3

Highly enantioselective transfer hydrogenation catalysts that exhibit extraordinary turnover rates and lifetimes were developed recently by Noyori and co-workers.[68, 69] Two of these remarkable catalysts are presented in Figure 1.3.

Under reaction conditions (isopropyl alcohol and a base such as KOH) the active catalyst containing a RuH and a NH site is formed. The transition state for these metal-ligand bifunctional catalysts was shown computationally to involve a six-member ring

system (Figure 1.3) whereby hydride transfer from RuH and proton transfer from NH occur simultaneously.[70] The mechanism does not require formation of metal alkoxides or carbonyl-metal coordination complexes in the catalytic cycle.

1.4 Hydrogen activation ability of transition metal complexes

The fundamental investigations in the field were done by Kubas and coworkers some decades ago. Before Kubas' discovery, the dihydrogen η^2-H_2 complex was assumed to be unobservable intermediate in dihydride formation. In 1983 $W(CO)_3(P\textit{i}Pr_3)_2(H_2)$ was isolated and exemplified as the first η^2-H_2 complex.[71] The neutron diffraction investigations revealed that H−H distance is elongated to 0.89 Å from 0.75 Å in free H_2, indicating the bond is only partially broken.

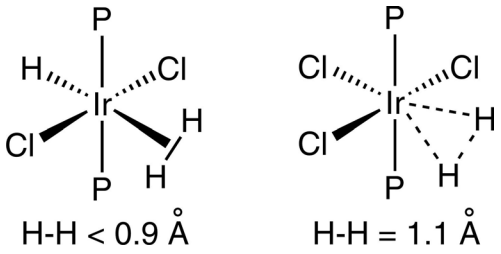

Figure 1.4

The bonding in M−H_2 and other σ-bond complexes is stabilized by backdonation from a filled metal *d* orbital to the σ* orbital of the H−H bond. Backdonation is crucial in activating the H−H bond towards homolytic cleavage to dihydride ligands. If the backbonding becomes too strong, e.g. if more electron donating co-ligands are put on M, the σ-bond cleaves to form a dihydride because of overpopulation of $H_2\sigma^*$. For example, strong π-acceptors such as CO greatly reduce backdonation, and H−H distance is normally < 0.9 Å in complexes with CO *trans* to H_2. In the contrary, complexes with mild σ-donor ligands such as H_2O *trans* to H_2 or π-donors such as Cl, have elongated H−H bonds (0.96-1.34 Å) (Figure 1.4).[72] Most of these structure and bonding principals were accurately modulated computationally. The interplay between experiment and theory in M(η^2-H_2) and M−H systems has been remarkably effective.[73]

Back-bonding from M to the H−H σ* orbital has widely been accepted to control the H−H distance along the reaction coordinate toward OA and confers stability to H_2 complexes; e.g. poor back-bonding fragments such as $Cr(CO)_5$ give thermally unstable H_2 complexes.[74-76] As a good example, two complexes $Mo(R_2PCH_2CH_2PR_2)_2(CO)$ (R = Ph, Et) can be considered (Scheme 1.6).[72, 77, 78]

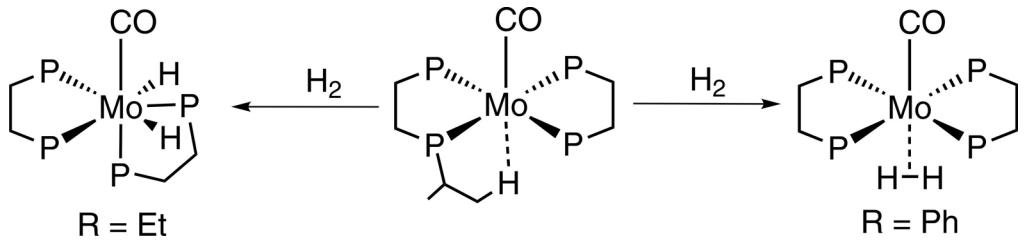

Scheme 1.6 Influence of substituents on hydrogen activation reactivity.

Complex $Mo(dppe)_2(CO)$ bears two dppe (1,2-bis(diphenilphosphanyl)ethane) ligands which possess less electron donating capability than related depe (1,2-bis(diethylphosphanyl)ethane) diphosphin in $Mo(depe)_2(CO)$. In consequence, complex $Mo(dppe)_2(CO)$ can coordinate a hydrogen molecule elongating a H−H bond, whereas $Mo(depe)_2(CO)$ is able to homolytically cleave H−H molecule forming a stable dihydride complex at room temperature.

1.5 Objectives of the work

The aim of the project is to develop a catalytic system based on cheap metals, molybdenum and tungsten. As it was discussed before, some efforts in this direction have been done. Bullock reported catalytic system with molybdenum and metals which showed catalytic activity towards ketone hydrogenation. However, the activity of the catalysts still remains very low and is incomparable with precious metal catalytic systems. Nevertheless, Bullock and co-workers demonstrated that the ionic complexes such as $[M(CO)_2Cp(PR_3)(\eta^1\text{-}Et_2C{=}O)][BAr^F{}_4]$ are able to activate hydrogen at room temperature leading to the formation of a cationic dihydride $[M^+(H)_2]$.[55, 56] The dihydride is involved in catalytic cycle and can deliver hydrogen to the substrate via ionic transfer mechanism.

A synthesis of a series of transitional metal hydrides was reported by our group.[21, 38, 47-54, 79-87] The influence of electronic and steric effects of the ligand sphere on the ionicity of metal-hydride bond and, consequently, on reactivity of the hydride was unambiguously demonstrated. The crucial influence was proven to have a ligand located in *trans* position to the hydride atom due to strong *trans* influence.[88-91] The studies in our group showed that nitrosyl group in *trans* position to the hydride is very efficient in promotion of hydride transfer reaction with unsaturated compounds.

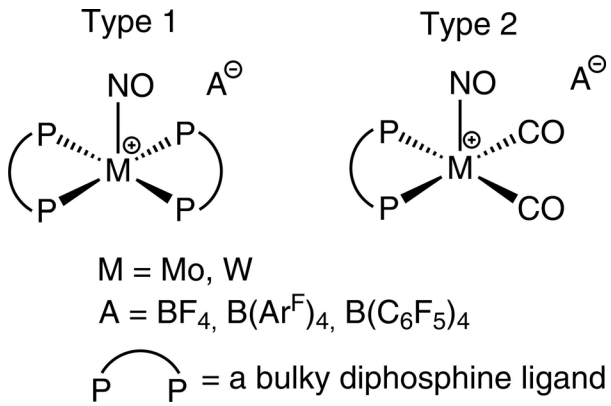

Figure 1.5

On the other hand Kubas reported the enormous influence of the equatorial ligands on the hydrogen activation capability of the complexes (see chapter 1.4). The electron-donating bulky diphosphine ligands such as $iBu_2PCH_2CH_2PiBu_2$ or $Et_2PCH_2CH_2PEt_2$ (depe) exhibited the observable increasing of the reactivity in hydrogen activation reaction. We came to the similar conclusion. The increasing of the number of phosphine ligands as well as bulkiness of the phosphine ligands results in enhanced hydride activity.

Summarizing all, we designed two types of nitrosyl complexes, which in our opinion might have activity towards hydrogenation of unsaturated compounds (Figure 1.5). The type 1 is related to the Kubas' complexes $M(R_2PCH_2CH_2PR_2)(CO)$.[77, 78, 92] Thus, it contains a nitrosyl instead of carbonyl ligand that might cause sufficient enhancement in the system properties. The type 2 was developed to facilitate the approach of the substrate, which was presumably sterically hindered in the type 1 molecules. We used 1,3-bis(diisopropylphosphanyl)propane (dippp), 1,2-

bis(diisopropylphosphanyl)ethane (dippe), 1,1'-bis(diphenylphosphino)ferrocene) (dippf), 1,2-bis(dicyclogexylphosphanyl)ethane (dcype), 1,2-bis(diethylphosphanyl)-ethane (depe) and 1,2-bis(diphenilphosphanyl)ethane (dppe) as a bulky diphosphine ligand. We chose BF_4^-, $BAr^F{}_4^-$ (Ar^F = 3,5-bis(trifluoromethyl)phenyl), $B(C_6F_5)_4^-$ as counterions due to their stability and non-coordinative ability.[93-96] The synthesis development and the investigation of the chemical and catalytic properties of the complexes obtained are to be reported in this dissertation.

2 Complexes of the Type [M(P∩P)$_2$(NO)][A]

2.1 Introduction

Homogeneous catalysis of ketone hydrogenation is mainly accomplished with ruthenium and rhodium complexes. A mechanism related to Wilkinson hydrogenations of olefins is anticipated, where initial binding of the ketone to the metal, subsequent insertion of the ketone into the M–H bond and reductive elimination of the alcohol are key steps.[29] An alternative reaction course for ketone hydrogenations is ionic hydrogenation, which does not require primary insertion into the M−H bond, rather heterolytic splitting of the H_2 molecule and transfer of a proton (H^+) and a hydride (H^-) to the ketone.[24, 31] Molybdenum and tungsten dihydride complexes are thought to bear both these functions in the same molecule acting as proton and hydride donors at the same time.[34, 97, 98] In 1994 Bullock and co-workers showed that transition metal monohydrides are capable of providing an H_2 equivalent in the presence of acids. $HW(CO)_3Cp$ and other metal hydrides were used for the stoichiometric ionic hydrogenation of alkenes,[37] alkynes[33] and ketones.[41] Such stoichiometric reactivity studies led to the development of a series of Mo and W catalysts for the homogeneous hydrogenation of ketones.

Related to the described chemistry, hydride transfer reactions between $HM(CO)_2Cp(PR_3)$ (M = Mo, W; R = Me, Ph, Cy) and $[H(Et_2O)_2][BAr^F{}_4]$ in the presence of $Et_2C{=}O$ gave ketone complexes $[M(CO)_2Cp(PR_3)(\eta^1\text{-}Et_2C{=}O)][BAr^F{}_4]$ [Ar^F = 3,5-bis(trifluoromethyl)phenyl] and Et_2HCOH. The ketone complexes were shown to be catalyst precursors for the homogeneous hydrogenation of various ketones.[55, 56] Mechanistic experiments supported the proposed ionic hydrogenation mechanism that involves proton transfer from a cationic dihydride $[M^+(H)_2]$. There are neutral $16e^-$ complexes of the type $M(CO)(R_2PCH_2CH_2PR_2)_2$ (M = W, Mo, R = Ph, Bz, Et, *i*Bu) stabilized by an agostic M···H−C interaction, which can cleave the H_2 molecule forming dihydride molybdenum complexes.[92, 99-101] These can be considered as analogues of dihydride intermediate complexes in the catalytic cycle proposed by Bullock.[57, 102]

We in our group are interested in the development of systems that are capable of activating the hydrogen molecule in a heterolytic fashion. For that purpose we designed a system bearing besides two alkyl diphosphanes a nitrosyl ligand situated *trans* to a vacant site of the metal center. We supposed that the nitrosyl ligand might effect weakening of any *trans* M–H bond via its *trans* influence. In this chapter we report the preparation and characterization of complexes of the type [M(P∩P)$_2$(NO)$^+$] (M = Mo, W; P∩P = *i*Pr$_2$PCH$_2$CH$_2$P*i*Pr$_2$, Ph$_2$PCH$_2$CH$_2$PPh$_2$, Et$_2$PCH$_2$CH$_2$PEt$_2$ and Cy$_2$PCH$_2$CH$_2$PCy$_2$) and studies of them in hydrogen activation reaction.

2.2 Synthesis of molybdenum and tungsten chlorides [M(dippe)$_2$(NO)Cl] (M = Mo, W)

Previously two main methods were described to prepare molybdenum or tungsten complexes bearing a nitrosyl ligand, four phosphine ligands and one chloride ligand. The first one is based on substitution of the carbonyl groups in the complex [M(NO)(CO)$_4$(ClAlCl$_3$)] (M = Mo, W) with the corresponding phosphines at high temperature.[53] However, this method was found not to be very efficient. The heating of the mixture of [M(NO)(CO)$_4$(ClAlCl$_3$)] during 10 days at 160 °C with excess of the dippe ligand led to the formation of the desired products, but the yield achieved were low in both molybdenum and tungsten cases due to the formation of the asymmetric complexes containing two non-substituted carbonyl groups. The prolonged reaction time does not significantly enhance the yield of the products.

Another route to the desired molecules involves the substitution of two weakly coordinated CH$_3$CN ligands in the complex [M(NO)(CH$_3$CN)$_2$Cl$_3$] (M = Mo, W) by phosphine ligands and consequently elimination of two chlorides with 1% sodium amalgam in the presence of the phosphine ligands.[85, 103] This method showed more promising results in comparison with the one described above.

The tungsten complex [W(NO)(CH$_3$CN)$_2$Cl$_3$] interacts with excess of the dippe ligand at room temperature forming the yellow crystalline compound [(dippe)W(NO)(Cl)$_3$(dippe)(Cl)$_3$(NO)W(dippe)] (**1**) (Scheme 2.1). The ^{31}P {^{1}H} NMR spectrum of **1** showed two broad paramagnetic signals with the integration ratio 2:1 at

59.2 ppm and 11.6 ppm identifying the presence of two chemically different phosphorus atoms in the molecule. The ^{1}H NMR spectra of **1** showed broad paramagnetic signals from 3.00 to 1.00 ppm. The IR spectrum of **1** showed a strong band at 1609 cm^{-1} attributed to ν(NO) stretching vibration.

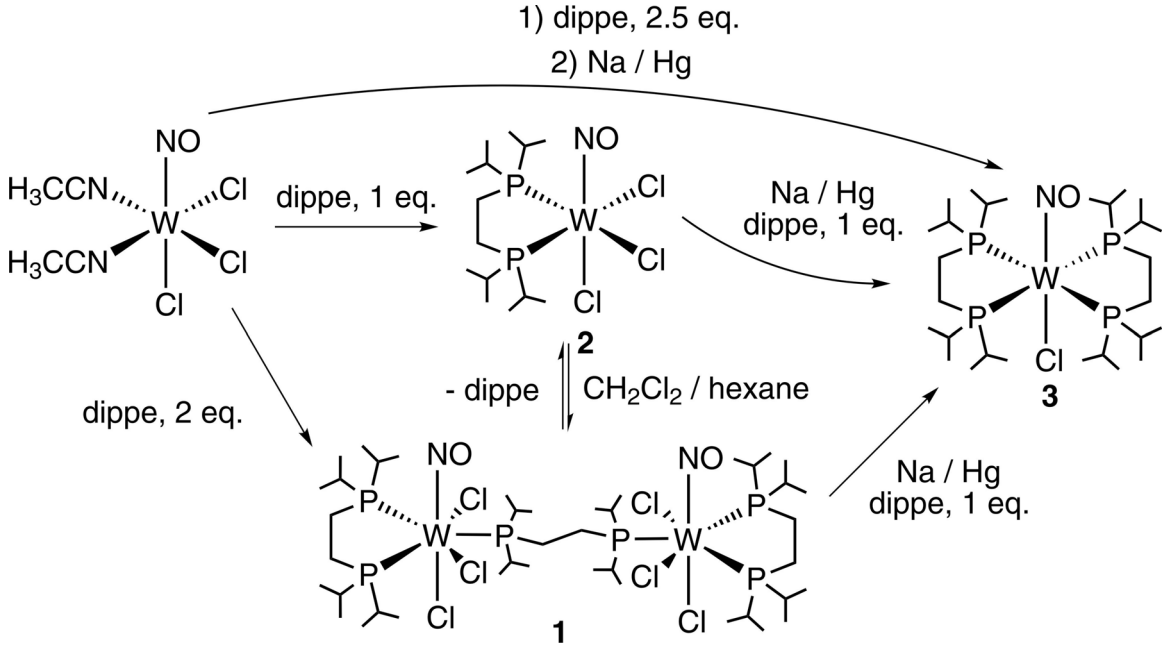

Scheme 2.1

The molecular structure of compound **1** was unambiguously established by X-ray diffraction analysis. Figure 2.1 shows an ORTEP drawing of the complex **1**. The X-ray data collection and processing parameters are presented in the Experimental Part. Compound **1** crystallizes in the centrosymmetric space group P2$_1$/c. The dinuclear species lie on a center of symmetry in the middle of the P−CH$_2$−CH$_2$−P bridge, which made it possible to refine only one half of the molecule. Two dichloromethane solvate molecules co-crystallized with the compound. The coordination sphere around tungsten can be described as distorted pentagonal bipyramid. Two phosphorus atoms of the bidentate ligand, as well as one phosphorus atom from the bridging phosphine and two chloride atoms do not lie in one plane. The three phosphorus atoms are slightly bent towards the NO ligand (angle Cl2−W1−P3 is 93.30(3)°, angle Cl2−W1−P2 is 91.14(3)°), whereas the chlorides Cl1 and Cl3 towards the Cl2 atom (angle Cl2−W1−Cl1 is 82.93º). The NO ligand and the Cl2 chloride atom are located *trans*. The W1–P3 bond was found to be

significantly elongated in comparison with two other tungsten–phosphorus bonds (Table 2.1).

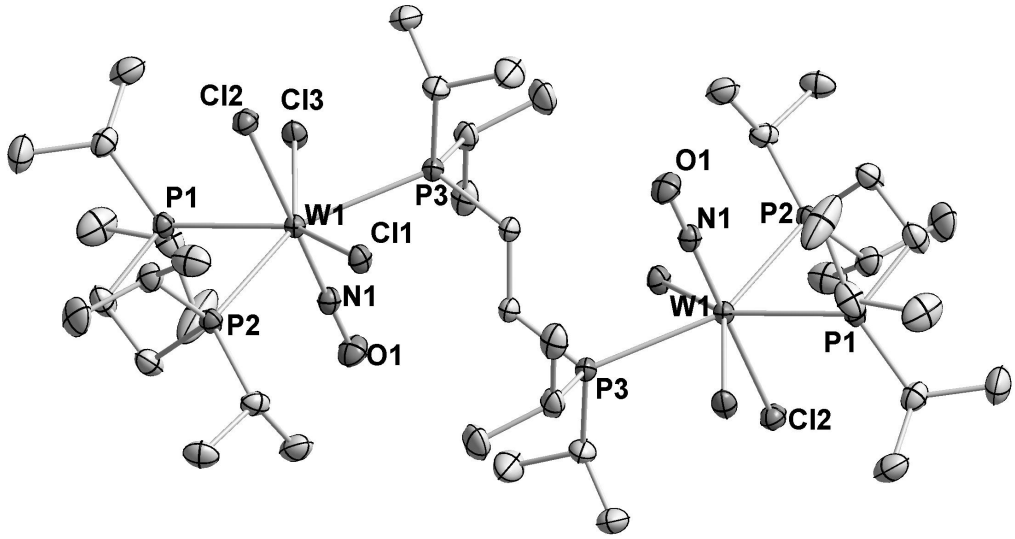

Figure 2.1 An ORTEP drawing of **1**. Displacement ellipsoids are drawn at the 50% probability level. All hydrogen atoms have been omitted for clarity.

Table 2.1 Selected Bond Lengths [Å] and Bond Angles [°] of **1**.

Bond lengths			
W1−N1	1.7826(3)	W1−P2	2.5979(7)
W1−Cl3	2.4449(8)	W1−P1	2.6584(9)
W1−Cl1	2.4741(9)	W1−P3	2.6894(8)
W1−Cl2	2.4995(8)	W1−O1	2.9837(23)
Bond angles			
N1−W1−Cl3	95.5(1)	N1−W1−P1	93.41(9)
N1−W1−Cl1	97.42(9)	N1−W1−P3	87.33(9)
N1−W1−Cl2	179.36(9)	W1−Cl3−Cl1	142.09(3)
N1−W1−P2	88.4(1)	W1−Cl3−Cl2	84.59(3)

Slow hexane diffusion into a CH_2Cl_2 solution of **1** resulted in crystallization of two different crystalline compounds. One of them was identified as compound **1** and another as W(dippe)(NO)Cl_3 (**2**). The formation of the six-coordinative species at

ambient temperature points to the presence of an equilibrium between six and seven coordinated complexes **1** and **2** in solution (Scheme 2.1). This equilibrium also demonstrated that the bridging phosphine is bound weakly to the metal center. Compound **2** can be directly prepared by the reaction of $[W(NO)(CH_3CN)_2Cl_3]$ and dippe in a stoichiometric ratio.

The ^{31}P $\{^1H\}$ NMR of **2** revealed in contrast to **1** a sharp diamagnetic singlet at 58.6 ppm that indicates the presence of chemically equivalent phosphorus atoms. The ^1H NMR spectra of **2** exhibited two multiplet resonances for the –C*H* protons of the isopropyl groups at 2.92 and 2.66 ppm. A multiplet attributed to the methylene protons was observed at 2.36 ppm. The IR spectrum of **2** showed a strong band at 1642 cm^{-1} attributed to the ν(NO) stretching vibration.

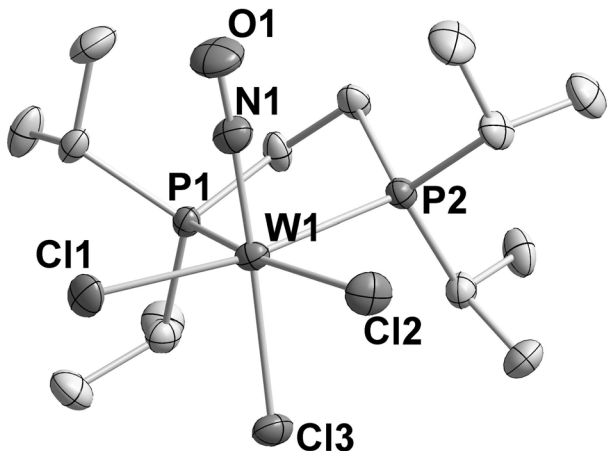

Figure 2.2 An ORTEP drawing of complex **2**. Displacement ellipsoids are drawn with 50% probability. Hydrogen atoms are omitted for clarity.

A X-ray diffraction study confirms the *trans* structure of **2**. An ORTEP drawing of **2** is presented in Figure 2.2. Selected bond distances and angles are summarized in Table 2.2. **2** crystallizes in the non centrosymmetric space group $Pca2_1$ and displays octahedral coordination geometry. The average tungsten-phosphorus bond equals to 2.565 Å that is shorter than the mean metal-phosphorus distance of **1**. The nitrogen atom N1 is slightly bent towards the chloride atom Cl3. The angle N1–W1–Cl3 is 173.59(12)°. One of the phosphorus atoms is slightly bent towards Cl3 atom. The P1–W1–Cl3 angle is

88.44(3)°. In contrast P2 phosphorus atom is bent towards NO group and the angle P2–W1–Cl3 is 95.66(3)°. The chloride atom Cl1 and Cl2 are slightly bent to Cl3 atom.

Table 2.2 Selected Bond Lengths [Å] and Bond Angles [°] of **2**.

Bond lengths			
W1−N1	1.775(4)	W1−P2	2.544(1)
W1−Cl3	2.454(1)	W1−P1	2.587(1)
W1−Cl1	2.351(1)	N1−O1	1.197(5)
W1−Cl2	2.344(1)	W1−O1	2.968(4)
Bond angles			
N1−W1−Cl2	92.70(13)	N1−W1−P1	96.49(12)
N1−W1−Cl1	90.46(12)	Cl2−W1−Cl1	118.53(4)
N1−W1−Cl3	173.59(12)	P2−W1−P1	75.29(3)
N1−W1−P2	89.57(12)	O1−N1−W1	174.0(4)
Cl3−W1−P1	88.44(3)	Cl3−W1−P2	95.66(3)

Either complex **1** or **2** interact with excess of 1% sodium amalgam in the presence of the dippe ligand forming **3** (Scheme 2.1). Based on this observation a one-pot reaction seamed feasible, whereby a small excess of dippe was used, immediately followed by reduction with 1% sodium amalgam of W(NO)(CH_3CN)$_2$Cl$_3$ in THF, which resulted in an increase of the overall yield.

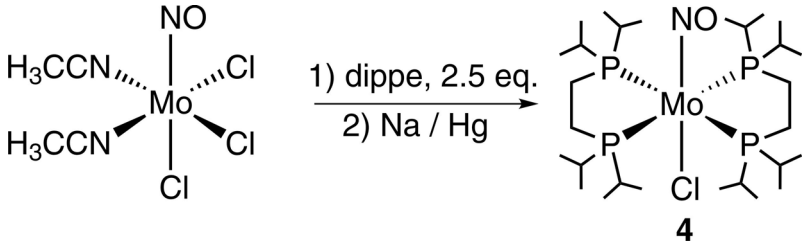

4

Scheme 2.2

Indeed, the consecutive addition of 2.5 equivalent of the dippe ligand and excess of sodium amalgam (1%) to a THF solution of the [W(CH_3CN)$_2$(NO)Cl$_3$] species revealed formation of the chloride **3** (Scheme 2.1), which was isolated in 85% yield. The

yield achieved in the two-step reaction to **3** was 60%. The molybdenum analogue, complex **4** was prepared in the similar way (Scheme 2.2) without isolation of the intermediate product in 80% yield.

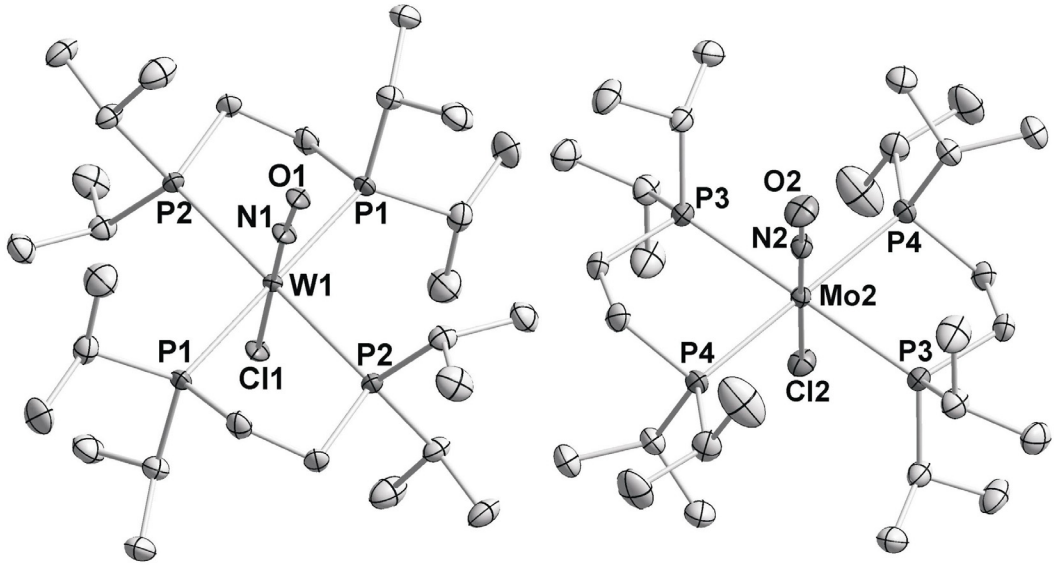

Figure 2.3 ORTEP drawings of one crystallographically independent molecule of **3** and **4**. Displacement ellipsoids are drawn at the 50% probability level. The NO/Cl disorder and all hydrogen atoms have been omitted for clarity.

Table 2.3 Selected Bond Lengths [Å] and Bond Angles [°] of **3**.

Bond lengths			
W1−N1	1.761(5)	N1−O1	1.241(8)
W1−P1	2.4971(8)	W1−P2	2.5403(7)
W1−Cl1	2.5179(19)	W2−P3	2.5381(7)
W2−N2	1.795(5)	W2−Cl2	2.4842(16)
N2−O2	1.229(6)	W2−P4	2.4864(7)
Bond angles			
N1−W1−P1	88.55(17)	P1−W1−P2	78.93(2)
N1−W1−P1	91.45(17)	Cl1−W1−P2	96.04(5)
P1−W1−Cl1	92.90(5)	O1−N1−W1	175.6(6)
N1−W1−Cl1	178.48(17)	N1−W1−P2	84.70(17)

The ^{31}P {^{1}H} NMR spectra exhibited single resonances at 44.5 ppm for **3** and at 59.9 ppm for **4**, which indicated the presence of four equivalent phosphorus atoms in each complex. The ^{1}H NMR spectrum of **3** and **4** showed two multiplets at 2.62 and 2.49 ppm and at 2.69 and 2.51 ppm, respectively, attributed to the –C*H* protons of the isopropyl groups. The bridging CH_2 protons displayed multiplets at 1.63 ppm for **3** and at 1.79 ppm for **4**. The IR spectra revealed strong bands attributed to NO vibrations at 1516 cm^{-1} for **3** and at 1527 cm^{-1} for **4**.

Table 2.4 Selected Bond Lengths [Å] and Bond Angles [°] of **4**.

Bond lengths			
Mo1–N1	1.766(4)	Mo2−P4	2.5007(5)
Mo2−N2	1.796(4)	Mo1−Cl1	2.5450(15)
Mo1−P1	2.5110(5)	Mo2−Cl2	2.5120(14)
Mo1−P2	2.5601(4)	Mo2−P3	2.5569(4)
Bond angles			
N1−Mo1−Cl1	178.35 (9)	P1−Mo1−P2	79.085(15)
N2−Mo2−Cl2	177.83(9)	N1−Mo1−P2	95.36(9)
P1−Mo1−Cl1	87.28(4)	N1−Mo1−P2	84.64(9)

X-ray diffraction studies of **3** and **4** confirmed the spectroscopically derived *trans* structures. ORTEP drawings of the complexes are presented in Figure 2.3. The selected atom bond lengths and angles are summarized in the Tables 2.3 and 2.4.

The asymmetric units of **3** and **4** are composed of two independent halves of the M(NO)(dippe)$_2$Cl molecules (M = Mo, W) with the metal centres lying on crystallographic centres of symmetry. In both structures the *trans* NO and Cl groups are disordered. The four phosphorus atoms are in-plane with the tungsten or molybdenum coordination centres. The average metal-phosphorus bond lengths are 2.515(2) Å for **3** and 2.532(1) Å for **4** respectively, which are slightly longer than those of [W(dmpe)$_2$(NO)Br] (2.427(2) Å)[87] and [W(dmpe)$_2$(O)(Cl)][ClO$_4$][104] (2.481(6) Å) or of [Mo(dmpe)$_2$(NO)Cl][53] (2.446(1) Å) and [Mo(depe)$_2$(N)(Cl)] (2.489(2) Å),[86] which can be explained in terms of the higher steric congestion of the dippe ligand. The average metal-

chloride bond lengths are 2.501(2) Å for **3** and 2.529(1) Å for **4**, which are shorter than the metal-chloride bond lengths of related complexes, which are, for instance, 2.539(5) Å in [W(dmpe)$_2$(O)(Cl)][ClO$_4$][104] and 2.556(1) Å in [W(dmpe)$_2$(Cl)(CH)][B(C$_6$F$_5$)$_4$][105] or 2.772(2) Å in [Mo(depe)$_2$(N)(Cl)].[86] Only in [Mo(dmpe)$_2$(NO)Cl][53] the Mo–Cl bond (2.488(1) Å) is shorter than in **4**.

2.3 Preparation of molybdenum and tungsten hydrides [M(dippe)$_2$(NO)(H)] (M = Mo, W)

Treatment of [W(dippe)$_2$(NO)Cl] (**3**) with 5 eq. of LiBH$_4$ in Et$_3$N at room temperature resulted in the formation of the [W(dippe)$_2$(Cl)(NO···LiBH$_4$)] complex (**5**) (Scheme 2.3). The ^{31}P {^{1}H} NMR spectrum of **5** exhibited a singlet at 43.0 ppm, which would be in agreement with a planar arrangement of the phosphorus atoms. In addition to the signals of dippe ligands the ^{1}H NMR spectrum exhibited a quintet at 0.20 ppm ($^1J_{BH}$ = 79.8 Hz), which is attributed to protons of the B*H*$_4$ unit. The IR spectrum showed an intense absorption band at 1489 cm^{-1} assigned to the ν(NO) stretching vibration (Table 2.5). The difference of 27 cm^{-1} in the wavenumbers of the ν(NO) of **3** and **5** accounts for the fact that the N–O bond order of the adduct **5** becomes lowered by Li coordination with respect to **3**. A similar tendency was observed in molybdenum nitrosyl complexes.[106] For instance, the difference of 49 cm^{-1} in the stretching vibration frequency of the nitrosyl group was identified for the pair Mo(dmpe)$_2$(Cl)(NO) / [Mo(dmpe)$_2$(Cl)(NO)](LiHBEt$_3$) (dmpe = 1,2-bis(dimethylphosphanyl)ethane).

Table 2.5 IR stretching vibrations of the ν(NO) in **3**, **4**, **5**, **6**, **7**, **8** and ν(MH) in **6**, **7** and **8**.

	ν(NO), cm^{-1}	ν(MH), cm^{-1}
3	1516	
4	1527	
5	1489	
6	1459	1672
7	1492	1671
8	1500	1670

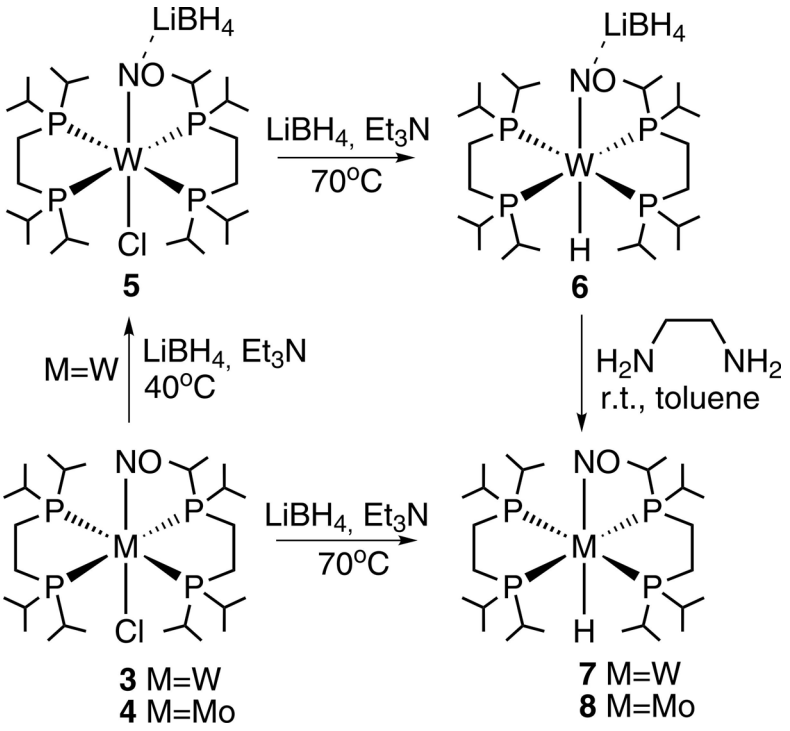

Scheme 2.3

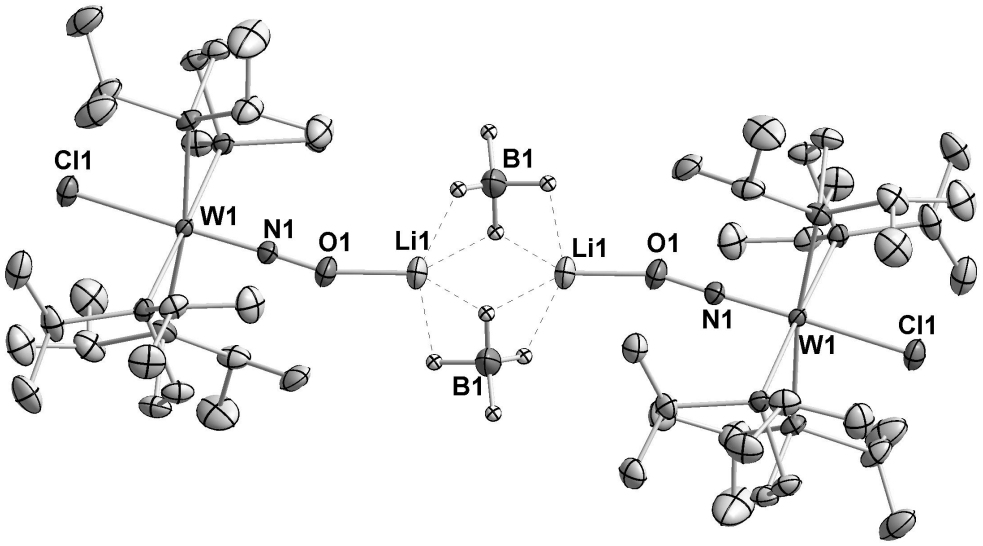

Figure 2.4 An ORTEP drawing of [W(dippe)$_2$(Cl)(NO···LiBH$_4$)] (**5**). Displacement ellipsoids are drawn at the 50% probability level. Selected hydrogen atoms have been omitted for clarity.

Table 2.6 Selected Bond Lengths [Å] and Bond Angles [°] of **5**.

Bond lengths			
W1−N1	1.764(4)	W1−P3	2.5372(13)
W1−P4	2.4949(13)	W1−P2	2.5501(13)
W1−Cl1	2.5083(12)	O1−N1	1.256(5)
W1−P1	2.5176(12)	O1−Li1	1.826(9)
B1−Li1	2.364(12)		
Bond angles			
Cl−W1−N1	178.79(13)	N1−W1−P1	92.39(13)
N1−O1−Li1	161.6(4)	P4−W1−P1	178.67(4)
N1−W1−P4	88.92(13)	Cl1−W1−P1	86.43(4)
P4−W1−Cl1	92.26(4)	N1−W1−P3	92.71(13)

Suitable single crystals for a X-ray diffraction study were obtained by slow diffusion of hexane into a benzene solution of **5**. The crystal structure of **5** can be seen as a dimer of two molecules of **5** bridged by a $(LiBH_4)_2$ unit (Figure 2.4) with an unique Li–O_{NO} interaction.[106, 107] The lithium ion is attached to the O_{NO} atom with an angle of 161.6(4)°. The average W–P and W–Cl distances were found to approximately equal to the corresponding bond lengths in **3** (Table 2.6).

When the temperature of the reaction to **5** was increased to 70 °C, the $LiBH_4$ bound hydride complex [W(dippe)$_2$(H)(NO···$LiBH_4$)] (**6**) was formed. The ^{31}P {^1H} NMR spectrum of **6** showed a singlet resonance at 62.8 ppm. In the ^1H NMR spectrum, besides a set of multiplets which are attributed to dippe ligands, a characteristic multiplet of hydride ligand was observed at -2.91 ppm ($^2J_{HP}$ = 26.0 Hz). In addition a quadruplet corresponding to BH_4 was detected at 0.15 ppm ($^1J_{BH}$ = 82.2 Hz). The IR spectrum revealed an intensive absorption band of NO stretching vibration at 1460 cm^{-1} and a band of W–H stretching vibration at 1673 cm^{-1}. A monocrystal of **6** suitable for X-ray diffraction analysis was obtained by slow hexane diffusion to the concentrated benzene solution of complex **6**. An ORTEP drawing and selected bond distances of **6** are presented in Figure 2.5 and in Table 2.7. The crystal structure of **6** revealed similarities

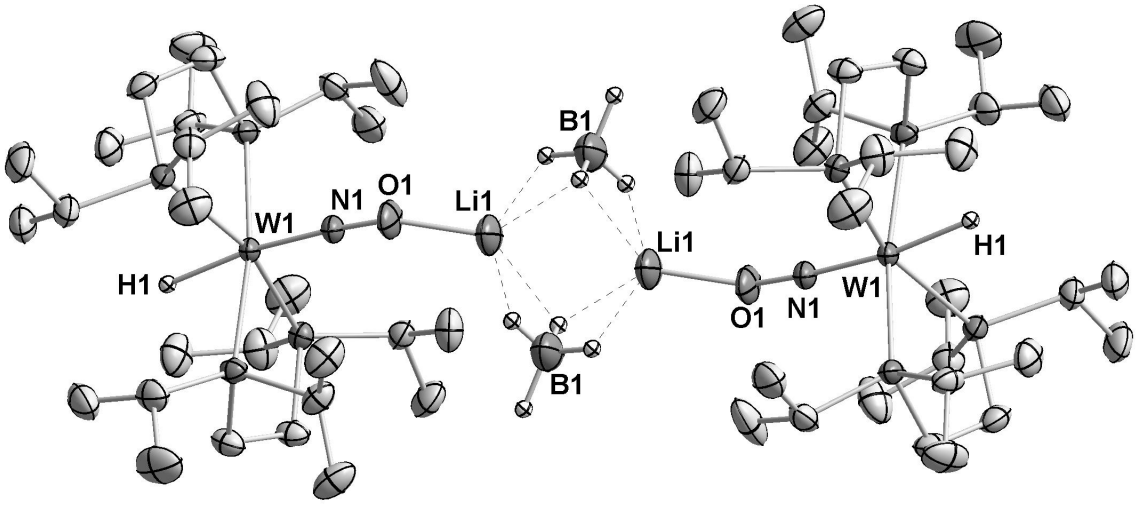

Figure 2.5 An ORTEP drawing of [W(dippe)$_2$(H)(NO···LiBH$_4$)] (**6**). Displacement ellipsoids are drawn at the 50% probability level. Selected hydrogen atoms have been omitted for clarity.

Table 2.7 Selected Bond Lengths [Å] and Bond Angles [º] of **6**.

Bond lengths			
W1−H1	1.79(3)	Li1−B1^{i}	2.377(5)
W1−N1	1.7986(15)	W1−P2	2.4712(4)
N1−O1	1.251(2)	W1−P4	2.4988(4)
O1−Li1	1.847(4)	W1−P3	2.4991(4)
Li1−B1	2.436(5)	W1−P1	2.5126(4)
Bond angles			
N1−W1−P2	93.35(5)	P2−W1−P3	98.277(15)
N1−W1−P4	96.13(5)	P4−W1−P3	79.756(16)
P2−W1−P4	170.498(15)	N1−W1−P1	99.72(5)
N1−W1−P3	97.79(5)	P2−W1−P1	78.826(14)
P4−W1−P1	100.203(15)	P3−W1−P1	162.386(16)
N1−W1−H1	171.2(8)	P2−W1−H1	77.9(8)
W1−N1−O1	175.22(15)	N1−O1−Li1	150.8(2)
O1−Li1−B1	126.4(2)	O1−Li1−B1^{i}	130.6(2)

with the one of **5**. Identical to **6** two W(dippe)$_2$(H)(NO) species are bridged through (LiBH$_4$)$_2$. The hydride ligand was located *trans* to the NO group.

To obtain the hydride complex **7** ethylenediamine was added to the toluene solution of **6** at room temperature, which resulted in quantitative precipitation of [Li(en)$_2$BH$_4$].[108] The ^{31}P {^{1}H} NMR spectrum of **7** revealed a sharp singlet at 64.4 ppm demonstrating chemically identical phosphorus atoms. Besides the multiplets at 2.47 and 2.10 ppm attributed to the chemically different protons of the dippe methylene groups and sets of resonances for the diastereotopic of the isopropyl methyl groups, a characteristic H_W quintet was observed in the ^{1}H NMR spectrum at -3.38 ppm ($^2J_{PH}$ = 24.8 Hz). The IR spectrum of **7** showed a weak band at 1671 cm^{-1} attributed to the ν(WH) vibration and a strong ν(NO) band at 1492 cm^{-1} (Table 2.5). In analogy to the pair of chloride complexes **3** and **5**, the ν(NO) bands of **6** and **7** differ in their position by 27 cm^{-1} indicating again a lower NO bond order for **6** caused by Li coordination.[107]

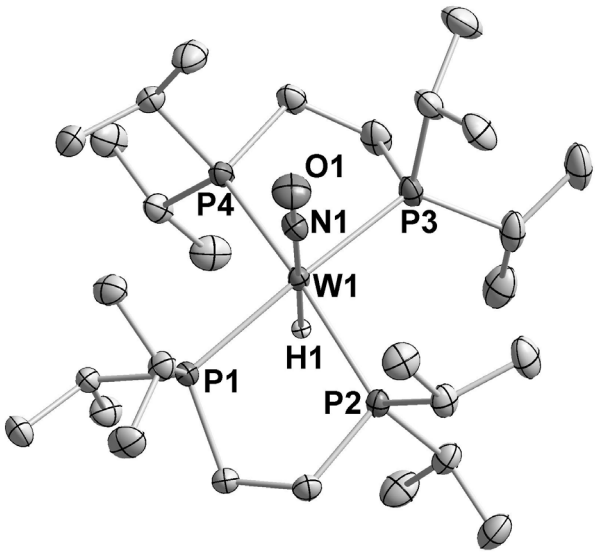

Figure 2.6 An ORTEP drawing of complex [W(dippe)$_2$(NO)H] (**7**). Displacement ellipsoids are drawn at the 50% probability level. All hydrogen atoms except H1 have been omitted for clarity.

Compound **7** crystallizes in the centrosymmetric space group Pccn. Similar to the structure of **3**, **4** displays a pseudo-octahedral coordination geometry (Figure 2.6). Four phosphorus atoms of the dippe ligands are in-plane with the tungsten center. The mean

W–P distance amounts to 2.4826(6) Å, which is slightly shorter than the corresponding distances in **3**. The hydride ligand was located in the Fourier difference map and its coordinates and isotropic thermal parameter could be freely refined. The W–H bond length was found to be 1.88(3) Å. Considering its high standard deviations it falls into the same range of elongated hydride bonds, like for instance that of W(PMe)$_3$(NO)(H)[52] (1.93(3) Å) and of W(dmpe)$_2$(CMes)(H) (2.00(4) Å).[82]

Table 2.8 Selected Bond Lengths [Å] and Bond Angles [°] of **7**.

Bond lengths			
W1−N1	1.807(2)	W1−P4	2.4893(6)
W1−H1	1.89(3)	W1−P2	2.5074(6),
W1−P3	2.4645(6)	O1−N1	1.231(3)
W1−P1	2.4691(6)		
Bond angles			
N1−W1−P3	93.61(6)	P3−W1−P4	78.64(2)
N1−W1−P1	92.85(6)	P1−W1−P4	100.381(19)
P3−W1−P1	173.54(2)	N1−W1−H1	177.5(11)
N1−W1−P4	97.57(7)	P3−W1−H1	85.5(11)
P1−W1−H1	88.0(11)	P4−W1−H1	79.9(11)

Notably, the transformation of **3** into **7** can be carried out stepwise with isolation of intermediates or in a one-pot procedure, which led to an enhanced overall yield.

A molybdenum hydride **8** analogous to **7** was obtained via the reaction of **4** with $LiBH_4$ in Et_3N as a solvent at 70 °C. Under these conditions the hydride **8** was the only product. A $LiBH_4$ adduct of **8** is supposed to be less tight than **6** and would therefore be expected to undergo facile cleavage in the presence of NEt_3. Application of excess of $LiBH_4$ did apparently not lead to noticeable adduct formation (*vide infra*) rather it led to considerable increase of the yield of **8**, which was presumably effected by a shift of the Cl^-/hydride exchange equilibrium toward the hydride site. To assure the lower Lewis basicity of **8** in comparison with **7**, **8** was treated in an unique experiment with excess of $LiBH_4$ using Et_2O as a non-coordinating solvent[106, 107]. Stirring the reaction mixture

overnight did not reveal the appearance of any new ν(NO) band at lower wavenumbers and is in agreement with the observation that only staring materials were isolated. The ^{31}P {^{1}H} NMR of **8** exhibited a sharp signal at 85.8 ppm proving the presence of chemically equivalent phosphorus ligands. Besides the expected multiplets attributed to dippe ligands, the ^{1}H NMR spectrum displayed a quintet for the hydride ligand at -3.80 ppm ($^2J_{PH}$ = 24.8 Hz). In the region of 2000 to 1400 cm^{-1} the IR spectrum of **8** revealed two strong bands at 1670 cm^{-1} ν(MoH) and 1500 cm^{-1} ν(NO). Based on these spectroscopic data **8** was assigned to a *trans* structure similar to **7**.

2.4 Reactivity of hydrides [M(dippe)$_2$(NO)H] (M = W, Mo) towards CO$_2$ gas

As it was reported earlier for compounds structurally related to **7** and **8**, the hydride transfer reaction to unsaturated compounds occurs very smoothly at room temperature.[47, 86] There are several examples of alcoholate formation through ketone or aldehydes insertion into the M−H bond, which mechanistically proceeds via a hydride transfer step .[43, 109, 110] However, the initially expected reaction of **7** or **8** with ketones was found not to lead to any product (Scheme 2.4).

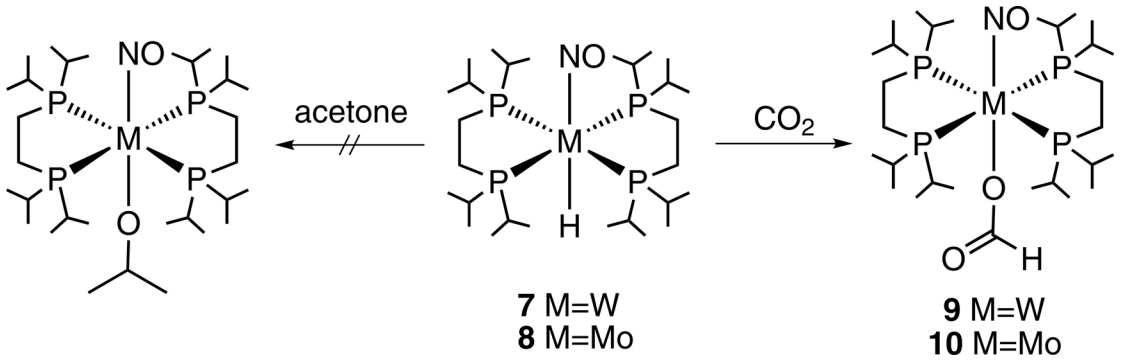

7 M=W
8 M=Mo

9 M=W
10 M=Mo

Scheme 2.4

Although a variety of ketones, as well as the high temperature conditions (up to 80 °C) were tried, only a singlet of the starting material was observed in the ^{31}P {^{1}H} NMR spectra indicating no reaction between **7** or **8** and the ketones had occurred. This

can be explained in terms of a too large steric congestion of the dippe ligands, shielding the hydride atom and preventing the substrate to approach it.

However, the reaction of hydrides **7** and **8** with CO_2 gas led to formation of the formate compounds **9** and **10**. Immediately after the NMR tube containing toluene solution of **7** or **8** was filled with CO_2 gas, the color of the solution turned from bright to pale yellow. The ^{31}P $\{^1H\}$ NMR spectra ensured the full conversion. A singlet was observed at 49.3 ppm for **9** and at 63.2 ppm for **10**, which indicated no significant change in the phosphine coordination sphere. Besides the multiplets for the dippe ligands, the ^1H NMR spectra exhibited a singlet at 8.25 ppm (**9**) and at 8.39 ppm (**10**) attributed to the formate proton. The ^{13}C $\{^1H\}$ spectra showed a characteristic signal for formate carbon atoms at 165.7 ppm (**9**) and at 166.4 ppm (**10**). Strong bands for ν(C=O) and ν(NO) stretching vibration were observed in the IR spectra at 1631 and 1512 cm^{-1} (**9**); 1627 and 1526 cm^{-1} (**10**).

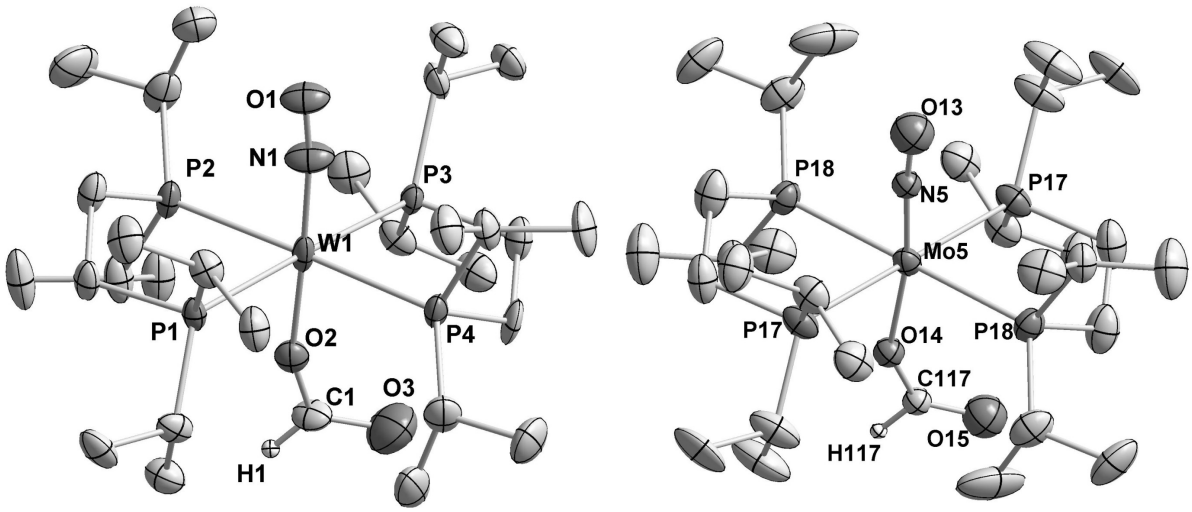

Figure 2.7 An ORTEP drawing of **9** and **10**. Displacement ellipsoids are drawn at the 50% probability level. Selected hydrogen atoms have been omitted for clarity.

X-ray diffraction studies confirmed the structures of **9** and **10**. ORTEP drawings of the compounds are presented in Figure 2.7. Selected bond distances and angles are summarized in Tables 2.9 and 2.10.

Table 2.9 Selected Bond Lengths[Å] and Bond Angles [°] of **9**.

Bond lengths			
W1−N1	1.887(8)	W1−P2	2.503(2)
W1−O2	2.032(6)	W1−P1	2.531(2)
W1−P4	2.485(2)	W1−P3	2.526(2)
N1−O1	1.210(9)	C1−O3	1.295(13)
Bond angles			
W1−N1−O2	177.9(3)	N1−W1−P1	88.0(3)
W1−O2−C1	160.0(7)	N1−W1−P3	94.5(3)
P2−W1−P3	101.31(7)	N1−W1−P4	90.6(3)
N1−W1−P2	90.7(3)	P1−W1−P2	78.91(7)

Table 2.10. Selected Bond Lengths[Å] and Bond Angles [°] of **10**.

Bond lengths			
Mo5−N5	1.8449(1)	Mo5−P17	2.5437(1)
Mo5−O14	2.0637(1)	C117−H117	0.93(4)
Mo5−P18	2.5106(1)	O14−C117	1.270(4)
N5−O13	1.220(3)		
Bond angles			
N5−Mo5−O13	175.4(9)	N5−Mo5−P18	88.7(3)
Mo5−O14−C117	149.4(9)	N5−Mo5−P17	98.0(3)
P17−Mo5−P18	100.8(5)	O14−C117−O15	131.3(15)

Compound **9** crystallizes in the non-centrosymmetric space group $P2_1$. Two crystalographically independent molecules were found in the asymmetric unit. Similar to the hydride **7**, **9** displays a pseudo-octahedral coordination geometry, in which four phosphorus atoms are in-plane with the tungsten center. The mean tungsten-phosphorus bond length equals to 4.511(2) Å that is in accord with the tungsten-phosphorus distances of the starting hydride **7**. The nitrosyl and formate ligand are located *trans*.

10 crystallizes in the centrosymmetric space group P-1. Five independent molecules are in the asymmetric unit and one lies on a center of symmetry. In analogy to

9 compound **10** displays a pseudo-octahedral coordination geometry: four phosphorus atoms are in-plane with the molybdenum metal center, whereas the nitrosyl and the formate ligand disposed *trans*.

2.5 Reaction of [M(dippe)$_2$(NO)H] (M = W, Mo) with [H(Et$_2$O)$_2$][BAr$^F_4$]

The counterion $[BAr^F_4]^-$ is classified as non-coordinating[93, 94] allowing in many cases observation of dihydrogen complexes obtained upon protonation of transition metal hydrides.[36] The weakly coordinating dihydrogen ligand can not be replaced by the $[BAr^F_4]^-$ anion, which is still weaker in electron donation. If dihydrogen ligands are weakly bound as in **7a**, they might be released as H_2 leaving a vacant site behind. In a formal ligand substitution process the H_2 ligand can normally be replaced by other small molecules.

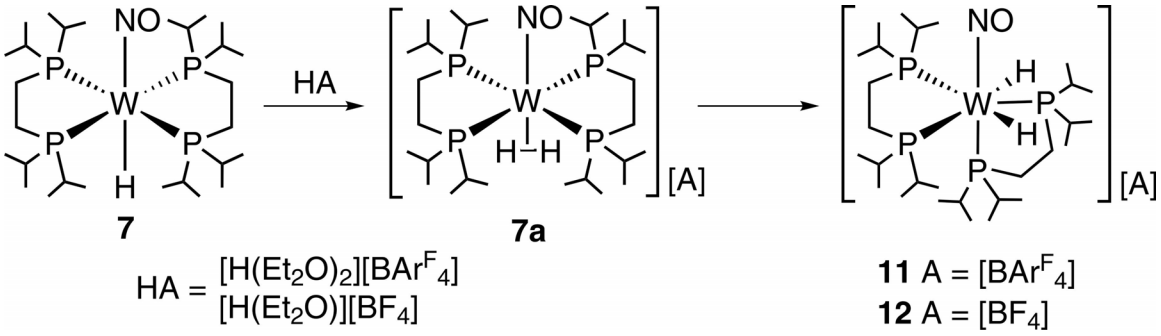

Scheme 2.5

The tungsten hydride **7** reacts with $[H(Et_2O)_2][BAr^F_4]$ forming presumably first the dihydrogen complex **7a**, which then undergoes oxidative addition to the seven-coordinated pentagonal bipyramidal dihydride $[W(dippe)_2(NO)H_2][BAr^F_4]$ (**11**) (Scheme 2.5). **11** was isolated in a good yield as a colorless powder. The $^{31}P\{^1H\}$ NMR exhibits three triplets with an integration ratio 1:2:1 at 66.8, 59.5 and 25.2 ppm attributed to three chemically different types of phosphorus atoms, from which one phosphorus position is equatorial, one axial and two phosphorus positions are chemically equivalent and equatorial. Besides signals for the dippe ligand, the ^1H NMR spectrum of **11** revealed a multiplet for hydride protons. In the $^1H\{^{31}P\}$ spectrum one singlet at 1.76 ppm was

attributed to the chemically equivalent hydride atoms. An IR spectrum of **11** revealed a band at 1613 cm^{-1} attributed to a ν(NO) stretching vibration. No bands could be assigned to ν(WH) vibrations, which are presumably of too low intensity.

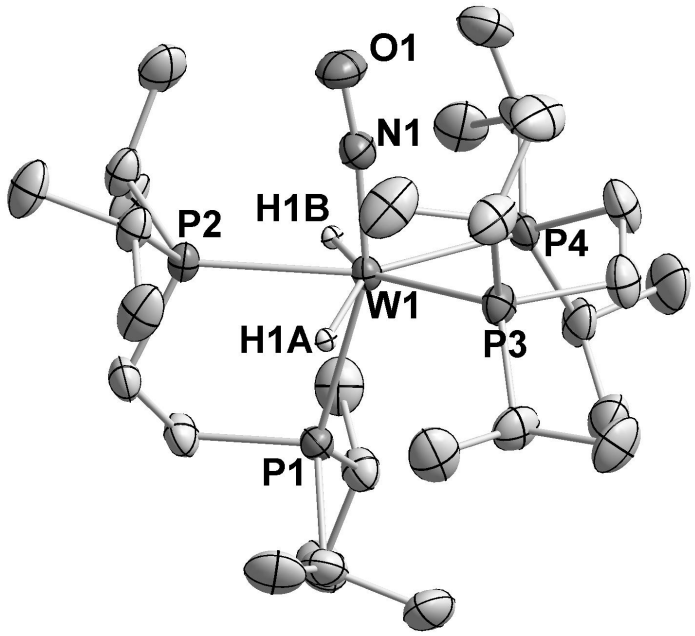

Figure 2.8 An ORTEP drawing of [W(dippe)$_2$(H)$_2$(NO)][BAr$^F{}_4$] (**11**). Displacement ellipsoids are drawn at the 50% probability level. Only the main residue (without the counterion) and selected H atoms is shown.

The structure of **11** was confirmed by a X–ray diffraction study (Figure 2.8). **11** crystallized in the centrosymmetric space group P2$_1$/c. The molecular structure of **11** showed the spectroscopically derived pseudo-pentagonal bipyramid. The coordination geometry is even distorted from an ideal C$_s$ symmetry with the planes of the two chelating ligands P3–W–P4 and P1–W–P2 amounting to 80.53(3)°. The P1–W–N1 angle of the equatorial/axial chelate equals 160.84(8)° (Table 2.11), which demonstrates together with the long W–P1 bond distance of 2.6849(8) Å that P1 is only weakly bound to the tungsten center presumably due to the strong *trans* influence[36, 111] of the NO group

Table 2.11 Selected Bond Lengths[Å] and Bond Angles [°] of **11**.

Bond lengths			
W1−H1A	1.62(4)	W1−P4	2.5363(7)
W1−H1B	1.66(4)	W1−P3	2.5496(7)
W1−N1	1.79(3)	W1−P1	2.6849(8)
W1−P2	2.4810(7)	N1−O1	1.206(4)
Bond angles			
N1−W1−P2	82.68(9)	P4−W1−P3	78.43(3)
N1−W1−P4	92.22(9)	N1−W1−P1	160.83(9)
N1−W1−P3	86.76(9)	P2−W1−P1	78.85(3)
N1−W1−H1A	102.3(15)	P4−W1−H1A	142.1(15)
N1−W1−H1B	93.3(14)	P3−W1−H1B	151.4(14)

expecting high lability of the axial P1. Temperature dependent ^{31}P $\{^1H\}$ NMR studies showed however that the structure **11** remained static up to 100 °C, since the spectra did not reveal any significant change upon warming up. In addition substitution with coordinating solvents such as THF or acetone did apparently not occur to a significant extent. The two hydride ligands were located in a Fourier difference map and were fully refined. The average W–H distance of **11** is quite short (1.64(4) Å), not perturbed by any *trans* influence like in **7**, where the W1−H1 distance was found to be 0.25 Å longer.

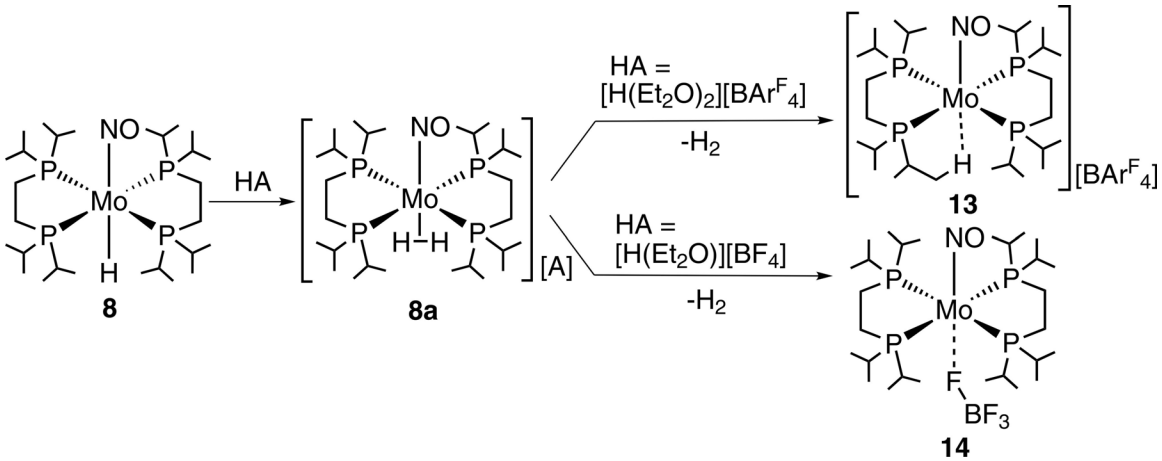

Scheme 2.6

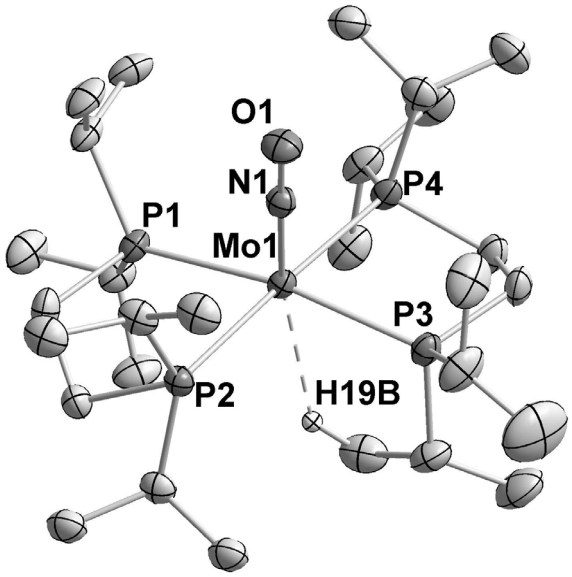

Figure 2.9 An ORTEP drawing of [Mo(dippe)$_2$(NO)][BAr$^F{}_4$] (**13**). Only the main residue is shown without the counterion and selected H atoms.

Table 2.12 Selected Bond Lengths[Å] and Bond Angles [°] of **13**.

Bond lengths			
Mo1−N1	1.767(3)	Mo1−P2	2.5231(10)
Mo1−H19B	2.4524(3)	Mo1−P1	2.5368(9)
Mo1−P3	2.473(1)	N1−O1	1.199(4)
Mo1−P4	2.5189(10)		
Bond angles			
N1−Mo1−P3	96.90(10)	P4−Mo1−P2	177.01(3)
N1−Mo1−P4	90.91(9)	N1−Mo1−P1	96.98(10)
P3−Mo1−P4	78.27(3)	P3−Mo1−P1	166.12(3)
N1−Mo1−P2	91.96(9)	P4−Mo1−P1	101.72(3)
P3−Mo1−P2	100.56(3)	P2−Mo1−P1	78.75(3)

The formally sixteen electron complex **13** was prepared similar to compound **11** via the reaction of the hydride **8** with [H(Et$_2$O)$_2$][BAr$^F{}_4$] presumably with the dihydrogen complex **8a** as a short-lived intermediate (Scheme 2.6). **13** was isolated as a green powder. The ^{31}P {^{1}H} NMR spectrum showed a singlet at 72.0 ppm that indicated

chemical equivalence of the four phosphorus atoms. The ^{1}H NMR spectrum of **13** displayed several multiplets in the region of 2.55 – 0.50 ppm assigned to resonances of the dippe ligands. No special resonance was observed for an agostic hydrogen, which was based on the X-ray diffraction study of **13** (*vide infra*). The agostic hydrogen is anticipated to undergo rapid exchange with the other H_{Me} atoms of the isopropyl groups.[111] The fast exchange is also indicated by variable-temperature ^{31}P {^{1}H} NMR spectra, which showed only a single resonance in the temperature range from 193 to 298 K. The IR spectrum of **13** displayed a ν(NO) band at 1591 cm^{-1}.

An ORTEP representation of the molecular structure of **13** is presented in Figure 2.9. Compound **13** adopts a square pyramidal geometry, in which four phosphorus atoms form the square base of the pyramid. It is worthwhile mentioning that the Mo1–P3 bond length is shorter (2.473(1) Å) (Table 2.12) than the other three M−P distances presumably because this P atom bears the substituent with the agostic hydrogen. Recently it was published a DFT energy partitioning scheme for agostic bonds,[112, 113] from which it became evident that several geometric distortions contribute to the total energy of the agostic binding. For comparison, the Mo····H−C distance of **13** is 2.45 Å, which is considerably shorter than the related distance of Mo(CO)(Ph$_2$PCH$_2$CH$_2$Ph$_2$)$_2$ (2.98 Å)[78, 114] but is longer than that of 2.20 Å reported for the Mo(CO)(iBu$_2$PCH$_2$CH$_2$iBu$_2$)$_2$ complex.[77]

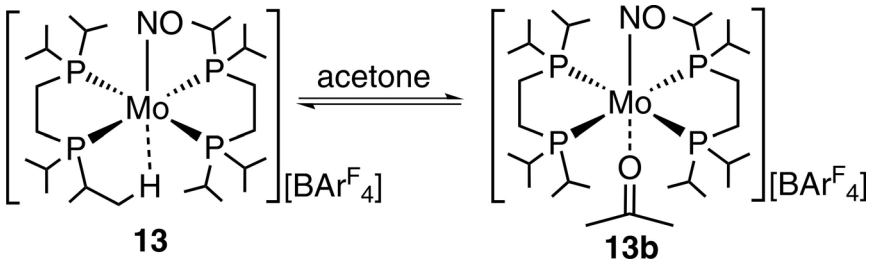

13 **13b**

Scheme 2.7

Apparently, the weakly agostic Mo···H–C interaction can be readily displaced by donor solvent molecules that are suited to enter the sterically congested coordinated sphere. Based on NMR spectroscopic evidence, THF for instance does enter the "hole". However, using of acetone leads to significant broadening of the unique signal at room

temperature. At 40 °C a sharp singlet was observed. At -40 ºC this signal splits into two sharp singlets at 61.5 and 60.0 ppm. The ^{31}P {^{1}H} NMR spectra of **13** in various THF/acetone mixtures revealed dependence of the signal's integrals on the acetone concentration. This observation pointed to an equilibrium operating at room temperature with dynamics fast on the NMR time scale (Scheme 2.7).

2.6 Reaction of [M(dippe)$_2$(NO)H] (M = W, Mo) with [H(Et$_2$O)][BF$_4$].

The tungsten hydride **7** interacts with [H(Et$_2$O)][BF$_4$] acid forming **12** structurally related to **11** (Scheme 2.5). **12** were isolated as a colorless powder. The ^{31}P {^{1}H} NMR of **12** exhibited three triplets with an integration ratio 1:2:1 at 69.2, 61.9 and 27.3 ppm indicating three chemically different phosphorus atoms. In ^{1}H {^{31}P} NMR spectra a singlet attributed to the hydride atoms can be found at 1.76 ppm. A monocrystal X-ray diffraction investigation fully confirmed the structure of **12**. An ORTEP drawing is presented in Figure 2.10, the selected bond length and angles are summarized in Table 2.13.

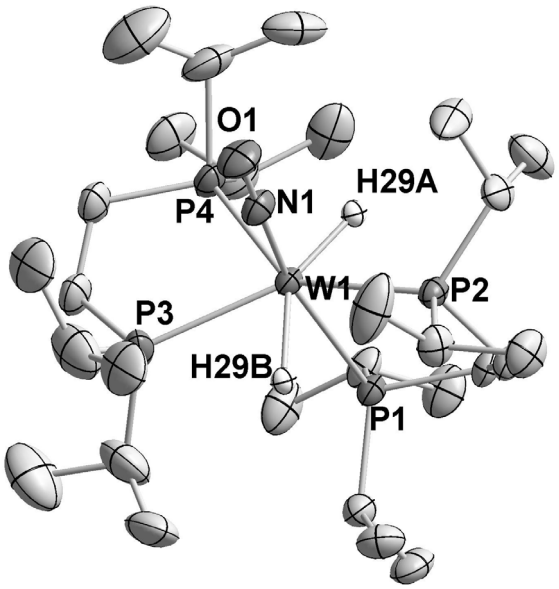

Figure 2.10 An ORTEP drawing of [W(dippe)(H)$_2$(dippe)(NO)][BF$_4$] (**12**). Displacement ellipsoids are drawn at the 50% probability level. Selected hydrogen atoms have been omitted for clarity.

Table 2.13 Selected Bond Lengths[Å] and Bond Angles [°] of **12**.

Bond lengths			
W1−N1	1.797(3)	W1−P4	2.5474(10)
W1−P1	2.6816(9)	N1−O1	1.203(4)
W1−P2	2.4919(9)	W1−H29A	1.57(4)
W1−P3	2.5399(11)	W1−H29B	1.80(4)
Bond angles			
P1−W1−N1	166.17(10)	P2−W1−H29A	69.0(15)
P2−W1−P3	142.68(4)	P2−W1−H29B	75.8(4)
P2−W1−P4	138.58(3)	N1−W1−P1	166.17(10)
N1−W1−H29B	98.0(14)	P2−W1−P1	78.61(3)
P2−W1−H29B	75.8(14)	P2−Mo1−P1	99.88(4)

The reaction of **8** and [H(Et$_2$O)][BF$_4$] was carried out in Et$_2$O at room temperature and was completed within minutes. After the acid was added the red [Mo(dippe)$_2$(NO)(FBF$_3$)] complex **14** started to precipitate. In accord with the general observation that the kinetic sites of protonations of hydride complexes are the hydride ligands,[36] we assume primary formation of the dihydrogen complex **8a**, which apparently is unstable and decays with substitution of the H_2 ligand by the BF_4^- anion to form **14** (Scheme 2.6). In the ^{31}P {^1H} NMR spectrum of **14** a singlet was observed at 64.5 ppm, which revealed that the square of phosphorus ligands of **8** retained. The ^{19}F NMR spectrum showed two singlets at -157.8 and -157.9 ppm with an integration ratio of 1:3. The non-equivalence of the fluorine atoms accounts for strong counterion coordination and suppressed coordination dynamics of the BF_4^- anion proceeding normally with hopping between the fluorine substituents.

The X–ray diffraction study of **14** corroborated the BF_4^- coordination. An ORTEP drawing of the crystal structure of **14** is given in Figure 2.11. The selected bond lengths and angles are presented in Table 2.14.

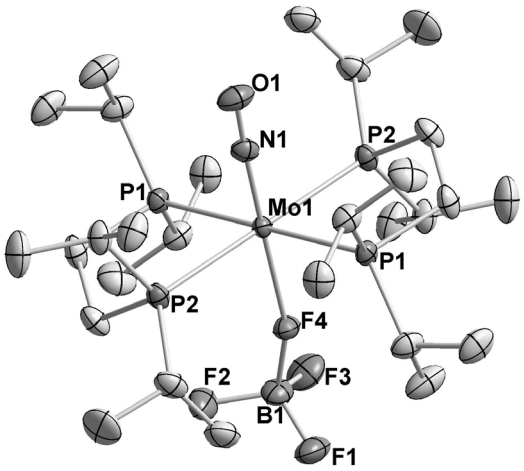

Figure 2.11 An ORTEP drawing of [Mo(dippe)$_2$(NO)(FBF$_3$)] (**14**). Displacement ellipsoids are drawn at the 50% probability level. All hydrogen atoms have been omitted for clarity.

Table 2.14 Selected Bond Lengths[Å] and Bond Angles [°] of **14**.

Bond lengths			
Mo1−N1	1.770(8)	B1−F1	1.360(9)
Mo1−F4	2.265(6)	B1−F2	1.373(9)
Mo1−P1	2.5549(8)	B1−F3	1.377(10)
Mo1−P2	2.5197(6)	B1−F4	1.487(11)
Bond angles			
N1−Mo1−F4	177.3(5)	N1−Mo1−P1	95.6(4)
N1−Mo1−P2	89.3(4)	F4−Mo1−P1	86.83(19)
F4−Mo1−P2	91.4(2)	P2−Mo1−P1	101.32(2)
B1−F4−Mo1	161.6(6)	O1−N1−Mo1	177.4(11)

14 crystallized in the centrosymmetric space group P-1. The molybdenum atom lies on a center of inversion with a positional disorder between the *trans* NO and BF_4^- groups. The average Mo–P bond length is 2.535(1) Å, which is similar to the corresponding distances in **14**. In comparison with the W–F bonds of analogous structures, the Mo1–F4 bond distance of 2.265(6) Å in **14** is slightly longer than the

corresponding bond in W(PMe$_3$)(CO)$_3$(NO)(BF$_4$) (2.169(11) Å)[115] or in W(H)(CO)$_3$(PCy$_3$)$_2$(BF$_4$) (2.15(2) Å).[116] Nevertheless, the B1−F4 bond distance of

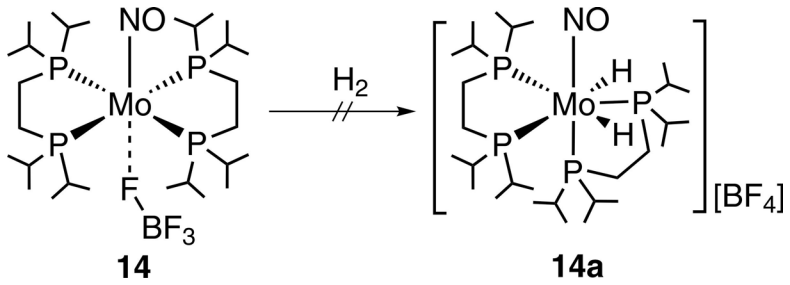

14 **14a**

Scheme 2.8

1.487(11) is significantly longer than the other B−F bonds in the range 1.36-1.38(1), which indicates a strong interaction between the counter-ion and the metal center. This could explain the failure to substitute the counterion by pressurizing a THF solution of **14** even with 3 bar of hydrogen gas (Scheme 2.8).

2.7 Equilibrium Reaction of [Mo(dippe)$_2$(NO)][BAr$^F{}_4$] (13) with hydrogen gas

Filling a NMR tube with 1.8 bar of H_2 gas led to an immediate colour change of the THF solution of **13** from green to yellow. In the ^{31}P $\{^1$H$\}$ NMR spectrum a set of three triplets at 89.5, 76.1 and 42.4 ppm appeared with the integration ratio 1:2:1 assigned to the formation of [Mo(dippe)$_2$(H)$_2$(NO)][BAr$^F{}_4$] (**13a**) with three non-equivalent types of phosphorus atoms. Additionally the ^{1}H NMR spectrum of **13a** showed a characteristic multiplet at 0.32 ppm at room temperature, which became a singlet in the decoupled ^{1}H $\{^{31}$P$\}$ spectrum. A comparison with the NMR data of **11** allowed the conclusion that **13** can react with hydrogen gas to form **13a** presumably via the intermediacy of **8a** (Scheme 2.9).

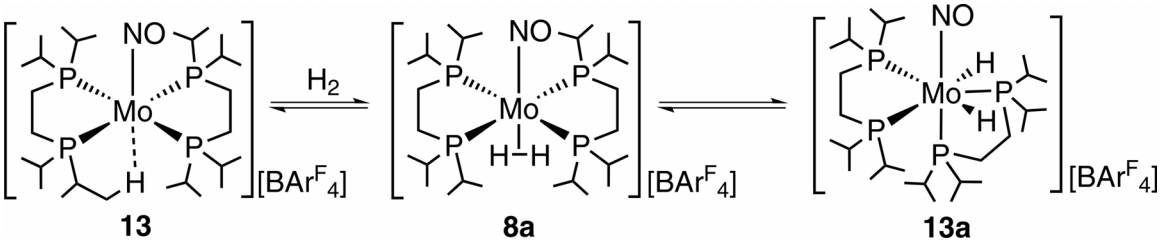

Scheme 2.9

The equilibrium formation of **13** could be traced to H_2 pressures of approximately 0.2 bar. Lower H_2 pressures caused considerable broadening of the singlet of **13** in the ^{31}P $\{^1H\}$ NMR spectrum. We think that this observation can be interpreted in terms of a slowing of the H_2 equilibrium and that low H_2 pressures lead to a preference of the **13**/**8a** equilibrium appearing with signal averaging of both species close in rates to the NMR time scale (Scheme 2.9). In contrast to **11** neither the dihydride **13a** nor the dihydrogen complex **8a** could be isolated from solution due to their instability in the absence of H_2. The dependence of integration ratio of **13a**/**13** *vs.* hydrogen pressure (Figure 2.12) allowed calculating the equilibrium constant that equals to 2.6 ± 0.1 bar^{-1} at 25 °C.

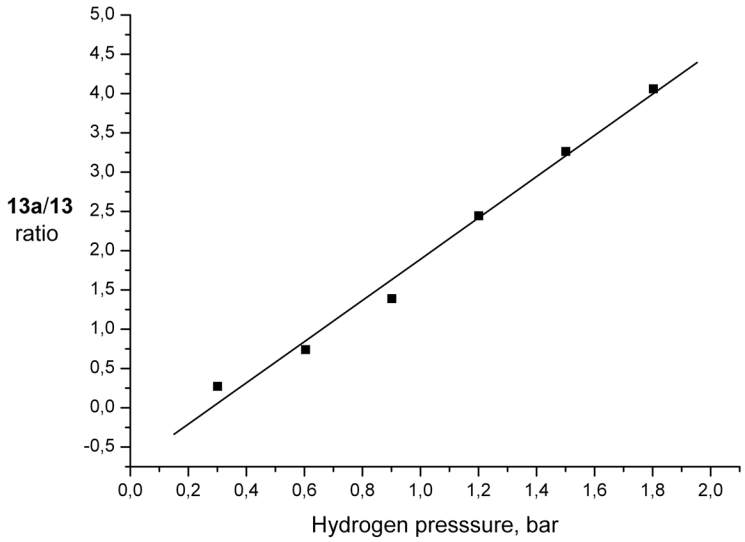

Figure 2.12 Integration ratio of the **13a**/**13** signals *vs.* hydrogen pressure. The linear regression allows to calculate an equilibrium constant of 2.6 ± 0.1 bar^{-1} at 25 °C.

Based on a comparison with the related species Mo(CO)($R_2PCH_2CH_2PR_2$)$_2$, R = Ar, Et, iBu[100] obtained by Kubas and co-workers it can be concluded that the "*trans* ligand" located *trans* to the weakly coordinated H_2 ligand has a great influence on the position of the H_2/dihydrogen equilibrium. It was demonstrated earlier that the donating ability of the chelating phosphine plays a major role. For instance, all complexes with R = Ar with lower donating abilities showed no tendency to form the dihydride complexes. In the case of R = Et, iBu the dihydride complexes could be isolated in pure form. It is remarkable that all H_2 complexes of the Mo(CO)($R_2PCH_2CH_2PR_2$)$_2$ series with CO as a *trans* ligand interact strongly with H_2, while **13a** loses the interaction with H_2 instantaneously, once the H_2 concentration falls below a certain limit. The *trans* NO exerts a stronger *trans* influence than CO which labilizes the π acceptor H_2 ligand by a π acceptor competition. A labilized H_2 ligand could however bring about enhanced reactivity.

2.8 Catalytic hydrogenation of acetone-d$_6$

Ionic hydrogenations of unsaturated compounds require addition of H^+ from an acid and H^- from a hydride source.[30, 33] The traditional mechanism for ketone hydrogenations involves coordination of the ketone to the metal, followed by insertion of the ketone into a metal-hydrogen bond.[29] In the molybdenum or tungsten cases the ketone insertion occurs mostly very smoothly, but the formed alcoholate complexes were shown to be often significantly stable.[52, 53, 85, 86] Only a few examples of catalytic ionic hydrogenations of ketones[55, 56] or imines[85] with molybdenum or tungsten catalysts were reported earlier.

The reaction between the molybdenum hydride complex **8** with [H(Et_2O)$_2$][BAr^F_4] in deuterated acetone led to a singlet resonance at 3.90 ppm which was attributed to the partially deuterated isopropanol (CD_3)$_2$C*H*OH.[117] Comparing the integration of the alcohol and the $BAr^F_4{}^-$ aryl signals we could conclude that the amount of alcohol formed was the same as the amount of the acid added. However, when the mixture was pressurized with 2 bar of H_2 and heated to 60 °C it led to an increased alcohol signal, which was quantified by integration of this signal with reference to the

aryl signals of the counterion. This observation pointed to catalytic behavior and we therefore reacted **13** by dissolving in acetone-d_6 and pressurizing with 2 bar of H_2. The formation of the partially deuterated isopropanol was quantitatively pursued by ^{1}H NMR spectroscopy. The catalytic performance can be judged from the plot of the turn-over numbers (TON) *vs.* time (Figure 2.13).

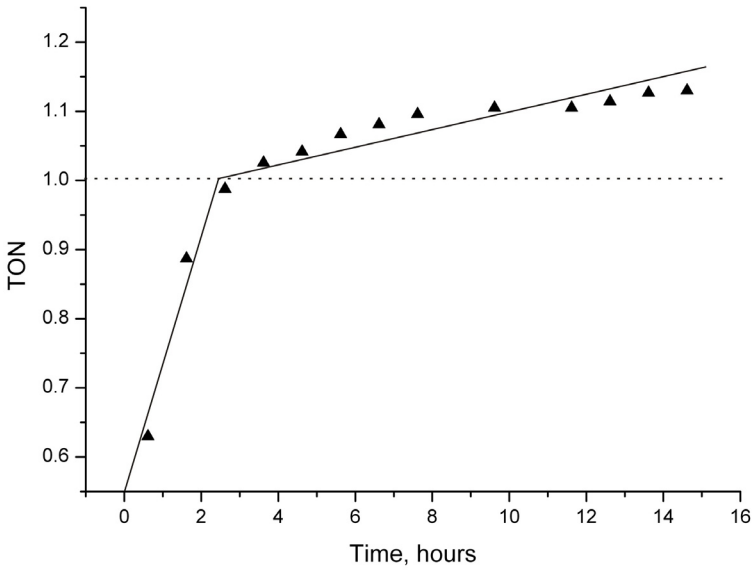

Figure 2.13 The catalytic activity of complex **13** in acetone hydrogenation at 60 °C and 2 bar of H_2. The linear approximation was carried out to demonstrate the jump in the reaction rate.

Other substrates (acetophenone, benzophenone, propionaldehyde, pivaldehyde) were also tested in hydrogenations using **13** as a catalyst. Variations of the conditions in these reactions, such as different pressures of H_2, different solvents including neat media did not reveal formation of any respective alcohol. We suppose that the bulky dippe ligands shield and additionally protect the molybdenum center.

2.9 Preparation of W(dppe)$_2$(NO)Cl (15) and reaction with AlCl$_3$

The consecutive treatment of W(NO)(CHCN)$_2$Cl$_3$ with 2.5 equivalent of the dppe ligand and 1% sodium amalgam led to the formation of W(dppe)$_2$NOCl (**15**) with yield of 63% (Scheme 2.10). The ^{31}P {^{1}H} NMR spectrum of **15** displayed a singlet at 39.4 ppm,

that stresses the presence of chemically identical phosphorus atoms in the molecule. Besides the set of the phenyl group multiplets in the region 7.30 − 7.00 ppm in the ^{1}H NMR spectrum of **15**, two multiplets at 2.68 and 2.36 ppm were attributed to the methylene protons of the ligand bridge. The IR spectra exhibited a strong band assigned to a nitrosyl stretching vibration at 1524 cm^{-1}.

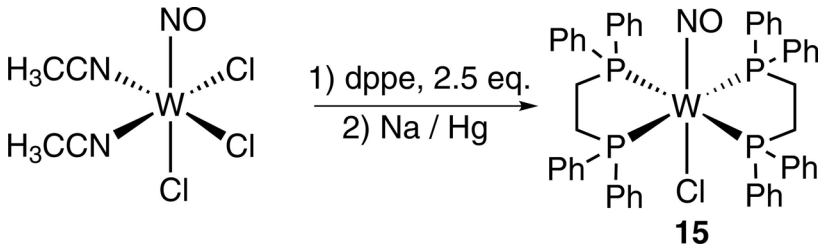

Scheme 2.10

Crystals of **15** suitable for X-ray investigation were obtained by slow diffusion of hexane into a saturated CH_2Cl_2 solution of **15**. An ORTEP drawing of the compound is presented in Figure 2.14. Selected bond distances and angles are summarized in Table 2.15.

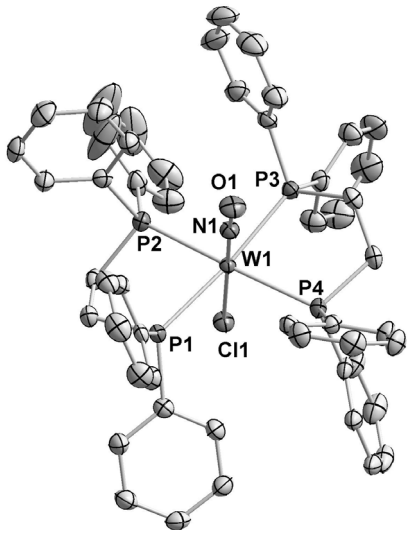

Figure 2.14 An ORTEP drawing of **15**. Displacement ellipsoids are drawn at the 50% probability level. The disorder between the Cl and NO ligands in *trans* and all hydrogen atoms have been omitted for clarity.

15 crystallizes in the centrosymmetric space group C2/c. Like **3,** compound **15** displays pseudo-octahedral geometry with phosphorus atoms of the dppe ligands in-plane with the tungsten center. Disorder between the NO and Cl ligands in *trans* position was observed. The mean metal-phosphorus bond distance amounts to 2.496(1) Å, which is slightly shorter than in **3** (2.515(2) Å). The tungsten-chloride bond is also shorter in **15** (2.501(2) Å) than in **3** (2.518(2) Å), presumably due to weaker electron donation of the dppe ligand in comparison with the dippe ligand.

Table 2.15 Selected Bond Lengths [Å] and Bond Angles [°] of **9**.

Bond lengths			
W1−N1	1.795(8)	W1−P1	2.5011(9)
N1−O1	1.231(9)	W1−P3	2.4626(10)
W1−P4	2.5000(9)	W1−Cl1	2.501(2)
W1−P2	2.4842(9)		
Bond angles			
P2−W1−P1	79.03(3)	N1−W1−P2	96.23(15)
N1−W1−Cl1	177.5(4)	N1−W1−P3	82.70(15)
P3−W1−P4	79.71(3)	Cl1−W1−P1	93.84(12)
P3−W1−P1	173.80(3)	P2−W1−P4	174.17(3)

With the aim to prepare the corresponding hydride, **15** was treated with excess of $LiBH_4$ in Et_3N at 70 °C analogous to **7** and **8** (Scheme 2.11). Monitoring of the reaction mixture by ^{31}P $\{^1H\}$ NMR spectroscopy did not reveal formation of any product as only the signal of the starting material was detected. The increase in temperature to 110 °C led to the decomposition of the starting material. Other hydride sources ($LiAlH_4$, KH + 18-crown-6, $LiHAl(tBuO)_3$), as well as variations of the solvents were tested to achieve the transformation of the chloride **15** to the hydride complex. In all cases no reaction was observed.

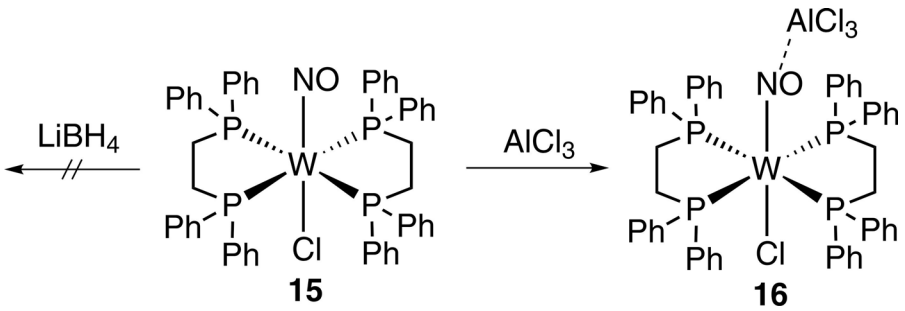

Scheme 2.11

There are some examples in the literature where the chloride atom was activated via coordination with $AlCl_3$. The Lewis acid can either attach to the chloride atoms elongating the metal-chloride bond[118] or even cleave the metal-chloride bond forming an ionic species with $AlCl_4^-$ (or $Al_2Cl_7^-$) counterion.[84, 119] However, the reaction between **15** and $AlCl_3$ did not reveal the activation of the chloride ligand. Instead of desired complex, **16** was isolated, in which $AlCl_3$ was found to be coordinated to the nitrosyl group (Scheme 2.11).

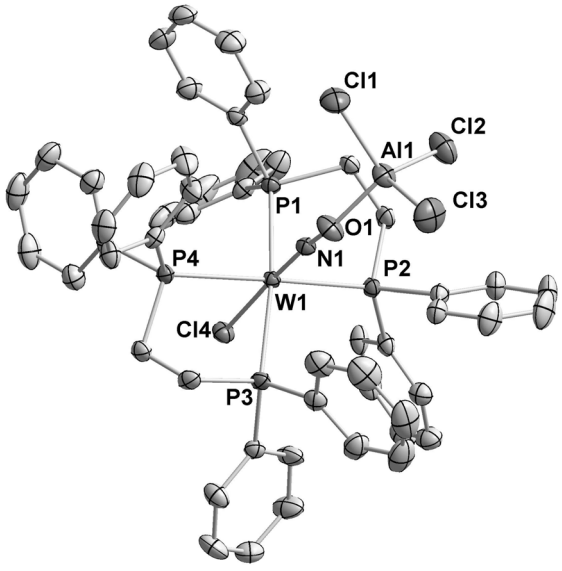

Figure 2.15 An ORTEP drawing of **16**. 50% probability displacement ellipsoids are shown. The co-crystallized complex **15** and hydrogen atoms are omitted for clarity.

Table 2.16 Selected Bond Lengths [Å] and Bond Angles [°] of **16**.

Bond lengths			
W1−N1	1.7542(14)	W1−P1	2.5145(4)
N1−O1	1.3085(17)	W1−P3	2.5425(5)
W1−P4	2.5196(5)	W1−Cl4	2.4416(4)
W1−P2	2.5205(5)	O1−Al1	1.7710(14)
Bond angles			
P2−W1−P1	79.343(15)	N1−W1−P1	94.37(5)
N1−W1−Cl4	176.09(5)	O1−N1−W1	172.53(13)
P2−W1−P3	103.056(15)	N1−O1−Al1	138.96(12)
N1−W1−P1	94.37(5)	P1−W1−P4	97.760(15)

The ^{31}P {^{1}H} NMR spectrum of **16** exhibited a singlet resonance at 34.9 ppm, that is different from the starting complex **15** and indicated the chemically equivalent phosphorus atoms. Besides sets of multiplets in the range from 7.46 to 6.81 ppm for the phenyl protons and two multiplets at 2.85 and 2.57 ppm attributed to methylene protons of the diphosphine bridge. A characteristic quartet and triplet of Et_2O were detected in the ^{1}H NMR spectrum of **16**. The integration ratio of the ether protons and the protons of the complex were in agreement with the formulation of **16**·Et_2O. The IR spectrum of **16** showed a strong nitrosyl band at 1484 cm^{-1} that appears lower than in **15** because of $AlCl_3$ molecule coordinated to the nitrosyl group.[106, 107]

Interestingly, the crystal structure obtained by X-ray study does not fully match the spectroscopic data. The asymmetric unit of the crystals, obtained by slow diffusion of cyclohexane into the concentrated dichloromethane solution of **16**, contains one W(dppe)$_2$Cl(NO···$AlCl_3$) (**16**) molecule, one half of W(dppe)$_2$Cl(NO) (**15**) (the metal center lies on a center of symmetry) and one solvent molecule (CH_2Cl_2). Presumably this is due to $AlCl_3$ dissociating during crystal growth that leading to the co-crystallized structure of the **15** and **16**.

An ORTEP drawing of **16** is given in Figure 2.15. Selected bond lengths and angles are presented in Table 2.16. The structure of **16** displays pseudo-octahedral coordination around the tungsten center. The four phosphorus atoms are located in-plane

and the chloride is located *trans* to the NO ligand. The mean phosphorus-tungsten bond length is 2.5242(5) Å, shorter than that of **15** (2.496(1) Å). The tungsten-chloride bond was found to be significantly shorter in **16** than in **15** (2.4416(4) Å *vs.* 2.501(2) Å) due to a stronger electron accepting ability of the NO···$AlCl_3$. The aluminum-oxygen bond length is 1.7710(14) Å.

2.10 Preparation of Mo(depe)$_2$(NO)H and its reaction with [H(Et$_2$O)$_2$][BAr$^F{}_4$]

Compound Mo(depe)(NO)Cl (**17**) was prepared similar to **3** starting from $Mo(NO)(CH_3CN)_2Cl_3$ with 83% yield (Scheme 2.12). As it was shown for **3** and **4** there is no need for the isolation of the intermediate product after the initial reaction of the phosphine ligand with the $Mo(NO)(CH_3CN)_2Cl_3$ complex. A ^{31}P $\{^1H\}$ NMR pursuit of the reaction was performed to trace the different behavior of the depe and dippe ligands.

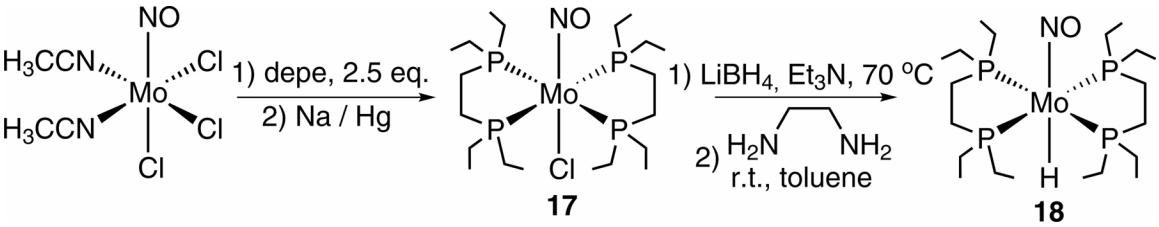

Scheme 2.12

The ^{31}P $\{^1H\}$ NMR investigation revealed a doublet at 61.5 ppm ($^2J_{PP}$ = 87.3 Hz) and a triplet at 27.4 ppm ($^2J_{PP}$ = 87.3 Hz) for the intermediate complex in the ratio 2:1, which indicated two chemically different phosphorus atoms in the coordination sphere. In all probability the reaction between $Mo(NO)(CH_3CN)_2Cl_3$ and the depe ligand had led to the formation of the species structurally close to **1** with one diphosphine bridging two metal centers. Reduction of the intermediate complex with 1% sodium amalgam in the presence of the depe ligand smoothly yielded **17** with chemically equivalent phosphorus atoms. The ^{31}P $\{^1H\}$ spectrum of complex **17** exhibited the singlet at 52.4 ppm indicating the chemical equivalence of the phosphorus atoms. The ^1H $\{^{31}P\}$ NMR spectrum showed a characteristic multiplet for the bridging methylene protons. The signals of methyl groups

were observed as triplets at 1.17 ($^1J_{HH}$ = 80.5 Hz) and 1.12 ($^1J_{HH}$ = 76.1 Hz). A band attributed to a nitrosyl stretching vibration was found in the IR spectrum of **17** at 1532 cm^{-1}.

Complex **17** was treated with excess of $LiBH_4$ in Et_3N to prepare the corresponding hydride (Scheme 2.12). Similar to the procedure for **7** the residue was extracted with toluene after the evaporation of Et_3N. According to the ^{1}H NMR spectroscopy (a characteristic quartet at 0.36 ppm ($^1J_{BH}$ =81.4 Hz)) the adduct was isolated, in which $LiBH_4$ is coordinated to the nitrosyl group (structurally related to **6**). Addition of ethylendiamine to the toluene solution of the adduct caused quantitative precipitation of $[Li(en)_2][BH_4]$ and afforded the hydride **18**. The NMR spectroscopic data for **18** are similar to hydrides **7** or **8**. A singlet resonance of the identical phosphorus atoms of the depe ligand was observed at 70.6 ppm in the ^{31}P {^{1}H} NMR spectrum of **18**. The ^{1}H NMR spectrum showed a quintet at 4.78 ppm ($^1J_{PH}$ = 28.8 Hz). The IR spectrum revealed a strong band at 1542 cm^{-1} attributed to the ν(MoH) stretching vibration and a band of the nitrosyl ligand at 1500 cm^{-1}.

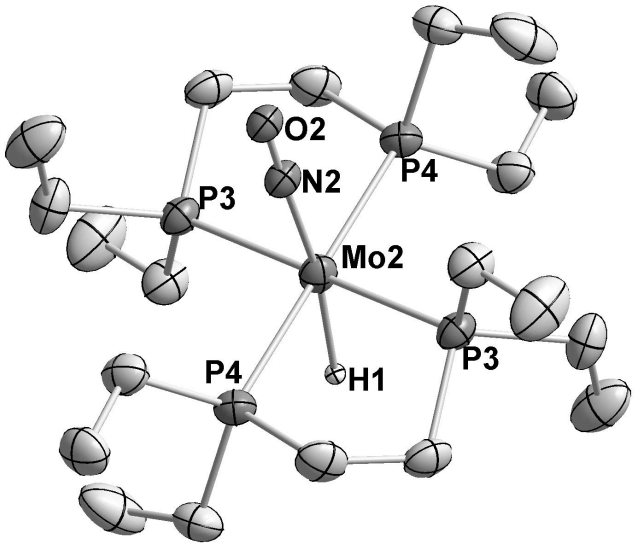

Figure 2.16 An ORTEP drawing of **18**. Displacement ellipsoids are drawn at the 50% probability level. The disorder of NO/H and selected hydrogen atoms have been omitted for clarity.

Table 2.17 Selected Bond Lengths [Å] and Bond Angles [°] of **18**.

Bond lengths			
Mo2−N2	1.909(6)	Mo2−P3	2.470(1)
Mo2−H1	1.76(3)	Mo2−P2	2.4759(10)
N2−O2	1.084(7)	Mo2−P1	2.4847(9)
Mo2−P4	2.4776(10)		
Bond angles			
P3−Mo2−P4	79.18(3)	P4−Mo2−H1	80.31(2)
N2−Mo2−H1	170.43(18)	N2−Mo2−P4	90.58(18)
N2−Mo2−P3	101.31(7)	O2−N1−Mo2	178.0(5)
N2−Mo2−P4	89.42(18)	P3−Mo2−H1	91.75(2)

A X-ray analysis confirmed the *trans* structure of **18**. **18** crystallizes in the centrosymmetric space group P-1. The asymmetric unit consists of two independent molecules, for which the metal center lies on an inversion center. The NO/H atoms are desordered. The phosphorus atoms are in-plane with the molybdenum metal center. The mean metal-phosphorus bond distance equals to 2.477(1) Å, that is 0.02 Å longer than the mean distance in the related complexes Mo(dmpe)$_2$(NO)Cl or Mo(dmpe)$_2$(NO)(H−BH$_3$) (dmpe = 1,2-bis(dimethylphosphino)ethane),[53] probably due to the bigger steric congestion of the ethyl groups as compared to methyl substituents.

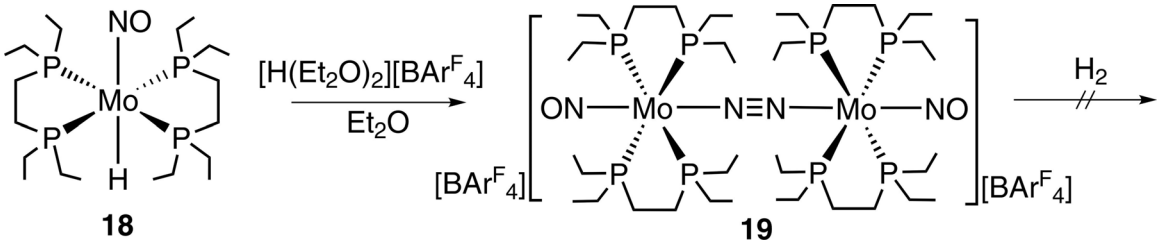

Scheme 2.13

The reaction between **18** and the [H(Et$_2$O)$_2$][BAr$^F_4$] acid was carried out to obtain a complex similar to **13**. The red crystalline compound [(Mo(NO)(depe)$_2$)$_2$(μ-N$_2$)][BAr$^F_4$]$_2$ (**19)** was isolated in 75% yield. The ^{31}P{^{1}H} NMR spectrum of **19** showed a

singlet resonance at 48.7 ppm indicating one type of phosphorus atom in the coordination. The ^{1}H NMR spectra exhibited multiplet resonances at 2.03 (8H), 1.93 (4H) and 1.82 (4H) ppm attributed to the methylene protons of depe ethyls and a characteristic multiplet of bridging methylenes at 1.73 ppm. Methyl resonances appeared at 1.25 and 1.18 ppm as well as complicated multiplets. In the IR spectrum of **19** a strong nitrosyl band was observed at 1572 cm^{-1}. No band could be observed for ν(NN) stretching mode presumably due to a symmetrically bridged nitrogen. Such coordination of N_2 causes the lack of any dipole moment associated with the vibration mode. The similar phenomenon was reported by Kubas *et al.* for $[Mo(CO)(Et_2PC_2H_4PEt_2)_2]_2(\mu\text{-}N_2)$,[77] which was structurally characterized. The Raman spectra of **19** exhibited a strong band at 1597 cm^{-1} attributed to NN stretch. For comparison, ν(NN) Raman bands were found at 1681 cm^{-1} for $[ArN_3N]Mo\text{-}N{=}N\text{-}Mo[ArN_3N]$ (Ar = 4-*t*BuC_6H_4)[120] and at 1630 cm^{-1} for $[Ar(R)N]_3Mo\text{-}N{=}N\text{-}Mo[N(R)Ar]_3$ (R = $C(CD_3)_2CH_3$, Ar = 3,5-$C_6H_3Me_2$).[121]

Comparing the spectroscopic data of **19** with those of Kubas' complex, we could propose **19** to possess a structure with a bridging N_2 ligand between two molybdenum centers as shown in Scheme 2.13. The element analysis fully matched the theoretical values confirming the composition of **19**. An X-ray diffraction analysis could not be carried out on **19** due to the fact that all crystals grow led to diffraction patterns, which could not be resolved.

Complex **19** showed no reaction with hydrogen gas as it was observed for related $[Mo(depe)_2(CO)]_2(N_2)$.[77] However, the intensive heating of Kubas' complex led to liberation of N_2 and formation of $Mo(depe)_2(CO)$ with agostic interaction *trans* to CO. Contrary to this heating of **19** under similar conditions did not result in N_2 release. Presumably NO ligand causes stronger binding of N_2 to the molybdenum center than it was observed for Kubas' complex.

2.11 Reaction of Mo(dippe)$_2$(NO)Cl with AgBF$_4$

However, complex **13** could be prepared via a protonation of **8** with $[H(Et_2O)_2][BAr^F{}_4]$ acid, this route to the vacant site seemed to be limited by inaccessibility of the intermediate hydride complex. Therefore other routes were carried

out avoiding the hydride complexes and attempting direct access to a "vacant site" molecules starting from the chloride complexes. Although the reaction between tungsten chloride complex W(dippe)$_2$(CPh)Cl and NaBAr$^F_4$ led to the formally 16e$^-$ complex [W(CPh)(dippe)$_2$][BAr$^F_4$][122], the substitution of the chloride in **4** by NaBAr$^F_4$ or by $NaBF_4$ could not be accomplished. Presumably, the strong π acceptor NO interacts with the strong π donor Cl forming via a push-pull π interaction a strong NO/Cl axis. The push-pull effect is normally stronger than the *trans* labializing effect of NO, which are denoted *trans* influence and *trans* effect.

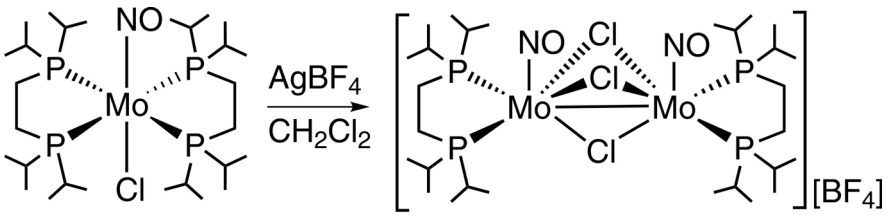

4 **20**

Scheme 2.14

There are some examples in the literature using the $AgBF_4$ reagent for rupture of Mo−Cl bond.[123-125] The advantage of the reagent is that it can cleave a metal-halogen bond at ambient conditions due to a strong chemical affinity of silver to halogens. At the same time Ag^+ is a strong oxidant that might cause side reactions. Therefore, a reaction mixture has to be protected from light to avoid the formation of by-products. In spite of this precaution, the interaction of **4** with $AgBF_4$ in CH_2Cl_2 at room temperature led to the formation of the mixture, in which compound **20** is the major, but no unique product (according to the $^{31}P\ \{^1H\}$ NMR spectroscopy) (Scheme 2.14).

The complex **20** readily crystallized from THF which allowed its isolation in pure form. The $^{31}P\ \{^1H\}$ NMR spectrum of the diamagnetic compound **20** exhibited a singlet resonance at 68.2 ppm. This indicated the presence of the chemically equivalent phosphorus atoms at the both sides of the dinuclear molecule. The ^1H NMR spectrum showed two multiplets for the isopropyl C−*H* protons at 2.43 and 2.35 ppm. A multiplet attributed to phosphine methylene resonances was found at 2.28 ppm. A singlet resonance at -154.9 ppm was observed in the $^{19}F\ \{^1H\}$ NMR spectrum of **20** that proved

the presence of a non-coordinated BF_4^- moiety. The IR spectrum of **20** revealed strong ν(NO) bands at 1654 and 1630 cm^{-1}.

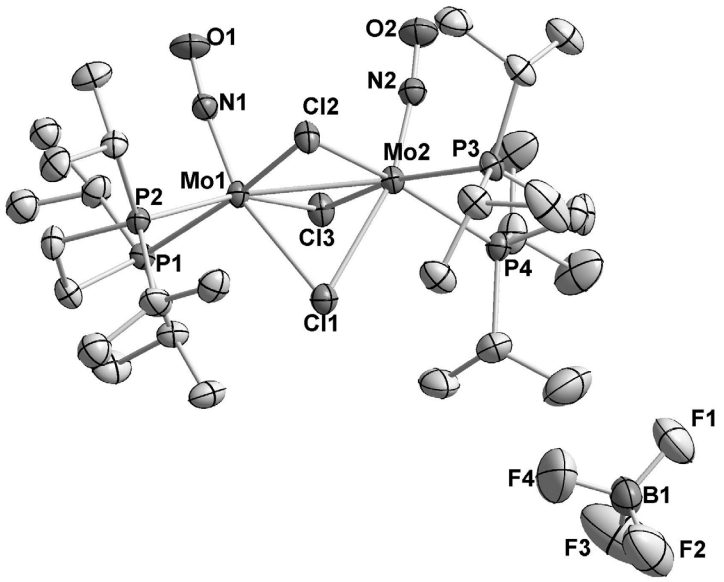

Figure 2.17 An ORTEP drawing of **20**. Displacement ellipsoids are drawn at the 50% probability level. All hydrogen atoms have been omitted for clarity.

Based on spectroscopic evidence it was concluded that **20** bears symmetrically bound dippe ligands, as well as a nitrosyl group in the coordination sphere. But the definitive structure was eventually based on a X-ray diffraction study. Monocrystals suitable for a X-ray diffraction study were grown by slow cooling of a concentrated THF solution. **20** crystallizes in the centrosymmetric space group P-1 and was found to adopt a dinuclear structure with two molybdenum centers held together by three bridging chloride atoms (Figure 2.17). Each metal center has a distorted octahedral coordination geometry, in which two chlorides and two phosphorus atoms are "in-plane" with the molybdenum atom. The nitrosyl ligand and Cl1 chloride atom are not located strictly *trans*. The N1−Mo1−Cl1 angle amounts to 162.26(7)°. The metal-metal bond distance is 2.8118(3) Å that is slightly longer than the bond length in the related complexes $Mo_2Cl_6(PEt_3)_3$ (2.753 (2) Å), $Mo_2Cl_6(PMe_2Ph)_3$ (2.6582 (5) Å)[126], $[PHMe_3]$-$[Mo_2Cl_7(PMe_3)_2]$ (2.7171 (3) Å).[127] It indicates the relative weak interaction between metal centers denoted as ligand enforced metal-metal bond. It is also interesting that Mo1−Cl1 (2.5721(6)) bond length is longer than other two, Mo1−Cl2 (2.4588(6) Å) and

Mo1−Cl3 (2.4447(6) Å) (Table 2.18). The mean molybdenum-phosphorus bond in **20** is 2.530 (1) Å.

Table 2.18 Selected Bond Lengths [Å] and Bond Angles [°] of **20**.

Bond lengths			
Mo1−N1	1.767(2)	Mo1−Cl1	2.5721(6)
Mo1−Cl3	2.4447(6)	Mo1−Mo2	2.8118(3)
Mo1−Cl2	2.4588(6)	Mo2−N2	1.763(2)
Mo1−P2	2.5273(7)	Mo2−Cl2	2.4538(6)
Mo1−P1	2.5312(6)	Mo2−Cl3	2.4574(6)
Mo2−P3	2.5402(6)	Mo2−P(4)	2.5221(7)
N1−O1	1.187(3)	N2−O2	1.198(3)
Bond angles			
N1−Mo1−Cl3	94.71(7)	Cl2−Mo1−P2	86.42(2)
N1−Mo1−Cl2	90.76(7)	N1−Mo1−P1	89.75(7)
Cl3−Mo1−Cl2	108.81(2)	Cl3−Mo1−P1	85.42(2)
N1−Mo1−P2	97.16(7)	Cl2−Mo1−P1	165.66(2)
Cl3−Mo1−P2	160.56(2)	P2−Mo1−P1	79.30(2)
N1−Mo1−Cl1	162.26(7)	Cl3−Mo1−l1	77.10(2)
Cl2−Mo1−Cl1	77.37(2)	P2−Mo1−Cl1	95.23(2)
P1−Mo1−Cl1	105.02(2)	N1−Mo1−Mo2	105.34(7)
Cl3−Mo1−Mo2	55.213(14)	Cl2−Mo1−Mo2	55.002(15)

2.12 Preparation of [Mo(dcype)(dippe)(NO)][BAr$^F{}_4$] and its reaction with hydrogen gas

The steric demand of bidentate ligands can be determined by their bite angle (for phosphorus ligands the P−M−P angle) and additionally by the cone angles at each phosphorus side. The dcype ligand with a large bite angle than the dippe was chosen to increase the tendency for dissociation of one “leg” of the diphosphine ligand in the targeted [Mo(dcyppe)$_2$(NO)][BAr$^F{}_4$] complex in comparison with complex **13**. However,

a synthetic access to the starting complex Mo(dcyppe)$_2$(NO)Cl was not found. Either the method used for the preparation of **4** or the substitution of CO in Mo(NO)(CO)$_4$(Cl-AlCl$_3$)[53] did not lead to the desired product. We supposed that two bulky dcype ligands are not fitting around the Mo center, because of too high steric congestion of the cyclohexyl substituents.

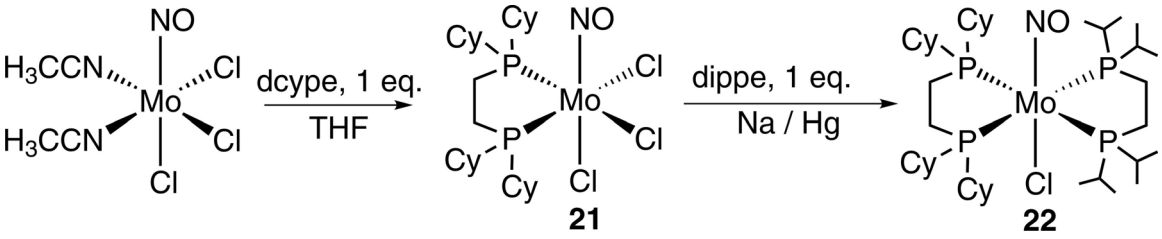

Scheme 2.15

But in a preliminary experiment, in which Mo(CH$_3$CN)$_2$(NO)Cl$_3$ was treated with the mixture of the dcype and dippe ligands in the presence of 1% sodium amalgam, formation of the mixed-ligand complex Mo(dcype)(dippe)(NO)Cl (**22**) was found in the mixture with **4**. We presumed that the substitution of CH$_3$CN molecules by the dcype ligand and consequent reduction of two chlorides with 1% sodium amalgam in the presence of only dippe could lead to the isolation of **22** without the formation of the side product **4**.

Complex Mo(dcype)(NO)Cl$_3$ (**21**) precipitated from the solution after the addition of the dcype to the THF solution of Mo(CH$_3$CN)$_2$(NO)Cl$_3$ (Scheme 2.15). **21** was isolated as a green powder in 55% yield. The singlet resonance at 70.4 ppm in the ^{31}P {^{1}H} NMR spectrum of **21** indicated the chemically equivalent phosphorus atoms in the molecule. The IR spectrum of **21** showed a ν(NO) strong band at 1676 cm^{-1}.

Compound **21** was characterized by X-ray diffraction analysis (Figure 2.18, Table 2.19). **21** crystallizes in the centrosymmetric space group Pbca. The asymmetric unit consists of two crystallographically independent molecules and one CH$_2$Cl$_2$ solvent molecule in a ratio 4:1. One molecule (Mo1) exhibited a positional disorder between the *trans* NO and Cl groups. The second molecule (Mo2) showed a disordered ethane group of the bidentate phosphine ligand. **21** displays pseudo-octahedral coordination geometry with two phosphorus and two chloride atoms located in-plane with the molybdenum

center. The mean phosphorus-molybdenum bond length is 2.569(2) Å, which is in the same range that was reported for the related complexes $MoOCl_3(PMe_3)_2$ (2.5629(7) Å)[128] and $MoOCl_3$(dppe) (dppe = 1,2-bis(diphenylphosphino)ethane) (2.587(1) Å)[129]. The average bond distance of the equatorial chloride-metal amounts to 2.351(2) Å, which is longer than the axial one (2.4531(19) Å) presumably due to the influence of *trans* nitrosyl group.

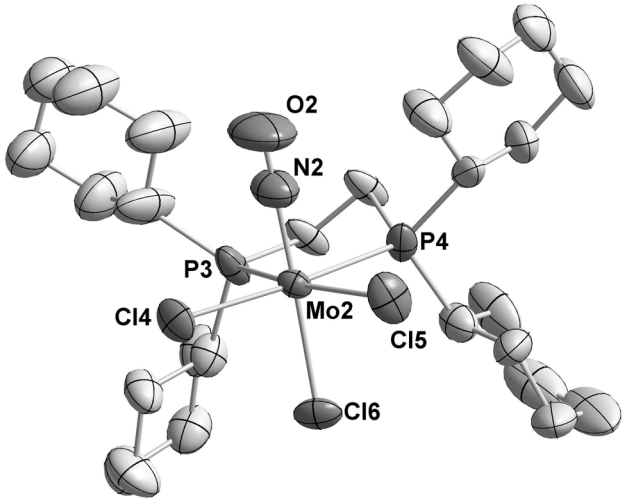

Figure 2.18 An ORTEP drawing of **21**. Displacement ellipsoids are drawn at the 50% probability level. The disorder of NO/Cl and selected hydrogen atoms have been omitted for clarity.

Table 2.19 Selected Bond Lengths [Å] and Bond Angles [°] of **21**.

Bond lengths			
N2−Mo2	1.815(8)	P3−Mo2	2.573(2)
Cl4−Mo2	2.3497(19)	P4−Mo2	2.5646(19)
Cl5−Mo2	2.353(2)	N2−O2	1.133(10)
Cl6−Mo2	2.4531(19)		
Bond angles			
O2−N2−Mo2	173.2(10)	Cl4−Mo2−Cl5	115.26(8)
N2−Mo2−Cl4	90.3(3)	N2−Mo2−Cl6	178.2(3)
N2−Mo2−Cl5	94.0(3)	P4−Mo2−P3	76.36(7)
N2−Mo2−P4	91.5(3)	N2−Mo2−P3	91.3(3)

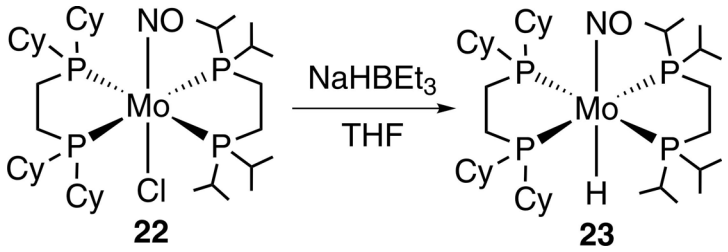

Scheme 2.16

Mo(dcype)(dippe)(NO)Cl (**22**) was obtained via the reaction of **21** and sodium amalgam in the presence of the dippe ligand (Scheme 2.15). **22** was isolated as a pale-yellow powder in 72% yield. The ^{31}P {^{1}H} NMR spectrum of **22** revealed two doublets of doublets at 59.6 and 54.0 ($^{2}J_{PP}$ = 120.6 Hz) indicating that two different bidentate phosphorus ligands are bound to the molybdenum metal center. The ^{31}P, ^{1}H NMR correlation spectrum revealed a signal at 59.6 ppm to be attributed to the dippe ligand and another one at 54.0 ppm to the dcype ligand, correspondingly. The IR spectrum of **22** showed a strong ν(NO) band at 1527 cm^{-1}.

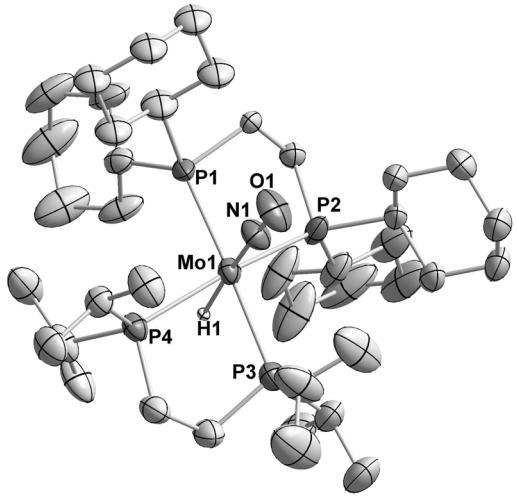

Figure 2.19 An ORTEP drawing of **23**. Displacement ellipsoids are drawn at the 50% probability level. The disorder of the dcype bridge and of one cyclohexyl group as well as the selected hydrogen atoms have been omitted for clarity.

Table 2.20 Selected Bond Lengths [Å] and Bond Angles [°] of **23**.

Bond lengths			
N1−O1	1.220(4)	P3−Mo1	2.4759(11)
N1−Mo1	1.807(3)	P4−Mo1	2.531(1)
P1−Mo1	2.5018(11)	Mo1−H1	1.83(3)
P2−Mo1	2.4869(11)		
Bond angles			
N1−Mo1−H1	175.3(10)	P3−Mo1−P4	78.45(4)
P1−Mo1−P4	101.85(4)	N1−Mo1−P3	95.91(11)
P2−Mo1−P4	166.13(4)	N1−Mo1−P2	95.04(11)
O1−N1−Mo1	179.6(4)	P2−Mo1−H1	86.8(10)
P1−Mo1−H1	93.1(10)	P4−Mo1−H1	79.3(10)

Although the combination of $LiBH_4$ and Et_3N was successfully used for the preparation of the hydride complex **7**, **8** and **18**, this set of the reagents was found not to be suitable for the preparation of Mo(dcype)(dippe)(NO)H (**23**) apparently due to the instability of the starting chloride **22** under the reaction condition. Instead of the $LiBH_4$ and Et_3N combination, the hydride reagent $NaHBEt_3$ was applied as an alternative hydride donor. The treatment of **22** with $NaHBEt_3$ in THF solution at room temperature afforded the hydride **23** in a good yield (67%) (Scheme 2.16). Similarly to **22** the $^{31}P\{^1H\}$ spectrum of **23** showed two doublets of doublets at 86.2 ($^2J_{PP}$ = 99.0 Hz) and at 77.5 ($^2J_{PP}$ = 99.0) ppm. The ^1H NMR spectrum of **23** exhibited a quintet for the hydride ligand at -4.12 ppm ($^2J_{PH}$ = 27.5 Hz). In the IR spectrum of **23** a strong hydride band appeared at 1573 cm^{-1} and a signal at 1500 cm^{-1} was attributed to the nitrosyl vibration.

The X-ray structure analysis fully confirmed the spectroscopically derived structure (Figure 2.19, Table 2.20). **23** crystallized in the centrosymmetric space group $P2_1/c$. The dippe and dcype ligand are arranged equatorially whereby nitrosyl and chloride *trans*. It is interesting to note that one of the molybdenum-phosphorus bond lengths of the dippe ligand is 0.06 Å longer than the other ones. Presumably steric pressure of the "bumping" isopropyl and cyclohexyl groups causes this distortion. The atoms of these substituents on the side of the P "square" are packed without visible steric

interaction. The molybdenum-hydride bond distance equals to 1.83(3) Å and is very long; a "normal" Mo−H bonds are observed in the range of 1.6 to 1.65 Å. One should, however, take into account that such bonds have high standard deviations in X-ray diffraction studies. Compared the bond length of **23** is in the same range with the Mo−H distance of **18** (1.79(4) Å).

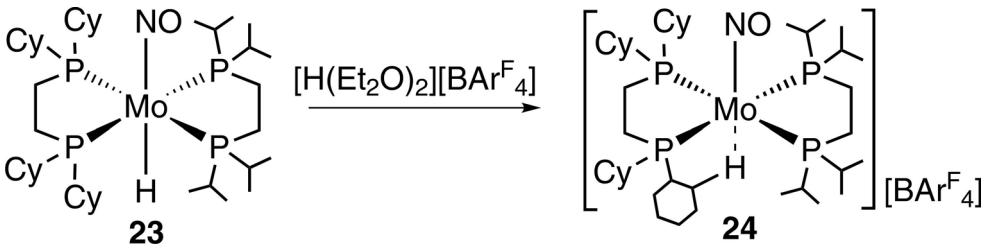

23 **24**

Scheme 2.17

In analogy to the previously described complex **7**, the hydride **23** interacts with the $[H(Et_2O)_2][BAr^F{}_4]$ acid forming complex **24**, which bears a weak agostic interaction (Scheme 2.17). The $^{31}P\{^1H\}$ spectrum of **24** revealed the two doubles of doublets at 73.4 ($^2J_{PP}$ = 99.2 Hz) and 77.5 ppm ($^2J_{PP}$ = 99.2 Hz) indicating that the "equatorial" phosphorus atom arrangement is preserved in **24**. In contrast to **13** a resonance for the agostic hydrogen was observed in the ^1H NMR spectrum of **24** at -0.27 ppm. According to the ^{13}C, ^1H NMR correlation the agostic proton belongs to a cyclohexyl group of the dcype ligand. Presumably, possessing a larger steric congestion than the isopropyl group, the cyclohexyl substituents are not capable to undergo rapid exchanging in solution as it was observed for complex **13**. That makes the agostic proton visible in the ^1H NMR spectrum at room temperature. The IR spectrum of **24** showed a nitrosyl band at 1589 cm^{-1}.

A single-crystal X-ray diffraction study was carried out on **24** (Figure 2.20, Table 2.21), which crystallizes in the centrosymmetric space group P-1. The asymmetric unit contains the molybdenum cation and its $[BAr^F{}_4]^-$ counter-ion. Similar to **13** complex **24** adopts a square pyramidal geometry, in which four phosphorus atoms form the square base of the pyramid. The X-ray structure analysis confirmed that the agostic hydrogen atom belongs to cyclohexyl group. In **24** the agostic bond length equals to 2.56 Å that is longer than the related distance in **13** (2.46 Å). The P3 phosphorus which bears the

substituent with agostic hydrogen atom is located closer to the molybdenum center than three other as it was also observed for **13**.

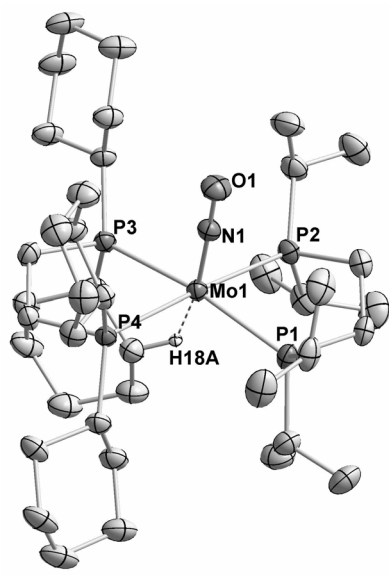

Figure 2.20 An ORTEP drawing of **24**. Only the main residue is shown without the counterion and selected H atoms.

Table 2.21 Selected Bond Lengths [Å] and Bond Angles [°] of **24**.

Bond lengths			
N1−O1	1.212(2)	P3−Mo1	2.4722(6)
N1−Mo1	1.7569(19)	P4−Mo1	2.5160(6)
P1−Mo1	2.5162(6)	H18A−Mo1	2.5603(2)
P2−Mo1	2.5337(6)		
Bond angles			
O1−N1−Mo1	178.66(18)	N1−Mo1−P2	92.29(6)
N1−Mo1−P3	97.01(6)	P3−Mo1−P2	101.02(2)
N1−Mo1−P4	92.01(6)	P4−Mo1−P2	175.65(2)
P3−Mo1−P4	79.13(2)	P1−Mo1−P2	79.59(2)
P3−Mo1−P1	169.94(2)	H18−Mo1−N1	157.53(6)

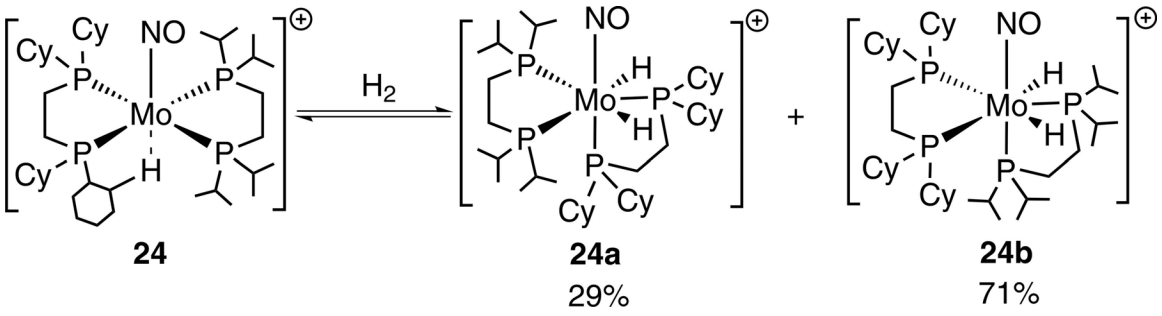

Scheme 2.18

In analogy to **13** complex **24** is capable of activating hydrogen gas (Scheme 2.18). Pressurizing the THF solution of **24** with 1.8 bar of H_2 led to a color change from green to yellow. The ^{31}P $\{^1H\}$ NMR spectrum of the reaction mixture exhibited two sets of triplets at 89.7, 66.7, 41.8 ppm and 81.1, 76.5, 32.7 ppm and two doublets of doublets attributed to the starting material **24** (Figure 2.21). The integration ratio between these sets of signals depended on the hydrogen pressure, therefore we have to assume an equilibrium reaction as it was reported before for **13**.

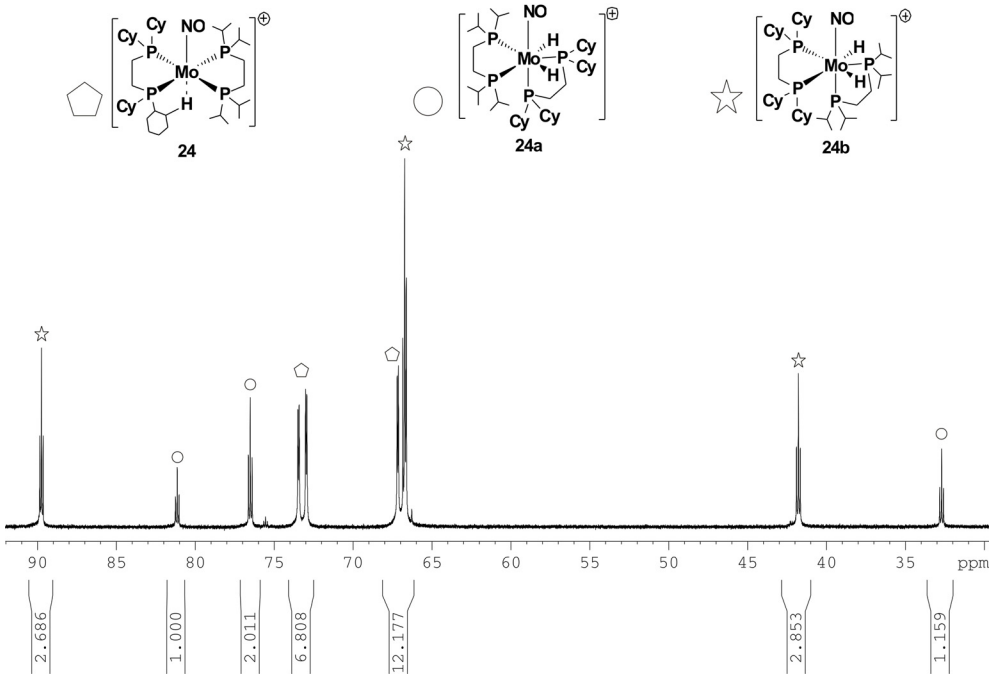

Figure 2.21 The ^{31}P $\{^1H\}$ NMR spectrum of the reaction of **24** with H_2 gas. All signals are schematically assigned to the corresponding compounds.

The ratio between reaction products **24a** and **24b** was found to be 71:29 according to the integration of the ^{31}P $\{^1H\}$ NMR spectrum. To assign the signals a ^{13}P, ^1H NMR correlation spectrum was measured. This indicated that the resonance at 41.8 ppm in the ^{31}P $\{^1H\}$ NMR spectrum and the doublets of methyl groups at 0.95 and 0.87 ppm in the ^1H $\{^{31}P\}$ NMR spectrum to belong to the dippe ligand. Consequently, the dippe ligand is more prone to go axial/equatorial than the related dcype, in spite of the fact that only cyclohexyl substituent forms the agostic interaction in **24**.

2.13 Conclusion

An improved method for the preparation of the starting chlorides **3**, **4**, **15**, **17** was developed. The reaction was carried out in-one-pot fashion without isolation of the intermediate products of the diphosphine ligand and $M(CH_3CN)_2(NO)Cl_3$ (M = Mo, W) reaction with a significant increase in the overall yields.

$LiBH_4$ as a hydride donor and an appropriate amine suited to complex the lithium cation were shown to be a suitable combination to prepare the hydride complexes **7**, **8** and **18** starting from the corresponding chlorides.

The hydride transfer reactions of **7** and **8** onto ketones was found not to result in any product, presumably due to the large steric demand of isopropyl groups preventing access to the hydride ligand. The formate complexes **9** and **10** were obtained by insertion of CO_2 gas, that is less sterically hindered and electronically more polarizable than ketones, into M−H bond.

The tungsten hydride **7** reacts with the acid $[H(Et_2O)_2][BAr^F{}_4]$ to form the seven-coordinate cationic dihydride complex **11** that is stable at various temperatures. The analogous molybdenum complex **13a** was found to be unstable and could be traced only in solution under H_2. It deliberately looses H_2 at room temperature to form the sixteen electron complex **13** bearing a weak agostic interaction.

In the presence of the $[BF_4]^-$ anion, the H_2 ligand in **8a** undergoes substitution to form **14**. In contrast to this observation the $[BF_4]^-$ and the $[BAr^F{}_4]^-$ counterions were able to stabilize the seven-coordinated tungsten dihydride cation in the form of **11** and **12** salts.

Complex **13** was found to catalyze hydrogenation of acetone with the formation of isopropanol. Attempts to hydrogenate other ketonic substrates were not successful presumably due to the too great steric congestion exerted by the dippe ligands.

The substitution of isopropyl groups with phenyl, making the diphosphine ligand less electron donating, caused the strengthening of W−Cl bond in **15** and as a consequence the corresponding hydride could not be prepared. Attempts to activate the W−Cl bond via interaction with the Lewis acid $AlCl_3$ led to $AlCl_3$ coordination onto the nitrosyl group. The adduct **16** was isolated as a product of the reaction.

Substitution of the dippe ligand by the depe also affected the reactivity of the complexes. Thus, the reaction of the hydride **18,** which is structurally related to **8,** and $[H(Et_2O)_2][BAr^F{}_4]$ acid led to the formation of **19** bearing a N_2 ligand bridging the molybdenum centers, whereas **13** possessing an agostic interaction was obtained in a similar reaction as for **8**.

Attempts were made to create reaction conditions avoiding the hydride formation and generating a "vacant site" at molybdenum. However, the reaction between **4** and $AgBF_4$ led to formation of the unexpected dinuclear complex **20**, in which two metal centers are connected by three Cl atoms.

To increase the on-off behavior of the diphosphine substituent, the dcype ligand was used that is more bulky than the dippe ligand. The preparation of the symmetric Mo(dcype)$_2$(NO)Cl could not be accomplished. Instead the asymmetrically substituted chloride complex **22** was obtained by the reduction of Mo(dcype)(NO)Cl_3 with 1% sodium amalgam in the additional presence of the dippe ligand. Since complex **22** is unstable under the condition, which was applied in the preparation of **8**, the alternative hydride reagent $NaBHEt_3$ was chosen. The reaction between **23** and $[H(Et_2O)_2][BAr^F{}_4]$ acid resulted in the $16e^-$ complex **24**, which analogously to **13** bears an agostic cyclohexyl substituent. The reaction of **24** with hydrogen gas furnished a mixture of two seven-coordinated dihydride isomers, which were found to be in equilibrium with the starting complex. Based on the interpretation of ^{31}P, ^{1}H NMR correlation studies, it was concluded that the dippe ligand prefers the axial/equatorial position more than the dcype ligand.

3 Complexes of the Type [M(P∩P)(CO)$_2$(NO)][A]

3.1 Introduction

Homogenous hydrogenations are crucial in the production of numerous fine chemicals. Wilkinson or Osborn type catalysts[17] are normally used involving formal homolytic splitting of H_2.[29] These types of catalytic transformations are particularly suited for the hydrogenation of olefinic compounds. "Ionic hydrogenation", operating with heterolytic cleavage of H_2, constitutes a principally new approach.[30, 31] They involve hydride (H^-) or proton (H^+) as a H_2 equivalent transferring these to the substrate.[24] Various catalytic systems enable efficient hydrogenations of ketones[68, 130, 131] and imines[7, 61, 132-134] via Wilkinson / Osborn type or ionic hydrogenations. However, most of these processes are presently based on precious metals, which require tedious catalyst recycling for economical and toxicity reasons. Therefore a global research approach has been initiated to develop non-precious metal catalysts.[67, 135] Bullock *et al.* reported some molybdenum and tungsten complexes $[Cp(CO)_2M(L)]^+[A]^-$ (M = Mo, W; L = phosphine, carbene; A = BAr^F_4 (Ar^F = 3,5-$(CF_3)_2C_6H_3$), $B(C_6F_5)_4$) that showed catalytic activity in ketone hydrogenation,[55-57, 102, 136] but the TOF values achieved were still quite low. Mechanistic studies supported the "ionic hydrogenation" pathway with proton before hydride transfer.[31] Furthermore in related systems Kubas *et al.* demonstrated the crucial influence of phosphine substitutions on the hydrogen activation via their electron donating capability.[100, 101, 137, 138] For example, the complexes Mo(CO)-(iBu$_2$PCH$_2$CH$_2$PiBu$_2$)$_2$ bearing strong electron donating ligands can split the H_2 molecule at ambient temperature forming a dihydride $Mo(H)_2$ species, whereas the structurally similar $Mo(CO)(Ph_2PCH_2CH_2PPh_2)_2$ complex coordinates the hydrogen molecule possessing an elongated H−H bond. In isoelectronic cationic bis(diposphine)nitrosyl molybdenum and tungsten complexes the H_2 ligand is oxidatively added to form dihydride complexes.[139] H_2 complexes are normally more acidic than the corresponding dihydride complexes. Therefore the earlier species are preferably involved in heterolytic splitting via deprotonation and the latter foster catalyses of the Wilkinson type. The

presence of nitrosyl ligands is expected to reduce the binding strength of H_2 ligands and enhance their acidity thus promoting heterolytic splitting of H_2.[47, 51] In addition we would expect for the deprotonated dihydrogen complexes the weakening of the resulting metal-hydride bonds to facilitate hydride transfers onto unsaturated compounds.[52, 140]

Based on this we supposed that the diphosphine nitrosyl complexes of the type [M(NO)(P∩P)(CO)$_2$(L)][A] (M = Mo, W; L = labile ligand) might render catalytic ionic hydrogenation systems, particularly prone for imine hydrogenations with proton before hydride transfer characteristics.

3.2 Synthesis of molybdenum and tungsten complexes of the Type [M(dippp)(CO)$_2$(NO)(THF)][A] (M = Mo, W, A = BAr$^F{}_4$ or B(C$_6$F$_5$)$_4$)

The addition of 1 equivalent of the dippp ligand (dippe = 1,3-bis(diisopropyl-phosphino)propane) to a THF solution of the M(CO)$_4$(NO)ClAlCl$_3$ (M = Mo, W) revealed formation of the chloride compounds M(dippp)(NO)(CO)$_2$(Cl) (M = Mo, **25a** and M = W, **26a**) (Scheme 3.1), which were isolated in 75% and 95% yield, respectively.

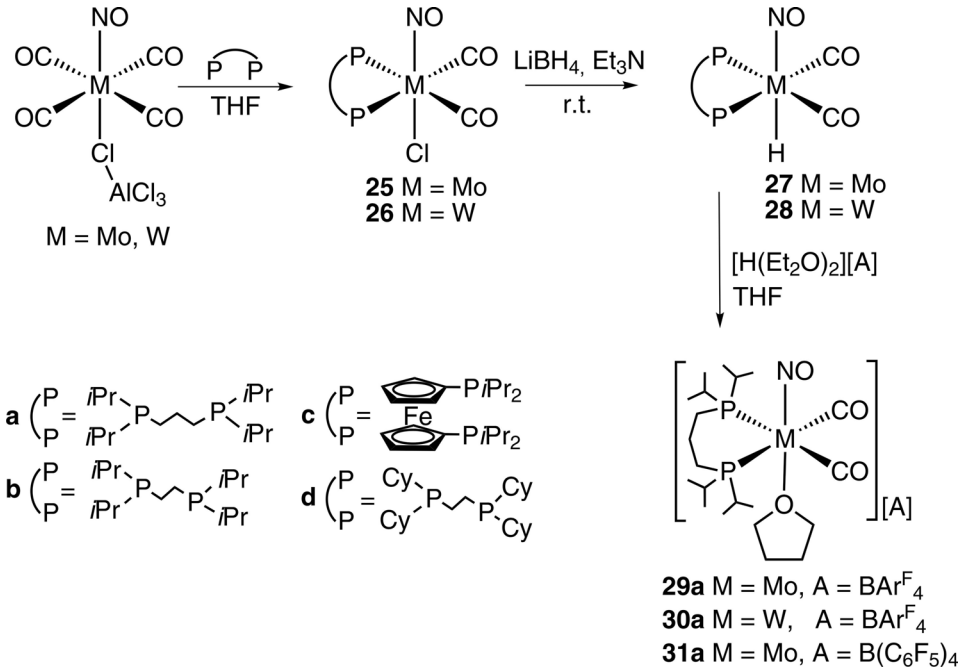

Scheme 3.1

The ^{31}P {^{1}H} NMR spectra exhibited single resonances at 21.5 ppm for **25a** and at 7.6 ppm for **26a**, which indicated the presence of two equivalent phosphorus atoms in each complex. The ^{1}H NMR spectra of **25a** and **26a** showed two multiplets at 2.36 and 2.27 ppm and at 2.44 and 2.36 ppm, respectively, attributed to the –C*H* protons of the isopropyl groups. In the ^{13}C {^{1}H} spectra the characteristic signals of carbonyl ligands appeared as doublet of doublets at 215.9 ppm ($^2J_{CP}$ = 22.9 Hz) for **25a** and at 211.4 ppm ($^2J_{CP}$ = 15.1 Hz) for **26a**. The IR spectra revealed strong bands at 2019, 1950 cm^{-1} (ν(CO)), 1610 cm^{-1} (ν(NO)) for **25a** and at 2007, 1929 cm^{-1} (ν(CO)), 1610 cm^{-1} (ν(NO)) for **26a**. The X–ray diffraction studies of **25a** and **26a** confirmed the spectroscopically derived pseudo-octahedral structures. ORTEP drawings of **25a** and **26a** are presented in Figure 3.1. Selected bond lengths and angles are summarized in Tables 3.1 and 3.2.

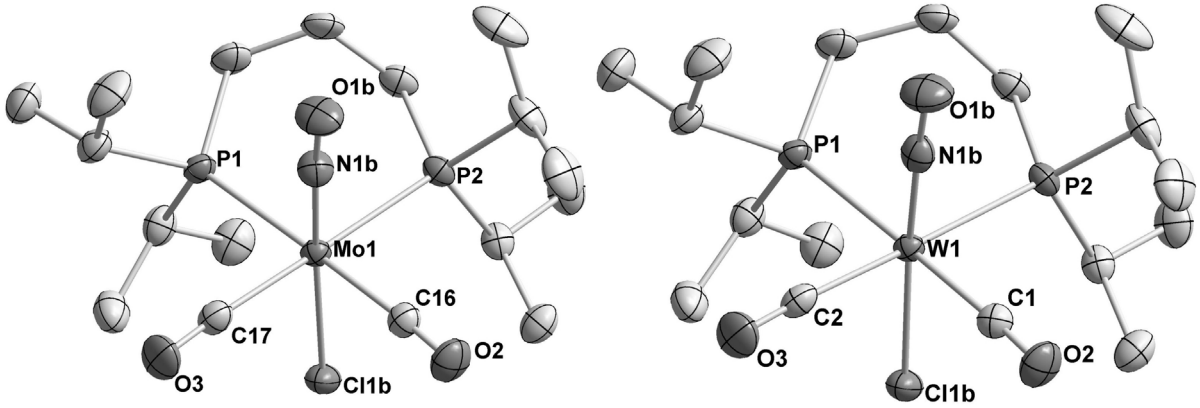

Figure 3.1 ORTEP drawings of M(dippp)(NO)(CO)$_2$(Cl) (M = Mo, **25a** and M = W, **26a**). Displacement ellipsoids are drawn at the 50% probability level. All hydrogen atoms have been omitted for clarity.

The structures of **25a** and **26a** display a geometry with one Cl atom *trans* to the nitrosyl group, which are disordered in both complexes. The phosphorus atoms and the two carbon atoms of the carbonyl groups are in-plane with the metal. The average Mo−P and W−P bond distances are 2.5678(5) and 2.5598(7) Å, respectively, which are slightly longer than, for instance, those of W[C(4-NH$_2$C$_6$H$_4$)]Cl(CO)$_2$(dppe) (2.540(2) Å)[141], [W(CMes)(CO)$_2$(dppe)$_2$Cl][SbF$_6$] (2.538(7) Å)[83] and (dppe)(CO)$_2$(ClW≡CCH=C)-(cyclopentyl)[90] (2.531(1) Å). Only in WCl(CO)$_2$(dppf)(CPh) the W–P bond (2.584(1) Å) is longer than in **26a**.[142]

Table 3.1 Selected Bond Lengths [Å] and Bond Angles [°] of **25a**.

Bond lengths			
P1−Mo1	2.5780(5)	N1B−O1B	1.218(12)
P2−Mo1	2.5576(4)	C17−O3	1.130(2)
Mo1−N1B	1.816(8)	C16−O(2)	1.134(2)
Mo1−Cl1B	2.449(2)	C17−Mo1	2.0431(19)
C16−Mo1	2.0340(19)		
Bond angles			
N1B−Mo1−C16	87.4(2)	Cl1B−Mo1−P2	92.58(5)
N1B−Mo1−C17	90.5(2)	N1B−Mo1−P1	91.7(2)
C16−Mo1−C17	89.75(7)	C16−Mo1−P1	177.91(5)
N1B−Mo1−Cl1B	173.0(2)	C17−Mo1−P1	88.37(5)
C16−Mo1−Cl1B	86.06(7)	Cl1B−Mo1−P1	94.75(5)
C17−Mo1−Cl1B	86.92(7)		

Table 3.2 Selected Bond Lengths [Å] and Bond Angles [°] of **26a**.

Bond lengths			
P2−W1	2.5519(6)	C1−O2	1.132(3)
P1−W1	2.5679(7)	C1−W1	2.026(3)
Cl1B−W1	2.436(4)	C2−O3	1.142(3)
N1B−W1	1.828(8)	C2−W1	2.030(3)
N1B−O1B	2.0340(19)		
Bond angles			
O2−C1−W1	177.4(3)	C1−W1−Cl1B	86.46(11)
O3−C2−W1	176.5(3)	C2−W1−Cl1B	87.76(11)
N1B−W1−C1	87.0(4)	N1B−W1−P2	89.9(3)
N1B−W1−C2	90.3(3)	C1−W1−P2	91.97(8)
C1−W1−C2	89.53(10)	C2−W1−P2	178.48(8)
N1B−W1−Cl1B	173.2(4)	Cl1B−W1−P2	92.13(8)

Treatment of the chlorides **25a** and **26a** with 5eq. of $LiBH_4$ in Et_3N at room temperature resulted in the formation of the hydride complexes **3a** and **4a** (Scheme 3.1).[139] The ^{31}P $\{^1H\}$ NMR spectra of **27a** and **28a** exhibited singlets at 41.1 ppm for **27a** and 20.9 ppm for **28a**, which indicated equivalent phosphine ligands. Besides multiplets attributed to the resonance of the dippp protons characteristic triplets of the hydride ligands were observed in the ^1H NMR spectra at -2.28 ppm ($^2J_{PH}$ = 24.0 Hz) for **27a** and at -1.19 ppm ($^2J_{PH}$ = 24.0 Hz) for **28a**. In the ^{13}C $\{^1H\}$ spectra doublet of doublets at 226.0 ppm ($^2J_{CP}$ = 10.7Hz) (**27a**) and at 2l7.7 ppm ($^2J_{CP}$ = 14.1 Hz) (**28a**) were assigned to the carbonyl ligands. The IR spectra of **27a** and **28a** revealed strong bands at 1983, 1910 (ν(CO)), 1653 (ν(MoH)), 1570 (ν(NO)) cm^{-1} and at 1976, 1898 (ν(CO)), 1726 (ν(WH)), 1568 (ν(NO)) cm^{-1} respectively.

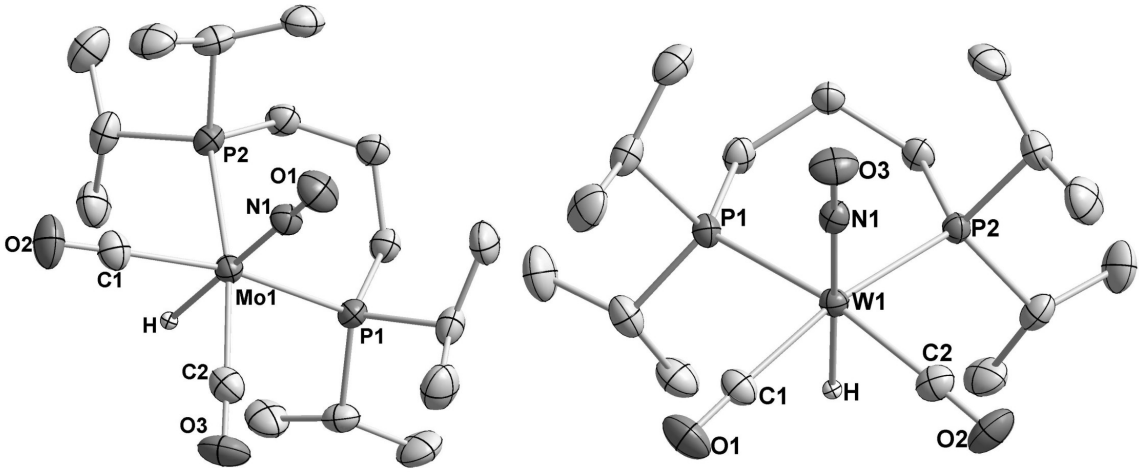

Figure 3.2 ORTEP drawings of M(dippp)(NO)(CO)$_2$(H) (M = Mo, **27a** and M = W, **28a**). Displacement ellipsoids are drawn at the 50% probability level. Selected hydrogen atoms have been omitted for clarity.

X-ray diffraction studies were carried out on **27a** and **28a** (Figure 3.2, Tables 3.3 and 3.4). Similarly to the starting chloride compounds **25a** and **26a**, the hydride compounds **27a** and **28a** display pseudo-octahedral coordination geometries with the phosphorus atoms of the dippp ligand and the two carbonyl ligands in-plane with the metal center and the hydride ligand located *trans* to the nitrosyl group. Structurally related bond distances of **27a** and **28a** are similar to those of chlorides **25a** and **26a**.

Table 3.3 Selected Bond Lengths [Å] and Bond Angles [°] of **27a**.

Bond lengths			
C1−O2	1.136(4)	N1−Mo1	1.829(2)
C1−Mo1	2.017(3)	P1−Mo1	2.5368(7)
C2−O3	1.136(3)	P2−Mo1	2.5347(7)
C2−Mo1	2.017(3)	Mo1−H	1.66(3)
N1−O1	1.190(3)		
Bond angles			
O2−C1−Mo1	178.7(3)	N1−Mo1−P2	98.19(7)
O3−C2−Mo1	178.7(3)	C1−Mo1−P2	165.47(8)
N1−Mo1−C1	95.79(11)	N1−Mo1−P1	98.89(8)
N1−Mo1−C2	96.30(10)	C1−Mo1−P1	165.21(8)
C1−Mo1−C2	88.07(13)	C2−Mo1−P1	88.52(9)

Table 3.4 Selected Bond Lengths [Å] and Bond Angles [°] of **28a**.

Bond lengths			
C1−O1	1.143(3)	N1−W1	1.8266(17)
C1−W1	2.013(2)	P1−W1	2.5280(6)
C2−O2	1.145(3)	P2−W1	2.5269(5)
C2−W1	2.012(2)	W1−H	1.67(3)
N1−O3	1.210(2)		
Bond angles			
O1−C1−W1	178.3(2)	N1−W1−P2	98.40(6)
O2−C2−W1	178.3(2)	C2−W1−P2	88.15(7)
N1−W1−C2	95.75(8)	C1−W1−P2	165.88(7)
N1−W1−C1	95.63(8)	N1−W1−P1	97.90(5)
C2−W1−C1	88.81(10)	C2−W1−P1	166.34(7)
C1−W1−P1	89.23(7)	P2−W1−P1	90.473(16)

Treatment of **27a** and **28a** with 1 eq. of $[H(Et_2O)_2][BAr^F{}_4]$[143-145] (Ar^F = 3,5-$(CF_3)_2C_6H_3$) in THF afforded $[M(dippp)(NO)(CO)_2(THF)][BAr^F{}_4]$ M = Mo, **29a** and M = W, **30a** (Scheme 3.1), which were isolated in 69% yield. The ^{31}P $\{^1H\}$ NMR showed singlets at 17.6 ppm (**29a**) and 8.8 ppm (**30a**). In the ^1H NMR spectra of **29a** and **30a** characteristic multiplet resonances of the THF ligand appeared with the proton chemical shifts different of those from the free molecule. The ^{13}C $\{^1H\}$ NMR revealed carbonyl resonance at 214.1 ppm ($^2J_{CP}$ = 16.7 Hz) for **29a** and at 211.6 ppm ($^2J_{CP}$ = 15.06 Hz) for **30a**. Strong bands were observed in the IR spectra at 2044, 1978 (ν(CO)), 1682 (ν(NO)) cm^{-1} for **29a** and at 2027, 1953 (ν(CO)), 1666 (ν(NO)) cm^{-1} for **30a**.

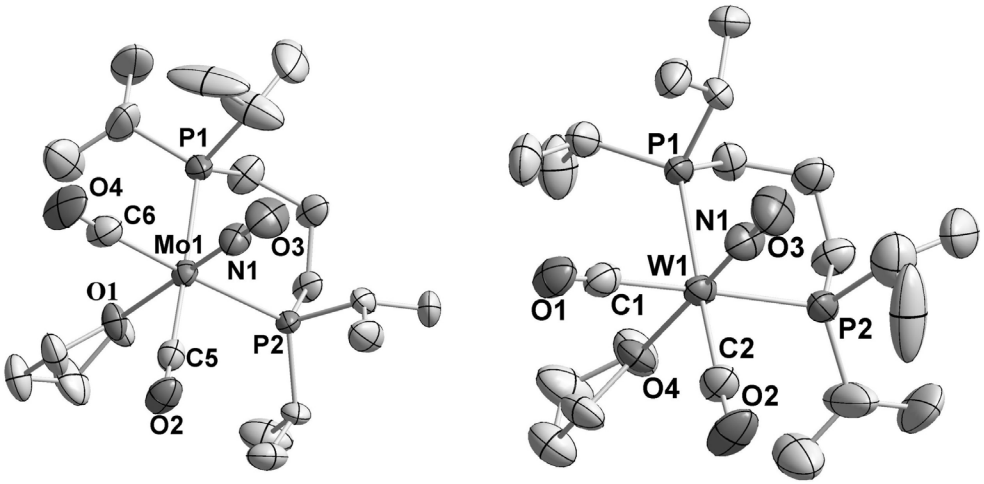

Figure 3.3 ORTEP drawings of $[M(dippp)(NO)(CO)_2(THF)][BAr^F{}_4]$ (M = Mo, **29a** and M = W, **30a**). Displacement ellipsoids are drawn at the 50% probability level. Only the main residues (without counterions and free solvent molecules) are shown. Hydrogen atoms have been omitted for clarity.

The X-ray diffraction studies of **29a** and **30a** (Figure 3.3, Tables 3.5 and 3.6) revealed pseudo-octahedral environment of the metal centers similar to the hydride and chloride complexes **25a**, **26a**, **27a** and **28a** with two phosphorus atoms of the dippp ligands and the carbonyl ligands in-plane with the metal center. The average M−P bond distances of 2.588(2) Å (**29a**) and 2.571(2) Å (**30a**) are slightly longer than the corresponding bond lengths in **27a** and **28a**. Coordination of one THF molecule on the metal center occurred with the M−O bond lengths of 2.241(4) Å for **29a** and 2.223(4) Å

Table 3.5 Selected Bond Lengths [Å] and Bond Angles [°] of **29a**.

Bond lengths			
O1−C1	1.434(8)	C5−O2	1.122(8)
N1−O3	1.188(7)	C5−Mo1	2.060(7)
N1−Mo1	1.780(6)	C6−O4	1.122(9)
P1−Mo1	2.5824(19)	O1−Mo1	2.242(4)
P2−Mo1	2.5840(16)		
Bond angles			
N1−Mo1−C6	87.1(3)	C5−Mo1−O1	86.9(2)
N1−Mo1−C5	87.5(3)	N1−Mo1−P1	91.3(2)
C6−Mo1−C5	87.6(3)	C6−Mo1−P1	90.0(2)
N1−Mo1−O1	173.3(2)	C5−Mo1−P1	177.45(19)
C6−Mo1−O1	89.0(3)	O1−Mo1−P1	94.08(12)
N1−Mo1−P2	91.28(19)	C6−Mo1−P2	177.7(2)
P1−Mo1−P2	88.40(5)	C5−Mo1−P2	93.89(18)

Table 3.6 Selected Bond Lengths [Å] and Bond Angles [°] of **30a**.

Bond lengths			
C1−O1	1.084(8)	N1−W1	1.790(5)
C1−W1	2.078(7)	O4−W1	2.223(4)
C2−O2	1.127(8)	P1−W1	1.122(9)
C2−W1	2.029(7)	P2−W1	2.5708(18)
N1−O3	1.181(7)		
Bond angles			
N1−W1−C2	86.8(3)	P2−W1−P1	88.55(5)
C2−W1−C1	87.3(3)	O4−W1−P1	92.10(12)
N1−W1−O4	173.8(2)	C1−W1−P1	93.37(19)
C2−W1−O4	89.7(3)	C2−W1−P1	178.1(2)
C1−W1−O4	87.0(2)	N1−W1−P1	91.48(19)

for **30a**. In the complex (μ-H)$W_2(CO)_7(THF)_2(NO)$[146] the THF molecules *trans* to the nitrosyl ligand possess a W−O bond distance of 2.205(5) Å that is slightly shorter than in **30a**.

The reaction of **27a** with $[H(Et_2O)_2][B(C_6F_5)_4]$ produced the cationic complex $[Mo(dippp)(NO)(CO)_2(THF)][B(C_6F_5)_4]$ (**31a**). The NMR and IR spectra revealed **29a** and **31a** having been structurally related species. The ^{31}P $\{^1H\}$ NMR spectrum exhibited a singlet resonance at 16.5 ppm for dippp ligand. The ^{13}C $\{^1H\}$ NMR spectrum showed a doublet of doublets at 214.0 ppm ($^2J_{CP}$ = 22.1 Hz) attributed to the carbonyl ligands. The IR spectrum of **31a** displayed two ν(CO) strong bands at 2038, 1970 cm^{-1} and a ν(NO) band at 1668 cm^{-1}. However, the element analysis did not match the theoretical ratio presumably due to the fact that **31a** was not isolated in crystalline form. We supposed that the excess of THF in the substance, which could not removed even in vacuum, prevented **31a** from crystallization.

3.3 Synthesis of the Molybdenum Hydrides of the type Mo(P∩P)(CO)$_2$(NO)(H)

The influence of the phosphine ligands on the reactivity of the complexes was attempted to be approached by the preparation of the series of the molybdenum hydrides with different phosphine ligands (Scheme 3.1). The starting chlorides **25b**, **25c** and **25d** were prepared by the reaction of $Mo(CO)_4(NO)ClAlCl_3$ with the corresponding diphosphine ligands in THF at room temperature. Then the chlorides were treated with excess of $LiBH_4$ in Et_3N to afford the hydrides complexes **27b**, **27c** and **27d**. The NMR and IR spectra revealed the close structural relationship of **25b**, **25c**, **25d** with **25a** and **27b**, **27c, 27d** with **27a**. All the spectroscopic data are summarized in Table 3.7.

25d and **27b** were additionally characterized by X-ray diffraction analyses. ORTEP drawings of **25d** and **27b** are shown in Figures 3.4. Selected bond lengths and distances are presented in Tables 3.8 and 3.9. Similar to **25a** the structure of **25d** displayed pseudo-octahedral coordination geometries with two phosphine atoms and two carbonyls are in-plane together with the molybdenum center. The asymmetric unit of **25d** contains one half of the molecule, since the metal center lies on a crystallographic two-

fold axis. Consequently, the *trans* Cl and NO ligands are positionally disordered with the occupancy ratio 0.5. The Mo−P bond length amounts to 2.5319(7) Å, which is slightly shorter than the ones in **25a** complex presumably due to the smaller bite angle of dcyde ligand in comparison with the dippp derivative.[147] The similar tendency can be observed comparing bond lengths in the pair **27a** and **27b**. The mean Mo−P bond distance in **27b** equals to 2.513 Å, whereas Mo−P bond length in **27a** was found to be 2.546 Å.

Table 3.7 Selected Spectroscopic Data for **25b, 25c, 25d, 27b, 27c** and **27d**.

Compound	δ(M−*P*) [ppm]	δ(M−*H*) [ppm] (*J* [Hz])	δ(*C*O) ppm (*J* [Hz])	IR vibration frequency [cm^{-1}] ν(CO)		ν(MH)	ν(NO)
25b	61.1		217.1 (10.7)	2020	1949		1611
25c	29.8		2l6.5 (18.1)	2021	1950		1610
25d	53.5		2l7.4 (10.7)	2022	1948		1614
27b	84.5	-3.44 (26.4)	226.8 (10.7)	1983	1910	1653	1570
27c	48.3	-1.20 (23.6)	226.2 (11.0)	1981	1902	1637	1574
27d	53.5	-3.25 (26.3)	227.1 (10.7)	1986	1920	1647	1574

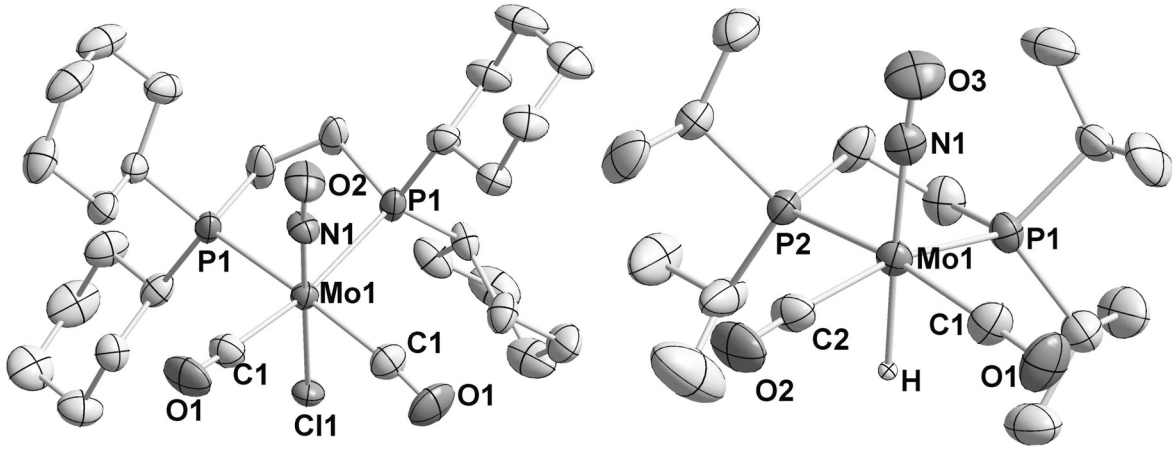

Figure 3.4 ORTEP drawings of Mo(dcype)(NO)(CO)$_2$(Cl) (**25d**) and Mo(dcype)(NO)(CO)$_2$(H) (**27b**). Displacement ellipsoids are drawn at the 50% probability level. Selected hydrogen atoms were omitted for clarity.

Table 3.8 Selected Bond Lengths [Å] and Bond Angles [°] of **25d**.

Bond lengths			
C1−O1	1.135(4)	P1−Mo1	2.5319(7)
C1−Mo1	2.044(3)	Cl1−Mo1	2.517(3)
N1−O2	1.195(6)	N1−Mo1	1.772(6)
Bond angles			
O1−C1−Mo1	171.9(3)	N1−Mo1−P1	94.71(18)
N1−Mo1−C1	83.89(19)	C1−Mo1−P1	95.89(9)
N1−Mo1−Cl1	179.38(16)	Cl1−Mo1−P1	85.76(7)
C1−Mo1−Cl1	96.46(11)		

Table 3.9 Selected Bond Lengths [Å] and Bond Angles [°] of **27b**.

Bond lengths			
C1−O1	1.148(4)	N1−O3	1.152(4)
C1−Mo1	2.007(3)	N1−Mo1	1.868(3)
C2−O2	1.136(4)	P1−Mo1	2.5054(8)
C2−Mo1	2.023(3)	P2−Mo1	2.5204(7)
Mo1−H	1.83(3)		
Bond angles			
O1−C1−Mo1	178.8(4)	C1−Mo1−C2	90.17(15)
O2−C2−Mo1	177.3(3)	N1−Mo1−P1	99.03(8)
O3−N1−Mo1	177.1(3)	C1−Mo1−P1	91.82(10)
N1−Mo1−C1	96.01(13)	C2−Mo1−P1	162.05(10)
N1−Mo1−C2	98.49(13)	N1−Mo1−P2	97.17(8)
C1−Mo1−P2	165.54(10)	C2−Mo1−P2	93.74(11)
P1−Mo1−P2	80.25(3)		

3.4 Imine hydrogenation

29a and **30a** were tested as catalysts in hydrogenation of PhCH=N(α-naphtyl) imine. The reaction was carried out at 10 atm of H_2 at 80 °C in C_6H_5Cl.[148] Hydrogenation catalysis was detectable in the case of using **29a** as a catalyst. However, the conversion of the reaction was found to amount to 5% only (Table 3.10). Kinetic pursuit demonstrated that the reaction proceeded well during the initial 30 min whereupon the catalyst was decomposed due to limited stability of the $[BAr^F_4]^-$ counterion.[149, 150] The $[B(C_6F_5)_4]^-$ counterion offers even lower tendency to coordinate and the possesses higher stability than corresponding $[BAr^F_4]^-$.[95]

Table 3.10 Catalytic Hydrogenation of PhCH=N(α-naphtyl).

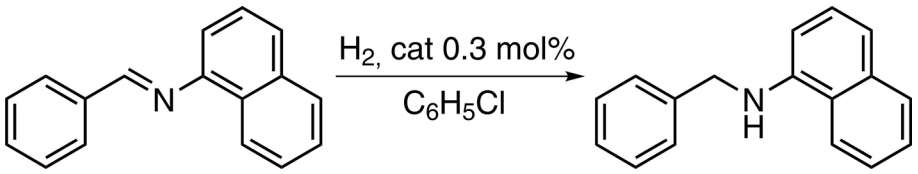

Entry	Catalyst	Pressure [bar]	Temperature [ºC]	Initial TOF [h^{-1}]	Conv.,%
1	**29a**	10	80	–	5
2	**27a**[a]	30	r.t.	106	>99
3	**31a**	30	r.t.	95	>99
4	**27b**[a]	30	r.t.	123	>99
5	**27c**[a]	30	r.t.	68	>99
6	**27d**[a]	30	r.t.	50	>99
7	**28a**[a]	30	r.t.	9	>99

[a] The mixture of a corresponding hydride and $[H(Et_2O)_2][B(C_6F_5)_4]$ was used as a catalyst.

Using of **31a** as a catalyst in the imine hydrogenation revealed 100% conversion and TOF value of 95 h^{-1} in the first hour at room temperature and at H_2 pressure of 30 bar (Table 3.10). An increase in temperature led to significantly lowered conversion presumably due to decomposition of the catalyst. It is worthwhile mentioning that no

hydrogenation was observed in a case of use of THF as a solvent. Moreover, experiments, in which THF was initially added to the reaction mixture in various amount, demonstrated dependence of the hydrogenation rate on the amount of the added solvent. We suppose that THF acts as a ligand and thereby blocks the catalytically crucial vacant site of the complex and consequently the catalytic turnovers. Hydrogenation without involving THF was realized by using of the pure hydride **27a** and $[H(Et_2O)_2][B(C_6F_5)_4]$ as a co-catalyst. Then solution of the substrate in C_6H_5Cl was added to this mixture and pressurized with 30 bar of H_2. This approach revealed a slightly higher hydrogenation rate (TOF = 105 h^{-1}) than when **31a** was applied as a catalyst. Tungsten complex **28a** also showed the catalytic performance in the hydrogenation of PhCH=N(α-naphtyl) (Table 3.10). Though the conversion of the reaction was comparable with the molybdenum catalyst, the hydrogenation rate was found to be considerably lower (TOF = 9 h^{-1}).

Table 3.11 Catalytic Hydrogenation of Imines with **27b** as a catalyst.

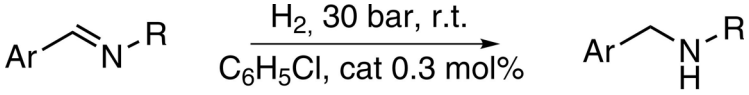

cat = **27b** + $[H(Et_2O)_2][B(C_6F_5)_4]$

Entry	Substrate	TOF, h^{-1}	Conversion,%
8	PhCH=N(α-naphtyl)	123	>99
9	PhCH=NPh	34	80
10	p-ClC_6H_4CH=NPh	74	96
11	p-ClC_6H_4CH=N-p-C_6H_4Cl	41	66
12	PhCH=NCH$(Ph)_2$	18	45
13	PhCH=NMes	84	>99
14	PhCH=N^{i}Bu	–	~0.3

Testing of the hydrides **27b**, **27c** and **27d** in PhCH=N(α-naphtyl) hydrogenations (Table 3.10) did not reveal a clear dependence of the activity on the bite angle of the phosphine ligands.[151] The lowest hydrogenation rate was founded for **27d** presumably due to steric bulk of the cyclohexyl substituent of the dcype ligand, which prevented the facile approach of PhCH=N(α-naphtyl) substrate to the metal center. **27c** bearing the

diphosphine with the largest bite angle[152] showed slightly higher activity (initial TOF 68 *vs.* 50 h^{-1}) in comparison with **27d**, which can be explained on the basis of the rigidity of the bridging ferrocene. Apparently the hydrogenations require the certain flexibility in the diphosphine backbone at some stage of the catalytic cycle. The hydrides **27a** and **27b** demonstrated significantly higher hydrogenation rate (initial TOF 106 h^{-1} for **27a**, 123 h^{-1} for **27b**). The hydride **27b** that showed the best catalytic performance was additionally tested in hydrogenations of the various imines. The results of these catalytic experiments are presented in Table 3.11.

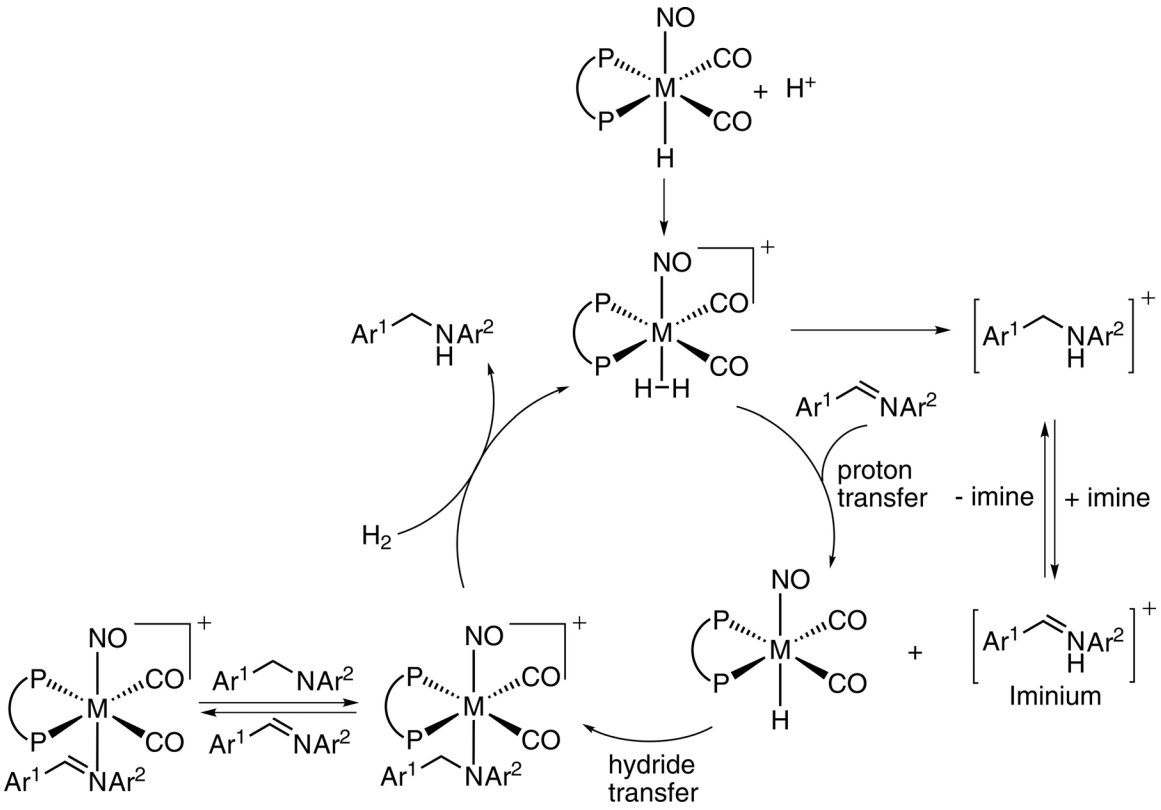

Scheme 3.2 A mechanism of imine hydrogenation.

A mechanism for the hydrogenation of imines with the Mo and W catalysts is presented in Scheme 2. The initial protonation of the hydride results in a short-lived dihydrogen complex,[35] which is the key species to drive the catalytic cycle. An iminium salt might then be formed by proton transfer from the acidic dihydrogen complex.[31, 134] Both the imine and amine product are expected to get involved in a protolysis equilibrium, requiring that the electrophilic iminium as a reactant is present in sufficient

concentration that a subsequent hydride transfer could become kinetically feasible. The deprotonation of the dihydrogen ligand comprises the heterolytic splitting step of H_2 and this presumably constitutes the rate limiting step. The highest hydrogenation rates were observed with more bulky substrates (entry 8 and 13, Table 3.11), which apparently facilitate the amine dissociation from the molybdenum center required for re-entry of H_2 into the cycle. Amine, imine and H_2 coordination have to be considered competitive.

Crucial to the course of the hydrogenation reaction is the formation of the iminium cation, which competes with the formation of ammonium salt produced from the protonation of the amine products. Tempelton *et al.* reported the influences of different substituents on the basicities of the imines and amines in tungsten complexes.[153] All imine/amine pairs with aryl substituents showed generally low basicities, but the imine was the stronger base. Conversely, the basicities of alkyl substituted imine/amine are generally higher with the amine more basic than the corresponding imine derivatives. Thus, we anticipated that the hydrogenation of aniline derivatives could be readily accomplished, since their imines are stronger bases than the amines and the iminium cation should therefore be available in kinetically relevant concentrations. In the case of alkylimine derivatives (entry 12 and 14, Table 3.11) we could not achieve satisfactory conversions probably due to the fact that the amine is the stronger base and would consume a great deal of the protons, thus blocking their involvement in the catalytic cycle. The alkyl amines would also be stronger ligands and could block the metal center, if not enough protons can be supplied to scavenge the amine as an ammonium salt. In the case of N alkyl substituted PhCH=NCHPh$_2$ the basicities of the amine and the imine are presumably in a comparable range, and the reaction was found to stop when a certain amount of amine is produced, which would be in accord with the given rationalization on the protolysis equilibrium.

The difference in pK_b of the pair PhCH=N*i*Bu/PhCH$_2$NH*i*Bu seems to be so high that only the amine is expected to be present in the protonated form. Indeed, the hydrogenation rate of this compound was zero. Presumably the low yield of the reaction of entry 11 with a chlorine containing substrate can be related to a blocking of the molybdenum center with chloride released during catalysis.[154]

3.5 Synthesis of molybdenum complexes bearing iPr$_3$P ligands

The reaction between Mo(CO)$_4$(NO)(Cl-AlCl$_3$) and two equivalents of P*i*Pr$_3$ at room temperature afforded Mo(P*i*Pr$_3$)$_2$(CO)$_2$(NO)Cl (25) in 61% yield (Scheme 3.3). The ^{31}P {^{1}H} NMR spectrum of **32** exhibited a singlet resonance at 48.5 ppm, which exhibited equivalent phosphorus atom arrangement. The ^{1}H {^{31}P} NMR spectrum of **32** showed a multiplet of -C*H* protons at 2.37 ppm and a doublet of methyl groups at 1.24 ppm ($^3J_{HH}$ = 64.1 MHz). In the ^{13}C {^{1}H} NMR spectrum a characteristic triplet was detected at 219.1 ppm ($^1J_{CP}$ = 9.0 Hz) attributed to the CO carbon atoms. As the signal of the carbonyl ligands appeared as a triplet, the structure of **32** was concluded to possess carbonyls ligands in *trans* position. The IR spectrum of **32** revealed strong ν(CO) bands at 1937 and 1867 cm^{-1}. A ν(NO) band was observed at 1616 cm^{-1}.

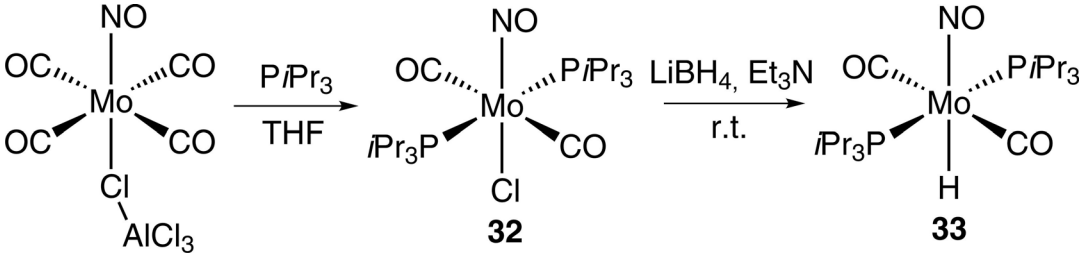

Scheme 3.3

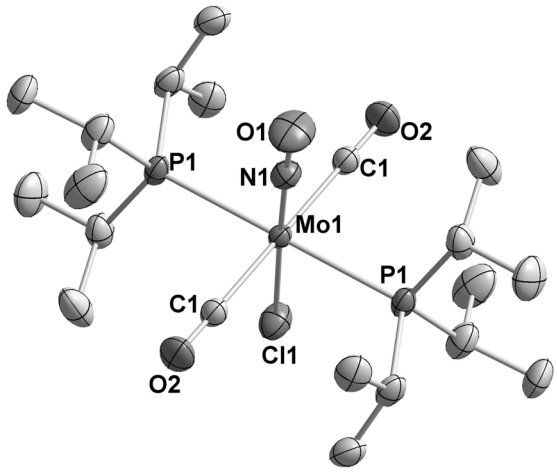

Figure 3.5 An ORTEP drawing of **32**. Displacement ellipsoids are drawn at the 50% probability level. The disorder between the *trans* Cl and NO ligands and all hydrogen atoms have been omitted for clarity.

A X-ray structure analysis was carried to establish the structure of **32** (Figure 3.5, Table 3.12). **32** crystallized in centrosymmetric space group P-1. The molybdenum atoms lie on centers of symmetry, which allowed to refine only one half of the molecule. As commonly observed, the *trans* nitrosyl and chloride groups are positionally disordered. The structure displays a distorted octahedron. Two phosphine and two carbonyl ligands are located *trans*. The metal-phosphorus bond length equals to 2.5628(4) Å. For comparison, in Mo(1,4-Ph_2N_4)(CO)$_2$(PPh_3)$_2$ and Mo(1,4-Ph_2N_4)(CO)$_2$(PEt_3)$_2$,[155] the complexes with *trans* phosphine ligands, molybdenum-bond distances are 2.494 (4) and 2.478 (2) Å that is significantly shorter than in **32**.

Table 3.12 Selected Bond Lengths [Å] and Bond Angles [°] of **32**.

Bond lengths			
N1−O1	1.262(5)	C1−O2	1.133(2)
N1−Mo1	1.799(4)	C1−Mo1	2.0624(16)
Cl1−Mo1	2.4844(17)	Mo1−P1	2.5628(4)
Bond angles			
N1−Mo1−C1	90.64(11)	C1−Mo1−P1	91.85(4)
C1−Mo1−Cl1	90.40(6)	Cl1−Mo1−P1	89.30(3)
N1−Mo1−P1	90.33(10)	O2−C1−Mo1	179.47(16)

There are only a few molybdenum or tungsten complexes,[156-158] in which two phosphine ligands are coordinated opposite to each other, rather than taking sites in *trans* position to electron accepting ligands (carbonyl, for example). Most likely, such arrangements are based on the steric demand of two bulky phosphines. This bulkiness of ligands might lead to their lability in the coordination sphere with the consequence of facile substitution. The reaction between **32** and PMe_3 occurs at room temperature leading to Mo(CO)(PMe_3)$_3$(NO)Cl[54] (Scheme 3.4). This can be considered as an example showing the reactivity of **32**.

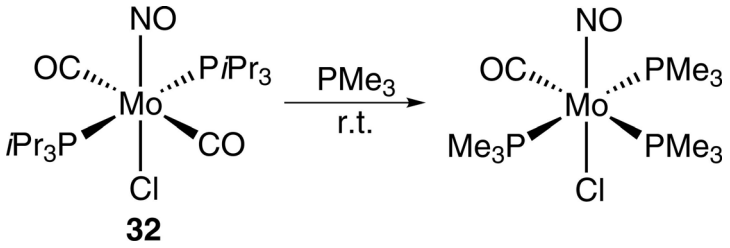

32

Scheme 3.4

The complex Mo(CO)(PMe$_3$)$_3$(NO)Cl was obtained via substitution of CO in Mo(CO)$_4$(NO)(Cl-AlCl$_3$) at 80 °C within two days. The reaction of **32** with PMe$_3$ was found (^{31}P {^{1}H} NMR monitoring) to be completed within minutes at room temperature with 100% conversion that demonstrated the lability of the phosphine ligands in **32**.

To prepare the hydride **33**, the chloride **32** was treated with LiBH$_4$ using Et$_3$N as a solvent. **33** was isolated as a yellow powder in 63% yield (Scheme 3.3). The ^{31}P {^{1}H} NMR spectrum of **33** revealed a singlet at 66.9 ppm indicating a similar structure as in the starting complex **32**. In the ^{1}H NMR spectrum a characteristic triplet for the hydride ligand was observed at -2.81 ppm ($^2J_{PH}$ = 24.1 Hz). A triplet at 228.9 ppm ($^2J_{CP}$ = 9.5 Hz) was observed for the carbonyl groups in the ^{13}C {^{1}H} NMR spectrum. The IR spectrum of **33** showed strong ν(CO) bands at 1905 and 1864 cm^{-1} and a ν(NO) band at 1570 cm^{-1}. A band for the ν(MoH) vibration was detected at 1637 cm^{-1}.

A X-ray structure analysis revealed the complex's structure to be similar to the structure of the initial chloride **32** (Figure 3.6, Table 3.13). **33** crystallized in the space group Pbca and displays pseudo-octahedral coordination geometry. Two phosphine and two carbonyl ligands are located in *trans* position. The hydride ligand was located *trans* to the nitrosyl group. The mean phosphorus-metal bond equals to 2.5164(4) Å, that is 0.05 Å shorter than in the initial chloride presumably due to a smaller size of the hydride ligand in comparison with the chloride. It is also worthwhile to mention that the phosphine and carbonyl ligands are bending towards the hydride ligand for the reason of the small size of this atom. For example, N1−Mo1−P1 angle is 95.92(4)° and N1−Mo1−C20 is 100.20(7)°.

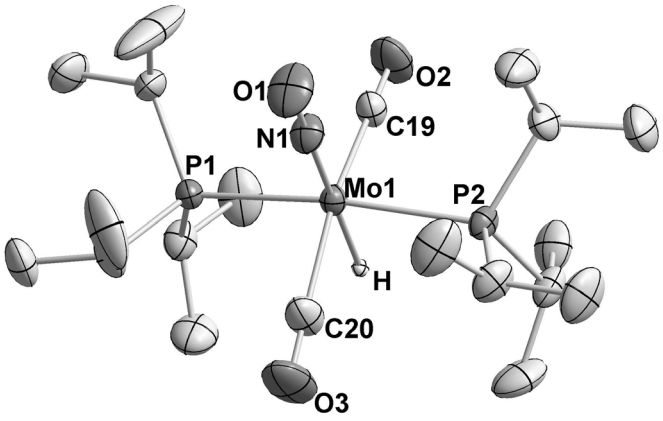

Figure 3.6 An ORTEP drawing of **33**. Displacement ellipsoids are drawn at the 50% probability level. The selected hydrogen atoms have been omitted for clarity.

Table 3.13 Selected Bond Lengths [Å] and Bond Angles [°] of **33**.

Bond lengths			
N1−O1	1.2014(16)	C20−Mo1	2.0335(19)
N1−Mo1	1.8238(13)	C19−Mo1	2.0287(16)
P1−Mo1	2.5187(4)	C19−O2	1.1335(19)
P2−Mo1	2.5141(4)	C20−O3	1.131(2)
Bond angles			
O1−N1−Mo1	179.44(14)	C19−Mo1−C20	160.82(7)
O2−C19−Mo1	177.04(15)	N1−Mo1−P2	94.27(4)
O3−C20−Mo1	176.8(2)	N1−Mo1−P1	95.92(4)
N1−Mo1−C19	98.98(6)	P2−Mo1−P1	169.809(13)
N1−Mo1−C20	100.20(7)	N1−Mo1−H	179.4(6)

The hydride complex **33** reacted with the $[H(Et_2O)_2][BAr^F{}_4]$ acid in THF forming an ionic six-coordinated complex **34** with THF molecule attached *trans* to the nitrosyl ligand (Scheme 3.5).The complex was isolated as a yellow powder in 82% yield. The $^{31}P\{^1H\}$ NMR spectrum of **34** exhibited a singlet resonance at 51.1 ppm. Beside signals attributed to the phosphine ligands, the ^1H NMR spectrum revealed characteristic multiplets of THF coordinated to metal center at 3.62 and 1.78 ppm, which differ in chemical shifts from free THF. In $^{13}C\{^1H\}$ NMR a triplet for the CO groups was

observed at 218.8 ppm ($^1J_{CP}$ = 8.8 Hz). The IR spectrum of **34** showed two strong bands at 1953 cm^{-1} (ν(CO)) and at 1679 cm^{-1} (ν(NO)).

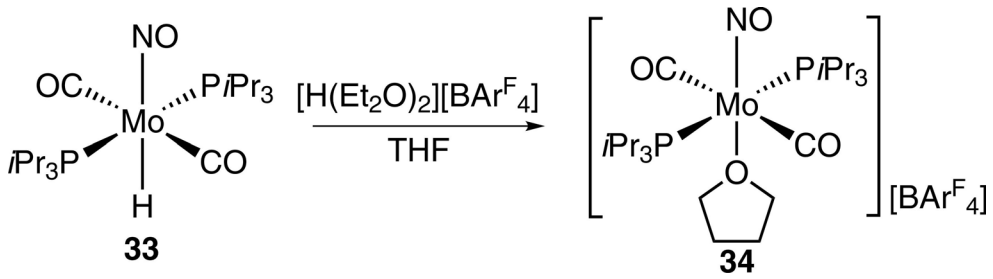

Scheme 3.5

A X-ray studies confirmed the structure of **34** (Figure 3.7, Table 3.14). **34** crystallized in the space group C 2/c. The molybdenum and the boron centers are located on special positions (two-fold axes), which allowed refinement of only half of each species. **27** retained grossly the coordination geometry of **26**: two phosphine and two carbonyls are located *trans*. The THF ligand was observed to be coordinated *trans* to the nitrosyl group. The metal-phosphorus bond distances are found to equal to 2.6005(6) that is significantly (0.1 Å) longer than in the starting hydride complex. O3−Mo1 bond distance is 2.264(3) Å that is approximately equal to the bond in **29a**.

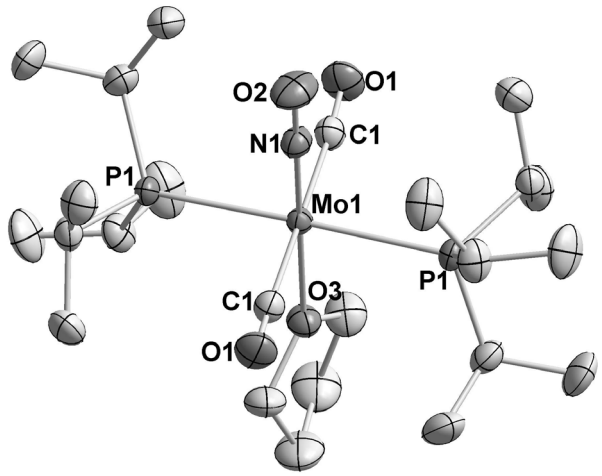

Figure 3.7 An ORTEP drawings of **34**. Displacement ellipsoids are drawn at the 50% probability level. All hydrogen atoms and [BAr$^F{}_4$]$^-$ counter-ion have been omitted for clarity.

Table 3.14 Selected Bond Lengths [Å] and Bond Angles [°] of **34**.

Bond lengths			
N1−O2	1.178(4)	C1−Mo1	2.061(3)
N1−Mo1	1.790(3)	C1−O1	1.135(4)
P1−Mo1	2.6005(6)	O3−Mo1	2.264(3)
Bond angles			
O2−N1−Mo1	180.000(1)	C1−Mo1−O3	90.70(8)
N1−Mo1−C1	89.30(8)	N1−Mo1−P1	90.934(16)
N1−Mo1−O3	180.000(1)	O3−Mo1−P1	89.066(16)
C1−Mo1−P1	85.60(8)	O1−C1−Mo1	175.1(3)

Complex **34**, as well as the hydride **33** were tested in hydrogenation of imines in combination with $[H(Et_2O)_2][B(C_6F_5)_4]$. Although **33** is a complex electronically and structurally related to hydrides **27**, no catalytic activity was observed. We suppose the reason for that is the overall instability of the complexes. The monodentate *i*Pr$_3$P phosphine which presumably binds significantly weaker to the molybdenum center than any diphosphine ligand could undergo dissociation that could lead to decomposition of the complex.

3.6 Conclusion

A series of the hydride complexes of the type M(P∩P)(CO)$_2$(NO)H (M =Mo, W) bearing bulky diphosphine ligands were prepared via the reaction of M(P∩P)(CO)$_2$(NO)Cl with $LiBH_4$ in Et_3N at room temperature. In combination with $[H(Et_2O)_2][B(C_6F_5)_4]$ the hydrides showed valuable catalytic performance towards the hydrogenation of imine PhCH=N(α-naphtyl). The widely used $[BAr^F{}_4]^-$ counterion apparently possesses too high coordinating ability. On the contrary $[B(C_6F_5)_4]^-$ anion leave 16e molybdenum or tungsten center and allow the exchange of weak ligands. The complex Mo(dippe)(CO)$_2$(NO)H (**27b**) displayed the best activity with an initial TOF of 123 h^{-1}. This hydride was also tested as a catalyst to hydrogenate various other imines. The hydrogenation rate depended mainly on the size of nitrogen substituent. The

analogous complex bearing two monodentate *i*Pr$_3$P phosphine ligands revealed no catalytic activity presumably due to low stability.

All observations were explained on the basis of an "ionic hydrogenation" pathway occurring with heterolytic cleavage of H_2 and "proton before hydride" transfer.

4 Complexes with chiral diphosphine ligands

4.1 Introduction

Selective chiral catalytic hydrogenation plays a major role in organic synthesis, in particular with respect to pharmaceutical applications as it allows to obtain high enantioselectivities. Among others the pioneering work was carried out by Dang and Kagan.[159-161] In 1971 they reported a synthesis of a C_2 chiral diphosphine ligand which was tested in several asymmetric reductions giving optical yields of up to 72%. Subsequent investigations revealed that optically stable bidentate phosphine ligands exhibit C_2 chirality in their carbon frameworks. They appeared to be among the most successful ligands employed in a variety of transition metal-catalyzed enantioselective hydrogenations. Thus, Dahlenburg *et al.* developed a route to the synthesis of chiral bidentate C_2-symmetric phosphorus ligands (1S,1S)-$C_5H_8(PR_2)_2$ (R = aryl, alkyl), [162-165] which were used in the preparation of a series of Rh and Pt complexes. The catalysts showed remarkable results in enantioselective hydrogenation of α-acetamidocinnamic acid.[166-169] According to Halpern *et al.* the catalytic cycle of this hydrogenation involves the formation of the intermediate hydride complex.[170-173] However, detailed mechanistic studies of how the hydride is transferred to unsaturated compounds was not yet discovered.

In our group the investigations of the reactivity of a chiral molybdenum hydride Mo[(S,S)-dmpcp]$_2$(NO)H ((*S*,*S*)-dmpcp = (1S,1S)-$C_5H_8(PMe_2)_2$) with the pro-chiral $PhC(O)CH_3$ ketone were carried out.[174] The nitrosyl group that is located *trans* to the hydride ligand causes the increasing of the Mo−H bond ionicity and facilitates the hydride transfer. In this chapter we discuss some experiments which were carried out to supplement the previously delivered results, as well as some attempts to improve the system, namely the preparation of Mo[(S,S)-dippcp)]$_2$(NO)H ((*S*,*S*)-dippcp = (1S,1S)-$C_5H_8(P\textit{i}Pr_2)_2$).

4.2 Synthesis of Mo[(S,S)-dmpcp]$_2$(NO)(OPh) (35)

The starting hydride Mo[(S,S)-dmpcp]$_2$(NO)(H) was prepared according to the method reported earlier.[174] The interaction between Mo[(S,S)-dmpcp]$_2$(NO)(H) and PhOH at room temperature resulted in the complex Mo[(S,S)-dmpcp]$_2$(NO)(OPh) (**35**) that was isolated in 78% yield (Scheme 4.1). The reaction was carried out in toluene and according to the ^{31}P {^{1}H} spectra was completed within minutes. The ^{31}P {^{1}H} NMR spectra of **35** revealed two triplets at 13.0 and 10.1 ppm ($^2J_{PP}$ = 21.6 Hz) that pointed to the fact that phosphorus framework of the molybdenum center was not changed during the reaction. Besides the signals of (*S*,*S*)-dmpcp ligand the ^{1}H NMR spectrum of **35** exhibited two triplets at 7.28 ($^3J_{HH}$ = 7.5 Hz), 6.68 ($^3J_{HH}$ = 7.0 Hz) and a doublet at 6.45 ($^3J_{HH}$ = 8.0 Hz) attributed to phenyl proton resonances. The IR spectrum of **35** showed a strong ν(NO) band at 1519 cm^{-1}.

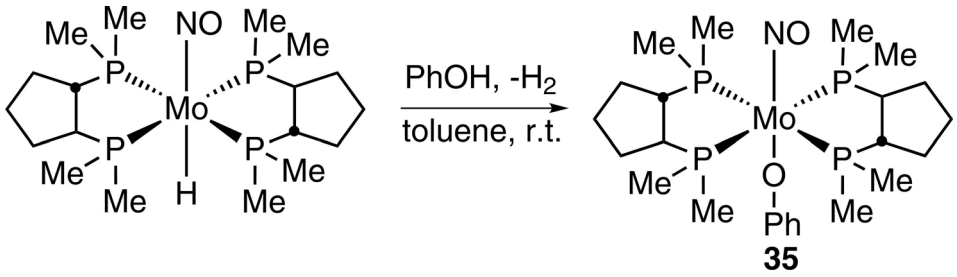

Scheme 4.1

A X-ray diffraction study fully confirmed the structure of complex **35**. An ORTEP drawing of **35** is presented in Figure 4.1. The selected bond lengths and angles are summarized in Table 4.1. **35** crystallized in P 2_1 2_1 2_1 space group. There are three independent molecules in one the asymmetric unit. Compound **35** adopts a pseudo-octahedral coordination geometry. Four phosphorus atoms are in-plane with the metal center, whereby the NO ligand is located *trans* to the PhO-moiety. The mean Mo−P bond distance is 2.463(1) Å that approximately equals to the Mo−P bond length in the starting hydride complex (2.442(1) Å). The X-ray diffraction study also unambiguously revealed the *S,S* chiral configuration of the diphosphine ligands around the metal center.

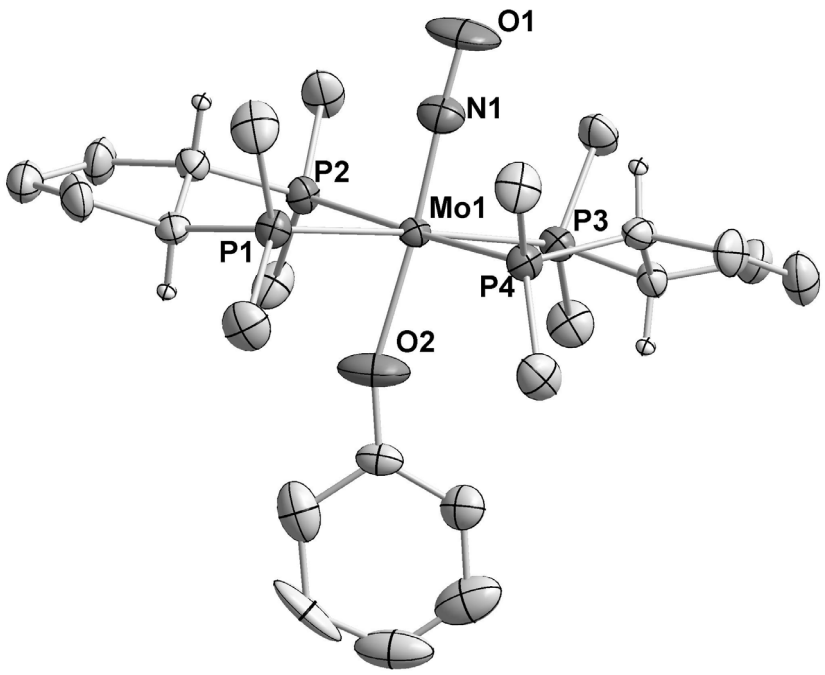

Figure 4.1 An ORTEP drawing of **35**. Displacement ellipsoids are drawn at the 50% probability level. The selected hydrogen atoms have been omitted for clarity.

Table 4.1 Selected Bond Lengths [Å] and Bond Angles [°] of **34**.

Bond lengths			
Mo1−N1	1.762(4)	Mo1−P2	2.4626(14)
Mo1−O2	2.090(4)	Mo1−P3	2.4751(14)
Mo1−P4	2.4549(14)	N1−O1	1.223(5)
Mo1−P1	2.4610(14)		
Bond angles			
N1−Mo1−O2	176.0(2)	O2−Mo1−P1	81.95(13)
N1−Mo1−P4	85.51(15)	P4−Mo1−P1	97.04(5)
O2−Mo1−P4	96.65(13)	N1−Mo1−P2	92.16(15)
N1−Mo1−P1	94.52(15)	O2−Mo1−P2	85.60(14)
P4−Mo1−P2	177.27(5)	N1−Mo1−P3	88.18(15)
P1−Mo1−P2	81.71(5)	O2−Mo1−P3	95.39(14)
P4−Mo1−P3	82.21(5)	P2−Mo1−P3	99.15(5)
P1−Mo1−P3	177.14(5)	O1−N1−Mo1	176.9(5)

4.3 Insertion reaction of Mo[(S,S)-dmpcp]$_2$(NO)(H) with acetophenone

The insertion reaction of Mo[(S,S)-dmpcp]$_2$(NO)(H) and the prochiral acetophenone occurs within minutes at room temperature in toluene.[174] Due to chirality of the starting hydride the product of the reaction, the alcoholate complex Mo[(S,S)-dmpcp]$_2$(NO)(MeO(H)Ph) exists in two diastereomers, which are distinguishable in the ^{1}H NMR spectra. The characteristic quartets of –PhC(*H*)O– protons appeared at 4.62 ppm for S isomer and at 4.57 ppm for R isomer. The integration furnished a ratio of the diastereomers of 1:1 for the reaction carried out at room temperature. Therefore the reaction was repeated under "kinetic control" that was experimentally found to be a temperature of -60 °C (Scheme 4.2). Below this temperature the reaction rate is close to zero. In this case the ratio of two diastereomers was calculated to amount 3:2 with predominance of the S isomer (Figure 4.2) This ratio correspondes to a de of 20% and the same ee value for the alcoholate.

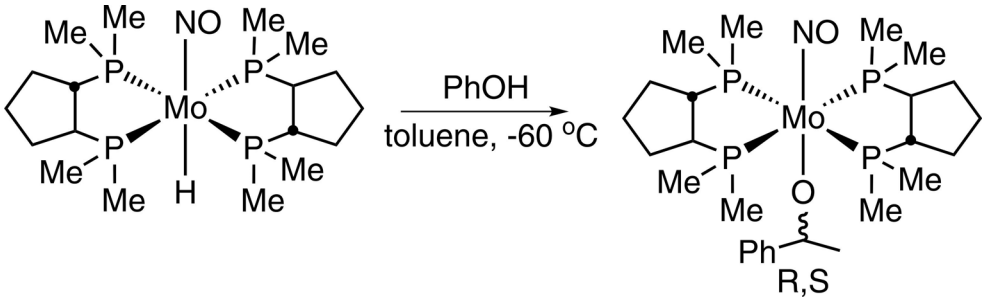

Scheme 4.2

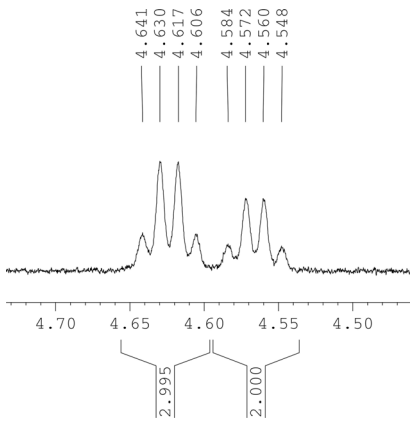

Figure 4.2 The ^{1}H NMR spectrum of **36**. The integration showes the ratio between two diasteriomers.

When the hydride Mo[(S,S)-dmpcp]$_2$(NO)(H), acetophenone and phenol were mixed at -60 °C (ionic hydrogenation conditions), the reaction was completed after several hours (following the ^{31}P {^1H} NMR spectra). The phenolate complex **35** and PhC(OH)CH$_3$ were formed in the reaction (Scheme 4.3). To determine the ee value of the formed phenylethanol all volatiles were distilled in vacuum and collected in a cooled receiver. Gas chromatography revealed an enantiomeric excess of 27% with predominance of the S isomer. The retention time was 6.227 min for S-phenylethanol and 6.355 min for R-phenylethanol.

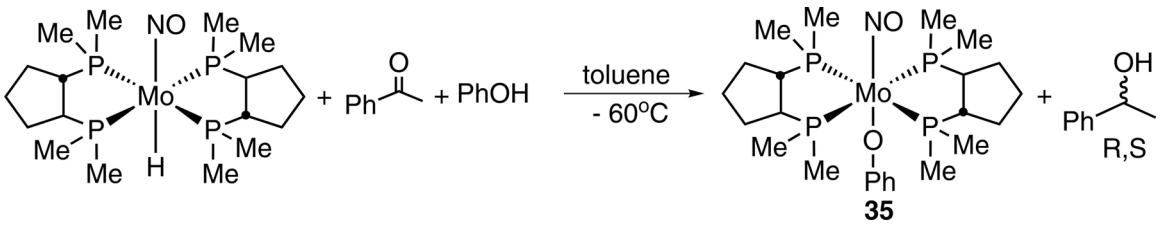

Scheme 4.3

Comparing the ee of the insertion reaction and the ee of the ionic hydrogenation reaction we see a slight increase in the ee, which might be interpreted in terms of a tighter packing in the relevant transition states of hydride transfers (Scheme 4.4). The hydrogen bound phenol leads to a withdrawal of electron density making the $C_{acetophenone}$ more electrophilic. Subsequently, the hydride gets closer the $C_{acetophenone}$ atom causing higher diastereomeric distinction.

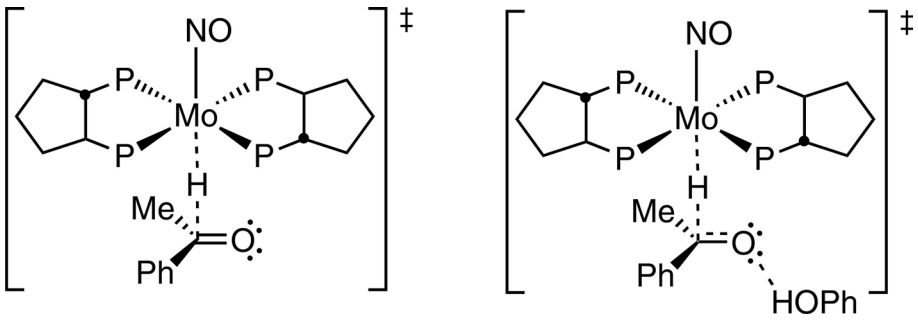

Scheme 4.4

4.4 Preparation of the (S,S)-dippcp) ligand

The dippcp ligand was prepared via interaction of (S,S)-$C_5H_8(PCl)_2$[164] with *i*PrMgCl by the procedure described in literature.[175] The product was isolated with 63% yield as a colorless liquid. The purity of the substance was controlled by NMR. The ^{31}P $\{^1H\}$ NMR spectra of the ligand revealed a singlet resonance at 12.4 ppm. The ^1H NMR spectra of the ((S,S)-dippcp) showed two multiplets at 1.84 and 1.60 ppm attributed to –C*H* protons of the isopropyl groups. A characteristic multiplet for protons of the bridging −C*H* groups were observed at 1.77 ppm.

4.5 Preparation and Reactivity of Mo[(S,S)-dippcp)]$_2$(NO)(Cl) (36) and Mo[(S,S)-dippcp)]$_2$(NO)(H) (37)

Complex Mo[(S,S)-dippcp)]$_2$(NO)(Cl) (**36**) was prepared in analogy to the procedure that was described before for chlorides **3** and **4** (Scheme 4.5). **36** was isolated as a yellow powder with an yield of 63%. It is interesting to note that ^{31}P $\{^1H\}$ NMR spectrum of **36** showed only a singlet resonance at 28.1 ppm although the ^{31}P $\{^1H\}$ spectrum of the structurally similar chloride complex Mo[(S,S)-dmpcp]$_2$(NO)(Cl) displayed two triplets.

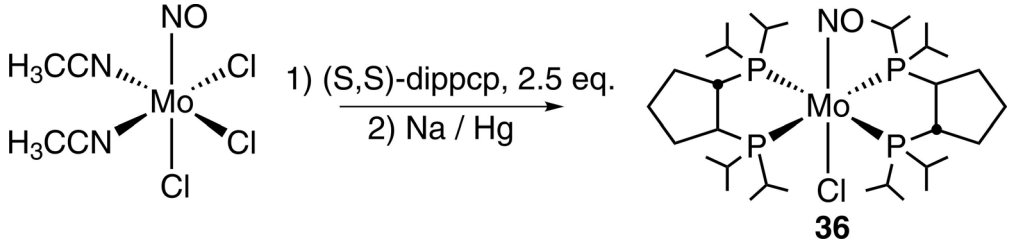

36

Scheme 4.5

Presumably, due to the larger steric congestion of the two (*S*,*S*)-dippcp ligands around the metal center, they undergo rapid change in their distorted ground state arrangement that resulted in the unique signal in the ^{31}P $\{^1H\}$ spectra. The variable temperature NMR investigation proved this idea. At -60 °C the phosphorus NMR singlet splitted into two multiplets and at -80 °C two triplets at 27.0 and 26.1 ppm ($^2J_{PP}$ = 14.0

Hz) became clearly distinguishable (Figure 4.3). The ^{1}H NMR spectrum of **36** exhibited a set multiplets attributed to the proton of the (*S*,*S*)-dippcp in the region from 2.90 to 1.20 ppm. The IR spectrum of **36** displayed a strong ν(NO) band at 1515 cm^{-1}. **36** could not be characterized by a X-ray diffraction analysis due to difficulty in preparing a suitable single crystal. However, comparing the spectroscopic data of **36** with those of previously obtained complexes **4** and of Mo[(S,S)-dmpcp]$_2$(NO)(Cl), it can be concluded that complex **36** indeed has a *trans* diphosphine structure as it is shown in Scheme 4.5.

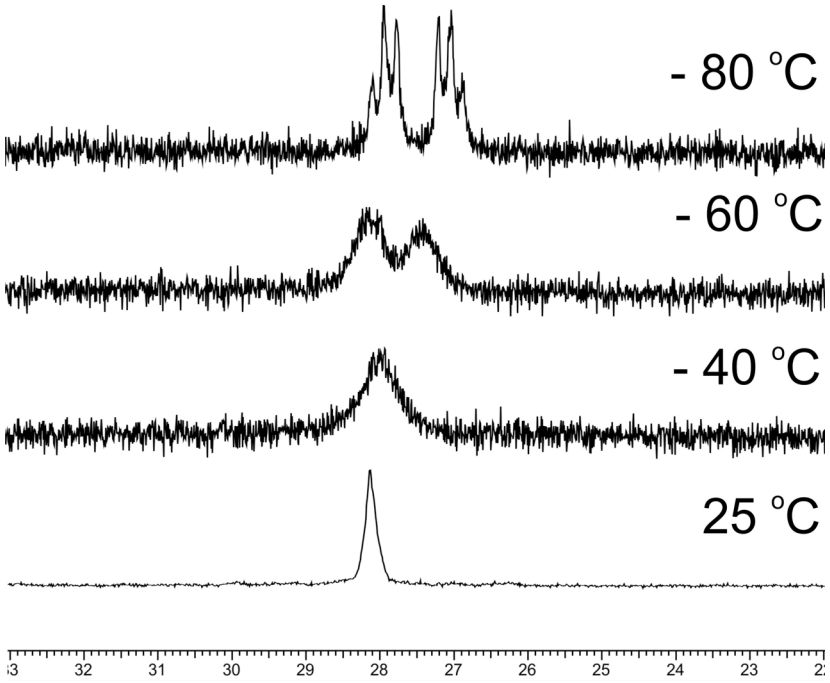

Figure 4.3 The ^{31}P {^{1}H} NMR spectra of **36** at different temperatures.

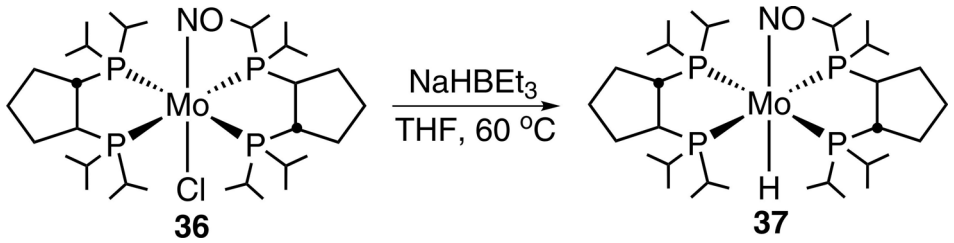

Scheme 4.6

A few hydride sources, such as $LiBH_4$, $LiAlH_4$, KH, $LiHAl(OtBu)_3$, were tried to prepare the hydride Mo[(S,S)-dippcp)]$_2$(NO)(H) (**37**). The only reagent that produced the desired product was found to be $NaHBEt_3$ (Scheme 4.6). The use of other reagents resulted in the decomposition of the starting material. In the ^{31}P $\{^1H\}$ NMR spectrum a singlet for the ((*S*,*S*)-dippcp free ligand was observed. Despite several attempts to find a suitable solvent for crystallization, the hydride **37** could not be isolated in a pure form. After the reaction between **36** and $NaHBEt_3$ an oily substance was isolated consisting of ~ 60% of hydride **37** and was contaminated with the (*S*,*S*)-dippcp compound and $NaHBEt_3$ (according to NMR spectroscopy). Further purification appears not to be possible, since the contaminations prevent the crystallization of the complex. The ^{31}P $\{^1H\}$ NMR spectrum revealed two triplets at 55.5 and 54.7 ppm ($^2J_{PP}$ = 14.9 Hz). It is worthwhile to mention that compound **37**, similar to Mo[(S,S)-dmpcp]$_2$(NO)(H), displays set of triplets at room temperature. Presumably, the less sterically demanding hydride ligand allows more compact packing of two bulky phosphines that results in Mo−P bond lengths shorter than in **36**. Shorter bonds are stronger and can not so easily be equilibrated by temperature as it was observed for **36**. The ^1H NMR spectrum exhibited a characteristic multiplet resonance for hydride ligand at -1.27 ppm.

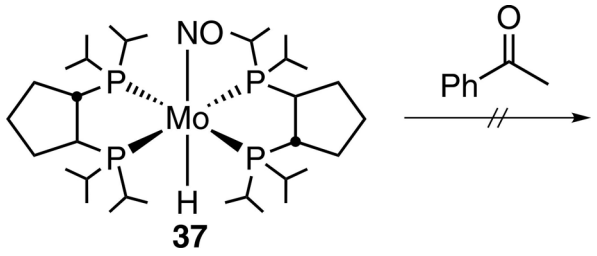

Scheme 4.7

Even though **37** was not isolated in pure form, it was still possible to investigate in NMR experiments its reactivity towards the pro-chiral ketone acetophenone. The ^{31}P $\{^1H\}$ revealed that no such reaction between **37** and $PhC(O)CH_3$ occured as it was observed for hydride **7** and **8** (Scheme 4.7). In all probability the bulky isopropyl groups shield the small hydride ligand from direct ketone approach.

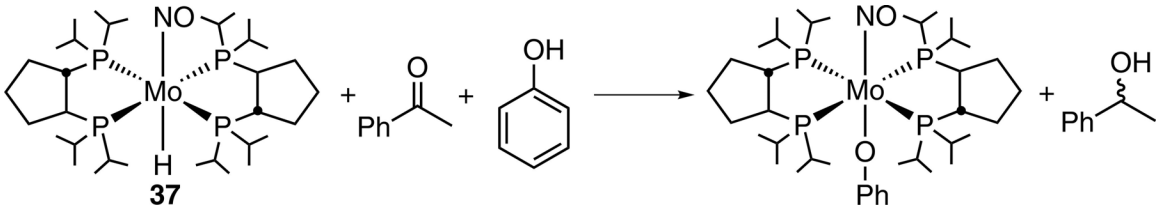

Scheme 4.8

The reaction between the hydride **37** and mixture of acetophenone and phenol[176] was carried out at -60 °C using toluene as a solvent (Scheme 4.8). According to $^{31}P\ \{^1H\}$ NMR spectroscopy the reaction was completed within some hours. Gas chromatography revealed an ee value for the alcohol to equal to 4%. The value is certainly lowered by the interaction of acetophenone with the contaminating $NaHBEt_3$, which led to an achiral reaction. Nevertheless, there was chiral induction and presumably even lower than the related reaction of $Mo[(S,S)\text{-}dmpcp]_2(NO)(H)$ due to a looser packing in the transition state.

4.6 Conclusion

Complex $Mo[(S,S)\text{-}dmpcp]_2(NO)(OPh)$ (**35**) was obtained via the reaction between $Mo[(S,S)\text{-}dmpcp]_2(NO)(H)$ and PhOH. The compound was isolated in 78% yield and fully characterized. The insertion reaction of $Mo[(S,S)\text{-}dmpcp]_2(NO)(H)$ with the prochiral acetophenone at -60°C showed diastereomeric selectivity towards S isomer. The two diastereomers were detected in ratio of 3:2. The insertion reaction of acetophenone in the presence of an acid resulted also in predominance of the S isomer of acetophenone. The ee value was calculated to be 27%.

The chloride complex $Mo[(S,S)\text{-}dippcp)]_2(NO)(Cl)$ (**36**) was prepared in a similar way as for **3** and **4**. The $^{31}P\ \{^1H\}$ NMR spectroscopy revealed that complex **36** undergoes a rapid conformational changes in solution at room temperature. Hydride **37** was obtained from the reaction between **36** and $NaHBEt_3$, but was not isolated in pure form due to presence of admixtures that prohibited the hydride crystallization. Hydride **37** was found not to react with $PhC(O)CH_3$, but reacted with acetophenone in the presence of phenol,

which is line with the observations that ionic hydrogenation are faster than the insertion reactions into metal-hydride bonds, upon which the ionic hydrogenations are based.

5 Summary

Two chloride complexes $M(dippe)_2(NO)Cl$ (M = W (**3**), Mo (**4**)) were synthesized via the reaction of $M(NO)(CH_3CN)_2(Cl)_3$ (M = W or Mo) with 2.5 eq. of the dippe ligand (dippe = 1,2-bis(diisopropylphosphanyl)ethane) followed by the reduction with 1% sodium amalgam. The related hydride complexes of the type $M(dippe)_2(NO)H$ (M = W (**7**), Mo (**8**),) were prepared via the reaction of **3** and **4** with $LiBH_4$. The nitrosyl group of tungsten complexes **3** and **7** were shown to be capable to coordinate $LiBH_4$ molecule forming stable adducts $W(dippe)_2(Cl)(NO\cdots LiBH_4)$ (**5**) and $W(dippe)_2(H)(NO\cdots LiBH_4)$ (**6**). The addition of ethylenediamine to a toluene solution of **6** led to rupture of the adduct **6** and afforded **7** in a good yield. Hydrides **7** and **8** were found not to react with simple ketones presumably due to two sterically hindered dippe ligands. The interaction between the hydrides and CO_2 resulted in the formation of the formate complexes $M(dippe)_2(NO)[OC(H)=O]$ (M = W (**9**), M = Mo (**10**)).

The reaction between **7** and $[H(Et_2O)][BF_4]$ produced the stable seven coordinated cationic dihydride $[W(dippe)(H)_2(dippe)(NO)][BF_4]$ (**12**). The reaction between **8** and $[H(Et_2O)][BF_4]$ leads to the formation of $[Mo(dippe)_2(NO)(FBF_3)]$ (**14)** in which BF_4^- was found to be coordinated to the metal centre. The $[H(Et_2O)_2][BAr^F{}_4]$ (Ar^F = 3,5-$(CF_3)_2C_6H_3$) acid interacts with **7** to generate a seven coordinated complex $[W(dippe)(H)_2(dippe)(NO)][BAr^F{}_4]$ (**11**) similar to **12**. In the reaction between **8** and $[H(Et_2O)_2][BAr^F{}_4]$, the $16e^-$ five coordinated complex $[Mo(dippe)_2(NO)][BAr^F{}_4]$ (**13**) was formed. A X-ray diffraction study revealed that **13** has a weak agostic interaction *trans* to the NO ligand. **13** was found to rapidly react with hydrogen gas at ambient condition forming the dihydride complex $[Mo(dippe)(H)_2(dippe)(NO)][BAr^F{}_4]$ (**13a**), which is unstable in the absence of H_2. The interaction between **13** and H_2 was found to be an equilibrium with K = 2.6 bar^{-1} at 25 °C. Complex **13** was tested in hydrogenation of acetone revealing a maximum TON of 7.

The complex $W(dppe)_2(NO)Cl$ (**15**) (dppe = 1,2-bis(diphenylphosphino)ethane) was prepared in a similar way to complex **4**. **15** could not be transformed to the corresponding hydride presumably due to weaker σ donation of the dppe ligands compared to the dippe that makes Mo−Cl bond stronger. $AlCl_3$ was used to activate the

Cl ligand. However, $AlCl_3$ was found not to interact with the chloride and the complex $W(dppe)_2(NO\cdots AlCl_3)Cl$ (**16**) was isolated after the reaction of **15** with $AlCl_3$ in CH_2Cl_2.

Hydride complex $Mo(depe)_2(NO)(H)$ (**18**) (depe = 1,2-bis(diethylphosphino)-ethane) were prepared in analogy to **8** isolating $Mo(depe)_2(NO)Cl$ as an precursor chloride. **18** reacts with $[H(Et_2O)_2][BAr^F{}_4]$ forming complex $[BAr^F{}_4]_2[Mo(NO)(depe)_2]_2(N_2)$ (**19**), which supposedly contains a N_2 ligand bridging to molybdenum centers *trans* to nitrosyl. The N_2 appears to be relatively strongly bound to the metal and could not be removed in vacuum under heating.

The attempt to avoid the hydride formation step and establish a direct route to the "vacant site" from chloride precursor was carried out. The interaction between **4** and $AgBF_4$ did not lead to the desired compound and resulted in the ionic complex $[(NO)(dippe)Mo(\mu\text{-}Cl)_3Mo(dippe)(NO)][BF_4]$ **20**, in which two molybdenum centers are bound with three (μ-Cl) ligands. The X-ray diffraction study revealed the interaction between molybdenum centers in the dinuclear complex.

The mixed-ligand Mo(dcype)(dippe)(NO)(Cl) (**20**) (dcype = 1,2-bis-(dicyclohexylphosphino)ethane) was obtained by reduction of $Mo(NO)(dcype)(Cl)_3$ (**21**) with 1% sodium amalgam. The corresponding hydride complex Mo(dcype)(dippe)(NO)(H) (**23**) was prepared using $NaHBEt_3$ as a hydride source. The formally $16e^-$ complex $[Mo(dcype)(dippe)(NO)][BAr^F{}_4]$ (**24**) was formed via interaction of **23** with $[H(Et_2O)_2][BAr^F{}_4]$. **24** was shown to bear an agostic interaction formed by cyclohexyl substituent. Analogously to **13** complex **24** is capable to activate H_2 molecule at room temperature. The interaction of **24** with H_2 gas resulted in the equilibrium mixture of three compounds: the initial complex **24** and two dihydride species **24a** and **24b** structurally similar to **13a**.

The reaction between $M(CO)_4(NO)(ClAlCl_3)$ (M = Mo, W) and sterically hindered diphosphines 1,3-bis(diisopropylphosphanyl)propane (dippp, **a**), 1,2-bis(diisopropylphosphanyl)ethane (dippe, **b**), 1,1'-bis(diisopropylphosphanyl)ferrocene) (dippf, **c**), 1,2-bis(dicyclohexylphosphanyl)ethane (dcype, **d**) produced the chlorides $M(P\cap P)(CO)_2(NO)Cl$ **25a**, **25b**, **25c**, **25d** (M = Mo) and **26a** (M = W). The chlorides were transformed to the corresponding hydrides **27a**, **27b**, **27c**, **27d** and **28a** via the

reaction with $LiBH_4$ in Et_3N at room temperature. The THF molybdenum complexes $[Mo(dippe)(CO)_2(NO)(THF)][BAr^F{}_4]$ **29a**, obtained via the reaction of **25a** with $[H(Et_2O)_2][BAr^F{}_4]$, was exemplarily tested in the hydrogenation of the imine PhCH=N(α-naphtyl), while the analogous tungsten complex **30a** displayed no activity in imine hydrogenation. Replacement of the $[BAr^F{}_4]^-$ counterion by the more stable $[B(C_6F_5)_4]^-$ anion greatly increased the catalytic activity. The *in situ* mixture of the hydrides **27a**, **27b**, **27c**, **27d**, **28a** and $[H(Et_2O)_2][B(C_6F_5)_4]$ improved hydrogenation activities. The hydride **27b** revealed the highest TOF value of 123 h^{-1} in the reduction of PhCH=N(α-naphtyl). The hydrogenation of the imines PhCH=NPh, p-ClC_6H_4CH=NPh, p-ClC_6H_4CH=N-p-C_6H_4Cl, PhCH=NCH$(Ph)_2$ and PhCH=NMes showed TOF values of 34, 74, 41, 18 and 84 h^{-1} at room temperature and H_2 pressure of 30 bar. A mechanism of ionic hydrogenation with "proton before hydride transfer" is anticipated.

Complex Mo[(S,S)-dmpcp]$_2$(NO)(OPh) ((S,S)-dmpcp = (1S,2S) 1,2-cyclo--pentanediylbis(dimethylphosphine) (**35**) was obtained by the reaction between Mo[(S,S)-dmpcp]$_2$(NO)(H) and PhOH in 78% yield.

The insertion reaction of acetophenone into Mo−H bond demonstrated that hydride complex Mo[(S,S)-dmpcp]$_2$(NO)(H) is prone to form preferentially an enantiomer with S configuration (ee 20%). The formation of S optical isomer of PhC(OH)CH_3 was shown to predominate over R isomer in the reaction of Mo[(S,S)-dmpcp]$_2$(NO)(H) with acetophenone in the presence of phenol. The ee value was found to be 27%.

The chloride complex Mo[(S,S)-dippcp)]$_2$(NO)(Cl) (**36**) ((S,S)-dippcp = (1S,2S) 1,2-cyclo-pentanediylbis(diisopropylphosphine) was obtained via a similar reaction that was used for the preparation of **4**. Although the hydride complex Mo[(S,S)-dippcp)]$_2$(NO)(H) (**37**) was unambiguously detected by NMR spectroscopy, the complex could not be isolated in pure form. The reason for this is presumably impurities contained in the material, which inhibits crystallization of the compound.

6 Experimental part

6.1 General consideration

Reagent grade benzene, toluene, pentane, diethyl ether and tetrahydrofuran were dried and distilled from sodium benzophenone ketyl prior to use. Acetone, NEt_3, acetophenone, ethylenediamine and CH_2Cl_2 were dried with CaH_2 and then distilled. Literature procedures were used to prepare the following compounds: 1,2-bis(diisopropylphosphanyl)ethane (dippe), 1,2-bis(dicyclohexylphosphanyl)ethane (dcype), 1,2-bis(diethylphosphanyl)ethane (depe) [175] 1,3-bis(diisopropylphosphanyl)-propane (dippp),[177] 1,1'-bis(diisopropylphosphino)ferrocene) (dippf),[178] (*S*,*S*)-dippcp = (1S,1S)-$C_5H_8(P\textit{i}Pr_2)_2$,[162-165] $M(NO)Cl_3(CH_3CN)_2$ (M = Mo, W),[179] $[H(Et_2O)_2][BAr^F{}_4]$,[93] $[H(Et_2O)_2][B(C_6F_5)_4]$[95] and $M(CO)_4(NO)(ClAlCl_3)$ (M = Mo, W).[180] Other reagents were purchased and used without further purification. All the manipulations were carried out under nitrogen using Schlenk techniques or a dry glovebox. IR spectra were obtained with Bio-Rad FTS-45 instrument. NMR spectra were measured with a Varian Mercury 200 spectrometer 81.0 MHz for $^{31}P\ \{^1H\}$, with Bruker-DRX 500 spectrometer at 500.2 MHz for ^1H, 202.5 MHz for $^{31}P\ \{^1H\}$, 125.8 MHz for $^{13}C\ \{^1H\}$ and Bruker-DRX 400 spectrometer at 400.1 MHz for ^1H, 162.0 MHz for $^{31}P\ \{^1H\}$, 100.6 MHz for $^{13}C\ \{^1H\}$. Chemical shifts for ^1H and $^{13}C\ \{^1H\}$ are given in ppm relatively to TMS ($SiMe_4$), the $^{31}P\ \{^1H\}$ NMR spectra were referenced to 98% external H_3PO_4. Elemental analyses: Leco CHN(S)-932 instrument. Transmitter CPT 2500 instrument. The mass spectra were recorded on a Varian Saturn 2000 spectrometer equipped with Varian 450-GC chromatograph. Gas flow (He): 1.0 ml/min. Temperature regime: 70 °C – 0.5 min hold, then 20 °C / min. The column parameters: VF-5ms 30.0m×0.25mm ID DF=0.25 mm.

The hydrogen pressure in catalytic reactions was monitored with "WIKA" Transmitter CPT 2500.

For the chiral GC Column Chirasil-DEX CB (Chrompak) 25m × 0.25 mm × 0.25 μm was used. Gas flow: 1.5 ml/min, helium. Standard condition: 100 °C – 3 min, than 15 °C / min. The machine: TRACE GC 2000 series.

6.2 Synthesis of complexes

6.2.1 Complexes bearing dippe ligands

Preparation of (dippe)W(NO)(Cl)$_3$(dippe)(Cl)$_3$(NO)W(dippe) (1)

To the solution of W(NO)(CH$_3$CN)$_2$Cl$_3$ (178 mg, 0.44 mmol) in 10 mL of THF the solution of dippe ligand (288 mg, 1.1 mmol, 2.5 eq.) in 5 mL THF was added. The reaction mixture was stirred 4 h at ambient temperature. Then the solvent was evaporated under low pressure. The residue was washed with hexane 3×10 mL and dried in vacuum.

Yield: 513.4 mg, 82%.

^{1}H NMR (202.5 MHz, CD_2Cl_2, 25 °C): δ 2.98 (m, 4 H, -PC*H*(CH$_3$)$_2$), 2.84 (m, 4 H, -PC*H*(CH$_3$)$_2$), 2.32–1.91 (m, 8 H, -PC*H*$_2$C*H*$_2$P-), 1.43−1.15 (m, 48 H, -C*H*$_3$).

^{31}P {^{1}H} NMR (80.9 MHz, CD_2Cl_2, 25 °C): 59.22 (s), 11.56 (s).

^{13}C {^{1}H} NMR (50.3 MHz, CD_2Cl_2, 25 °C): δ 23.95 (s), set of the multiplets from 20.32 till 19.01.

IR (cm^{-1}, ATR) 1609 (NO).

Anal. Calcd for $C_{43}H_{98}Cl_8N_2O_2P_6W_2$: C 34.15; H 6.53; N 1.85; Found: C 33.31; H 6.28; N 1.75.

Preparation of W(NO)(Cl)$_3$(dippe) (2)

To the solution of W(NO)(CH$_3$CN)$_2$Cl$_3$ (178 mg, 0.44 mmol) in 10 mL of THF the solution of the dippe ligand (115.3 mg, 0.44 mmol) in 5 mL THF was added. The reaction mixture was stirred 4 h at ambient temperature. Then the solvent was evaporated under low pressure. The residue was washed with hexane 3×10 mL and dried in vacuum.

Yield: 227.5 mg, 89%.

^{1}H NMR (202.5 MHz, CD_2Cl_2, 25 °C): δ 2.92 (m, 2 H, -PC*H*(CH$_3$)$_2$), 2.67 (m, 2 H, -PC*H*(CH$_3$)$_2$), 2.36 (m, 4 H, -PC*H*$_2$C*H*$_2$P-), 1.47−1.26 (m, 24 H, -C*H*$_3$).

^{31}P {^{1}H} NMR (80.9 MHz, CD_2Cl_2, 25 °C): δ 58.54 (s, $^1J_{WP}$ (d, satellites) = 216.4 Hz).

^{13}C {^{1}H} NMR (50.3 MHz, CD_2Cl_2, 25 °C): 27.54 (d, -P*C*H(CH$_3$)$_2$, $^1J_{CP}$ = 24.4 Hz), 26.47 (d, -P*C*H(CH$_3$)$_2$, $^1J_{CP}$ = 21.7 Hz), 19.69 (s, -*C*H$_3$), 19.18 (s, -*C*H$_3$), 18.43 (s, -*C*H$_3$), 18.05 (s, -*C*H$_3$). 17.87 (m, -P*C*H$_2$*C*H$_2$P-).

IR (cm^{-1}, ATR) 1642 (NO).

Anal. Calcd for $C_{43}H_{98}Cl_8N_2O_2P_6W_2$: C 28.86; H 5.54; N 2.40; Found: C 29.14; H 5.52; N 2.37.

General procedure for preparation of [M(P∩P)$_2$(NO)(Cl)] (3, 4, 15, 17, 36) (M = W and Mo, P∩P = dippe, depe, dppe and (*S*,*S*)-dippcp)

$MCl_3(CH_3CN)_2$ (M = Mo, W) (1.0 mmol) was solved in 20 mL of THF. To the stirred solution a ligand (2.5 mmol, 2.5 eq.) in 15 mL of THF was added. The reaction mixture was stirred 12 hours at the room temperature. Then 13.9 g of 1% sodium amalgam (6.0 mmol of Na) was added to the reaction mixture. Then the reaction mixture was stirred 12 hours. The color of the reaction mixture turned to bright-yellow. The solution with the precipitation was decanted from the amalgam. The solvent was removed under low pressure. The residue was extracted with CH_2Cl_2 until the extract solution became colorless. After removing of the solvent the residue was washed with hexane (3×10 mL) and dried in vacuum.

W(dippe)$_2$(NO)Cl (**3**)

Yield: 658 mg, 85%.

^{1}H NMR (400.1 MHz, CD_2Cl_2, 25 °C): δ = 2.62 (m, 4 H, -PC*H*$(CH_3)_2$), 2.49 (m, 4 H, -PC*H*$(CH_3)_2$), 1.63 (m, 8 H, -PC*H*$_2$C*H*$_2$P-), 1.24 (m, 24 H, -C*H*$_3$), 1.14 (m, 24 H, -C*H*$_3$).

^{31}P {^{1}H} NMR (162.0 MHz, CD_2Cl_2, 25 °C): δ = 44.1 (s, $^1J_{PW}$ (d, satellites) = 276.2 Hz)

^{13}C {^{1}H} NMR (100.6 MHz, CD_2Cl_2, 25 °C): δ = 29.6 (m, -P*C*H$_2$*C*H$_2$P-), 25.9 (m, -P*C*H$(CH_3)_2$), 20.6 (s, -PCH(*C*H$_3$)$_2$), 20.1 (s, -PCH(*C*H$_3$)$_2$), 19.8 (s, -PCH(*C*H$_3$)$_2$), 19.7 (s, -PCH(*C*H$_3$)$_2$).

IR (cm^{-1}, ATR) 1516 (NO).

Anal. Calcd for $C_{28}H_{64}ClNOP_4W$ C 43.45; H 8.33; N 1.81. Found C 43.90; H 9.01; N 1.78.

Mo(dippe)$_2$(NO)Cl (**4**)

Yield: 522 mg, 80%.

^{1}H NMR (400.1 MHz, CD_2Cl_2, 25 °C): δ = 2.64 (m, 4 H, -PC*H*$(CH_3)_2$), 2.47 (m, 4 H, -PC*H*$(CH_3)_2$), 1.76 (m, 8 H, -PC*H*$_2$C*H*$_2$P-), 1.32 (m, 24 H, -PCH(C*H*$_3)_2$), 1.23 (m, 24 H, -PCH(C*H*$_3)_2$).

^{31}P {^{1}H} NMR (162.0 MHz, CD_2Cl_2, 25 °C): δ = 59.9 (s).

^{13}C {^{1}H} NMR (100.6 MHz, CD_2Cl_2, 25 °C): δ = 28.5 (s, -P*C*H$(CH_3)_2$), 25.6 (s, -P*C*H$(CH_3)_2$), 20.5 (s, -PCH(*C*H$_3)_2$), 20.1 (s, -PCH(*C*H$_3)_2$), 19.9 (s, -PCH(*C*H$_3)_2$), 19.8 (s, -PCH(*C*H$_3)_2$), 17.8 (m, -P*C*H$_2$*C*H$_2$P-).

IR (cm^{-1}, ATR) 1528 (NO).

Anal. Calcd for $C_{28}H_{64}ClMoNOP_4$ C 49.02; H 9.40; N 2.04. Found C 49.24; H 9.58; N 1.96.

W(dppe)$_2$(NO)Cl (**15**)

Yield: 659.0 mg, 63%.

^{1}H NMR (500.1 MHz, CD_2Cl_2, 25 °C): set of multiplets from 7.30 till 7.03 (m, 40H, Ph), 2.68 (m, 4H, -PC*H*$_2$C*H*$_2$P-), 2.36 (m, 4H, -PC*H*$_2$C*H*$_2$P-).

^{31}P {^{1}H} NMR (202.5 MHz, CD_2Cl_2, 25 °C): δ 39.4 (s, $^{1}J_{PW}$ (d, satellites) = 293.0 Hz).

^{13}C {^{1}H} NMR (160.5 MHz, THF–d_8, 25 °C): δ 138.0 (m, i-Ph), 136.6 (m, i-Ph), 133.9 (m, o-Ph), 133.7 (m, o-Ph), 129.5 (s, p-Ph), 129.2 (s, p-Ph), 128.1 (t, m-Ph, $^{3}J_{PC}$ = 2.1 Hz), 127.7 (t, m-Ph, $^{3}J_{PC}$ = 2.1 Hz), 31.7 (dd, -P*C*H$_2$*C*H$_2$P-, $^{1}J_{PC}$ = 9.6 Hz).

IR (cm^{-1}, ATR) 1524 (NO).

Anal. Calcd for $C_{52}H_{48}ClNOP_4W$: C 59.70; H 4.62; N 1.34. Found: C 59.51; H 4.70; N 1.29.

Mo(depe)$_2$(NO)Cl (**17**).

Yield: 499 mg, 87%.

^{1}H {^{31}P} NMR (500.2 MHz, CD_2Cl_2, 25 °C): δ 1.98 (m, 4 H, -PC*H*$_2$CH$_3$), 1.95 (m, 4 H, -PC*H*$_2$CH$_3$), 1.87 (m, 4 H, -PC*H*$_2$CH$_3$), 1.76 (m, 4 H, -PC*H*$_2$CH$_3$), 1.62 (m, 8 H, -PC*H*$_2$C*H*$_2$P-), 1.17 (t, 12 H, -C*H*$_3$, $^{1}J_{HH}$ = 80.5 Hz), 1.12 (t, 12 H, -C*H*$_3$, $^{1}J_{HH}$ = 76.1 Hz).

^{31}P {^{1}H} NMR (202.5 MHz, CD_2Cl_2, 25 °C): δ 52.4 (s).

^{13}C {^{1}H} NMR (160.5 MHz, CD_2Cl_2, 25 °C): δ 22.1 (m, -P*C*H$_2$*C*H$_2$P-), 19.8 (m, -P*C*H$_2$CH$_3$), 18.6 (m, -P*C*H$_2$CH$_3$), 8.8 (s, -*C*H$_3$), 8.2 (s, -*C*H$_3$).

IR (cm^{-1}, ATR) 1532 (NO).

Anal. Calcd for $C_{20}H_{48}ClMoNOP_4$: C 41.86; H 8.43; N 2.44. Found: C 41.91; H 8.52; N 2.51.

Mo[(S,S)-dippcp)]$_2$(NO)Cl (**36**).

Yield: 513 mg, 63%.

^{1}H NMR (500.2 MHz, CD_2Cl_2, 25 °C): δ 2.90 (m, 4 H, C_5H_8), 2.66 (m, 8 H, C_5H_8), 2.59 (m, 2 H, -PC*H*$(CH_3)_2$), 2.49 (m, 1 H, -PC*H*$(CH_3)_2$), 2.25 (m, 2 H, -PC*H*$(CH_3)_2$), 2.22 (m, 2 H, -PC*H*$(CH_3)_2$), 1.89 (m, 4 H, C_5H_8), 1.52 − 1.20 (m, 48H, CH_3).

^{31}P {^{1}H} NMR (202.5 MHz, CD_2Cl_2, 25 °C): δ 28.1 (s).

^{13}C {^{1}H} NMR (160.5 MHz, CD_2Cl_2, 25 °C): δ 46.3 (m, -P*C*H), 46.1 (m, -P*C*H), 31.8 (m, CH_2), 31.7 (m, -P*C*H$(CH_3)_2$), 30.9 (m, -P*C*H$(CH_3)_2$), 26.9 (m, -P*C*H$(CH_3)_2$), 25.8 (m, -*C*H_2), 25.5 (m, *C*H_2), 21.5 (s, Me), 21.3 (s, Me), 21.0 (s, Me), 20.9 (s, Me), 20.8 (s, Me), 20.5 (s, Me), 20.3 (s, Me), 19.8 (s, Me).

IR (cm^{-1}, ATR) 1515 (NO).

Anal. Calcd for $C_{34}H_{72}ClMoNOP_4$: C 53.30; H 9.47; N 1.83. Found: C 53.21; H 9.87; N 2.05.

Preparation of [W(dippe)$_2$(Cl)(NO···LiBH$_4$)] (5)

To the mixture of W(dippe)$_2$(NO)Cl (**3**) (470 mg, 0.6 mmol) and $LiBH_4$ (73 mg, 3.4 mmol, 5eq.) of Et_3N (25 mL) was added. The reaction mixture was stirred 10 hours at 40 °C. Then Et_3N was evaporated at low pressure and the residue was extracted with toluene. The toluene solution was concentrated half to its original volume and cooled to -30 °C. The supernatant was decanted and the residue was washed with cooled hexane (2×5 mL) and dried in vacuum to afford **5** as a yellow powder.

Yield: 260 mg, 53%.

^{1}H NMR (400.1 MHz, C_6D_6, 25 °C): δ = 2.85 (m, 4 H, -PC*H*$(CH_3)_2$), 2.61 (m, 4 H, -PC*H*$(CH_3)_2$), 1.58 (m, 8 H, -PCH_2CH_2P-), 1.40 – 1.05 (m, 48 H, -CH_3), 0.20 (q, $^1J_{BH}$ = 82.0 Hz, LiBH_4).

^{31}P {^{1}H} NMR (162.0 MHz, C_6D_6, 25 °C): δ = 62.9 (s, $^1J_{PW}$ (d, satellites) = 280.1 Hz).

^{13}C {^{1}H} NMR (100.6 MHz, C_6D_6, 25 °C): δ = 29.6 (s, -P*C*H(CH$_3$)$_2$), 26.8 (s, -P*C*H(CH$_3$)$_2$), 21.0 (s, -PCH(*C*H$_3$)$_2$), 20.6 (s, -PCH(*C*H$_3$)$_2$), 20.2 (s, -PCH(*C*H$_3$)$_2$), 19.7 (s, -PCH(*C*H$_3$)$_2$), 18.4 (m, -P*C*H$_2$*C*H$_2$P-).

IR (cm^{-1}, ATR) 1489 (NO).

Anal. Calcd for $C_{28}H_{68}BClLiNOP_4W$ C 42.26; H 8.61; N 1.76. Found: C 42.59; H 8.76; N 1.89.

Preparation of [W(dippe)$_2$(H)(NO···LiBH$_4$)] (6)

Et$_3$N (20 mL) was added to the mixture of W(dippe)$_2$(NO)Cl (**3**) (470 g, 0.61 mmol) and LiBH$_4$ (73 mg, 3.4 mmol, 5 eq.). The suspension was stirred at 70 ºC until the starting material was consumed (^{31}P {^{1}H} NMR monitoring) (ca. 15 h). Then Et$_3$N was removed in vacuum and the residue was extracted with toluene. After removal of toluene the residue was washed with hexane (3×5 mL) and dried in vacuum.

Yield: 362 mg, 78%.

^{1}H NMR (400.1 MHz, C_6D_6, 25 °C): δ = 2.24 (m, 4 H, -PC*H*(CH$_3$)$_2$), 1.98 (m, 4 H, -PC*H*(CH$_3$)$_2$), 1.23 (m, 32 H, -C*H*$_3$ and -PC*H*$_2$C*H*$_2$P-), 1.01 (m, 12, H, -C*H*$_3$), 0.87 (m, 12, H, -C*H*$_3$), 0.15 (q, 4H, LiB*H*$_4$, $^{1}J_{BH}$ = 82.0 Hz), -2.91 (m, 1H, W–*H*, $^{2}J_{PH}$ = 26.3 Hz).

^{31}P {^{1}H} NMR (162.0 MHz, C_6D_6, 25 °C): δ = 63.8 (s, $^{1}J_{PW}$ (d, satellites) = 274.3 Hz).

^{13}C {^{1}H} NMR (100.6 MHz, C_6D_6, 25 °C): δ = 28.4 (s, -P*C*H(CH$_3$)$_2$), 25.7 (s, -P*C*H(CH$_3$)$_2$), 20.5 (s, -PCH(*C*H$_3$)$_2$), 20.3 (s, -PCH(*C*H$_3$)$_2$), 19.8 (s, -PCH(*C*H$_3$)$_2$), 19.1 (s, -PCH(*C*H$_3$)$_2$), 17.6 (m, -P*C*H$_2$*C*H$_2$P-).

IR (cm^{-1}, ATR) 1672 (WH) 1459 (NO).

Anal. Calcd for $C_{28}H_{69}BLiNOP_4W$ C 44.17; H 9.13; N 1.84. Found C 43.94; H 9.03; N 1.94.

Preparation of [W(dippe)$_2$(NO)H] (7)

Et$_3$N (30 mL) was added to the mixture of W(dippe)$_2$(NO)Cl (**3**) (774 mg, 1.0 mmol) and LiBH$_4$ (110 mg, 5.0 mmol, 5 eq.). The suspension was stirred at 70 °C until the starting material was consumed (^{31}P {^{1}H} NMR monitoring) (ca. 15 h). Then Et$_3$N was removed in vacuum and the residue was extracted with toluene. $NH_2CH_2CH_2NH_2$ (2 mL) was added to the toluene solution to remove LiBH$_4$ coordinated to the NO group. The

precipitate was filtered off. After removal of toluene in vacuum the residue was washed with hexane (3×5 mL) and dried in vacuum.

Yield: 510 mg, 69%.

^{1}H NMR (400.1, C_6D_6, 25 °C): δ = 2.47 (m, 4 H, -PC*H*$_2$C*H*$_2$P-), 2.10 (m, 4 H, -PC*H*$(CH_3)_2$), 1.36 (m, 24 H, -PCH(C*H*$_3)_2$) 1.15 (m, 12 H, -PCH(C*H*$_3)_2$), 1.04 (m, 12 H, -PCH(C*H*$_3)_2$), -3.38 (m, 1H, W–*H*, $^2J_{PH}$ = 24.8 Hz).

^{31}P {^{1}H} NMR (162.0 MHz, C_6D_6, 25 °C): δ = 64.5 (s, $^1J_{PW}$ (d, satellites) = 279.7 Hz).

^{13}C {^{1}H} NMR (160.5 MHz, C_6D_6, 25 °C): δ = 32.0 (m, -P*C*H$(CH_3)_2$), 30.0 (m, -P*C*H$(CH_3)_2$), 23.8 (m, -P*C*H$_2$*C*H$_2$P-), 21.2 (s, -PCH(*C*H$_3)_2$), 20.4 (s, -PCH(*C*H$_3)_2$), 20.3 (s, -PCH(*C*H$_3)_2$), 18.5 (s, -PCH(*C*H$_3)_2$).

IR (cm^{-1}, ATR) 1670 (WH) 1456 (NO).

Anal. Calcd for $C_{28}H_{65}NOP_4W$ C 45.47; H 8.86; N 1.89. Found C 45.66; H, 8.81; N 2.00.

Preparation of [Mo(dippe)$_2$(NO)H] (8)

To a mixture of Mo(dippe)$_2$(NO)Cl (**4**) (275 mg, 0.4 mmol) and $LiBH_4$ (28 mg, 2.0 mmol, 5 eq.) Et_3N (15 mL) was added. The suspension was stirred at 70 °C until the starting material was consumed (^{31}P {^{1}H} NMR monitoring) (ca. 15 hours). Then Et_3N was removed in vacuum and the residue was extracted with toluene. The toluene fractions were combined and the solvent was removed in vacuum. The remaining substance was washed with hexane (3×3 mL) and dried in vacuum.

Yield: 180 mg, 69%.

^{1}H NMR (200.2 MHz, C_6D_6, 25 °C): δ = 2.52 (m, 8 H, -PC*H*$_2$C*H*$_2$P-), 2.23 (m, 8 H, -PC*H*$(CH_3)_2$), 1.57−1.32 (m, 48 H, -C*H*$_3$), -3.80 (m, 1H, Mo–H, $^2J_{HP}$ = 28.3 Hz).

^{31}P {^{1}H} NMR (80.9 MHz, C_6D_6, 25 °C): δ = 85.8 (s).

^{13}C {^{1}H} NMR (160.5 MHz, C_6D_6, 25 °C): δ = 31.2 (m, -P*C*H$(CH_3)_2$), 28.9 (m, -P*C*H$(CH_3)_2$), 21.2 (m, -P*C*H$_2$*C*H$_2$P-), 21.0 (s, -PCH(*C*H$_3)_2$), 20.2 (s, -PCH(*C*H$_3)_2$), 20.1 (s, -PCH(*C*H$_3)_2$), 18.5 (s, -PCH(*C*H$_3)_2$).

IR (cm^{-1}, ATR) 1601 (WH) 1500 (NO).

Anal. Calcd for $C_{28}H_{65}NOP_4Mo$ C 51.61; H 10.05; N 2.15. Found C 51.72; H 10.00; N 2.14.

Preparation of M(dippe)$_2$(NO)(O(CH)O) (M = W (9), Mo (10))

Toluene (0.6 mL) was added onto Yang NMR tube containing M(dippe)$_2$(NO)H (M = W, Mo) (0.02 mmol). The NMR tube was filled with CO_2 gas (1.2 bar). Then the NMR tube was shaken. ^{31}P $\{^1H\}$ NMR monitoring revealed that the reaction occured within minutes. The solvent was removed in vacuum and the residue was washed with cold hexane.

Yield of **9**: 95%, 14.9 mg.

^{1}H NMR (400.1 MHz, C_6D_6, 25 °C): δ δ 8.25 (s, 1H, -O(C*H*)O), 2.68 (m, 4 H, -PC*H*$(CH_3)_2$), 2.49 (m, 4 H, -PC*H*$(CH_3)_2$), 1.88 (m, 4 H, -PC*H*$_2$C*H*$_2$P-), 1.59 (m, 4 H, -PC*H*$_2$C*H*$_2$P-), set of multiplets from 1.33 to 1.15 (m, 48 H, -C*H*$_3$).

^{31}P $\{^1$H$\}$ NMR (162.0 MHz, C_6D_6, 25 °C): δ = 49.3 (s, $^1J_{PW}$ (d, satellites) = 286.1 Hz).

^{13}C $\{^1$H$\}$ NMR (100.6 MHz, C_6D_6, 25 °C): δ 165.7 (s, -O(*C*H)O), 29.6 (quint, -P*C*H$(CH_3)_2$, $^1J_{CP}$ = 5.0 Hz), 25.9 (quint, -P*C*H$(CH_3)_2$, $^1J_{CP}$ = 4.0 Hz), 21.0 (s, -CH_3), 20.4 (quint, -PCH_2CH_2P-, $^1J_{CP}$ = 7.0 Hz), 20.3 (s, -CH_3), 20.0 (s, -CH_3), 19.7 (s, -CH_3).

IR (cm^{-1}, ATR) 1631 (OCO), 1512 (NO).

Anal. Calcd for $C_{29}H_{65}NO_3P_4W$: C, 44.45; H, 8.36; N, 1.79. Found: C, 44.53; H, 8.29; N, 1.71.

Yield of **10**: 91%, 12.7 mg.

^{1}H NMR (400.1 MHz, C_6D_6, 25 °C): δ 8.39 (s, 1 H, OC*H*O), 2.55 (m, 4 H, -PC*H*(CH_3)), 2.50 (m, 4 H, -PC*H*$(CH_3)_2$), 1.92 (m, 4 H, -PC*H*$_2$C*H*$_2$P-), 1.62 (m, 4 H, -PC*H*$_2$C*H*$_2$P-), set of multiplets from 1.30 to 1.01 (m, 48 H, -C*H*$_3$).

^{31}P $\{^1$H$\}$ NMR (162.0 MHz, C_6D_6, 25 °C): δ = 63.2 (s).

^{13}C $\{^1$H$\}$ NMR (100.6 MHz, C_6D_6, 25 °C): δ 166.4 (s, -O(*C*H)O), 28.5 (t, -P*C*H$(CH_3)_2$, $^1J_{CP}$ = 3.6 Hz), 25.4 (t, -P*C*H$(CH_3)_2$, $^1J_{CP}$ = 3.6 Hz), 20.7 (s, -CH_3), 20.2 (s, -CH_3), 20.0 (s, -CH_3), 19.7 (s, -CH_3), 18.0 (quint, -PCH_2CH_2P-, $^1J_{CP}$ = 7.2 Hz).

IR (cm^{-1}, ATR) 1627 (OCO), 1526 (NO).

Anal. Calcd for $C_{29}H_{65}MoNO_3P_4$: C, 50.07; H, 9.42; N, 2.01. Found: C, 49.98; H, 9.38; N, 2.03.

Preparation of [W(dippe)(H)$_2$(dippe)(NO)][BAr$^F{}_4$] (11)

To the mixture of W(NO)(dippe)$_2$H (**7**) (17.1 mg, 0.023 mmol) and [H(Et$_2$O)$_2$][BAr$^F{}_4$] (23.4 mg, 0.023 mmol) Et$_2$O (1.0 mL) was added. White precipitate was formed immediately. The precipitation was filtered off, washed with Et$_2$O (3×1 mL) and dried in vacuum.

Yield of **11**: 25.3 mg, 68%.

^{1}H {^{31}P} NMR (500.2 MHz, THF-d$_8$, 25 °C): δ = 7.80 (s, 8 H, o-BAr^F), 7.59 (s, 4 H, p-BAr^F), 2.67 (m, 2 H, -PC*H*(CH$_3$)$_2$), 2.59 (m, 2 H, -PC*H*(CH$_3$)$_2$), 2.32 (m, 4 H, -PC*H*$_2$C*H*$_2$P-), 2.22 (m, 2 H, -PC*H*(CH$_3$)$_2$), 2.15 (t, 2 H, -PC*H*$_2$C*H*$_2$P-), 1.99 (t, 2 H, -PC*H*$_2$C*H*$_2$P-), 1.89 (m, 2 H, -PC*H*(CH$_3$)$_2$), 1.76 (s, 2 H, W–(*H*)$_2$), 1.50 – 1.43 (m, 6 H, -C*H*$_3$), 1.41 (d, 6 H, C*H*$_3$, $^1J_{HH}$ = 65.2 Hz), 1.37 (d, 6 H, -C*H*$_3$, $^1J_{HH}$ = 65.3 Hz), 1.33 (d, 6 H, -C*H*$_3$, $^1J_{HH}$ = 65.2 Hz), 1.31 (d, 6 H, -C*H*$_3$, $^1J_{HH}$ = 65.3 Hz), 1.16 (d, 6 H, -C*H*$_3$, $^1J_{HH}$ = 65.2 Hz), 1.12 (d, 6 H, -C*H*$_3$, $^1J_{HH}$ = 65.2 Hz).

^{31}P {^{1}H} NMR (202.5 MHz, THF-d$_8$, 25 °C): δ = 69.3 (dt, $^2J_{PP}$= 5.5 Hz, $^2J_{PP}$= 17.7 Hz, $^1J_{WP}$ (d, satellites) = 144.0 Hz), 61.9 (dd, $^2J_{PP}$= 23.7 Hz, $^2J_{PP}$= 17.7 Hz, $^1J_{WP}$ (d, satellites) = 158.0 Hz), 27.6 (dt, $^2J_{PP}$= 23.7 Hz, $^2J_{PP}$= 5.5 Hz, $^1J_{WP}$ (d, satellites) = 96.0 Hz).

^{13}C {^{1}H} NMR (160.5 MHz, THF-d$_8$, 25 °C): δ = 163.0 (quart, $^1J_{BC}$ = 50.5 Hz, i-BAr$^F{}_4$), 135.6 (s, o-BAr$^F{}_4$), 130.1 (m, m-BAr$^F{}_4$), 125.5 (quart, $^1J_{CF}$ = 273.1 Hz, *C*F$_3$), 118.4 (s, p-BAr$^F{}_4$), 29.8 (s, -P*C*H(CH$_3$)$_2$), 29.7 (s, -P*C*H(CH$_3$)$_2$), 29.5 (s, -P*C*H(CH$_3$)$_2$), 29.4 (s, -P*C*H(CH$_3$)$_2$), 29.3 (s, -P*C*H(CH$_3$)$_2$), 29.2 (s, -P*C*H(CH$_3$)$_2$), 26.5 (s, -P*C*H(CH$_3$)$_2$), 26.3 (s, -P*C*H(CH$_3$)$_2$), 24.7 (m, -P*C*H(CH$_3$)$_2$), 23.2 (m, -P*C*H(CH$_3$)$_2$), 20.5 (s, -PCH(*C*H$_3$)$_2$), 20.4 (s, -PCH(*C*H$_3$)$_2$), 20.3 (s, -PCH(*C*H$_3$)$_2$), 20.2 (s, -PCH(*C*H$_3$)$_2$), 19.6 (s, -PCH(*C*H$_3$)$_2$), 19.5 (s, -PCH(*C*H$_3$)$_2$), 19.2 (s, -PCH(*C*H$_3$)$_2$), 18.6 (s, -PCH(*C*H$_3$)$_2$) ppm.

^{19}F {^{1}H} NMR (376.5 MHz, THF-d$_8$, 25 °C): δ = -64.5 (s, C*F*$_3$) ppm.

IR (cm^{-1}, ATR) 1613 (NO).

Anal. Calcd for $C_{60}H_{78}NBF_{24}OP_4W$ C 44.93; H 4.90; N 0.87. Found C 44.99; H 4.86; N 0.89.

Preparation of [W(dippe)(H)$_2$(dippe)(NO)][BF$_4$] (12)

To the solution of W(NO)(dippe)$_2$H (**7**) (25.0 mg, 0.034 mmol) in 3 mL of Et$_2$O 57% solution of HBF$_4$·Et$_2$O was added dropwise (~ 7 µl). A white precipitate was formed

immediately. The precipitate was filtered off, washed with Et_2O (3×1 mL) and dried in vacuum.

Yield: 18.7 mg, 67%.

^{1}H {^{31}P} NMR (500.2 MHz, THF-d_8, 25 °C): δ = 2.65 (m, 2 H, -PC*H*$(CH_3)_2$), 2.59 (m, 2 H, -PC*H*$(CH_3)_2$), 2.43 (m, 4 H, -PCH_2CH_2P-), 2.31 (m, 2 H, -PC*H*$(CH_3)_2$), 2.24 (m, 2 H, -PCH_2CH_2P-), 2.20 (m, 2 H, -PCH_2CH_2P-), 2.02 (m, 2 H, -PC*H*$(CH_3)_2$), 1.91 (m, -PC*H*$(CH_3)_2$), 1.76 (s, 2H, W–(*H*)$_2$), 1.48–1.43 (m, 6 H, -CH_3), 1.39 – 1.32 (m, 12H, -CH_3), 1.18−1.13 (m, 6 H, -CH_3).

^{31}P {^{1}H} NMR (202.5 MHz, THF-d_8, 25 °C): δ = 69.2 (dt, $^{2}J_{PP}$= 5.8 Hz, $^{2}J_{PP}$= 17.7 Hz, $^{1}J_{WP}$ (d, satellites) = 144.5 Hz), 61.9 (dd, $^{2}J_{PP}$= 23.1 Hz, $^{2}J_{PP}$= 17.7 Hz, $^{1}J_{WP}$ (d, satellites) = 160.6 Hz), 27.3 (dt, $^{2}J_{PP}$= 23.1 Hz, $^{2}J_{PP}$= 5.8 Hz, $^{1}J_{WP}$ (d, satellites) = 99.8 Hz).

^{13}C {^{1}H} NMR (160.5 MHz, THF-d_8, 25 °C): δ = 29.4 (m, -P*C*H$(CH_3)_2$), 26.3 (d, -P*C*H$(CH_3)_2$), $^{1}J_{CP}$ = 13.1 Hz), 24.7 (t, $^{1}J_{CP}$ = 18.7 Hz), 23.5 (dd, -P*C*H_2CH_2P-, $^{1}J_{CP}$ = 26.3 Hz), 23.0 (dd, -P*C*H_2CH_2P-, $^{1}J_{CP}$ = 22.9 Hz), 20.6 (s, -CH_3), 20.5 (s, -CH_3), 20.3 (s, -CH_3), 20.0 (s, -CH_3), 19.6 (s, -CH_3), 19.6 (s, -CH_3), 19.3 (d, -CH_3, $^{2}J_{CP}$ = 1.3 Hz), 18.6 (d, -CH_3, $^{2}J_{CP}$ = 1.7 Hz).

^{19}F {^{1}H} NMR (376.5 MHz, THF-d_8, 25 °C): δ = -155.3 (s, -CF_3).

IR (cm^{-1}, ATR) 1584 (NO), 1462 (WH).

Anal. Calcd for $C_{28}H_{66}NBF_4OP_4W$ C 40.65; H 8.04; N 1.69. Found C 40.82; H 7.97; N 1.60.

Preparation of [Mo(dippe)$_2$(NO)][BAr$^{F}_4$] (13)

To the mixture of Mo(dippe)$_2$(NO)H (**8**) (50.0 mg, 0.077 mmol) and [H(Et_2O)$_2$][BAr$^{F}_4$] (77.8 mg, 0.077 mmol) THF (5 mL) was added. After the hydrogen emission stopped (few minutes), the solvent was removed in vacuum. The green residue was washed with pentane (3×5 mL).

Yield: 107.3 mg, 92%.

^{1}H NMR (500.2 MHz, THF-d_8, 25 °C): δ = 7.79 (s, 8 H, o-Ph), 7.57 (s, 4 H, p-Ph), 2.64 (m, 4 H, -PC*H*$(CH_3)_2$), 2.45 (m, 4 H, -PC*H*$(CH_3)_2$), 2.08 (s, 8 H, -PCH_2CH_2P-), 1.40–1.20 (m, 36 H, -CH_3), 0.60 (m, 12 H, -CH_3).

^{31}P {^{1}H} NMR (202.5 MHz, THF-d_8, 25 °C): δ = 73.6 (s).

^{13}C {^{1}H} NMR (100.6 MHz, THF-d_8, 25 °C): δ = 163.0 (quart, $^{1}J_{BC}$ = 50.1 Hz, i-BAr^{F}_4), 135.8 (s, o-BAr^{F}_4), 130.1 (m, m-BAr^{F}_4), 125.5 (quart, $^{1}J_{CF}$ = 273.1 Hz, -*C*F_3), 118.4 (s, p-BAr^{F}_4), 28.6 (m, -P*C*H(CH_3)$_2$), 19.9 (s, -PCH(*C*H_3)$_2$), 19.4 (s, -PCH(*C*H_3)$_2$), 19.1 (s, -PCH(*C*H_3)$_2$), 18.9 (t, -P*C*H_2*C*H_2P-, $^{1}J_{CP}$ = 7.2 Hz).

^{19}F {^{1}H} NMR (376.5 MHz, THF-d_8, 25 °C): δ = -65.43 (s, -C*F*$_3$).

IR (cm^{-1}, ATR) 1591 (NO).

Anal. Calcd for $C_{60}H_{76}BF_{24}NOP_4Mo$ C 47.60; H 5.06; N 0.93. Found C 47.62; H 5.10; N 0.97.

Reaction [Mo(dippe)$_2$(NO)][BAr^{F}_4] (13) with H_2 gas.

15.0 mg of [Mo(NO)(dippe)$_2$][BAr^{F}_4] (**13**) was placed in an Young NMR tube. Then THF-d_8 (0.7 mL) was added. The NMR tube was filled with 1.8 bar of H_2 gas. After the NMR tube was shaken the colour of the solution changed from green to yellow. The estimated conversion was 80% (according to the ^{31}P {^{1}H} NMR).

^{1}H {^{31}P} NMR (500.2 MHz, THF-d_8, 25 °C): δ = 7.80 (s, 8 H, o-BAr^{F}), 7.59 (s, 4 H, p-BAr^{F}), 2.63 (m, 2 H, -PC*H*(CH_3)$_2$), 2.57 (m, 4 H, -PC*H*(CH_3)$_2$), 2.28 (m, 4 H, -PC*H*$_2$C*H*$_2$P-), 2.19 (m, 2 H, -PC*H*(CH_3)$_2$), 2.11 (m, 2 H, -PC*H*$_2$CH_2P-), 1.88 (m, 2 H, -PCH_2C*H*$_2$P-), 1.49 – 1.29 (m, 36 H, -C*H*$_3$), 1.15 – 1.09 (m, 36 H, -C*H*$_3$), 0.32 (s, 2 H, Mo – (*H*)$_2$).

^{31}P {^{1}H} NMR (202.5 MHz, THF-d_8, 25 °C): δ = 87.5 (t, $^{2}J_{PP}$= 22.4 Hz), 73.7 (t, $^{2}J_{PP}$ = 22.4 Hz), 39.9 (t, $^{2}J_{PP}$= 24.0 Hz).

^{13}C {^{1}H} NMR (100.6 MHz, THF-d_8, 25 °C): δ = 163.0 (quart, $^{1}J_{BC}$ = 50.3 Hz, i-BAr^{F}_4), 135.8 (s, o-BAr^{F}_4), 130.1 (m, m-BAr^{F}_4), 125.5 (quart, $^{1}J_{CF}$ = 273.1 Hz, -*C*F_3), 118.4 (s, p-BAr^{F}_4), 29.9 (d, -PC*H*(CH_3)$_2$, $^{1}J_{CP}$ = 26.2 Hz), 29.2 (t, -PC*H*(CH_3)$_2$, $^{1}J_{CP}$ = 11.9 Hz), 28.8 (t, -PC*H*(CH_3)$_2$, $^{1}J_{CP}$ = 8.3 Hz), 26.1 (d, -PC*H*(CH_3)$_2$, $^{1}J_{CP}$ = 10.9 Hz), 24.0 (t, -P*C*H$_2$*C*H$_2$P-, $^{1}J_{CP}$ = 17.9 Hz), 22.7 (dd, -P*C*H$_2$CH$_2$P-, $^{1}J_{CP}$ = 9.5 Hz), 21.3 (dd, -P*C*H$_2$CH$_2$P-, $^{1}J_{CP}$ = 8.3 Hz), 20.5 (s, -PCH(*C*H_3)$_2$), 20.3 (s, -PCH(*C*H_3)$_2$), 20.1 (s, -PCH(*C*H_3)$_2$), 20.0 (s, -PCH(*C*H_3)$_2$), 19.6 (s, -PCH(*C*H_3)$_2$), 19.5 (s, -PCH(*C*H_3)$_2$), 19.2 (s, -PCH(*C*H_3)$_2$), 18.6 (s, -PCH(*C*H_3)$_2$).

Preparation of [Mo(dippe)$_2$(NO)][BF$_4$] (14)

To the solution of Mo(NO)(dippe)$_2$H (**8**) (56.0 mg, 0.086 mmol) in 5 mL of Et_2O 57% ether solution of [H(Et_2O)][BF_4] was added dropwise until the emision of H_2 gas had stopped (~ 15 µl). Then the reaction mixture was stirred for 2 hours. The ether solution was decanted from the red precipitate formed, and then the precipitate was extracted with diethyl ether until the solution became colorless. The combined organic fractions were concentrated in vacuum to a volume of ~10 mL volume and cooled to -30 ºC. The precipitate formed was filtered off, washed with cooled diethyl ether and dried in vacuum.

Yield: 46.4 mg, 73%.

^{1}H {^{31}P} NMR (500.2 MHz, THF-d_8, 25 °C): δ = 2.59 (m, 4 H, -PC*H*(CH_3)$_2$), 2.42 (m, 4 H, -PC*H*(CH_3)$_2$), 1.96 (m, 4 H, -PCH_2CH_2P-), 1.83 (m, 4 H, -PCH_2CH_2P-), 1.37 (d, 12 H, -CH_3, $^1J_{HH}$ = 7.1 Hz), 1.35 (d, 12 H, -CH_3, $^1J_{HH}$ = 7.1 Hz), 1.22 (d, 12 H, -CH_3, $^1J_{HH}$ = 7.0 Hz), 1.20 (d, 12 H, -CH_3, $^1J_{HH}$ = 7.1 Hz).

^{31}P {^{1}H} NMR (202.5 MHz, THF-d_8, 25 °C): δ = 64.5 (s).

^{13}C {^{1}H} NMR (160.5 MHz, THF-d_8, 25 °C): δ = 29.2 (m, -P*C*H(CH_3)$_2$), 24.8 (m, -P*C*H(CH_3)$_2$), 20.8 (s, -PCH(*C*H_3)$_2$), 20.2 (s, -PCH(*C*H_3)$_2$), 20.0 (s, -PCH(*C*H_3)$_2$), 19.7 (s, -PCH(*C*H_3)$_2$), 17.7 (m, -P*C*H_2*C*H_2P-).

^{19}F {^{1}H} NMR (376.5 MHz, THF-d_8, 25 °C): δ = -156.8 (s, -*F*BF_3), 156.9 (s, -FB*F*$_3$).

IR (cm^{-1}, ATR) 1560 (NO).

Anal. Calcd for $C_{28}H_{64}BF_4MoNOP_4$ C 45.60; H 8.75; N 1.90. Found C 45.47; H 8.68; N 1.98.

Preparation of [(dippe)(NO)Mo(µ-Cl)$_3$Mo(NO)(dippe)][BF$_4$] (20)

To the vessel covered with aluminum foil to protect the reaction mixture from light Mo(diippe)$_2$(NO)Cl (**4**) (30 mg 0.044 mmol) and $AgBF_4$ (8.6 mg, 0.044 mmol) were placed. Then 10 mL of CH_2Cl_2 were added. The reaction mixture was stirred for 30 min, the precipitate formed was filtered off and the solvent was removed under reduced pressure. The residue was dissolved in 5 mL of THF and the solution was cooled at -30 °C giving red crystals.

Yield: 11.3 mg, 52%.

^{1}H {^{31}P} NMR (500.2 MHz, CD_2Cl_2, 25 °C): δ 2.43 (m, 4 H, -PC*H*$_2$C*H*$_2$P-), 2.35 (m, 4 H, -PC*H*$(CH_3)_2$), 2.28 (s, 4 H, -PC*H*$_2$C*H*$_2$P-), 1.53 (d, 12 H, -C*H*$_3$, $^{1}J_{HH}$ = 3.1 Hz), 1.46 (d, 12 H, -C*H*$_3$, $^{1}J_{HH}$ = 3.1 Hz), 1.22 (d, 12 H, -C*H*$_3$, $^{1}J_{HH}$ = 7.0 Hz), 1.18 (d, 12 H, -C*H*$_3$, $^{1}J_{HH}$ = 7.0 Hz).

^{31}P {^{1}H} NMR (200.5 MHz, THF-d_8, 25 °C): δ 68.2 (s).

^{13}C {^{1}H} NMR (100.6 MHz, CD_2Cl_2, 25 °C): δ = 29.7 (s, -P*C*H$_2$(CH$_3$)$_2$), 27.8 (s, -P*C*H(CH$_3$)$_2$), 21.8 (s, -PCH(*C*H$_3$)$_2$), 20.9 (s, -PCH(*C*H$_3$)$_2$), 20.3 (s, -PCH(*C*H$_3$)$_2$), 19.8 (s, -PCH(*C*H$_3$)$_2$), 18.8 (m, -P*C*H$_2$*C*H$_2$P-).

^{19}F {^{1}H} NMR (188.5 MHz, THF-d_8, 25°C) -154.9 (s, B*F*$_4$).

IR (cm^{-1}, ATR) 1654, 1630 (NO).

Anal. Calcd for $C_{28}H_{71}BCl_3F_4Mo_2N_2O_2P_4$: C 34.43; H 7.33; N 2.87. Found: C 34.69; H 7.59; N 2.76.

6.2.2 Complex with dppe ligands

Preparation of W(dppe)$_2$(NO···AlCl$_3$)Cl (16)

To the suspension of W(dppe)$_2$(NO)Cl (**15)** (52.3 mg, 0.05 mmol) in 2 mL of Et_2O the solution of $AlCl_3$ (20.0 mg, 0.15 mmol, 3 eq.) in 3 mL of Et_2O was added at room temperature. The reaction mixture was stirred for 5 hours, then the precipitate was filtered, washed with Et_2O (3×2 mL) and dried in vacuum.

Yield: 47.2 mg, 80%.

^{1}H NMR (400.1 MHz, CD_2Cl_2, 25 °C): set of multiplets from 7.46 till 6.81 (m, 40 H, Ph), 2.85 (m, 4H, -PC*H*$_2$C*H*$_2$P-), 2.57 (m, 4H, -PC*H*$_2$C*H*$_2$P-).

^{31}P {^{1}H} NMR (202.5 MHz, CD_2Cl_2, 25 °C): δ 34.9 (s, $^{1}J_{PW}$ (d, satellites) = 280.2 Hz).

^{13}C {^{1}H} NMR (160.5 MHz, THF-d_8, 25 °C): δ 135.2 (m, i-Ph), 134.3 (m, i-Ph), 134.2 (m, o-Ph), 133.8 (m, o-Ph), 130.9 (s, p-Ph), 130.0 (s, p-Ph), 129.5 (t, m-Ph, $^{3}J_{PC}$ = 2.0 Hz), 128.2 (t, m-Ph, $^{3}J_{PC}$ = 2.0 Hz), 32.2 (m, -P*C*H$_2$*C*H$_2$P-, $^{1}J_{PC}$ = 10.0 Hz).

IR (cm^{-1}, ATR) 1484 (NO).

Anal. Calcd for $C_{52}H_{48}AlCl_4NOP_4W$: C 52.95; H 4.10; N 1.19. Found: C 53.06; H 4.24; N 1.10.

6.2.3 Complexes bearing depe ligands

Preparation of $Mo(depe)_2(NO)H$ (18)

20 mL of Et_3N was added to the mixture of $Mo(depe)_2(NO)Cl$ (**17**) (250 mg, 0.44 mmol) and $LiBH_4$ (47 mg, 2.2 mmol, 5 eq.). The suspension was stirred at 60 °C until the starting material was no longer observed (^{31}P $\{^1H\}$ NMR monitoring). Then Et_3N was removed under low pressure and the residue was extracted with toluene. 1 mL of $NH_2CH_2CH_2NH_2$ was added to the toluene solution to remove $LiBH_4$ coordinated to the NO group. The precipitate formed was filtrate off. After removing of toluene under reduced pressure, the residue was dissolved in 10 mL of hexane and cooled to -30°C affording yellow crystals.

Yield: 185.0 mg, 79%.

^1H $\{^{31}P\}$ NMR (500.2 MHz, C_6D_6, 25 °C): δ 1.88 (m, 4 H, -PC*H*$_2$CH$_3$), 1.79 (m, 4 H, -PC*H*$_2$CH$_3$), 1.67 (m, 4 H, -PC*H*$_2$CH$_3$), 1.46 (m, 4 H, -PC*H*$_2$CH$_3$), 1.36 (s, 8 H, -PC*H*$_2$C*H*$_2$P-), 1.27 (t, 12 H, -C*H*$_3$, $^1J_{HH}$ = 7.0 Hz), 1.12 (t, 12 H, -C*H*$_3$, $^1J_{HH}$ = 6.0 Hz), 4.78 (quintet, Mo−H, $^1J_{PH}$ = 28.8 Hz).

^{31}P $\{^1H\}$ NMR (202.5 MHz, C_6D_6, 25 °C): δ 70.57 (s).

^{13}C $\{^1H\}$ NMR (160.5 MHz, C_6D_6, 25 °C): δ 25.6 (m, -P*C*H$_2$CH$_3$), 25.3 (m, -P*C*H$_2$*C*H$_2$P-), 24.0 (m, -P*C*H$_2$CH$_3$), 9.2 (s, -*C*H$_3$), 8.6 (s, -*C*H$_3$).

IR (cm^{-1}, ATR) 1545, (MoH), 1500 (NO).

Anal. Calcd for $C_{20}H_{49}MoNOP_4$: C 44.53; H 9.16; N 2.60. Found: C 44.71; H 9.30; N 2.79.

Preparation of $[\{Mo(NO)(depe)_2\}_2(N_2)][BAr^F{}_4]_2$ (19)

To the mixture of $Mo(NO)(depe)_2H$ (**18**) (45.0 mg, 0.072 mmol) and $[H(Et_2O)_2][BAr^F{}_4]$ (72.6 mg, 0.072 mmol) 10 mL of diethyl ether was added. The red precipitate formed after 2 hours of stirring was filtered off, washed with diethyl ether (2×2 mL) and dried in vacuum.

Yield: 75.0 mg, 75%.

^1H NMR (500.2 MHz, THF-d_8, 25 °C): δ 7.79 (s, 8 H, o-BAr^F), 7.58 (s, 4 H, p-BAr^F), 2.03 (m, 8 H, -PC*H*$_2$CH$_3$), 1.93 (m, 4 H, -PC*H*$_2$CH$_3$), 1.82 (m, 4 H, -PC*H*$_2$CH$_3$), 1.73 (s, 8 H, -PC*H*$_2$C*H*$_2$P-), 1.25 (m, 12 H, -C*H*$_3$), 1.18 (m, 12 H, -C*H*$_3$).

^{31}P {^{1}H} NMR (202.5 MHz, THF-d_8, 25 °C): δ 48.7 (s).

^{13}C {^{1}H} NMR (160.5 MHz, THF-d_8, 25 °C): δ 163.0 (quart, $^{1}J_{BC}$ = 50.1 Hz, i-BAr^{F}_{4}), 135.6 (s, o-BAr^{F}_{4}), 130.1 (m, m-BAr^{F}_{4}), 125.5 (quart, $^{1}J_{CF}$ = 273.0 Hz, CF_3), 118.4 (s, p-BAr^{F}_{4}), 22.2 (m, -P*C*H_2CH_3), 19.3 (m, -P*C*H_2*C*H_2P-), 18.8 (m, -P*C*H_2CH_3), 8.8 (s, -*C*H_3), 8.0 (s, -*C*H_3).

IR (cm^{-1}, ATR) 1572 (NO).

Raman (cm^{-1}): 1596 (NN).

Anal. Calcd for $C_{104}H_{120}B_2F_{48}Mo_2N_4O_2P_8$: C 44.12; H 4.27; N 1.98. Found: C 43.78; H 4.19; N 1.91.

6.2.4 Complexes bearing dippe and dcype ligands

Mo(dcype)Cl_3(NO) (21)

The solution of $Cy_2PCH_2CH_2PCy_2$ (211 mg, 0.5 mmol) in 10 mL of THF was added dropwise to the solution of $Mo(CH_3CN)_2Cl_3(NO)$ (157 mg, 0.5 mmol) in 10 mL of THF. The reaction mixture was stirred for 2 hours. A green precipitate was formed during that time. The precipitate was filtered off, washed with THF (3×5 mL) and dried in vacuum.

Yield of **21**: 148.0 mg, 55%.

^{1}H NMR (500.2 MHz, CD_2Cl_2, 25 °C): δ set of multiplets from 2.6 to 1.2.

^{31}P {^{1}H} NMR (202.5 MHz, THF-d_8, 25 °C): δ 70.5 (s).

^{13}C {^{1}H} NMR (160.5 MHz, THF–d_8, 25 °C): δ 39.1 (m, -P*C*H<), 37.6 (m, -P*C*H<), 29.8 (s, Cy), 28.9 (s, Cy), 28.2 (s, Cy), 27.9 (s, Cy), 27.4 (s, Cy), 27.2 (s, Cy), 19.2 (m, >P*C*H_2*C*H_2P<).

IR (cm^{-1}, ATR) 1676, 1660 (NO).

Anal. Calcd for $C_{29}H_{65}MoNO_3P_4$: C, 47.68; H, 7.39; N, 2.14. Found: C, 47.45; H, 7.25; N, 1.97.

Mo(dcype)(dippe)(NO)Cl (22)

The amalgam (10.7 g) containing 1% of sodium (107.0 mg, 4.64 mmol, 5 eq.) was added to the suspension of Mo(dcype)Cl_3(NO) (**21**) (304.0 mg, 0.46 mmol) in 15 mL

THF. Then the solution of dippe ligand (121.5 mg, 0.46 mmol) in 10 mL THF was added immediately after amalgam. The reaction mixture was stirred for 10 h. Then the suspension formed was removed from the amalgam, and filtered through celite. The residue on the celite was washed with THF until the solution became colorless. The solvent was removed from the combined THF fraction under reduced pressure. The residue was washed with pentane (3×5 mL) and dried in vacuum.

Yield: 284 mg, 72%.

^{1}H NMR (500.2 MHz, THF-d_8, 25 °C): δ sets of multiplets from 2.6 to 1.2.

^{31}P {^{1}H} NMR (202.5 MHz, THF-d_8, 25 °C): δ 59.6 (dd, (iPr)$_2$PCH$_2$CH$_2$P(iPr)$_2$, $^{2}J_{PP}$ = 135.8 Hz), 54.0 (dd, (Cy$_2$PCH$_2$CH$_2$PCy$_2$, $^{2}J_{PP}$ = 135.8 Hz).

^{13}C {^{1}H} NMR (160.5 MHz, THF-d_8, 25 °C): δ 39.6 (d, -P*C*H<, $^{1}J_{PC}$ = 15.7 Hz), 36.6 (d, -P*C*H<, $^{1}J_{PC}$ = 10.1 Hz), 31.2 (d, -PCH(CH$_2$)$_2$(*C*H$_2$)$_2$CH), $^{3}J_{PC}$ = 3.2 Hz), 30.4 (s, -PCH(CH$_2$)$_2$(CH$_2$)$_2$*C*H)), 30.3 (d, -PCH(CH$_2$)$_2$(*C*H$_2$)$_2$CH), $^{3}J_{PC}$ = 3.2 Hz), 30.0 (s, -PCH(CH$_2$)$_2$(CH$_2$)$_2$*C*H)), 29.2 (d, -P*C*H(CH$_3$)$_2$, $^{1}J_{CH}$ = 16.5 Hz), 28.8 (d, -PCH(*C*H$_2$)$_2$(CH$_2$)$_2$CH), $^{2}J_{PC}$ = 12.4 Hz), 28.5 (d, -PCH(*C*H$_2$)$_2$(CH$_2$)$_2$CH), $^{2}J_{PC}$ = 9.5 Hz), 26.2 (d, -P*C*H(CH$_3$)$_2$, $^{1}J_{CH}$ = 11.1 Hz), 20.6 (s, -PCH(*C*H$_3$)$_2$), 20.4 (s, -PCH(*C*H$_3$)$_2$), 20.1 (s, -PCH(*C*H$_3$)$_2$), 20.0 (s, -PCH(*C*H$_3$)$_2$), 18.3 (t, >P*C*H$_2$*C*H$_2$P<, $^{1}J_{PC}$ = 17.7 Hz), 17.9 (t, >P*C*H$_2$*C*H$_2$P<, $^{1}J_{PC}$ = 17.7 Hz).

IR (cm^{-1}, ATR) 1527 (NO).

Anal. Calcd for $C_{40}H_{80}ClMoNOP_4$: C 56.76; H 9.53; N 1.65. Found: C 56.50; H 9.41; N 1.46.

Mo(dcype)(dippe)(NO)H (23)

The 1 M solution of NaHBEt$_3$ (0.53 mL, 0.53 mmol, 3 eq.) was added to the solution of Mo(dcype)(dippe)(NO)H (**22**) (150 mg, 0.18 mmol) in 10 mL THF. The reaction mixture was stirred until the starting material was consumed (^{31}P {^{1}H} NMR monitoring). Then THF was removed under reduced pressure, and the residue was dissolved in 5 mL of toluene. 1 mL of NH$_2$CH$_2$CH$_2$NH$_2$ was added to the toluene solution to remove NaHBEt$_3$ coordinated to the NO group. The precipitate formed was filtered off and the toluene was removed in vacuum. The residue was extracted with

hexane. The combined hexane fractions were concentrated to one third of the original volume and cooled to -30 °C.

Yield: 96 mg, 67%.

^{1}H NMR (500.2 MHz, THF-d_8, 25 °C): δ sets of multiplets from 2.6 to 1.2, -4.12 (quintet, Mo–*H*, $^{2}J_{PH}$ = 27.5 Hz).

^{31}P {^{1}H} NMR (202.5 MHz, THF-d_8, 25 °C): δ 86.2 (dd (AB), (*i*Pr)$_2$PCH$_2$CH$_2$P(*i*Pr)$_2$, $^{2}J_{PP}$ = 99.0 Hz, 17.6 Hz), 77.5 (dd (AB), Cy$_2$PCH$_2$CH$_2$PCy$_2$, $^{2}J_{PP}$ = 99.0 Hz, 17.6 Hz).

^{13}C {^{1}H} NMR (160.5 MHz, THF-d_8, 25 °C): δ 42.0 (d, -P*C*H<, $^{1}J_{PC}$ = 17.0 Hz), 40.3 (d, -P*C*H<, $^{1}J_{PC}$ = 14.8 Hz), 31.6 (d, -P*C*H(CH$_3$)$_2$, $^{1}J_{CH}$ = 18.1 Hz), 30.5 (s, Cy) 29.95 (s, Cy), 29.7 (s, Cy), 29.0 (d, -P*C*H(CH$_3$)$_2$, $^{1}J_{CH}$ = 16.4 Hz), 28.9 (s, Cy), 28.6 (t, >P*C*H$_2$*C*H$_2$P<, $^{1}J_{PC}$ = 13.8 Hz), 27.76 (s, Cy), 25.7 (s, Cy), 21.5 (t, >P*C*H$_2$*C*H$_2$P<, $^{1}J_{PC}$ = 18.3 Hz), 21.2 (d, -PCH(*C*H$_3$)$_2$, $^{2}J_{PC}$ = 5.9 Hz), 20.3 (d, -PCH(*C*H$_3$)$_2$, $^{2}J_{PC}$ = 4.8 Hz), 20.0 (d, -PCH(*C*H$_3$)$_2$, $^{2}J_{PC}$ = 4.0 Hz), 18.4 (d, -PCH(*C*H$_3$)$_2$, $^{2}J_{PC}$ = 6.3 Hz).

IR (cm^{-1}, ATR) 1537 (MoH), 1500(NO).

Anal. Calcd for $C_{40}H_{81}MoNOP_4$: C 59.17; H 10.06; N 1.73. Found: C 59.55; H 10.20; N 1.84.

[Mo(dippe)(dcype)(NO)][BAr$^{F}_4$] (24)

3 mL of Et$_2$O was added to the mixture of Mo(dippe)(dcype)(NO)H (47.4 mg, 0.0585 mmol) and [H(Et$_2$O)$_2$][BAr$^{F}_4$] (59.2 mg, 0.0585 mmol). After the evolution of H_2 gas had stopped the reaction mixture was stirred for 30 min. Then the solvent was removed in vacuum. 3 mL of pentane was added to the residue, and then Et$_2$O was added dropwise until the oil was completely solved. The mixture was cooled to -30 °C to afford green powder that was filtered off and dried in vacuum.

Yield: 55.8 mg, 57%.

^{1}H NMR (500.2 MHz, ClC_6D_5, 25 °C): δ 8.40 (s, 8 H, o-BAr^{F}), 7.78 (s, 4 H, p-BAr^{F}), 2.50 (m, 2 H, -PC*H*(CH$_3$)), sets of multiplets from 2.4 to 0.95, 0.72 (m, -C*H*$_3$), -0.27 (m, agostic H).

^{31}P {^{1}H} NMR (202.5 MHz, ClC_6D_5, 25 °C): δ 73.4 (dd (AB), (*i*Pr)$_2$PCH$_2$CH$_2$P(*i*Pr)$_2$, $^{2}J_{PP}$ = 99.2 Hz, 16.0 Hz), 77.5 (dd (AB), Cy$_2$PCH$_2$CH$_2$PCy$_2$, $^{2}J_{PP}$ = 99.2 Hz, 16.0 Hz).

^{13}C {^{1}H} NMR (160.5 MHz, ClC_6D_5, 25 °C): δ 159.4 (quart, $^{1}J_{BC}$ = 50.0 Hz, i-BAr^F_4), 132.0 (s, o-BAr^F_4), 126.5 (m, m-BAr^F_4), 121.9 (quart, $^{1}J_{CF}$ = 273.2 Hz, -*C*F_3), 114.8 (s, p-BAr^F_4), 36.92 (d, -P*C*H<, $^{1}J_{PC}$ =22.9 Hz), 36.4 (d, -P*C*H<, $^{1}J_{PC}$ = 18.3 Hz), 27.16 (d, -P*C*H$(CH_3)_2$, $^{1}J_{CH}$ = 24.7 Hz), 26.5 (s, Cy), 25.7 (s, Cy), 25.5 (d, Cy, $^{2}J_{PC}$= 8.4 Hz), 24.3 (t, >P*C*H_2*C*H_2P<, $^{1}J_{PC}$ = 15.2 Hz), 23.8 (s, Cy), 23.5 (d, -P*C*H$(CH_3)_2$, $^{1}J_{CH}$ = 17.7 Hz), 23.0 (s, Cy), 16.2 (s, -PCH(*C*$H_3)_2$), 16.0 (s, -PCH(*C*$H_3)_2$), 15.55 (s, -PCH(*C*$H_3)_2$), 15.2 (s, -PCH(*C*$H_3)_2$), 14.3 (m, >P*C*H_2*C*H_2P<).

IR (cm^{-1}, ATR) 1589 (NO).

Anal. Calcd for $C_{72}H_{92}BF_{24}MoNOP_4$: C 51.66; H 5.54; N 0.84. Found: C 51.83; H 5.61; N 0.79.

6.2.5 Complexes bearing a diphosphine ligand and two carbonyls

General procedure for the synthesis of M(P∩P)$(CO)_2$(NO)Cl, 25a, 25b, 25c, 25d and 26a

The solution of a diphosphine ligand (1.0 mmol) in 10 mL of THF was added to the solution of $M(CO)_4ClAlCl_3$ (M= Mo, W) (1.0 mmol) in 15 mL of THF. The reaction mixture was stirred for 10 h at room temperature. Then the solvent was removed in vacuum. The residue was extracted with Et_2O. The combined Et_2O fractions were concentrated to the half of the original volume and cooled to -30 °C. The precipitation formed was filtered off and dried in vacuum.

Mo(dippp)$(CO)_2$(NO)Cl (**25a**)

Yield: 372.2 mg, 75%.

^{1}H NMR (400.1 MHz, CD_2Cl_2, 25 °C): δ 2.36 (m, 2 H, -PC*H*$(CH_3)_2$), 2.27 (m, 2 H, -PC*H*$(CH_3)_2$), 2.12 (m, 4 H, -PCH_2C*H*$_2$$CH_2$P-), 1.90 (m, 8 H, -PC*H*$_2$$CH_2$C*H*$_2$P-), set of the multiplets from 1.33 to 1.25 (24 H, -C*H*$_3$).

^{31}P {^{1}H} NMR (162.0 MHz, CD_2Cl_2, 25 °C): δ 21.5 (s).

^{13}C {^{1}H} NMR (100.6 MHz, CD_2Cl_2, 25 °C): δ 2l5.9 (dd, CO, $^{2}J_{CP}$ = 22.7 Hz), 27.4 (m, -P*C*H$(CH_3)_2$), 26.6 (m, -P*C*H$(CH_3)_2$), 21.9 (m, -P*C*$H_2$$CH_2$*C*$H_2$P-), 20.0 (m, -P$CH_2$*C*$H_2$$CH_2$P-), 19.9 (s, -*C*$H_3$), 19.7 (s, -*C*$H_3$), 19.1 (s, -*C*$H_3$).

IR (cm^{-1}, ATR) 2019, 1950 (CO), 1610 (NO).

Anal. Calcd for $C_{17}H_{35}ClMoNO_3P_2$: C 41.27; H 7.13; N 2.83. Found: C 41.08; H 7.04; N 2.69.

Mo(dippe)$(CO)_2$(NO)Cl (**25b**).

Yield: 205.9 mg, 43%.

^{1}H NMR (400.1 MHz, CD_2Cl_2, 25 °C): δ 2.41 (m, 2 H, -PC*H*$(CH_3)_2$), 2.30 (m, 2 H, -PC*H*$(CH_3)_2$), 1.94 (m, 4 H, -PCH_2CH_2P-), set of the multiplets from 1.37 to 1.23 (24 H, -CH_3).

^{31}P {^{1}H} NMR (162.0 MHz, CD_2Cl_2, 25 °C): δ 61.1 (s).

^{13}C {^{1}H} NMR (100.6 MHz, CD_2Cl_2, 25 °C): δ 217.0 (dd, CO, $^2J_{CP}$ = 10.7 Hz), 25.6 (m, -P*C*H$(CH_3)_2$, 24.0 (m, -P*C*H$(CH_3)_2$, 22.9 (dd, -P*C*$H_2C$$H_2$P-, $^1J_{CP}$ = 14.3 Hz), 20.5 (s, -*C*H_3), 20.3 (s, -*C*H_3), 20.2 (s, -*C*H_3), 18.6 (s, -*C*H_3).

IR (cm^{-1}, ATR) 2020, 1949 (CO), 1611 (NO).

Anal. Calcd for $C_{16}H_{32}ClMoNO_3P_2$: C 40.05; H 6.72; N 2.92. Found: C 40.21; H 6.63; N 2.81.

Mo(dippf)$(CO)_2$Cl, (**25c**)

Yield: 406.8 mg, 64%.

^{1}H NMR (400.1 MHz, CD_2Cl_2, 25 °C): δ 4.56 (s, 2 H, Cp), 4.45 (s, 2 H, Cp), 4.44 (s, 2 H, Cp), 4.41 (s, 2 H, Cp), 2.55 (m, 4 H, -PC*H*$(CH_3)_2$), set of the multiplets from 1.55 to 1.23 (24H, CH_3).

^{31}P{^{1}H} NMR (162.0 MHz, CD_2Cl_2, 25 °C): δ 29.8 (s).

^{13}C {^{1}H} NMR (100.6 MHz, CD_2Cl_2, 25 °C): δ 2l6.5 (dd, CO, $^2J_{CP}$ = 18.1 Hz), 76.4 (m, P–*C*$(CH)_2(CH)_2$), 75.6 (t, P–C(*C*$H)_2(CH)_2$, $^2J_{CP}$ = 5.0 Hz), 75.3 (t, P–C(*C*$H)_2(CH)_2$, $^2J_{CP}$ = 4.0 Hz), 71.7 (t, P–C$(CH)_2$(*C*$H)_2$, $^2J_{CP}$ = 2.0 Hz), 71.4 (t, P–C$(CH)_2$(*C*$H)_2$, $^2J_{CP}$ = 2.0 Hz), 29.2 (t, -P*C*H$(CH_3)_2$, $^1J_{CP}$ = 8.03 Hz), 28.7 (t, -P*C*H$(CH_3)_2$, $^1J_{CP}$ = 9.0 Hz), 20.9 (s, -*C*H_3), 20.5 (s, -*C*H_3), 19.8 (s, -*C*H_3), 18.8 (s, -*C*H_3).

IR (cm^{-1}, ATR) 2021, 1950 (CO), 1610 (NO).

Anal. Calcd for $C_{24}H_{36}ClNO_3P_2FeMo$: C, 45.34; H, 5.71; N, 2.20. Found: C, 45.23; H, 5.80; N, 2.15.

Mo(dcype)$(CO)_2$(NO)Cl, (**25d**)

Yield: 265.6 mg, 83%.

^{1}H NMR (500.2 MHz, CD_2Cl_2, 25 °C): δ set of multiplets from 2.2 to 1.1.

^{31}P {^{1}H} NMR (202.5 MHz, CD_2Cl_2 25 °C): δ 53.5 (s).

^{13}C {^{1}H} NMR (160.5 MHz, CD_2Cl_2, 25 °C): δ 2l7.4 (dd, CO, $^2J_{CP}$ = 10.7 Hz), 35.9 (m, -P*C*H$(CH_2)_2(CH_2)_2$CH), 34.0 (m, -P*C*H$(CH_2)_2(CH_2)_2$CH), 30.7 (s, Cy), 30.6 (s, Cy), 30.3 (s, Cy), 29.1 (s, Cy), 28.1 (m, Cy), 27.8 (m, Cy), 27.7 (m, Cy), 26.7 (s, Cy), 26.6 (s, Cy), 21.0 (dd, -P*C*H_2*C*H_2P-, $^1J_{CP}$ = 14.3 Hz).

IR (cm^{-1}, ATR) 2022, 1948 (CO), 1614 (NO).

Anal. Calcd for $C_{28}H_{48}ClMoNO_3P_2$: C, 52.54; H, 7.56; N, 2.19. Found: C, 52.38; H, 7.47; N, 2.15.

W(dippp)$(CO)_2$(NO)Cl (**26a**)

Yield: 550.0 mg, 95%.

^{1}H NMR (400.1 MHz, CD_2Cl_2, 25 °C): δ 2.44 (m, 2 H, -PC*H*$(CH_3)_2$), 2.36 (m, 2 H, -PC*H*$(CH_3)_2$), 2.17 (m, 2 H, -PCH_2C*H*$_2$$CH_2$P-), 1.97 (m, 4 H, -PC*H*$_2$$CH_2$C*H*$_2$P-), set of the multiplets from 1.35 to 1.25 (24 H, C*H*$_3$).

^{31}P {^{1}H} NMR (162.0 MHz, CD_2Cl_2, 25 °C): δ 7.6 (s, $^1J_{PW}$ (d, satellites) = 240.8 Hz).

^{13}C {^{1}H} NMR (100.6 MHz, CD_2Cl_2, 25 °C): δ 2l1.4 (dd, CO, $^2J_{CP}$ = 15.5 Hz), 27.9 (m, -P*C*H$(CH_3)_2$), 27.1 (m, -P*C*H$(CH_3)_2$), 21.4 (m, -P*C*$H_2$$CH_2$*C*$H_2$P-), 20.5 (m, -P$CH_2$*C*$H_2$$CH_2$P-), 20.0 (s, -*C*$H_3$), 19.7 (s, -*C*$H_3$), 19.2 (s, -*C*$H_3$), 19.1 (s, -*C*$H_3$).

IR (cm^{-1}, ATR) 2007, 1929 (CO), 1599 (NO).

Anal. Calcd for $C_{17}H_{34}ClNO_3P_2W$: C, 35.10; H, 5.89; N, 2.41. Found: C, 35.38; H, 5.99; N, 2.40.

General procedure for the synthesis M(P∩P)$(CO)_2$(NO)H, 27a, 27b, 27c, 27d, 28a.

To the mixture of Mo(P∩P)$(CO)_2$(NO)Cl (0.25 mmol) and $LiBH_4$ (27.5 mg, 1.25 mmol) 10 mL of Et_3N was added. The reaction mixture was stirred at room temperature until the starting material was consumed (^{31}P {^{1}H} NMR monitoring) (~ 10 h). The Et_3N

was removed in vacuum. The residue was extracted with benzene until the extracted solution became colorless. The extrats were combined and the benzene was evaporated. Then other hexane extraction was carried out until the extraction solution was colorless. The hexanes fraction were combined and concentrated to half to the original volume and cooled to -30°C. The precipitate formed was filtered off and dried in vacuum.

Mo(dippp)$(CO)_2$(NO)H, (**27a**)

Yield: 76.8 mg, 67%.

^{1}H NMR (400.1 MHz, C_6D_6, 25 °C): δ set of the multiplets from 1.82 to 1.62 (4 H, -PC*H*$(CH_3)_2$), set of the multiplets from 1.62 to 1.28 (6H, -PCH_2CH_2CH_2P-), set of the multiplets from 1.15 to 0.79 (24 H, -CH_3), -2.28 (t, 1 H, Mo–*H*, $^2J_{PH}$ = 24.0 Hz).

^{31}P {^{1}H} NMR (162.0 MHz, C_6D_6, 25 °C): δ 41.1 (s).

^{13}C {^{1}H} NMR (100.6 MHz, C_6D_6, 25 °C): δ 226.0 (dd, CO, $^2J_{CP}$ = 10.7 Hz), 29.2 (t, -P*C*H$(CH_3)_2$, $^1J_{CP}$ = 10.7 Hz), 27.6 (t, -P*C*H$(CH_3)_2$, $^1J_{CP}$ = 13.1 Hz), 22.7 (t, -PCH$_2$*C*H$_2$CH$_2$P-, $^2J_{CP}$ = 4.8 Hz), 20.0 (t, -P*C*H$_2$CH$_2$*C*H$_2$P-, $^1J_{CP}$ = 9.5 Hz), 19.6 (s, -*C*H$_3$), 18.8 (s, -*C*H$_3$), 18.8 (s, -*C*H$_3$), 17.5 (s, -*C*H$_3$).

IR (cm^{-1}, ATR) 1983, 1910 (CO), 1653 (MoH), 1570 (NO).

Anal. Calcd for $C_{17}H_{37}MoNO_3P_2$: C, 44.26; H, 8.08; N, 3.04. Found: C, 44.27; H, 7.99; N, 3.10.

Mo(dippe)$(CO)_2$(NO)H (**27b**)

Yield: 59.4 mg, 53%.

^{1}H NMR (400.1 MHz, C_6D_6, 25 °C): δ 1.78 (m, 2 H, -PC*H*$(CH_3)_2$), 1.67 (m, 2 H, -PC*H*$(CH_3)_2$), 1.18 (m, 4 H, -PCH_2CH_2P-), set of the multiplets from 1.09 to 0.81 (24 H, CH_3), -3.43 (t, 1 H, Mo–*H*, $^2J_{PH}$ = 26.3 Hz).

^{31}P {^{1}H} NMR (162.0 MHz, C_6D_6, 25 °C): δ 84.5 (s).

^{13}C {^{1}H} NMR (100.6 MHz, C_6D_6, 25 °C): δ 226.8 (dd, CO, $^2J_{CP}$ = 10.7 Hz), 28.3 (m, -P*C*H$(CH_3)_2$, 26.7 (m, -P*C*H$(CH_3)_2$, 22.5 (dd, -P*C*H$_2$*C*H$_2$P-, $^1J_{CP}$ = 15.50 Hz), 19.7 (s, -*C*H$_3$), 19.5 (s, -*C*H$_3$), 19.3 (s, -*C*H$_3$), 18.8 (s, -*C*H$_3$).

IR (cm^{-1}, ATR) 1983, 1910 (CO), 1653 (MoH), 1570 (NO).

Anal. Calcd for $C_{16}H_{35}MoNO_3P_2$: C 42.96; H 7.89; N 3.13. Found: C 42.71; H 7.79; N 3.18.

Mo(dippf)$(CO)_2$(NO)H, (**27c**)

Yield:74.6 mg, 49%.

^{1}H NMR (400.1 MHz, C_6D_6, 25 °C): δ 4.17 (s, 2 H, Cp), 4.03 (s, 2 H, Cp), 4.01 (s, 2 H, Cp), 3.98 (s, 2 H, Cp), 2.12 (m, 4 H, -PC*H*$(CH_3)_2$), set of the multiplets from 1.27 to 0.96 (24H, C*H*$_3$), -1.20 (t, 1 H, Mo–*H*, $^2J_{PH}$ = 23.6 Hz).

^{31}P{^{1}H} NMR (162.0 MHz, C_6D_6, 25 °C): δ 48.2 (s).

^{13}C {^{1}H} NMR (100.6 MHz, C_6D_6, 25 °C): δ 226.2 (dd, CO, $^2J_{CP}$ = 11.0 Hz), 76.9 (m, P -*C*$(CH)_2(CH)_2$), 75.3 (t, P -C(*C*H$)_2$(CH$)_2$, $^2J_{CP}$ = 4.0 Hz), 74.9 (t, P–C(*C*H$)_2$(CH$)_2$, $^2J_{CP}$ = 4.0 Hz), 71.0 (t, P–C(CH$)_2$(*C*H$)_2$, $^2J_{CP}$ = 2.0 Hz), 70.9 (t, P–C(CH$)_2$(*C*H$)_2$, $^2J_{CP}$ = 2.0 Hz), 29.2 (dd, -P*C*H$(CH_3)_2$, $^1J_{CP}$ = 9.0 Hz), 26.5 (dd, -P*C*H$(CH_3)_2$, $^1J_{CP}$ = 10.0 Hz), 20.0 (s, -*C*H$_3$), 19.8 (s, -*C*H$_3$), 19.1 (s, -*C*H$_3$), 19.1 (s, -*C*H$_3$).

IR (cm^{-1}, ATR) 1983, 1902 (CO), 1637 (MoH), 1574 (NO).

Anal. Calcd for $C_{24}H_{37}FeMoNO_3P_2$: C, 47.94; H, 6.20; N, 2.33. Found: C, 47.80; H, 6.11; N, 2.27.

Mo(dcype)$(CO)_2$(NO)H (**27d**)

Yield: 95.6 mg, 63%.

^{1}H NMR (400.1 MHz, C_6D_6, 25 °C): set of multiplets from 2.2 to 1.1, -3.25 (t, 1H, Mo–*H*, $^2J_{PH}$ = 26.3 Hz).

^{31}P {^{1}H} NMR (162.0 MHz, C_6D_6, 25 °C): δ 53.5 (s).

^{13}C {^{1}H} NMR (100.6 MHz, C_6D_6, 25 °C): δ 227.1 (dd, CO, $^2J_{CP}$ = 10.7 Hz), 38.0 (m, -P*C*H<, 37.0 (m, -P*C*H<, 29.9 (s, -Cy), 29.8 (s, -Cy), 29.2 (s, -Cy), 28.9 (s, -Cy), 27.8 (m, -Cy), 26.8 (s, -Cy), 26.6 (s, -Cy), 22.6 (dd, -P*C*H$_2$*C*H$_2$P-, $^1J_{CP}$ = 15.5 Hz).

IR (cm^{-1}, ATR) 1986, 1920 (CO), 1647 (MoH), 1574 (NO).

Anal. Calcd for $C_{28}H_{51}MoNO_3P_2$: C, 55.35; H, 68.46; N, 2.31. Found: C, 55.17; H, 8.34; N, 2.26.

W(dippp)$(CO)_2$(NO)H (**28a**)

Yield: 84.0 mg, 61%.

^{1}H NMR (400.1 MHz, C_6D_6, 25 °C): δ 1.93 (m, 4 H, -PC*H*$(CH_3)_2$), 1.61 (m, 2 H, -$PCH_2CH_2CH_2P$-), set of the multiplets from 1.26 to 1.15 (20H, -C*H*$_3$), 0.93 (m, 4H, -CH_3), -1.19 (t, W–H, $^2J_{PH}$ = 24.0 Hz).

^{31}P {^{1}H} NMR (162.0 MHz, C_6D_6, 25 °C): δ 20.9 (s, $^1J_{PW}$ (d, satellites) = 243.8 Hz).

^{13}C {^{1}H} NMR (100.6 MHz, C_6D_6, 25 °C): δ 2l7.7 (dd, CO, $^2J_{CP}$ = 14.1 Hz), 29.7 (m, -P*C*H$(CH_3)_2$, 28.4 (m, -P*C*H$(CH_3)_2$, 23.8 (t, -$PCH_2CH_2CH_2P$-, $^2J_{CP}$ = 4.0 Hz), 21.0 (dd, -$PCH_2CH_2CH_2P$-, $^1J_{CP}$ = 9.0 Hz), 19.9 (s, -*C*H_3), 19.0 (s, -*C*H_3), 19.0 (s, -*C*H_3), . 17.6 (s, -*C*H_3).

IR (cm^{-1}, ATR) 1976, 1898 (CO), 1726 (WH), 1568 (NO).

Anal. Calcd for $C_{17}H_{35}NO_3P_2W$: C, 37.31; H, 6.45; N, 2.56. Found: C, 37.45; H, 6.50; N, 2.50.

Procedure for the synthesis of [M(dippp)$(CO)_2$(NO)(THF)][BAr^F_4] 29a and 30a

To a solution of M(dippp)$(CO)_2$H (M = Mo, W) (0.043 mmol) in 2 mL of THF the solution of [H$(Et_2O)_2$][BAr^F_4] (43.8 mg, 0.043 mmol) in 2 mL of THF was slowly added at room temperature. The reaction mixture was stirred for 2 hours. Then the solvent was evaporated in vacuum. 2 mL of hexane were added to the residue, and then Et_2O was added to the suspension dropwise until the solid was completely dissolved. The solution was cooled to -30°C to afford the precipitation. The precipitate was filtered and dried in vacuum.

[Mo(dippp)$(CO)_2$(NO)(THF)][BAr^F_4] (**29a**)

Yield: 41.4 mg, 69%.

^{1}H NMR (400.1 MHz, THF-d_8, 25 °C): δ 7.79 (s, 8 H, o-Ph), 7.57 (s, 4 H, p-Ph), 3.62 (m, 4H, THF), 2.48 (m, 4H, -PC*H*$(CH_3)_2$), 2.23 (m, 4H, -P*C*H_2CH_2C*H*$_2$P-), 1.91 (m, 2H, -PCH_2C*H*$_2CH_2$P-), 1.77 (m, 4H, THF), set of the multiplets from 1.39 to 1.28 (24H, -C*H*$_3$).

^{31}P {^{1}H} NMR (162.0 MHz, THF-d_8, 25 °C): δ 17.7 (s).

^{13}C {^{1}H} NMR (100.6 MHz, THF-d_8, 25 °C): δ 214.1 (dd, CO, $^{2}J_{CP}$ = 16.7 Hz), 163.0 (quart, i-BAr^{F}_4, $^{1}J_{BC}$ = 50.0 Hz,), 135.8 (s, o-BAr^{F}_4), 130.1 (m, m-BAr^{F}_4), 125.5 (quart, -CF_3 $^{1}J_{CF}$ = 273.4 Hz,), 118.4 (s, p-BAr^{F}_4), 68.2 (s, THF), 27.9 (m, -P*C*H$(CH_3)_2$), 26.4 (s, THF), 22.5 (t, -P*C*$H_2$$CH_2$*C*$H_2$P-, $^{2}J_{CP}$ = 8.3 Hz), 20.4 (s, -*C*H_3), 20.1 (s, -PCH_2*C*$H_2$$CH_2$P-), 19.4 (s, -*C*$H_3$), 19.1 (s, -*C*$H_3$), 18.7 (s, -*C*$H_3$).

IR (cm^{-1}, ATR) 2044, 1978 (CO), 1682 (NO).

Anal. Calcd for $C_{53}H_{54}BF_{24}MoNO_3P_2$: C, 45.68; H, 3.91; N, 1.01. Found: C, 45.61; H, 3.78; N, 1.00.

[W(dippp)$(CO)_2$(NO)(THF)][BAr^{F}_4] (**30a**)

Yield: 44.1 mg, 69%.

^{1}H NMR (500.2 MHz, THF-d_8, 25 °C): δ 7.79 (s, 8 H, o-Ph), 7.57 (s, 4 H, p-Ph), 3.62 (m, THF), 2.61 (m, 4H, -PC*H*$(CH_3)_2$), 2.28 (m, 4H, -PC*H*$_2$$CH_2$C*H*$_2$P-), 1.93 (m, 2H, -PC$H_2$C*H*$_2$$CH_2$P-), 1.77 (m, 4H, THF), set of the multiplets from 1.40 to 1.29 (24H, -C*H*$_3$).

^{31}P {^{1}H} NMR (202.6 MHz, THF-d_8, 25 °C): δ 8.8 (s, $^{1}J_{PW}$ (d, satellites) = 246.3 Hz).

^{13}C {^{1}H} NMR (125.8 MHz, THF-d_8, 25 °C): δ 211.6 (dd, CO, $^{2}J_{CP}$ = 15.1 Hz), 163.0 (quart, i-BAr^{F}_4, $^{1}J_{BC}$ = 50.0 Hz,), 135.8 (s, o-BAr^{F}_4), 130.1 (m, m-BAr^{F}_4), 125.5 (quart, -CF_3, $^{1}J_{CF}$ = 273.3 Hz,), 118.4 (s, p-BAr^{F}_4), 68.4 (s, THF), 28.6 (m, -P*C*H$(CH_3)_2$), 26.6 (s, THF), 22.3 (m, -P*C*$H_2$$CH_2$*C*$H_2$P-), 20.8 (s, -PC$H_2$*C*$H_2$$CH_2$P-), 20.7 (s, -*C*$H_3$), 19.5 (s, -*C*$H_3$), 19.4 (s, -*C*$H_3$), 18.9 (s, -*C*$H_3$).

IR (cm^{-1}, ATR) 2027, 1953 (CO), 1666 (NO).

Anal. Calcd for $C_{49}H_{48}BF_{24}MoNO_3P_2$: C, 45.68; H, 3.91; N, 1.01. Found: C, 44.48; H, 3.99; N, 0.97.

Preparation of [Mo(dippp)$(CO)_2$(NO)(THF)][$B(C_6F_5)_4$] (31a)

The solution of [$H(Et_2O)_2$][$B(C_6F_5)_4$] (37.1 mg, 0.043 mmol) in 2 mL of THF was slowly added to a solution of Mo(dippp)$(CO)_2$H (0.043 mmol) in 2 mL of THF at room temperature. The reaction mixture was stirred for 2 hours. Then the solvent was evaporated in vacuum to afford oil that was used without further purification.

^{1}H NMR (400.1 MHz, THF-d_8, 25 °C): δ 3.37 (m, 4H, THF), 2.59 (m, 4H, -PC*H*$(CH_3)_2$), 2.23 (m, 4H, -PCH_2CH_2CH_2P-), 1.91 (m, 2H, -PCH_2CH_2CH_2P-), 1.77 (m, 4H, THF), set of the multiplets from 1.38 to 1.28 (24H, -CH_3).

^{31}P {^{1}H} NMR (162.0 MHz, THF-d_8, 25 °C): δ 16.5 (s).

^{13}C {^{1}H} NMR (125.8 MHz, THF-d_8, 25 °C): δ 214.0 (dd, CO, $^{2}J_{CP}$ = 22.1 Hz), 149.0 (br d, $^{1}J_{CF}$ = 235.9 Hz, o-C_6F_5), 139.1 (dm, $^{1}J_{CF}$ = 242.1 Hz, p-C_6F_5), 137.0 (dm, $^{1}J_{CF}$ = 244.1 Hz, m-C_6F_5), 125.7 (br m, i-C_6F_5), 68.10 (s, THF), 28.0 (m, -P*C*H$(CH_3)_2$), 26.0 (s, THF), 22.6 (t, -P*C*H_2CH_2*C*H_2P-, $^{2}J_{CP}$ = 8.0 Hz), 20.5 (s, -*C*H_3), 20.2 (s, -PCH_2*C*H_2CH_2P-), 19.5 (s, -*C*H_3), 19.2 (s, -*C*H_3), 18.8 (s, -*C*H_3).

IR (cm^{-1}, ATR) 2038, 1970 (CO), 1668 (NO).

The elemental analysis did not match to the calculated value due to the presence of the solvent in a non-stoichiometric ratio.

6.2.6 Complexes bearing two P*i*Pr$_3$ and two carbonyl ligands

Mo(P*i*Pr$_3$)$_2$(NO)(CO)$_2$Cl (32)

To the solution of Mo(NO)$(CO)_4ClAlCl_3$ (0.367 g, 0.90 mmol) in 5 mL of THF the solution of P*i*Pr_3 (0.541 g, 3.376 mmol, 3.75 equiv.) in 10 mL of THF were added. The reaction mixture was evacuated and then stirred for 36 h at room temperature. Then the solvent was removed under vacuum. The residue was extracted with Et_2O until the extract solution became colorless. The residue after Et_2O removel was extracted with hexane. The combined hexane fractions were concentrated to half to the volume and cooled to -30^{o}C. The precipitate formed was filtered off and dried in vacuum.

Yield: 310 mg, 61%.

^{1}H {P^{31}} NMR (500.2 MHz, benzene-d_6, 25 °C): δ 2.37 (m, 12 H, -C*H*$(CH_3)_2$), 1.24 (d, 64 H, -CH(C*H*$_3)_2$, $^{3}J_{HH}$ = 64.1 MHz).

^{31}P {^{1}H} NMR (202.5 MHz, benzene-d_6, 25 °C): δ 48.55 (s).

^{13}C {^{1}H} NMR (160.5 MHz, benzene-d_6, 25 °C): δ 219.14 (t, CO, $^{1}J_{CP}$ = 9.0 Hz), 25.42 (t,-*C*H$(CH_3)_2$, $^{1}J_{CP}$ = 10.3), 19.80 (-CH(*C*H$_3)_2$).

IR (cm^{-1}, ATR) 1937, 1867 (CO), 1616 (NO).

Anal. Calcd for $C_{20}H_{44}ClMoNO_3P_2$: C, 44.49; H, 8.21; N, 2.59. Found: C, 44.41; H, 8.56; N, 2.69.

$Mo(PiPr_3)_2(NO)(CO)_2H$ (33)

10 mL of Et_3N was added to the mixture of $Mo(PiPr_3)_2(NO)(CO)_2Cl$ (200.0 mg, 0.371 mmol) and $LiBH_4$ (40.0 mg, 1.86 mmol, 5 eq.). The solution became immediately red. The reaction mixture was stirred overnight at room temperature. Then Et_3N was removed in vacuum. The residue was extracted with benzene and then, after removal of the solvent, with hexane. The combined hexane extracts were concentrated until the precipitation started and then cooled to -30°C to afford a hazel powder.

Yield: 118 mg, 63%.

^{1}H NMR (500.2 MHz, benzene-d_6, 25 °C): δ 2.15 (m, 12 H, -C*H*$(CH_3)_2$), 1.86 (m, 64 H, -CH(C*H*$_3)_2$), -2.81 (t, 1H, Mo–H, $^2J_{PH}$ = 24.1 Hz).

^{31}P {^{1}H} NMR (202.5 MHz, benzene-d_6, 25 °C): δ 66.89 (s).

^{13}C {^{1}H} NMR (160.5 MHz, benzene-d_6, 25 °C): δ 228.9 (t, CO, $^2J_{CP}$ = 9.5 Hz), 27.33 (t,-*C*H(CH_3), $^1J_{CP}$ = 10.9), 19.80 (s,-CH(*C*$H_3)_2$).

IR (cm^{-1}, ATR) 1905, 1864 (CO), 1637 (MoH), 1570 (NO).

Anal. Calcd for $C_{20}H_{45}MoNO_3P_2$: C, 47.52; H, 8.97; N, 2.77. Found: C, 47.83; H, 9.07; N, 2.83.

$Mo(PiPr_3)_2(NO)(CO)_2(THF)BAr^F{}_4$ (34)

The solution of $[H(Et_2O)_2][BAr^F{}_4]$ (53.6 mg, 0.053 mmol) in 2 mL of THF was slowly added dropwise to the solution of $Mo(PiPr_3)_2(NO)(CO)_2H$ (26.8 mg, 0.053 mmol) in 2 mL of THF at room temperature. Then the reaction mixture was stirred for 2 hours. After removal of the solvent the residue was washed with hexane 3×2 mL and dried in vacuum.

Yield: 59.2 mg, 82%.

^{1}H {P^{31}} NMR (500.2 MHz, THF-d_8, 25 °C): δ 7.79 (s, 8 H, o-Ph), 7.57 (s, 4 H, p-Ph), 3.62 (m, THF), 1.78 (m, THF), 2.54 (m, 12 H, -C*H*$(CH_3)_2$), 1.44 (d, 64 H, -CH(C*H*$_3)_2$, $^3J_{HH}$ = 7.0 Hz).

^{31}P {^{1}H} NMR (202.5 MHz, THF-d_8, 25 °C): δ 51.1 (s).

^{13}C {^{1}H} NMR (160.5 MHz, THF-d_8, 25 °C): δ 218.8 (t, CO, $^{1}J_{CP}$ = 8.8 Hz), 163.0 (quart, $^{1}J_{BC}$ = 50.1 Hz, i-BAr^{F}_{4}), 135.81 (s, o-BAr^{F}_{4}), 130.1 (m, m-BAr^{F}_{4}), 125.5 (quart, $^{1}J_{CF}$ = 273.0 Hz, -CF_3), 118.4 (s, p-BAr^{F}_{4}), 26.44 (t, -*C*H$(CH_3)_2$, $^{1}J_{CP}$ = 10.8), 19.87 (s, -CH(*C*$H_3)_2$).

IR (cm^{-1}, ATR) 1953 (CO), 1679 (NO).

Anal. Calcd for $C_{56}H_{64}BF_{24}MoNO_4P_2$: C, 46.72; H, 4.48; N, 0.97. Found: C, 47.01; H, 4.79; N, 1.10.

6.2.7 Complexes bearign chiral ligands

Mo[(S,S)-dmpcp]$_2$(OPh)(NO) (35)

The solution of PhOH (2.0 mg, 0.022 mmol) in toluene (1 mL) was added to the solution of Mo[(S,S)-dmpcp]$_2$(H)(NO) (10.0 mg, 0.020 mmol) in 1 mL of toluene. The reaction mixture was stirred at room temperature for 1 h, whereupon the reaction complete (^{1}P {^{1}H} NMR monitoring). The solvent was removed under reduced pressure. The residue was washed with hexane and dried in vacuum to afford a yellow powder.

Yield: 9.3 mg, 78%.

^{1}H NMR (500.2 MHz, benzene-d_6, 25 °C): δ 7.28 (t, m-Ph, $^{3}J_{HH}$ = 7.5 Hz), 6.68 (t, p-Ph, $^{3}J_{HH}$ = 7.0 Hz), 6.45 (d, o-Ph, $^{3}J_{HH}$ = 8.0 Hz), 2.0 − 1.8 (m, 16H, C_5H_8), 1.35 (m, 6H, PMe_2), 1.33 (m, 6H, PMe_2), 1.29 (m, 6H, PMe_2), 1.07 (m, 6H, PMe_2).

^{31}P {^{1}H} NMR (202.5 MHz, benzene-d_6, 25 °C): δ 13.0, 10.1 (2t, $^{2}J_{PP}$ = 21.6 Hz)

^{13}C {^{1}H} NMR (160.5 MHz, benzene-d_6, 25 °C): δ 129.2 (s, OPh), 120.0 (s, OPh), 112.6 (s, OPh), 51.3, 50.6 (2m, PCH), 31.3 (s, $(CH_2)_2C$*H*$_2$), 22.6, 22.3 (2m, (C*H*$_2)_2CH_2$), 14.6, 14.4, 8.9, 8.2 (4m, PMe_2).

IR (cm^{-1}, ATR) 1519 (NO).

Anal. Calcd for $C_{24}H_{45}MoNO_2P_4$: C 48.09, H 7.57, N 2.34. found: C 48.30, H 7.61, N 2.55.

Insertion reaction of Mo[(S,S)-dmpcp]$_2$(NO)(H) with acetophenone

Mo[(S,S)-dmpcp]$_2$(H)(NO) (30.0 mg, 0.059 mmol) were placed in the NMR tube, than 0.4 mL of toluene-d_8 was added to dissolve the hydride. On the another side of the

tube the solution of $PhC(O)CH_3$ (7.1 mg, 0.059 mmol) in 0.4 mL toluene-d_8 was placed. Then the tube was closed with a teflon cap. Without mixing the solution the tube was taken out from the glovebox and immediately cooled up to -60°C. The temperature was kept at -60°C during 4 hours. After that time the reaction was completed as no signal of the starting hydride was observed in the $^{31}P\{^1H\}$ NMR spectra. Without further isolation the ^1H NMR was measured to determine the ratio of diasteriomers. The spectroscopic yield was found to be 100%. The ee of 20% was determined from the intergration ratio of the characteristic quartets of –PhC(*H*)O− protons appeared in the ^1H NMR spectra at 4.62 ppm for S isomer and at 4.57 ppm for R isomer.[174]

Insertion reaction of Mo[(S,S)-dmpcp]$_2$(NO)(H) with acetophenone and phenol

Mo[(S,S)-dmpcp]$_2$(H)(NO) (27.3 mg, 0.054 mmol) were placed into a NMR tube, then 0.4 mL of toluene was added to dissolve the hydride. On the another side of the tube the mixture of PhOH (5.0 mg, 0.054 mmol) and $PhC(O)CH_3$ (6.43 mg, 0.054 mmol) in 0.4 mL toluene was placed. Then the tube was closed with a teflon cap. Without mixing the solution the tube was taken out from the glovebox and immediately cooled up to -60 °C. The temperature was kept at -60 °C during 6 h to make sure that the reaction is complete. All volatile materials were transferred into a receiver cooled with liquid nitrogen by distillation in vacuum. An ee of 27% was determined after the reaction by GC using a chiral column. The retention time was 6.227 min for S-phenylethanol and 6.355 min for R-phenylethanol.

Preparation of the (S,S)-dippcp ligand

The (S,S)-dippcp ligand was obtained via reaction of (S,S)-$C_5H_8(PCl)_2$[164] (5.4 g, 0.02 mol) with *i*PrMgCl (6 eq.) according to procedure described in the literature.[175]
Yield: 3.80 g, 63%.

^{1}H NMR (500.2 MHz, $CDCl_3$, 25 °C): δ 1.84 (m, 2 H, -PC*H*$(CH_3)_2$), 1.78 (m, 4 H, C_5H_8), 1.60 (m, 2 H, -PC*H*$(CH_3)_2$), 1.59 (m, 2 H, C_5H_8), 1.17 (m, 4 H, C_5H_8) 1.09 − 0.98 (m, 64 H, CH_3).

^{31}P {^{1}H} NMR (202.5 MHz, $CDCl_3$, 25 °C): δ 12.4 (s).

^{13}C {^{1}H} NMR (160.5 MHz, $CDCl_3$, 25 °C): δ 29.3 (t, $^{2}J_{PC}$ = 3.0 Hz, CH_2), 27.1 (t, $^{3}J_{PC}$ = 2.0 Hz, CH_2), 22.6 (m, -P*C*H), 21.7 (t, $^{1}J_{PC}$ = 8.0 Hz, -P*C*H$(CH_3)_2$), 20.8 (s, Me), 20.7 (s, Me), 20.7 (s, Me), 20.6 (s, Me), 20.5 (s, Me), 20.5 (s, Me), 20.4 (s, Me), 20.3 (s, Me), 20.0 (t, $^{1}J_{PC}$ = 5.0 Hz, -P*C*H$(CH_3)_2$).

Insertion reaction of Mo[(S,S)-dippcp]$_2$(NO)(H) (36) with acetophenone and phenol

20 mg of the oily substance containing aprox. 12 mg (0.016 mmol) of Mo[(S,S)-dippcp]$_2$(NO)(H) (**36**) was dissolved in 0.4 mL of toluene. The solution was placed into the NMR tube. On the other side of the tube the mixture of PhOH (1.5 mg, 0.016 mmol) and PhC(O)CH_3 (1.9 mg, 0.016 mmol) in 0.4 mL toluene was placed. Then the tube was closed with a teflon cap. Without mixing the solution the tube was taken out from the glovebox and immediately cooled to -60 °C. The temperature was kept at -60 °C during 6 h to make sure that the reaction is complete. All volatile materials were transferred into a receiver cooled with liquid nitrogen by distillation in vacuum. An ee of 4% was determined by GC using a chiral column. The retention time was 6.227 min for S-phenylethanol and 6.355 min for R-phenylethanol.

6.3 Catalytic experiments

6.3.1 Catalytic hydrogenation of acetone-d$_6$

[Mo(dippe)$_2$(NO)][BAr$^F_4$] (13.7 mg, 0.009 mmol) were placed in Young's NMR tube. 0.6 mL of acetone-d$_6$ was added. The mixture was pressurized with 2.0 bar of hydrogen gas and heated at 60 °C. The reaction progress was monitored with the ^{1}H NMR spectrometry taking spectra every hour. The singlet resonance of the BAr$^F_4$ counterion at 7.66 ppm was taken as a reference signal to calculate the formation rate of the isopropyl alcohol.

6.3.2 General procedure for catalytic imine hydrogenation

The solution of a substrate (2.0 mmol) in C_5H_5Cl (5 mL) was added to the mixture of the M(P∩P)$(CO)_2$(NO)H complex (0.006 mmol, 0.3 mol.%) and $[H(Et_2O)_2][B(C_6F_5)_4]$ (5.0 mg, 0.006 mmol). The mixture was placed in the autoclave and pressurized with 30 bar of hydrogen gas. The monitoring of pressure diminution was carried out to measure the reaction rate. When no pressure changes were observed, the reaction mixture was taken out of the autoclave and filtered through silica gel. Without any further purification a GS-MS spectra were measured to determine the conversion of the hydrogenation reactions and identify the product. PhCH=N(α-naphtyl): rt = 10.532 min, m/z = 231; $PhCH_2NH$(α-naphtyl): rt = 10.607 min, m/z = 233; PhCH=NPh: rt = 7.460 min, m/z = 181; $PhCH_2NHPh$: rt = 7.695 min, m/z = 183; p-ClC_6H_4CH=NPh: rt = 8.636 min, m/z = 215; p-$ClC_6H_4CH_2NHPh$: rt = 8.989 min, m/z = 217; p-ClC_6H_4CH=N-*p*-C_6H_4Cl: rt = 9.639 min, m/z = 249; p-$ClC_6H_4CH_2NH$-p-C_6H_4Cl: rt = 10.114 min, m/z = 251; PhCH=N$CHPh_2$: rt = 10.589 min, m/z = 271; $PhCH_2NHCHPh_2$: rt = 10.386 min, m/z = 273; PhCH=NMes: rt = 8.301 min, m/z = 223; $PhCH_2$NHMes: rt = 8.491 min, m/z = 225; PhCH=N*i*Bu: rt = 4.876 min, m/z = 161; $PhCH_2$NH*i*Bu: rt = 5.756 min, m/z = 163.

6.4 X-ray structure analyses

All crystals were grown and prepared under an atmosphere of dry nitrogen in a glove box due to sensitivity of the compounds to air and moisture. Intensity data were collected at 183(2) K on a Stoe IPDS diffractometer (Imaging Plate Detector System with graphite-monochromated MoK_α radiation, λ = 0.71073 Å)[181] and on an Oxford Xcalibur diffractometer (4-circle kappa platform, Ruby CCD detector, and a single wavelength Enhance X-ray source with MoK_α radiation, λ = 0.71073 Å)[182]. The selected suitable single crystals were mounted using polybutene oil on the top of a glass fiber fixed on a goniometer head and immediately transferred to the diffractometer. The crystal structures were solved with SHELXS-97[183] using direct methods. The structure refinements were performed by full-matrix least-squares on F^2 with SHELXL-97.[183] The program PLATON[184] was used to check the results of the X-ray analyses. All hydrogen atoms

were placed on ideal positions and refined with fixed isotropic displacement parameters using a riding model.

Table 6.1 Summary of X-ray diffraction studies for **1** and **2**

	1	**2**
Empirical formula	$C_{28}H_{64}ClNOP_4W$	$C_{14}H_{32}Cl_3NOP_2W$
Formula weight	773.97	582.54
Temperature (K)	183(2)	183(2)
Wavelength (Å)	0.71073	0.71073
Crystal system, space group	Triclinic, P 1	Orthorhombic, $Pca2_1$
a (Å)	10.7933(14)	14.7278(5)
b (Å)	11.3598(16)	9.8789(7)
c (Å)	15.254(2)	14.3359(9)
α (deg)	89.951(17)	90
β (deg)	85.602(17)	90
γ (deg)	68.230(15)	90
Volume ($Å^3$)	1731.0(4)	14.3359(9)
Z, calculated density (g/cm)	2, 1.485	4, 1.855
Absorption coefficient (mm^{-1})	3.620	6.077
F(000)	796	1144
Crystal size (mm)	0.48 x 0.43 x 0.30	0.46 x 0.37 x 0.31
2θ scan range (deg)	3.29 to 25.00	2.86 to 29.99
Reflections collected	16869	25702
Reflections unique	5717	6008
Completeness to θ (%)	93.7	99.9
Absorption correction	Numerical	Numerical
Max./min. transmission	0.458 / 0.284	0.238 / 0.124
Data/restraints/parameters	5717 / 0 / 347	6008 / 1 / 207
Goodness-of-fit on F_2	1.055	0.981
Final R indices R1, wR2	0.0182, 0.0438	0.0283, 0.0576
R indices (all data) R1, wR2	0.0215, 0.0449	0.0310, 0.0581

Table 6.2 Summary of X-ray diffraction studies for **3** and **4**

	3	**4**
Empirical formula	$C_{28}H_{64}ClNOP_4W$	$C_{28}H_{64}ClMoNOP_4$
Formula weight	773.97	686.07
Temperature (K)	183(2)	183(2)
Wavelength (Å)	0.71073	0.71073
Crystal system, space group	Triclinic, P -1	Triclinic, P -1
a (Å)	10.7933(14)	10.8168(12)
b (Å)	11.3598(16)	11.3917(7)
c (Å)	15.254(2)	15.2248(12)
α (deg)	89.951(17)	89.893(6)
β (deg)	85.602(17)	85.617(7)
γ (deg)	68.230(15)	68.233(8)
Volume ($Å^3$)	1731.0(4)	1736.5(3)
Z, calculated density (g/cm)	2, 1.485	2, 1.312
Absorption coefficient (mm^{-1})	3.620	0.660
F(000)	796	732
Crystal size (mm)	0.48 x 0.43 x 0.30	0.44 x 0.31 x 0.10
2θ scan range (deg)	3.29 to 25.00	2.22 to 30.51
Reflections collected	16869	100479
Reflections unique	5717	10561
Completeness to θ (%)	93.7	99.6
Absorption correction	Numerical	Semi-empirical from equivalents
Max./min. transmission	0.458 / 0.284	1.00000 / 0.88885
Data/restraints/parameters	6851 / 0 / 402	10561 / 0 / 371
Goodness-of-fit on F_2	1.055	1.150
Final R indices R1, wR2	0.0182, 0.0438	0.0313, 0.0757
R indices (all data) R1, wR2	0.0215, 0.0449	0.0356, 0.0775

Table 6.3 Summary of X-ray diffraction studies for **5** and **6**

	5	**6**
Empirical formula	$C_{62}H_{142}B_2Cl_2Li_2N_2O_2P_8W_2$	$C_{56}H_{138}B_2Li_2N_2O_2P_8W_2$
Formula weight	1669.62	1522.62
Temperature (K)	183(2)	183(2)
Wavelength (Å)	0.71073	0.71073
Crystal system, space group	Monoclinic, P $2_1/c$	Triclinic, P -1
a (Å)	11.2516(12)	10.95100(10)
b (Å)	33.773(3)	11.27580(10)
c (Å)	11.4244(13)	15.7212(2)
α (deg)	90	85.2770(10)
β (deg)	112.980(12)	79.9990(10)
γ (deg)	90	73.7980(10)
Volume ($Å^3$)	3996.8(8)	1834.67(3)
Z, calculated density (g/cm)	2, 1.387	1, 1.378
Absorption coefficient (mm^{-1})	3.141	3.343
F(000)	1724	788
Crystal size (mm)	0.47 x 0.42 x 0.088	0.29 x 0.23 x 0.19
2θ scan range (deg)	2.24 to 25.00	2.26 to 30.51
Reflections collected	29577	97852
Reflections unique	6851	11194
Completeness to θ (%)	97.2	100.0
Absorption correction	Numerical	Semi-empirical from equivalents
Max./min. transmission	0.767 / 0.301	0.548 / 0.457
Data/restraints/parameters	6851 / 0 / 402	11194 / 0 / 370
Goodness-of-fit on F_2	1.250	1.097
Final R indices R1, wR2	0.0346, 0.0922	0.0181, 0.0474
R indices (all data) R1, wR2	0.0355, 0.0933	0.0211, 0.0489

Table 6.4 Summary of X-ray diffraction studies for **7** and **9**

	7	**9**
Empirical formula	$C_{28}H_{65}NOP_4W$	$C_{29}H_{65}NO_3P_4W$
Formula weight	739.53	783.54
Temperature (K)	183(2)	183(2)
Wavelength (Å)	0.71073	0.71073
Crystal system, space group	Orthorhombic, P c c n	Monoclinic, P 2_1
a (Å)	38.7832(3)	11.62950(10)
b (Å)	14.74120(10)	15.22860(10)
c (Å)	12.04370(10)	20.4436(2)
α (deg)	90	90
β (deg)	90	99.5789(8)
γ (deg)	90	90
Volume ($Å^3$)	6885.52(9)	3570.10(5)
Z, calculated density (g/cm)	8, 1.427	4, 1.458
Absorption coefficient (mm^{-1})	3.562	3.443
F(000)	3056	1616
Crystal size (mm)	0.39 x 0.37 x 0.30	0.26 x 0.15 x 0.07
2θ scan range (deg)	2.42 to 30.51	2.22 to 25.00
Reflections collected	111376	31502
Reflections unique	10516	11908
Completeness to θ (%)	100.0	99.9
Absorption correction	Semi-empirical from equivalents	Analytical
Max./min. transmission	1.00000 / 0.79839	0.806 / 0.595
Data/restraints/parameters	10516 / 0 / 336	11908 / 7 / 704
Goodness-of-fit on F_2	1.248	1.075
Final R indices R1, wR2	0.0237, 0.0485	0.0447, 0.1103
R indices (all data) R1, wR2	0.0310, 0.0546	0.0497, 0.1153

Table 6.5 Summary of X-ray diffraction studies for **10** and **11**

	10	**11**
Empirical formula	$C_{29}H_{65}MoNO_3P_4$	$C_{60}H_{78}BF_{24}NOP_4W$
Formula weight	695.64	1603.76
Temperature (K)	183(2)	183(2)
Wavelength (Å)	0.71073	0.71073
Crystal system, space group	Triclinic, P -1	Monoclinic, P $2_1/c$
a (Å)	10.8453(3)	12.24010(10)
b (Å)	23.7155(7)	14.69840(10)
c (Å)	31.2886(10)	37.7513(4)
α (deg)	96.445(3)	90
β (deg)	93.160(3)	98.5027(9)
γ (deg)	91.160(2)	90
Volume ($Å^3$)	7981.6(4)	6717.18(10)
Z, calculated density (g/cm)	9, 1.303	4, 1.586
Absorption coefficient (mm^{-1})	0.579	1.922
F(000)	3348	3232
Crystal size (mm)	0.18 x 0.13 x 0.04	0.33 x 0.18 x 0.14
2θ scan range (deg)	2.25 to 26.11	2.31 to 30.51
Reflections collected	98074	89016
Reflections unique	30443	20489
Completeness to θ (%)	95.8	99.9
Absorption correction	Semi-empirical from equivalents	Analytical
Max./min. transmission	0.977 / 0.955	0.793 / 0.634
Data/restraints/parameters	30443 / 2 / 1611	20489 / 3 / 861
Goodness-of-fit on F_2	0.818	1.036
Final R indices R1, wR2	0.0470, 0.0844	0.0378, 0.0935
R indices (all data) R1, wR2	0.1320, 0.0990	0.0558, 0.1043

Table 6.6 Summary of X-ray diffraction studies for **12** and **13**

	12	**13**
Empirical formula	$C_{28}H_{66}BF_4NOP_4W$	$C_{60}H_{76}BF_{24}MoNOP_4$
Formula weight	827.35	1513.85
Temperature (K)	183(2)	183(2)
Wavelength (Å)	0.71073	0.71073
Crystal system, space group	Tetragonal, P 4_1	Monoclinic, P $2_1/c$
a (Å)	11.1485(1)	13.0503(2)
b (Å)	11.1485(1)	18.6489(3)
c (Å)	29.5646(3)	28.5270(5)
α (deg)	90	90
β (deg)	90	94.8127(16)
γ (deg)	90	90
Volume ($Å^3$)	3674.56(6)	6918.2(2)
Z, calculated density (g/cm)	4, 1.496	4, 1.453
Absorption coefficient (mm^{-1})	3.360	0.386
F(000)	1696	3096
Crystal size (mm)	0.26 x 0.22 x 0.17	0.43 x 0.38 x 0.25
2θ scan range (deg)	2.58 to 32.57	2.30 to 28.00
Reflections collected	38822	51244
Reflections unique	13372	16629
Completeness to θ (%)	100.0	99.6
Absorption correction	Analytical	Analytical
Max./min. transmission	0.629 / 0.532	0.919 / 0.875
Data/restraints/parameters	13372 / 37 / 396	16629 / 17 / 896
Goodness-of-fit on F_2	1.034	1.042
Final R indices R1, wR2	0.0311, 0.0672	0.0509, 0.1249
R indices (all data) R1, wR2	0.0391, 0.0683	0.0915, 0.1607

Table 6.7 Summary of X-ray diffraction studies for **14** and **15**

	14	**15**
Empirical formula	$C_{28}H_{64}BF_4MoNOP_4$	$C_{105}H_{98}Cl_4N_2O_2P_8W_2$
Formula weight	737.43	2177.10
Temperature (K)	183(2)	183(2)
Wavelength (Å)	0.71073	0.71073 A
Crystal system, space group	Triclinic, P -1	Monoclinic, C 2/c
a (Å)	9.7151(2)	49.0802(5)
b (Å)	9.8928(3)	11.00910(10)
c (Å)	10.7503(3)	18.0405(2)
α (deg)	84.316(2) deg.	90
β (deg)	68.346(2) deg.	99.8778(10)
γ (deg)	69.732(2) deg.	90
Volume ($Å^3$)	900.34(5)	9603.30(17)
Z, calculated density (g/cm)	1, 1.360	4, 1.506
Absorption coefficient (mm^{-1})	0.585	2.689
F(000)	390	4376
Crystal size (mm)	0.20 x 0.14 x 0.05	0.33 x 0.22 x 0.14
2θ scan range (deg)	2.39 to 30.51	2.42 to 25.00
Reflections collected	26962	68671
Reflections unique	5497	8450
Completeness to θ (%)	99.9%	99.9
Absorption correction	Analytical	Semi-empirical from equivalents
Max./min. transmission	0.978 / 0.922	1.00000 and 0.60041
Data/restraints/parameters	5497 / 0 / 222	8450 / 4 / 563
Goodness-of-fit on F_2	1.241	1.123
Final R indices R1, wR2	0.0353, 0.1077	0.0278, 0.0771
R indices (all data) R1, wR2	0.0456, 0.1091	0.0325, 0.0820

Table 6.8 Summary of X-ray diffraction studies for **16** and **18**

	16	**18**
Empirical formula	$C_{158}H_{148}Al_2Cl_{13}N_3O_3P_{12}W_3$	$C_{20}H_{49}MoNOP_4$
Formula weight	3574.77	539.42
Temperature (K)	183(2)	183(2)
Wavelength (Å)	0.71073	0.71073
Crystal system, space group	Triclinic, P -1	Triclinic, P -1
a (Å)	14.1398(2)	8.2993(3)
b (Å)	15.2731(2)	10.3934(5)
c (Å)	17.8421(3)	17.0897(5)
α (deg)	92.0231(11)	104.275(3)
β (deg)	99.9789(13)	90.109(3)
γ (deg)	91.6355(11)	102.668(3)
Volume ($Å^3$)	3790.14(10)	1391.39(10)
Z, calculated density (g/cm)	1, 1.566	2, 1.288
Absorption coefficient (mm^{-1})	2.693	0.712
F(000)	1790	572
Crystal size (mm)	0.29 x 0.21 x 0.16	0.29 x 0.15 x 0.14
2θ scan range (deg)	2.32 to 30.51	2.46 to 25.00
Reflections collected	77193	17672
Reflections unique	22830	4820
Completeness to θ (%)	98.7	98.2
Absorption correction	Semi-empirical from equivalents	Analytical
Max./min. transmission	0.650 / 0.545	0.927 / 0.866
Data/restraints/parameters	22830 / 0 / 889	4820 / 0 / 261
Goodness-of-fit on F_2	0.964	1.070
Final R indices R1, wR2	0.0227, 0.0440	0.0488, 0.1460
R indices (all data) R1, wR2	0.0355, 0.0455	0.0558, 0.1504

Table 6.9 Summary of X-ray diffraction studies for **20** and **21**

	20	**21**
Empirical formula	$C_{28}H_{64}BCl_3F_4Mo_2N_2O_2P_4$	$C_{105}H_{194}Cl_{14}Mo_4N_4O_4P_8$
Formula weight	969.73	2704.46
Temperature (K)	183(2)	183(2)
Wavelength (Å)	0.71073	0.71073
Crystal system, space group	Triclinic, P -1	Orthorhombic, P b c a
a (Å)	8.4492(2)	28.6497(5)
b (Å)	15.5060(3)	15.3043(2)
c (Å)	16.3467(3)	30.3278(6)
α (deg)	75.176(2)	90
β (deg)	88.740(2)	90
γ (deg)	87.295(2)	90
Volume ($Å^3$)	2067.94(8)	13297.6(4)
Z, calculated density (g/cm)	2, 1.557	4, 1.351
Absorption coefficient (mm^{-1})	1.001	0.791
F(000)	996	5640
Crystal size (mm)	0.33 x 0.22 x 0.06	0.26 x 0.15 x 0.11
2θ scan range (deg)	2.41 to 30.51	2.37 to 25.68
Reflections collected	41040	73258
Reflections unique	12580	12534
Completeness to θ (%)	99.7	99.2
Absorption correction	Analytical	Analytical
Max./min. transmission	0.956 / 0.792	0.937 and 0.858
Data/restraints/parameters	12580 / 0 / 433	12534 / 67 / 639
Goodness-of-fit on F_2	1.020	1.065
Final R indices R1, wR2	0.0345, 0.0963	0.0753, 0.2297
R indices (all data) R1, wR2	0.0503, 0.1012	0.1014, 0.2454

Table 6.10 Summary of X-ray diffraction studies for **23** and **24**

	23	**24**
Empirical formula	$C_{40}H_{81}MoNOP_4$	$C_{72}H_{92}BF_{24}MoNOP_4$
Formula weight	811.88	1674.10
Temperature (K)	183(2)	183(2)
Wavelength (Å)	0.71073	0.71073
Crystal system, space group	Monoclinic, P $2_1/c$	Triclinic, P -1
a (Å)	11.9359(2)	13.3830(5)
b (Å)	22.8587(3)	14.0548(6)
c (Å)	16.1437(2)	20.6922(8)
α (deg)	90	86.437(3)
β (deg)	101.4022(12)	87.920(3)
γ (deg)	90	87.859(3)
Volume ($Å^3$)	4317.70(11)	3879.6(3)
Z, calculated density (g/cm)	4, 1.249	2, 1.433
Absorption coefficient (mm^{-1})	0.482	0.352
F(000)	1752	1724
Crystal size (mm)	0.18 x 0.18 x 0.10	0.36 x 0.30 x 0.23
2θ scan range (deg)	2.14 to 25.68	2.34 to 28.28
Reflections collected	36182	44357
Reflections unique	8197	19075
Completeness to θ (%)	99.9	99.0
Absorption correction	Semi-empirical from equivalents	Analytical
Max./min. transmission	0.953 / 0.889	0.957 and 0.939
Data/restraints/parameters	8197 / 13 / 432	19075 / 0 / 945
Goodness-of-fit on F_2	0.991	0.978
Final R indices R1, wR2	0.0503, 0.1213	0.0453, 0.1126
R indices (all data) R1, wR2	0.0855, 0.1355	0.0710, 0.1199

Table 6.11 Summary of X-ray diffraction studies for **25a** and **26a**

	25a	**26a**
Empirical formula	$C_{17}H_{34}ClMoNO_3P_2$	$C_{17}H_{34}ClNO_3P_2W$
Formula weight	493.78	581.68
Temperature (K)	183(2)	183(2)
Wavelength (Å)	0.71073	0.71073 A
Crystal system, space group	Orthorhombic, P 2_1 2_1 2_1	Orthorhombic, P 2_1 2_1 2_1
a (Å)	9.7411(1)	9.6673(1)
b (Å)	13.5632(2)	13.5489(1)
c (Å)	17.1379(2)	17.1950(2)
α (deg)	90	90
β (deg)	90	90
γ (deg)	90	90
Volume ($Å^3$)	2264.27(5)	2252.22(4)
Z, calculated density (g/cm)	4, 1.448	4, 1.716
Absorption coefficient (mm^{-1})	0.854	5.405
F(000)	1024	1152
Crystal size (mm)	0.52 x 0.28 x 0.18	0.42 x 0.29 x 0.27
2θ scan range (deg)	2.40 to 30.50	2.8 to 32.6
Reflections collected	27070	28444
Reflections unique	6897	8189
Completeness to θ (%)	99.9	99.9
Absorption correction	Analytical	Analytical
Max./min. transmission	0.87 / 0.70	0.327 / 0.180
Data/restraints/parameters	6897 / 2 / 262	8189 / 3 / 262
Goodness-of-fit on F_2	1.004	1.05
Final R indices R1, wR2	0.0236, 0.0480	0.020, 0.043
R indices (all data) R1, wR2	0.0286, 0.0489	0.023, 0.044

Table 6.12 Summary of X-ray diffraction studies for **27a** and **28a**

	27a	**28a**
Empirical formula	$C_{17}H_{35}MoNO_3P_2$	$C_{17}H_{35}NO_3P_2W$
Formula weight	459.34	547.24
Temperature (K)	183(2)	183(2)
Wavelength (Å)	0.71073	0.71073
Crystal system, space group	Orthorhombic, P 2_1 2_1 2_1	Orthorhombic, P 2_1 2_1 2_1
a (Å)	10.2002(1)	10.1851(1)
b (Å)	14.5065(2)	14.4862(1)
c (Å)	15.1319(2)	15.0675(1)
α (deg)	90	90
β (deg)	90	90
γ (deg)	90	90
Volume ($Å^3$)	2239.06(5)	2223.11(3)
Z, calculated density (g/cm)	4, 1.363	4, 1.635
Absorption coefficient (mm^{-1})	0.742	5.354
F(000)	960	1088
Crystal size (mm)	0.35 x 0.17 x 0.12 mm	0.32 x 0.21 x 0.16
2θ scan range (deg)	2.44 to 28.28	2.44 to 32.57
Reflections collected	24563	32374
Reflections unique	5557	8107
Completeness to θ (%)	99.9	100.0
Absorption correction	Analytical	Analytical
Max./min. transmission	0.94 and 0.86	0.625 / 0.415
Data/restraints/parameters	5557 / 0 / 229	8107 / 0 / 229
Goodness-of-fit on F_2	0.991	0.995
Final R indices R1, wR2	0.0321, 0.0708	0.0176, 0.0340
R indices (all data) R1, wR2	0.0370, 0.0720	0.0196, 0.0342

Table 6.13 Summary of X-ray diffraction studies for **29a** and **30a**

	29a	**30a**
Empirical formula	$C_{57}H_{62}BF_{24}MoNO_5P_2$	$C_{57}H_{62}BF_{24}NO_5P_2W$
Formula weight	1465.77	1553.67
Temperature (K)	183(2)	183(2)
Wavelength (Å)	0.71073	0.71073
Crystal system, space group	Orthorhombic, P 2_1 2_1 2_1	Orthorhombic, P 2_1 2_1 2_1
a (Å)	13.0684(2)	13.0842(2)
b (Å)	13.7481(2)	13.7606(2)
c (Å)	36.2825(8)	36.2178(5)
α (deg)	90	90
β (deg)	90	90
γ (deg)	90	90
Volume ($Å^3$)	6518.7(2)	6520.89(16)
Z, calculated density (g/cm)	4, 1.494	4, 1.583
Absorption coefficient (mm^{-1})	0.364	1.935
F(000)	2976	3104
Crystal size (mm)	0.33 x 0.18 x 0.16	0.36 x 0.30 x 0.22
2θ scan range (deg)	2.22 to 25.68	2.69 to 26.37
Reflections collected	59185	78446
Reflections unique	12338	13314
Completeness to θ (%)	99.9	99.9
Absorption correction	Semi-empirical from equivalents	Analytical
Max./min. transmission	0.943 / 0.849	0.726 / 0.614
Data/restraints/parameters	12338 / 208 / 860	13314 / 29 / 787
Goodness-of-fit on F_2	1.125	1.003
Final R indices R1, wR2	0.0730, 0.1597	0.0433, 0.1166
R indices (all data) R1, wR2	0.0908, 0.1665	0.0489, 0.1187

Table 6.14 Summary of X-ray diffraction studies for **25b** and **27d**

	25b	**27d**
Empirical formula	$C_{16}H_{33}MoNO_3P_2$	$C_{28}H_{48}ClMoNO_3P_2$
Formula weight	445.31	640.00
Temperature (K)	183(2)	183(2)
Wavelength (Å)	0.71073	0.71073
Crystal system, space group	Orthorhombic, P 2_1 2_1 2_1	Tetragonal, P 4_3 2_1 2
a (Å)	7.94395(12)	13.7908(1)
b (Å)	13.9479(2)	13.7908(1)
c (Å)	19.2640(3)	16.4899(2)
α (deg)	90	90
β (deg)	90	90
γ (deg)	90	90
Volume ($Å^3$)	2134.48(6)	3136.15(5)
Z, calculated density (g/cm)	4, 1.386	4, 1.355
Absorption coefficient (mm^{-1})	0.776	0.634
F(000)	928	1344
Crystal size (mm)	0.42 x 0.30 x 0.15	0.33 x 0.22 x 0.12
2θ scan range (deg)	2.57 to 30.50	2.88 to 30.50
Reflections collected	27362	39753
Reflections unique	6507	4785
Completeness to θ (%)	99.9	99.9
Absorption correction	Semi-empirical from equivalents	Semi-empirical from equivalents
Max./min. transmission	0.890 / 0.828	1.000 / 0.911
Data/restraints/parameters	6507 / 0 / 220	4785 / 0 / 177
Goodness-of-fit on F_2	1.000	1.217
Final R indices R1, wR2	0.0360, 0.0892	0.0365, 0.0830
R indices (all data) R1, wR2	0.0460, 0.0920	0.0403, 0.0839

Table 6.15 Summary of X-ray diffraction studies for **33** and **34**

	32	**33**
Empirical formula	$C_{20}H_{42}ClMoNO_3P_2$	$C_{20}H_{43}MoNO_3P_2$
Formula weight	537.88	503.43
Temperature (K)	183(2)	183(2)
Wavelength (Å)	0.71073	0.71073
Crystal system, space group	Triclinic, P -1	Orthorhombic, P b c a
a (Å)	8.7290(2)	15.9854(2)
b (Å)	8.7500(2)	13.4723(2)
c (Å)	9.4195(1)	23.9608(3)
α (deg)	94.681(1)	90
β (deg)	99.043(1)	90
γ (deg)	112.35(2)	90
Volume ($Å^3$)	649.21(10)	5160.20(12)
Z, calculated density (g/cm)	1, 1.376	8, 1.296
Absorption coefficient (mm^{-1})	0.750	0.650
F(000)	282	2128
Crystal size (mm)	0.34 x 0.30 x 0.19	0.41 x 0.33 x 0.26
2θ scan range (deg)	2.55 to 32.57	2.61 to 30.51
Reflections collected	14564	36055
Reflections unique	4718	7879
Completeness to θ (%)	99.7	99.9
Absorption correction	Analytical	Analytical
Max./min. transmission	0.91 / 0.85	0.87 / 0.82
Data/restraints/parameters	4718 / 0 / 148	7879 / 0 / 260
Goodness-of-fit on F_2	1.033	1.057
Final R indices R1, wR2	0.0309, 0.0801	0.0281, 0.0665
R indices (all data) R1, wR2	0.0329, 0.0811	0.0416, 0.0691

Table 6.16 Summary of X-ray diffraction studies for **34** and **35**

	34	**35**
Empirical formula	$C_{56}H_{62}BF_{24}MoNO_4P_2$	$C_{24}H_{45}MoNO_2P_4$
Formula weight	1437.76	599.43
Temperature (K)	183(2)	183(2)
Wavelength (Å)	0.71073	0.71073 A
Crystal system, space group	Monoclinic, C 2/c	Orthorhombic, P 2_1 2_1 2_1
a (Å)	18.3586(3)	8.9513(1)
b (Å)	17.6501(3)	17.9461(4)
c (Å)	19.2868(3)	54.8760(7)
α (deg)	90	90
β (deg)	95.515(1)	90
γ (deg)	90	90
Volume ($Å^3$)	6220.60(18)	8815.3(2)
Z, calculated density (g/cm)	4, 1.535	12, 1.355
Absorption coefficient (mm^{-1})	0.379	0.685
F(000)	2920	3768
Crystal size (mm)	0.50 x 0.35 x 0.24	0.15 x 0.12 x 0.08
2θ scan range (deg)	2.54 to 30.51	2.27 to 25.68
Reflections collected	23925	50499
Reflections unique	9487	16713
Completeness to θ (%)	99.8	99.9
Absorption correction	Analytical	Analytical
Max./min. transmission	0.93 / 0.89	0.955 / 0.932
Data/restraints/parameters	9487 / 0 / 410	16713 / 0 / 889
Goodness-of-fit on F_2	1.052	1.009
Final R indices R1, wR2	0.0544, 0.1531	0.0452, 0.0786
R indices (all data) R1, wR2	0.0768, 0.1632	0.0633, 0.0868

7 References

1. Hieber, W.; Leutert, F., *Naturwissenschaften* **1931,** *19*, 360.
2. Hieber, W.; Schulten, H., *Z. Anorg. Allg. Chem.* **1937,** *232*, 29.
3. Angelini, A.; Aresta, M.; Dibenedetto, A.; Pastore, C.; Quaranta, E.; Chierotti, M. R.; Gobetto, R.; Imre, P.; Graiff, C.; Tiripicchio, A., *Dalton Trans.* **2009**, 7924.
4. Clark, H. C.; Billard, C.; Wong, C. S., *J. Organomet. Chem.* **1979,** *173*, 341.
5. Pannetier, N.; Sortais, J. B.; Dieng, P. S.; Barloy, L.; Sirlin, C.; Pfeffer, M., *Organometallics* **2008,** *27*, 5852.
6. Sandoval, C. A.; Ohkuma, T.; Muniz, K.; Noyori, R., *J. Am. Chem. Soc.* **2003,** *125*, 13490.
7. Casey, C. P.; Bikzhanova, G. A.; Guzei, I. A., *J. Am. Chem. Soc.* **2006,** *128*, 2286.
8. Hayashi, A.; Yoshitomi, T.; Umeda, K.; Okazaki, M.; Ozawa, F., *Organometallics* **2008,** *27*, 2321.
9. Maruyama, Y.; Yoshiuchi, K.; Ozawa, F., *J. Organomet. Chem.* **2000,** *609*, 130.
10. Mimoun, H., *J. Org. Chem.* **1999,** *64*, 2582.
11. Albahily, K.; Al-Baldawi, D.; Gambarotta, S.; Koc, E.; Duchateau, R., *Organometallics* **2008,** *27*, 5943.
12. Cui, D. M.; Nishiura, M.; Tardif, O.; Hou, Z. M., *Organometallics* **2008,** *27*, 2428.
13. Labbe, A.; Carlotti, S.; Shcheglova, L.; Desbois, P.; Deffieux, A., *Polymer* **2006,** *47*, 3734.
14. Cann, K.; Cole, T.; Slegeir, W.; Pettit, R., *J. Am. Chem. Soc.* **1978,** *100*, 3969.
15. Brunet, J. J., *Chem. Rev.* **1990,** *90*, 1041.
16. Brunet, J. J., *Eur. J. Inorg. Chem.* **2000**, 1377.
17. Osborn, J. A.; Jardine, F. H.; Young, J. F.; Wilkinson, G. I., *J. Chem. Soc.* **1966**, 1711.
18. Koga, N.; Daniel, C.; Han, J.; Fu, X. Y.; Morokuma, K., *J. Am. Chem. Soc.* **1987,** *109*, 3455.
19. Halpern, J.; Harrod, J. F.; James, B. R., *J. Am. Chem. Soc.* **1961,** *83*, 753.
20. Schrock, R. R.; Osborn, J. A., *Chem. Commun.* **1970**, 567.

21. Chen, H. W.; Jolly, W. L.; Kopf, J.; Lee, T. H., *J. Am. Chem. Soc.* **1979,** *101*, 2607.

22. Sweany, R. L.; Owens, J. W., *J. Organomet. Chem.* **1983,** *255*, 327.

23. Bullock, M. R., *Comments Inorg. Chem.* **1991,** *12*, 1

24. Bullock, R. M., *Chem. Eur. J.* **2004,** *10*, 2366.

25. Abdur-Rashid, K.; Fong, T. P.; Greaves, B.; Gusev, D. G.; Hinman, J. G.; Landau, S. E.; Lough, A. J.; Morris, R. H., *J. Am. Chem. Soc.* **2000,** *122*, 9155.

26. Kristjansdottir, S. S.; Moody, A. E.; Weberg, R. T.; Norton, J. R., *Organometallics* **1988,** *7*, 1983.

27. Kristjansdottir, S. S.; Loendorf, A. J.; Norton, J. R., *Inorg. Chem.* **1991,** *30*, 4470.

28. Bullock, R. M.; Rappoli, B. J., *Chem. Commun.* **1989**, 1447.

29. Chaloner, P. A.; Esteruelas, M. A.; Jos, F.; Oro, L. A., *Homogeneous Hydrogenation*. Kluwer Academic Publishers: Dordrecht, 1994.

30. Kursanov, D. N.; Parnes, Z. N.; Loim, N. M., *Synthesis* **1974**, 633.

31. Berke, H., *ChemPhysChem* **2010,** *11*, 1837.

32. Dahlenburg, L.; Gotz, R., *Eur. J. Inorg. Chem.* **2004**, 888.

33. Luan, L.; Song, J. S.; Bullock, R. M., *J. Org. Chem.* **1995,** *60*, 7170.

34. Cheng, T.-Y.; Brunschwig, B. S.; Bullock, M. R., *J. Am. Chem. Soc.* **1998,** *120*, 13121.

35. Heinekey, D. M.; Oldham, W. J., *Chem. Rev.* **1993,** *93*, 913.

36. Kubas, G. J., *Metal Didydrogen and Bond Complexes: Structure, Theory and Reactivity*. Kluwer Academic/Plenum Publishers: New York, 2001.

37. Bullock, R. M.; Song, J. S., *J. Am. Chem. Soc.* **1994,** *116*, 8602.

38. Vanderzeijden, A. A. H.; Berke, H., *Helv. Chim. Acta* **1992,** *75*, 513.

39. Kao, S. C.; Spillett, C. T.; Ash, C.; Lusk, R.; Park, Y. K.; Darensbourg, M. Y., *Organometallics* **1985,** *4*, 83.

40. Gibson, D. H.; Elomrani, Y. S., *Organometallics* **1985,** *4*, 1473.

41. Song, J. S.; Szalda, D. J.; Bullock, R. M.; Lawrie, C. J. C.; Rodkin, M. A.; Norton, J. R., *Angew. Chem. Int. Ed.* **1992,** *31*, 1233.

42. Papish, E. T.; Rix, F. C.; Spetseris, N.; Norton, J. R.; Williams, R. D., *J. Am. Chem. Soc.* **2000,** *122*, 12235.

43. Smith, K. T.; Norton, J. R.; Tilset, M., *Organometallics* **1996,** *15*, 4515.

44. Song, J. S.; Szalda, D. J.; Bullock, R. M., *Inorg. Chim. Acta.* **1997,** *259*, 161.

45. Song, J. S.; Szalda, D. J.; Bullock, R. M., *J. Am. Chem. Soc.* **1996,** *118*, 11134.

46. Song, J. S.; Szalda, D. J.; Bullock, R. M., *Organometallics* **2001,** *20*, 3337.

47. Avramovic, N.; Höck, J.; Blacque, O.; Fox, T.; Schmalle, H. W.; Berke, H., *J. Organomet. Chem.* **2010,** *695*, 382.

48. Vanderzeijden, A. A. H.; Veghini, D.; Berke, H., *Inorg. Chem.* **1992,** *31*, 5106.

49. Vanderzeijden, A. A. H.; Bosch, H. W.; Berke, H., *Organometallics* **1992,** *11*, 2051.

50. Vanderzeijden, A. A. H.; Shklover, V.; Berke, H., *Inorg. Chem.* **1991,** *30*, 4393.

51. Höck, J.; Jacobsen, H.; Schmalle, H. W.; Artus, G. R. J.; Fox, T.; Amor, J. I.; Bath, F.; Berke, H., *Organometallics* **2001,** *20*, 1533.

52. Chen, Z.; Schmalle, H. W.; Fox, T.; Berke, H., *Dalton Trans.* **2005**, 580.

53. Fupei, L.; Schmalle, H. W.; Fox, T.; Berke, H., *Organometallics* **2003,** *22*, 3382.

54. Fupei, L.; Heiko, J.; Schmalle, H. W.; Fox, T.; Berke, H., *Organometallics* **2000,** *19*, 1950.

55. Bullock, M. R.; Voges Mark, H., *J. Am. Chem. Soc.* **2000,** *122*, 12594.

56. Voges, M. H.; Bullock, R. M., *J. Chem. Soc. Dalton.* **2002**, 759.

57. Kimmich, B. F. M.; Fagan, P. J.; Hauptman, E.; Bullock, R. M., *Chem. Commun.* **2004**, 1014.

58. Schlaf, M.; Ghosh, P.; Fagan, P. J.; Hauptman, E.; Bullock, R. M., *Angew. Chem. Int. Ed.* **2001,** *40*, 3887.

59. Guan, H. R.; Saddoughi, S. A.; Shaw, A. P.; Norton, J. R., *Organometallics* **2005,** *24*, 6358.

60. Guan, H. R.; Iimura, M.; Magee, M. P.; Norton, J. R.; Janak, K. E., *Organometallics* **2003,** *22*, 4084.

61. Guan, H. R.; Iimura, M.; Magee, M. P.; Norton, J. R.; Zhu, G., *J. Am. Chem. Soc.* **2005,** *127*, 7805.

62. Blum, Y.; Czarkie, D.; Rahamim, Y.; Shvo, Y., *Organometallics* **1985,** *4*, 1459.

63. Shvo, Y.; Czarkie, D.; Rahamim, Y.; Chodosh, D. F., *J. Am. Chem. Soc.* **1986,** *108*, 7400.

64. Shvo, Y.; Goldberg, I.; Czerkie, D.; Reshef, D.; Stein, Z., *Organometallics* **1997,** *16*, 133.

65. Samec, J. S. M.; Backvall, J. E., *Chem. Eur. J.* **2002,** *8*, 2955.

66. Casey, C. P.; Guan, H. R., *J. Am. Chem. Soc.* **2007,** *129*, 5816.

67. Bullock, R. M., *Angew. Chem. Int. Ed.* **2007,** *46*, 7360.

68. Noyori, R., *Angew. Chem. Int. Ed.* **2002,** *41*, 2008.

69. Noyori, R.; Yamakawa, M.; Hashiguchi, S., *J. Org. Chem.* **2001,** *66*, 7931.

70. Yamakawa, M.; Ito, H.; Noyori, R., *J. Am. Chem. Soc.* **2000,** *122*, 1466.

71. Kubas, G. J.; Ryan, R. R.; Swanson, B. I.; Vergamini, P. J.; Wasserman, H. J., *J. Am. Chem. Soc.* **1984,** *106*, 451.

72. Kubas, G. J., *Catal. Lett.* **2005,** *104*, 79.

73. Maseras, F.; Lledos, A.; Clot, E.; Eisenstein, O., *Chem. Rev.* **2000,** *100*, 601.

74. Perutz, R. N.; Turner, J. J., *J. Am. Chem. Soc.* **1975,** *97*, 4791.

75. Brown, C. E.; Ishikawa, Y.; Hackett, P. A.; Rayner, D. M., *J. Am. Chem. Soc.* **1990,** *112*, 2530.

76. Church, S. P.; Grevels, F. W.; Hermann, H.; Schaffner, K., *Chem. Commun.* **1985**, 30.

77. Luo, X. L.; Kubas, G. J.; Burns, C. J.; Butcher, R.; Bryan, J. C., *Inorg. Chem.* **1995,** *34*, 6538

78. Luo, X. L.; Kubas, G. J.; Burns, C. J.; Eckert, J., *Inorg. Chem.* **1994,** *33*, 5219.

79. Kundel, P.; Berke, H., *J. Organomet. Chem.* **1986,** *314*, C31.

80. Kundel, P.; Berke, H., *J. Organomet. Chem.* **1988,** *339*, 297.

81. Bannwart, E.; Jacobsen, H.; Furno, F.; Berke, H., *Organometallics* **2000,** *19*, 3605.

82. Furno, F.; Fox, T.; Schmalle, H. W.; Berke, H., *Organometallics* **2000,** *19*, 3620.

83. Bannwart, E.; Jacobsen, H.; Hubener, R.; Schmalle, H. W.; Berke, M., *J. Organomet. Chem.* **2001,** *622*, 97.

84. von Ahsen, B.; Bach, C.; Berkei, M.; Kockerling, M.; Willner, H.; Hagele, G.; Aubke, F., *Inorg. Chem.* **2003,** *42*, 3801.

85. Zhao, Y.; Schmalle, H. W.; Fox, T.; Blacque, O.; Berke, H., *Dalton Trans.* **2005**, 73.

86. Cugny, J.; Schmalle, H. W.; Fox, T.; Blacque, O.; Alfonso, M.; Berke, H., *Eur. J. Inorg. Chem.* **2006**, 540.

87. Avramovic, N.; Blacque, O.; Berke, H., *Acta Crystallogr., Sect. E: Struct. Rep. Online* **2008,** *64*, M242.

88. Jezowskatrzebiatowska, B.; Jezierski, A., *J. Mol. Struct.* **1978,** *46*, 197.

89. Lyne, P. D.; Mingos, D. M. P., *J. Chem. Soc. Dalton.* **1995**, 1635.

90. Zhang, L.; Gamasa, M. P.; Gimeno, J.; Carbajo, R. J.; LopezOrtiz, F.; Lanfranchi, M.; Tiripicchio, A., *Organometallics* **1996,** *15*, 4274.

91. Mitoraj, M. P.; Zhu, H.; Michalak, A.; Ziegler, T., *Int. J. Quantum Chem.* **2009,** *109*, 3379.

92. Kubas, G. J.; Burns, C. J.; Eckert, J.; Johnson, S. W.; Larson, A. C.; Vergamini, P. J.; Unkefer, C. J.; Khalsa, G. R. K.; Jackson, S. A.; Eisenstein, O., *J. Am. Chem. Soc.* **1993,** *115*, 569.

93. Brookhart, M.; Grant, B.; Volpe, A. F., *Organometallics* **1992,** *11*, 3920.

94. Alaimo, P. J.; Arndtsen, B. A.; Bergman, R. G., *J. Am. Chem. Soc.* **1997,** *119*, 5269.

95. Jutzi, P.; Muller, C.; Stammler, A.; Stammler, H. G., *Organometallics* **2000,** *19*, 1442.

96. Matsushita, N.; Kitagawa, H.; Mitani, T., *Synth. Met.* **1995,** *71*, 1933.

97. Cheng, T. Y.; Bullock, R. M., *J. Am. Chem. Soc.* **1999,** *121*, 3150.

98. Cheng, T. Y.; Bullock, R. M., *Organometallics* **2002,** *21*, 2325.

99. Kubas, G. J., *J. Organomet. Chem.* **2001,** *635*, 37.

100. Kubas, G. J.; Ryan, R. R.; Unkefer, C. J., *J. Am. Chem. Soc.* **1987,** *109*, 8113

101. Kubas, G. J.; Ryan, R. R.; Wrobleski, D. A., *J. Am. Chem. Soc.* **1986,** *108*, 1339.

102. Kimmich, B. F. M.; Fagan, P. J.; Hauptman, E.; Marshall, W. J.; Bullock, R. M., *Organometallics* **2005,** *24*, 6220.

103. Carmona, E.; Gutierrezpuebla, E.; Monge, A.; Perez, P. J.; Sanchez, L. J., *Inorg. Chem.* **1989,** *28*, 2120.

104. Cotton, F. A.; Llusar, R., *Acta Crystallogr., Sect. C: Cryst. Struct. Commun.* **1988,** *44*, 952.

105. van der Eide, E. F.; Piers, W. E.; Parvez, M.; McDonald, R., *Inorg. Chem.* **2007,** *46*, 14.

106. Fupei, L.; Schmalle, H. W.; Berke, H., *J. Organomet. Chem.* **2006,** *691*, 5655.

107. Fupei, L.; Schmalle, H. W.; Berke, H., *Eur. J. Inorg. Chem.* **2006**, 5081.

108. Giese, H. H.; Habereder, T.; Knizek, J.; Noth, H.; Warchhold, M., *Eur. J. Inorg. Chem.* **2001**, 1195.

109. Jana, A.; Roesky, H. W.; Schulzke, C., *Dalton Trans.* **2010,** *39*, 132.

110. Henderson, K. W.; Allan, J. F.; Kennedy, A. R., *Chem. Commun.* **1997**, 1149.

111. Brookhart, M.; Green, M. L. H., *J. Organomet. Chem.* **1983,** *250*, 395.

112. Mitoraj, M. P.; Michalak, A.; Ziegler, T., *Organometallics* **2009,** *28*, 3727.

113. Pantazis, D. A.; McGrady, J. E.; Besora, M.; Maseras, F.; Etienne, M., *Organometallics* **2008,** *27*, 1128.

114. Sato, M.; Tatsumi, T.; Kodama, T.; Hidai, M.; Uchida, T.; Uchida, Y., *J. Am. Chem. Soc.* **1978,** *100*, 4447.

115. Honeychuck, R. V.; Hersh, W. H., *Inorg. Chem.* **1989,** *28*, 2869.

116. Vandersluys, L. S.; Kubatmartin, K. A.; Kubas, G. J.; Caulton, K. G., *Inorg. Chem.* **1991,** *30*, 306.

117. Gottlieb, H. E.; Kotlyar, V.; Nudelman, A., *J. Org. Chem.* **1997,** *62*, 7512.

118. Gaudet, M. V.; Zaworotko, M. J.; Cameron, T. S.; Linden, A., *J. Organomet. Chem.* **1989,** *367*, 267.

119. Troyanov, S.; Pisarevsky, A.; Struchkov, Y. T., *J. Organomet. Chem.* **1995,** *494*, C4.

120. Greco, G. E.; Schrock, R. R., *Inorg. Chem.* **2001,** *40*, 3861.

121. Laplaza, C. E.; Johnson, M. J. A.; Peters, J. C.; Odom, A. L.; Kim, E.; Cummins, C. C.; George, G. N.; Pickering, I. J., *J. Am. Chem. Soc.* **1996,** *118*, 8623.

122. Zou, F. Synthesis, Catalytic Activity and Hydride Mobility of Tungsten Alkylidyne Hydride Complexes. University of Zurich, Zurich, 2005.

123. Carfagna, C.; Green, M.; Nagle, K. R.; Williams, D. J.; Woolhouse, C. M., *J. Chem. Soc. Dalton.* **1993**, 1761.

124. Legzdins, P.; Wassink, B., *Organometallics* **1988,** *7*, 482.

125. Gibson, D. H.; Owens, K.; Mandal, S. K.; Sattich, W. E.; Franco, J. O., *Organometallics* **1989,** *8*, 498.

126. Poli, R.; Mui, H. D., *Inorg. Chem.* **1991,** *30*, 65.

127. Cotton, F. A.; Luck, R. L., *Inorg. Chem.* **1989,** *28*, 182.

128. Limberg, C.; Buchner, M.; Heinze, K.; Walter, O., *Inorg. Chem.* **1997,** *36*, 872.

129. Isovitsch, R. A.; Fronczek, F. R.; Maverick, A. W., *Polyhedron* **1998,** *17*, 1617.

130. Fagan, P. J.; Voges, M. H.; Bullock, R. M., *Organometallics* **2010,** *29*, 1045.

131. Esteruelas, M. A.; Garcia-Yebra, C.; Onate, E., *Organometallics* **2008,** *27*, 3029.

132. Magee, M. P.; Norton, J. R., *J. Am. Chem. Soc.* **2001,** *123*, 1778.

133. Hou, G.; Gosselin, F.; Li, W.; McWilliams, C.; Sun, Y. K.; Weisel, M.; O'Shea, P. D.; Chen, C. Y.; Davies, I. W.; Zhang, X. M., *J. Am. Chem. Soc.* **2009,** *131*, 9882.

134. Liu, X. Y.; Venkatesan, K.; Schmalle, H. W.; Berke, H., *Organometallics* **2004,** *23*, 3153.

135. Bullock, M. R., *Handbook of Homogeneous Hydrogenation*. Wiley-VCH: Weinheim, 2007.

136. Wu, F.; Dioumaev, V. K.; Szalda, D. J.; Hanson, J.; Bullock, R. M., *Organometallics* **2007,** *26*, 5079.

137. Kubas, G. J.; Unkefer, C. J.; Swanson, B. I.; Fukushima, E., *J. Am. Chem. Soc.* **1986,** *108*, 7000.

138. Wasserman, H. J.; Kubas, G. J.; Ryan, R. R., *J. Am. Chem. Soc.* **1986,** *108*, 2294.

139. Dybov, A.; Blacque, O.; Berke, H., *Eur. J. Inorg. Chem.* **2010,** *2010*, 3328.

140. Liang, F.; Schmalle, H. W.; Fox, T.; Berke, H., *Organometallics* **2003,** *22*, 3382.

141. Yu, M. P. Y.; Mayr, A.; Cheung, K. K., *J. Chem. Soc. Dalton.* **1998**, 475.

142. Sekino, M.; Sato, M.; Nagasawa, A.; Kikuchi, K., *Organometallics* **1994,** *13*, 1451.

143. Johnson, L. K.; Killian, C. M.; Brookhart, M., *J. Am. Chem. Soc.* **1995,** *117*, 6414.

144. Campora, J.; Lopez, J. A.; Palma, P.; Valerga, P.; Spillner, E.; Carmona, E., *Angew. Chem. Int. Ed.* **1999,** *38*, 147.

145. Widenhoefer, R. A.; Vadehra, A.; Cheruvu, P. K., *Organometallics* **1999,** *18*, 4614.

146. Lee, M. K.; Huang, P. S.; Wen, Y. S.; Lin, J. T., *Organometallics* **1990,** *9*, 2181.

147. Tolman, C. A., *Chem. Rev.* **1977,** *77*, 313.

148. Chlorbenzene was used as a non-coordinative polar solvent with high boiling point. The non-polar solvent (benzene or toluene) are not able to dissolve the catalyst. Testing THF as a solvent revealed no product formation in the imine hydrogenation reaction.

149. Konze, W. V.; Scott, B. L.; Kubas, G. J., *Chem. Commun.* **1999**, 1807.

150. Salem, H.; Shimon, L. J. W.; Leitus, G.; Weiner, L.; Milstein, D., *Organometallics* **2008,** *27*, 2293.

151. Kranenburg, M.; Vanderburgt, Y. E. M.; Kamer, P. C. J.; Vanleeuwen, P. W. N. M.; Goubitz, K.; Fraanje, J., *Organometallics* **1995,** *14*, 3081.

152. Fey, N.; Harvey, J. N.; Lloyd-Jones, G. C.; Murray, P.; Orpen, A. G.; Osborne, R.; Purdie, M., *Organometallics* **2008,** *27*, 1372.

153. Vogeley, N. J.; White, P. S.; Templeton, J. L., *Organometallics* **2004,** *23*, 1378.

154. Lucht, B.; Poss, M. J.; Richmond, T. G., *J. Chem. Educ.* **1991,** *68*, 786.

155. Lee, S. W.; Trogler, W. C., *Organometallics* **1990,** *9*, 1470.

156. Smith, M. R.; Cheng, T. Y.; Hillhouse, G. L., *Inorg. Chem.* **1992,** *31*, 1535.

157. Smith, M. R.; Cheng, T. Y.; Hillhouse, G. L., *J. Am. Chem. Soc.* **1993,** *115*, 8638.

158. Miller, G. A.; Lee, S. W.; Trogler, W. C., *Organometallics* **1989,** *8*, 738.

159. Dang, T. P.; Kagan, H. B., *Chem. Commun.* **1971**, 481.

160. Kagan, H. B.; Dang, T. P., *J. Am. Chem. Soc.* **1972,** *94*, 6429.

161. Dumont, W.; Poulin, J.; Dang, T.; Kagan, H. B., *J. Am. Chem. Soc.* **1973,** *95*, 8295.

162. Eckert, C.; Dahlenburg, L.; Wolski, A., *Z. Naturforsch., B: J. Chem. Sci.* **1995,** *50*, 1004.

163. Dahlenburg, L.; Kaunert, A., *Acta Crystallogr., Sect. C: Cryst. Struct. Commun.* **1998,** *54*, 1016.

164. Dahlenburg, L.; Kaunert, A., *Eur. J. Inorg. Chem.* **1998**, 885.

165. Dahlenburg, L.; Kurth, V., *Eur. J. Inorg. Chem.* **1998**, 597.

166. Dahlenburg, L.; Becker, C.; Hock, J.; Mertel, S., *J. Organomet. Chem.* **1998,** *564*, 155.

167. Dahlenburg, L.; Eckert, C., *J. Organomet. Chem.* **1998,** *564*, 227.

168. Dahlenburg, L.; Kurth, V., *J. Organomet. Chem.* **1999,** *585*, 315.

169. Dahlenburg, L.; Herbst, K.; Berke, H., *J. Organomet. Chem.* **1999,** *585*, 225.

170. Chan, A. S. C.; Pluth, J. J.; Halpern, J., *J. Am. Chem. Soc.* **1980,** *102*, 5952.

171. Chan, A. S. C.; Halpern, J., *J. Am. Chem. Soc.* **1980,** *102*, 838.

172. Halpern, J., *Science* **1982,** *217*, 401.

173. Landis, C. R.; Halpern, J., *J. Am. Chem. Soc.* **1987,** *109*, 1746.

174. Zhao, Y. Chemistry of Molybdenum Nitrosyl Hydrides with Achiral or Chiral Phosphine Ligands. Universität Zürich, Zürich, 2005.

175. Burt, R. J.; Chatt, J.; Hussain, W.; Leigh, G. J., *J. Organomet. Chem.* **1979,** *182*, 203.

176. Phenol was used as a reagent initiating the ionic hydrogenation of acetophenone.

177. Lindner, E.; Schmid, M.; Wald, J.; Queisser, J. A.; Geprags, M.; Wegner, P.; Nachtigal, C., *J. Organomet. Chem.* **2000,** *602*, 173.

178. Kim, T. J.; Kim, Y. H.; Kim, Y. H.; Shim, S. C.; Kwak, Y. W.; Cha, J. S.; Lee, H. S.; Uhm, J. K.; Byun, S. I., *Bull. Korean Chem. Soc.* **1992,** *13*, 588.

179. Bencze, L.; Kohan, J., *Inorg. Chim. A-Lett.* **1982,** *65*, L17.

180. Seyferth, K.; Taube, R., *J. Organomet. Chem.* **1982,** *229*, 275.

181. *STOE & Cie, GmbH, Darmstadt*, Germany, 1999.

182. *Xcalibur CCD System; Oxford Diffraction Ltd: Abingdon, Oxfordshire*, England, 2007.

183. Sheldrick, G. M., *Acta Crystallogr., Sect. A: Found. Crystallogr.* **2008,** *64*, 112.

184. Spek, A. L., *J. Appl. Crystallogr.* **2003,** *36*, 7.

Acknowledgment

I would like to thank those people below…

My supervisor, Prof. Dr. Heinz Berke, for introducing me into an interesting research field; for his guidance, encouragement and support he provided through all these years working in his group.

I am grateful to people who helped me in leading my Ph.D. project:
Dr. Olivier Blacque, for so many crystallographic structures he solved for me
Dr. Thomas Fox, for huge number of NMR measurements he performed for me
Dr. Christian Frech, for a lot of discussions and text corrections
Dr. Koushik Venkatesan, for text corrections
Heinz Spring, for element analysis

The administration and technicians: Beatrice Spichtig, Tanja Spörri, Susanna Sprokkereef Hans-Peter Stalder, Manfred Jöhri, Sabine Stockhause, Dr. Fredinand Wild.

I am thankful to people with whom I worked in the glovebox for technical and scientific discussion as well as for the kind working atmosphere: Sergey Semenov, Thimokhin Ivan, Samir Barmen.

I am grateful to all members in the group of Prof. Dr. Heinz Berke for help and cooperation.

I thank the Swiss National Science Foundation for financial support.

The special thank to my lovely wife and my parents.

CURRICULUM VITAE

Personal information

Alexander Dybov
Waffenplatzstrasse 40
8002 Zurich
Switzerland
dybovalex@gmail.com
Mobile +41 76 278 49 41
Date of birth: 10 Aug 1984
Nationality: Russian

Goal / Motivation

A position in R&D department at that I can show my best sides and talents
(goals and solutions oriented personality, presenting experience, team player, high social competence, focused, creative, reliable, motivated)

Experience

Organic and organometallic synthesis, catalytic processes
Working in inert atmosphere (Shlenk technique and glovebox)
Routine NMR, IR and mass spectrometry, UV-vis
Experience in analytical chemistry
Basic knowledge concerning X – Ray analysis

Education

09/2006 - present	Ph.D. Student, Inorganic Chemical Institute, University of Zurich "Developing of a new catalytic system based on molybdenum and tungsten"
09/2001 - 07/2006	Chemical Department, Moscow State University named after Lomonosov, diploma with honour Master thesis: "Synthesis and study of chemical properties of β-diimine complex of aluminum"
09/2000 - 09/2001	Mathematic Kolmagorov school / Moscow, Russia

Working experience

05/2004 - 06/2006	Laboratory assistant, Organic laboratory at Moscow State University, Moscow, Russia

Languages

Russian: native
German: very good in speaking and writing
English: fluent in speaking and writing

Additional Skills

Experience in conducting of practical exercises for bachelor students
Good computer and software user: office programs (Word, Excel, Power Point); chemical programs (ChemDraw, ChemWindow), Outlook, different databank systems; graphical program (Corel Draw)
Experience in presenting in front of public
Experience in primitive glassblowing work

Publications

Dybov, A.; Blacque, O.; Berke, H., *Eur. J. Inorg. Chem.* **2010,** *2010*, 3328.

Dybov, A.; Blacque, O.; Berke, H., *Eur. J. Inorg. Chem.* "Molybdenum Nitrosyl Complexes and their Application in Catalytic Imine Hydrogenation", accepted.

Conferences attended

XIth International Seminar for Ph. D. Students on Organometallic and Coordination Chemistry, April 2008, Germany. Presentation.

XVIIIth EuCheMS Conference on Organometallic Chemistry, June 2009, Sweden. Poster.

8th Swiss Snow Symposium, Februar 2010, Parpan GR, Switzerland. Presentation.

Hobbies

Sport (water polo, swimming, skiing)
Chess (participated some Zurich tournaments and was awarded the prizes)

Referees

Prof. Dr. H. Berke, Professor at Universität Zürich, Anorganisch-chemisches Institut
Tel: +41 44 63 54681, E-mail: hberke@access.uzh.ch

Dr. Ch. Frech Oberassistent at Universität Zürich, Anorganisch-chemisches Institut
Tel: +41 44 63 54670, E-mail: chfrech@aci.uzh.ch